

IFM-GEOMAR

Leibniz - Institut für
Meereswissenschaften

Identification and quantification of suspended solids and their effects in modern marine recirculation systems

Dissertation

zur Erlangung des Doktorgrades
der Mathematisch-Naturwissenschaftlichen Fakultät
an der Christian-Albrechts-Universität zu Kiel

vorgelegt von

Jaime Orellana

Kiel, 2006

Referent: Prof. Dr. Dr. h.c. mult. Harald Rosenthal

Koreferent: Prof. Dr. Dietrich Schnack

Tag der mündlichen Prüfung: 29.01.2007

Zum Druck genehmigt:

Kiel, den

Der Dekan

Table of contents

	Summary	9
	Zusammenfassung	11
1	Introduction	13
1.1	General aspects towards aquaculture infrastructure	13
1.2	General background research on recirculating aquaculture systems (RAS)	14
1.3	Why are particles in RAS so harmful and their removal essential?	15
1.4	Solid removal in recirculation systems	18
1.5	Particle characteristics and size distribution	20
1.6	Objectives	22
2	Materials and Methods	25
2.1	Origin and characterisation of the fish material used in this study	25
2.1.1	Chronology of the scientific experimentations and relevant events related to this study	25
2.2	The recirculating aquaculture system (RAS)	25
2.2.1	Swirl separator: first step of suspended solids separation	30
2.2.2	Foam fractionator: second step of suspended solid separation	31
2.2.2.1	Enhanced foam fractionation with ozone	35
2.2.3	Biological filtration: nitrification	37
2.2.3	Rearing tanks	40
2.3	Secondary unit	41
2.3.1	Control of pH	41
2.4	Data recording of water physics in the RAS	42
2.4.1	Temperature and salinity in the system	42
2.4.2	Dissolved oxygen concentration	42
2.4.3	Measurement of pH values	42
2.4.4	Measuring points	43
2.5	Feed composition and feeding amount	43
2.6	Determination of growth, mortality, feed conversion ratio and condition factor	44
2.6.1	Growth	44
2.6.2	Specific growth rate	45
2.6.3	Mortality	45
2.6.4	Food conversion ratio	45
2.6.5	Condition factor	46
2.6.6	Grading	46
2.6.7	Fish quality	47
2.7	Determination of dissolved nutrients	49
2.7.1	Water sampling	49
2.7.2	Calibration of the analytical methods	51
2.7.3	Determination of total ammonia nitrogen (TAN) concentrations	51
2.7.3.1	Determination methods	51
2.7.3.2	Calibration of the measuring methods	53
2.7.4	Determination of nitrite-nitrogen (NO_2^- -N) concentrations	54
2.7.4.1	Determination method	54
2.7.4.2	Calibration of the measuring method	55
2.7.5	Determination of nitrate-nitrogen (NO_3^- -N) concentrations	56
2.7.5.1	Determination method	56
2.7.5.2	Calibration of the measuring method	57
2.7.6	Determination of the phosphorus (PO_4^{3-}) concentrations	59
2.7.6.1	Determination method	59

2.7.6.2	Calibration of the measuring method	59
2.8	Analysis of the solid waste	61
2.8.1	Solid waste in the swirl separator: sampling and preparation for analysis	61
2.8.2	Solid waste in the foam fractionator: sampling and preparation for analysis	63
2.8.3	Analysis for the determination of carbon and nitrogen content in the solids	63
2.8.4	Analysis for the determination of phosphorus content in the solids	63
2.8.5	Analysis for the determination of energy content in the solids	64
2.8.6	Analysis for the determination of ashfree organic content	65
2.9	Particle size analysis	65
2.10	Optical examination of particulate matter in the RAS	66
2.11	Bacteria in the RAS	66
2.11.1	Bacteria number, biomass and survival percentage	66
2.11.1.1	Method I: Total bacteria number and bacteria biomass	67
2.11.1.2	Method II: Heterotrophic plate count	69
2.11.2	Microscopic examination of bacteria	70
2.12	Water flow in the RAS	71
3	Results	73
3.1	Growth performance of <i>Dicentrarchus labrax</i>	74
3.1.1	Weight and length increment over time	74
3.1.2	Specific growth rate	77
3.1.3	Feeding and feed amount	79
3.1.4	Feed conversion ratio	81
3.1.5	Condition factor	81
3.1.6	Mortality	83
3.1.7	Fish yield and quality	84
3.2	Water physical characteristics in the culture system	86
3.2.1	Temperature and salinity	86
3.2.2	Dissolved oxygen concentration	87
3.2.3	pH in the culture system	88
3.3	Dissolved nutrients concentrations in the culture system	89
3.3.1	Water renewal (exchange)	89
3.3.2	Water quality in the outlet of the swirl separator	90
3.3.3	Water quality in the inlet and outlet of the biofilter (nitrification)	94
3.3.4	Water quality in the outlet of the foam fractionator	99
3.3.5	Water quality in the outlet of the additional biofilter	105
3.3.6	Water quality in the inlet of the fish tanks	109
3.4	Particulate matter in the culture system	112
3.4.1	Nutrients, organic and energy composition of the solid matter in the RAS	112
3.4.2	Description of particle shape and size	128
3.4.3	Particle size analysis	145
3.4.4	Bacteria in the system	148
3.4.5	The influence of ozone on particle size distribution and nutrients	156
3.4.6	Particle size analyses during the experiments with and without ozone treatment	164
3.4.6.1	Particle size analysis with ozone treatment	164
3.4.6.2	Particle size analysis without ozone treatment	167
3.4.7	Water flow in the RAS	170

4	Discussion	173
4.1	RAS conception and design in light of the state of the art	173
4.1.1	Design considerations in terms of efficient water transport and particle removal	174
4.2	Growth performance of European sea bass (<i>Dicentrarchus labrax</i>)	175
4.3	Performance of the biofiltration (nitrification)	180
4.4	Performance of the suspended solid separation	185
4.5	Particle characterization in effluent of the swirl separator	191
4.6	Particle size analysis	192
4.7	Bacteria in the RAS	194
4.7.1	Bacteria removal by counter-current foam stripping	194
4.7.2	The effect of ozone on total suspended solids in a RAS	198
4.8	Conclusions	202
5	References	205
	Annex	219
	Erklärung	
	Danksagung	
	Lebenslauf	

Summary

The proper management of suspended solids is one of the key factors determining the successful operation of recirculating aquaculture systems (RAS). In this thesis the qualitative and quantitative changes of total suspended solids (TSS) in a RAS were investigated, specifically addressing particle size distribution and removal efficiency for various size fractions of particles that were retained by the employed filtration units. The RAS configuration under study was designed to evaluate the performance of a system configuration that involved a two-step solid separation procedure (swirl separator and foam fractionation), each of them independent, however, partly affecting each others performance. The system was also designed to operate at low energy consumption and at a low water replacement.

European sea bass (*Dicentrarchus labrax*) was the target fish species reared over the main study period of 437 days. The performance of fish served as criteria to assess the functionality of the system in terms of fish growth and feed conversion efficiency. During the key investigational period the system was operated at a temperature of about 23°C. Water quality was continuously monitored and maintained within safe limits (ranges for the core study period: temperature 20°C to 24°C; salinity 20 to 25 psu; O₂ 6 to 8 mg*L⁻¹; pH 7 to 8; TAN 0.5 to 1.5 mg*L⁻¹; NO₂⁻-N 0.1 to 0.7 mg*L⁻¹). Water replacement in the system accounted on average about 1% per day of the total system volume. The two step solid separation techniques allowed to maintain fairly clear water conditions over the entire experimental period. The swirl separator worked effectively capturing solids coming from the fish tanks. The nutrient composition of the solids varied over time, depending on the nutrient content in the feed (nitrogen, carbon, phosphorous, ashfree organic, energy). Suspended solids were examined to determine shape and structure in samples from the swirl separator. Particle size distribution was studied by subsequent filtering samples from both, swirl separator and foam fractionator, through mesh sizes of 50µm, 100µm, 200µm, 400µm, 800µm, and 1600µm. Very fine particles were always captured (through scavenging with larger particle fractions). The results indicated that fines (<45 µm) dominated by number the particles removed. This is considered an important finding from a system management point of view. The removal of fine solids and bacterial biomass by counter-current foam stripping was determined. The use of ozone was beneficial in terms of enhanced foam formation, particle aggregation, subsequent removal of fines, and reduced bacterial counts.

The data collected during this study can be used to estimate the growth of European sea bass cultured in a RAS from juvenile stages to table-sized fish (300g). Data also allow estimates for calculating nutrient **inputs** (feed), feed composition, nutrient retention (fish growth and conversion) as well as **outputs** (soluble and particulate wastes). The results obtained provide also a base to estimate mass balances of solids produced in a RAS that integrates cost-effective treatment processes at a high rate of water re-use.

Zusammenfassung

Die effiziente Entfernung von im Wasser suspendierten, partikulären Feststoffen ist ein Schlüsselfaktor für den erfolgreichen Betrieb von Kreislaufanlagen. In der vorliegenden Arbeit wurden die Feststoffe in einem Kreislaufsystem (Recirculating Aquaculture System, RAS) für Fische (Wolfsbarsch, *Dicentrarchus labrax*) qualitativ und quantitativ analysiert, wobei insbesondere die Größenverteilung der Feststoffe und die Rückhaltung in den mechanischen Filtereinheiten. Die Untersuchungen dienten der Leistungsbestimmung Systemkomponenten und der Analyse ihre Wechselwirkungen. Die Systemkonfiguration schloss eine zweistufige, unabhängige Feststoffseparation (Wirbelstromseparator und Abschäumer) ein. Das Anlagenkonzept war auf einen insgesamt niedrigen Energie- und Wasserverbrauch ausgelegt.

Der europäische Wolfsbarsch (*Dicentrarchus labrax*) wurde 437 Tage in dem Kreislaufsystem untersucht. Die Wachstumsleistung und der Futterquotient der Fische dienten als Leistungskriterien für die Beurteilung der Funktionalität des Systems. In der Hauptuntersuchungsperiode betrug die Wassertemperatur im System 23 °C. Die Wasserqualität wurde kontinuierlich überwacht und in den biologisch sicheren Grenzen gehalten (Bereiche für die Hauptuntersuchungsperiode: Temperatur 20°C bis 24°C; Salzgehalt 20 bis 25; O₂ 6 bis 8 mg*L⁻¹; pH 7 bis 8; TAN 0.5 bis 1.5 mg*L⁻¹; NO₂⁻-N 0.1 bis 0.7 mg*L⁻¹). Der Wasseraustausch betrug im Mittel etwa 1% des Systemvolumens pro Tag. Über den gesamten Zeitraum konnten mit der verwendeten Technik „Klarwasserbedingungen“ aufrechterhalten werden. Der Wirbelstromseparator erfasste effizient die größere Partikelfraktion, die über den Versuchszeitraum in Abhängigkeit vom Futter variierende Nährstoffzusammensetzungen (Stickstoff- und Phosphorverbindungen) aufwies. Die Form und Größe der Partikel wurde mit verschiedenen Methoden untersucht. Die Partikelgrößenverteilung wurde anhand von Filterproben mit abnehmender Porenweite (50µm, 100µm, 200µm, 400µm, 800µm, und 1600µm) ermittelt. Dabei wurde auch die Feintrübe zwar erfasst (Anlagerung an größere Partikeln). In dem Kreislaufsystem dominierten deutlich Partikel mit einer Größe unterhalb 45µm. Diese Partikelfraktion konnte durch den Abschäumer erfasst und entfernt werden. Damit wurden auch Bakterien erfasst und die hygienischen Bedingungen im System nachhaltig verbessert. Die Verwendung von Ozon im Abschäumprozess war in Hinsicht auf eine verbesserte Schaumbildung, besserer Partikelseparation und einer Reduktion der Bakterienzahl fördernd.

Die in dieser Arbeit erzielten Ergebnisse und kontinuierlich aufgenommenen experimentellen Daten lieferten die Basis für die Beschreibung des Wachstums des europäischen Wolfsbarsches (juvenile bis Tellergröße (300g)). Darüber hinaus wurden Parameter für die numerische Abschätzung der gewichtsabhängigen Nahrungszufuhr (Futter, **Input**), der Futterzusammensetzung, der Nährstoffretention im Fisch (Wachstum und Futterverwertung), so wie die Exkretion (**Output**) von löslichen und partikelförmigen Stoffwechselendprodukten erarbeitet. Die Ergebnisse ermöglichen die Abschätzung der Mengen von Stoffwechselendprodukten, die in sekundären Komponenten so genannter integrierter Systeme als neue Ressourcen wieder verwendet werden können.

1 Introduction

1.1 General aspects towards aquaculture infrastructure

Conventional marine open farming systems have been a successful economic activity and still continues to expand. However, the industry did so by multiplying successful units particularly in open waters without due concern on environmental carrying capacity in receiving waters. This initial lack of concern has affected the environment and the image of aquaculture in many parts of the world (Rosenthal, 1994). Nowadays, farmers, enforced through national and regional regulations, have learned to mostly work in harmony with the environment; aquaculture is the only industry where the final product can be considered as a perfect bioindicator of the health status of the natural ecosystem in which the cultivated species thrive (Rosenthal, 1994). Environmental risk assessment (ERA), environmental impact assessment (EIA), and Best management practice (BMP), are some of the valuable tools for today's commercial and sustainable aquacultural development, thereby minimizing either ecological impacts or socio-economic failures. National policies have been implemented in many countries for the appropriate sustainable development of fish farming, although enforcement is still unsatisfactory in several parts of the world.

During the past years, however, the trend has also been to move from conventional open systems to high density and highly productive land-based recirculation systems, at least at experimental and pilot scale and in growing number of cases at commercial scale. These systems can be considered as artificial ecosystems with alternative production schemes compared to conventional systems, providing optimal natural conditions for organisms while being uncoupled from natural ecosystems. This trend has been triggered by several simultaneously acting factors which are coupled with the need for specialization, for example: (a) holding broodstocks under controlled conditions to secure timed maturation, (b) master larval development and growth, and (c) promote fingerling or juvenile production at fixed rates. Recirculating systems are increasingly considered for commercial application because of allowing independence from uncertainties in natural systems such as unpredictable temperature profiles over seasons, potential outbreaks of algal blooms and accidental pollution through increasing human activities, leading to increased competitive pressures from other water resource users.

1.2 General background research on recirculating aquaculture systems (RAS)

Recirculating systems for marine aquaculture (mariculture) have been investigated by many authors. Before the turn of the century the work was mainly descriptive and analytical as summarized by Rosenthal (1981) and further elaborated by many authors (Wickins, 1981; Muir, 1981; Murray *et al.*, 1981; LaBosmascus *et al.*, 1987; Russell and O'Brien, 1988; Bergheim *et al.*, 1991; Menasveta *et al.*, 1991; Sigholt *et al.*, 1993; Honda and Kikuchi, 1995; Baskerville-Bridges and Kling, 1996; House *et al.*, 1998; Lupatsch and Kissil, 1998; Van Gorder and Jug-Dujakovic, 1998). With the beginning of the new millennium numerous studies looked at overall system performance and on specific dynamics of individual processes and components (Blancheton, 2000; Chen *et al.*, 2000; Kim *et al.*, 2000; Lee *et al.*, 2000; Olivar *et al.*, 2000; Nijhof and Bovendeur, 1990; Lefebvre *et al.*, 2001; Perry *et al.*, 2001, Seo *et al.*, 2001; Timmons *et al.*, 2001; Thoman *et al.*, 2001; David *et al.*, 2002; Espinoza *et al.*, 2002; Borges *et al.*, 2003; Piedrahita, 2003; Barak *et al.*, 2003; Suantika *et al.*, 2003, Waller *et al.*, 2003a; Waller *et al.*, 2003b; Orellana *et al.*, 2005).

One of the key problems in RAS relates to the load of suspended solids and in particular to very fine particles. During the past ten years research on recirculation systems and its application in marine aquaculture has been extensive, with many studies considering technical aspects of system component design and their performance. Few employed the same fish species used in this study (Blancheton, 2000) while others mainly provided general overviews on systems and system components and their function (Timmons *et al.*, 2001; Van Gorder and Jug-Dujakovic, 1998; Espinoza *et al.*, 2002; David *et al.*, 2002; Borges *et al.*, 2003; Chen *et al.*, 2000; Piedrahita, 2003). The application of treatment units to solve biological needs like the removal of phosphorous (Barak *et al.*, 2003; House *et al.*, 1998), the control of denitrification processes (Lee *et al.*, 2000), the prediction of fish waste output (Lupatsch and Kissil, 1998), the nitrification performance and kinetic of biofilters (Seo *et al.*, 2001; Timmons *et al.*, 2001; Kim *et al.*, 2000; Chen *et al.*, 2006; Michaud *et al.*, 2006), and the nutrient budgets for specific species (Thoman *et al.*, 2001) have been extensively addressed with varying results. Considering the culture of new species (Perry *et al.*, 2001), the rearing of fish eggs and larvae in closed systems (Baskerville-Bridges and Kling, 1996; Olivar *et al.*, 2000), and the modelling of nutrient cycles under given system configurations differed appreciably from ours (Lefebvre *et al.*, 2001). These have also led to new insights in design criteria. With regard to the cultivation of live prey (Suantika *et al.*, 2003) the conceptual approaches

are much different compared to systems for conventional water treatment for common commercial species such as salmonids (Sharer *et al.*, 2005).

When assessing the present findings in light of the pertinent literature, the focus is particularly on the classification and quantification of particulate matter in marine RAS and obviously this issue has been addressed in the present study as well as in the scientific works by Franco-Nava *et al.* (2004a), Franco-Nava *et al.* (2004b), Waller *et al.* (2003a), and Orellana *et al.* (2005). The importance of TSS removal for system performance has always been an aspect of key concern and is specifically so in this study. Most investigations which concentrated around particle size distribution obviously studied freshwater systems (Chen *et al.*, 1993a; Chen *et al.*, 1993b; Chen *et al.*, 1994b; Han *et al.*, 1998; Patterson and Watts, 2003; Brinker and Rösch, 2005; Brinker *et al.*, 2005), tackling removal efficiencies (Viadero and Noblet, 2002; Ebeling *et al.*, 2003; Davidson and Summerfelt, 2005; Huggins *et al.*, 2005; Summerfelt and Penne, 2005;), focussing on nutrient determinations (Summerfelt and Penne, 2005; Viadero and Noblet, 2002), assessing the effect of system components on particle characteristics (McMillan *et al.*, 2003; Summerfelt and Penne, 2005; Veerapen *et al.*, 2002; Veerapen *et al.*, 2005), while also developing new sizing techniques (Brinker *et al.*, 2005). Similarly, the influence of ozone in the particle size distribution in freshwater (Krumins *et al.*, 2001) has also been conducted while a few earlier studies employed ozone in marine systems (Dwivedy, 1974; Schlesner und Rheinheimer, 1974; Rosenthal and Sander, 1975; Rosenthal and Westernhagen, 1976; Blogoslawski *et al.*, 1977; Ingols, 1978; Honn, 1979; Rosenthal and Otte, 1979; Rosenthal, 1981a, 1981b; Rosenthal and Krüner, 1985; Lin and Wu, 1996; Brazil *et al.*, 1998; Singh *et al.*, 1999). Colt (2006) listed the relevant limiting factors regarding water quality and remarked that these are not yet entirely understood and that the development of more relevant water quality criteria for reuse systems will require production-scale trials. This holds in particular for marine systems and this was the reason why the present study placed its central focus on such system.

1.3 Why are particles in RAS so harmful and their removal essential?

The presence and accumulation of particulate wastes in RAS (faeces, uneaten feed, and bacteria flocs) will impact negatively the water quality by affecting the performance efficiency of the water treatment units. High suspended solids load has many disadvantages:

- Particulate matter consumes oxygen during biological degradation which will decrease the availability of oxygen for fish in culture (Rosenthal, 1997; Davidson and Summerfelt, 2005).
- The brake down of organic wastes will increase the TAN concentration in the water affecting nitrification (Liao and Mayo, 1974; Spotte, 1979; Davidson and Summerfelt, 2005; Chen *et al.*, 2006). Small quantities of unionized ammonia can be toxic for epithelial tissues and disturb the elimination of protein metabolites across gills (Peters *et al.*, 1984).
- Solids support the growth of heterotrophic bacteria which can outgrow and compete with nitrifiers. The nitrification process is strongly inhibited by heterotrophic processes when high amounts of organic carbon are present (Zhu and Chen, 2001).
- Suspended solids offer an ideal temporary substrate for facultative pathogens while they try to find a final host. Bullock *et al.* (1994) inferred that suspended solids may be involved in bacteria gill disease (BGD) outbreak. Noble and Summerfelt (1996) described that beside opportunistic microorganisms, non-infectious problems prevail as high levels of suspended solids have caused mortalities in RAS.
- Particles can potentially clog biofilters and reduce their efficiency (Chen *et al.*, 1993; Rosenthal, 1997).
- Excessive solid loads can cause plugging within aeration columns, screens, and spray nozzles orifices, which could ultimately result in system failure (Davidson and Summerfelt, 2005).
- The organic C/N ratios in the water will negatively affect the efficiency of nitrifiers (Rosenthal, 1997; Ebeling *et al.*, 2006).
- The accumulation of solids can create anoxic conditions favourable for bacteria responsible for the production of geosmin and 2-methylisoborneol causing off-flavours in cultured fish (Tucker and Martin, 1991).

- Gill tissue can be damaged by particles (Rosenthal, 1997) during feeding, drinking, and breathing. Bullock *et al.* (1994) suspected that small suspended solids could irritate gill tissue and provide an injured surface for attachment of any bacteria (BGD) present in the water. Peters *et al.* (1984) found out that fin and gill lesions in rainbow trout were induced partly by the accumulation of excretory and decomposition products. Madetoja *et al.* (2000) showed that skin and mucus abrasion dramatically enhanced the invasion of pathogenic agents into the fish.
- Fish vision can be affected by high suspended solids load, disturbing the recognition of feed.

The proper management of suspended solids is one of the key factors determining the successful operation of recirculating systems because of the elucidated potential impacts. The relations between production rates and elimination rates of organic matter in a RAS are rather complex (Franco-Nava *et al.*, 2004). This has been partly studied by some authors (Avnimelech *et al.*, 1995; Leonard *et al.*, 2002) who highlighted the need for better knowledge of the nature of organic matter in order to apply a good strategy to control them (Franco-Nava *et al.*, 2004). Thus, technological and economic solutions should be based on a better understanding of the biological and chemical processes controlling not only nutrients but also particulate solid matter in recirculation systems.

The design of a RAS to achieve the desired solid elimination has to take the following aspects into consideration:

1. The more quickly solids are removed from the water the less time they have to break down and consequently less oxygen will be consumed by attached bacteria (Bullock *et al.*, 1994, 1997; Rosenthal, 1997; Davidson and Summerfelt, 2005). Long residence times for particles in the system will affect their size due to shear forces and microbial degradation. Substances are leaching faster from smaller particles than from big ones. Small particles, however, are more difficult to remove from the culture water because of size and the proximity to water density.
2. The methods to remove solids (sedimentation, filtration, and/or flotation) have to be able to eliminate particles over a wide range of sizes. Normally a combination of removal techniques are needed (Waller *et al.*, 2003a; Orellana *et al.*, 2005) specially for the elimination of fine solids fraction ($<20 \mu m$) that do not settle in conventional treatment processes such as gravity settling and microscreen, and

accumulate in the culture medium over time (Chen *et al.*, 1993; Chen *et al.*, 1994; Langer *et al.*, 1996; Rosenthal, 1997; Waller, 2001; Viadero and Noblet, 2002; Orellana *et al.*, 2005).

3. The size of fish and the water flow rates seem to be two closely related factors that determine the characteristic of solid waste and because fish size and feed size are known, these characteristics can largely be predicted. Small fish produce small particles and need high quantities of feed per unit weight in order to satisfy their energy requirements, while big fish produce larger particles and need less feed per unit of biomass, compensated for by a relatively lower growth rate (Franco-Nava *et al.*, 2004). The amount, characteristics, and size of solids indirectly determine the choice of methods for efficient removal.
4. High stocking densities are often aimed for (depending on the species) to boost the profitability of a RAS. High stocking densities allow more fish biomass to be produced per unit of culture. However, increasing stocking densities require a better management of solid removal and highly reliable removal techniques. Solid loads will increase rapidly. Waste removal from the system has to be efficient and becomes costly if mechanical means are no longer sufficient.

1.4 Solid removal in recirculation systems

The removal of suspended solids from RAS is a solid-liquid separation process. Such processes can be classified as sedimentation, filtration and flotation, according to the removal techniques. Sedimentation will depend on the difference in density between particles and water. The greater the density difference the faster will occur the settling of solid matter (Timmons *et al.*, 2001). Common sedimentation methods include clarifiers (settling tanks), settling tubes and hydrocyclones (swirl separators). Filtration processes can be accomplished with screens, granular media or porous filter media (Chen *et al.*, 1994). The separation of the solids from the water is controlled by the way particles are transported from the suspension onto the filter medium (Chen *et al.*, 1994; Timmons, *et al.*, 2001). In a flotation process, particles attach onto air bubbles and are separated from the water. This last technique has being described as foam fractionation and is repeatedly reported by several authors (Rosenthal and Sander, 1975; Mathews *et al.*, 1979; Rosenthal, 1981a; Rosenthal and Krüner, 1985; Chen *et al.*, 1993b; Sander, 1998; Boonyasuwat, 2003).

In selecting the appropriate process or a combination of processes for effectively controlling suspended solids in RAS, the required water quality to ensure fish welfare and optimal fish growth can be achieved while minimizing capital and operational costs. The technologies available for suspended solid removal in recirculating aquacultural applications are schematically presented in Figure 1. Each of these techniques targets on different ranges of particle sizes and can be combined to obtain different removal efficiencies in RAS depending on system purposes (*e.g.* broodstock holding, cultivation of live prey, hatchery, or grow-out). As can be seen from Figure 1, it is clear that the quantitative removal of fine solids ($<20 \mu\text{m}$) will demand special considerations when designing the respective RAS components. Therefore, a combination of removal techniques appears to have a determinant meaning for the quantitative elimination of a wide particle spectrum present in the culture water. Losordo *et al.* (1999) and Summerfelt (2002) described combinations of settling and mechanical filtration methods to cope with suspended solids. Waller (2000) and Waller *et al.* (2002) reported the combined use of swirl separator or drum filter with foam fractionation.

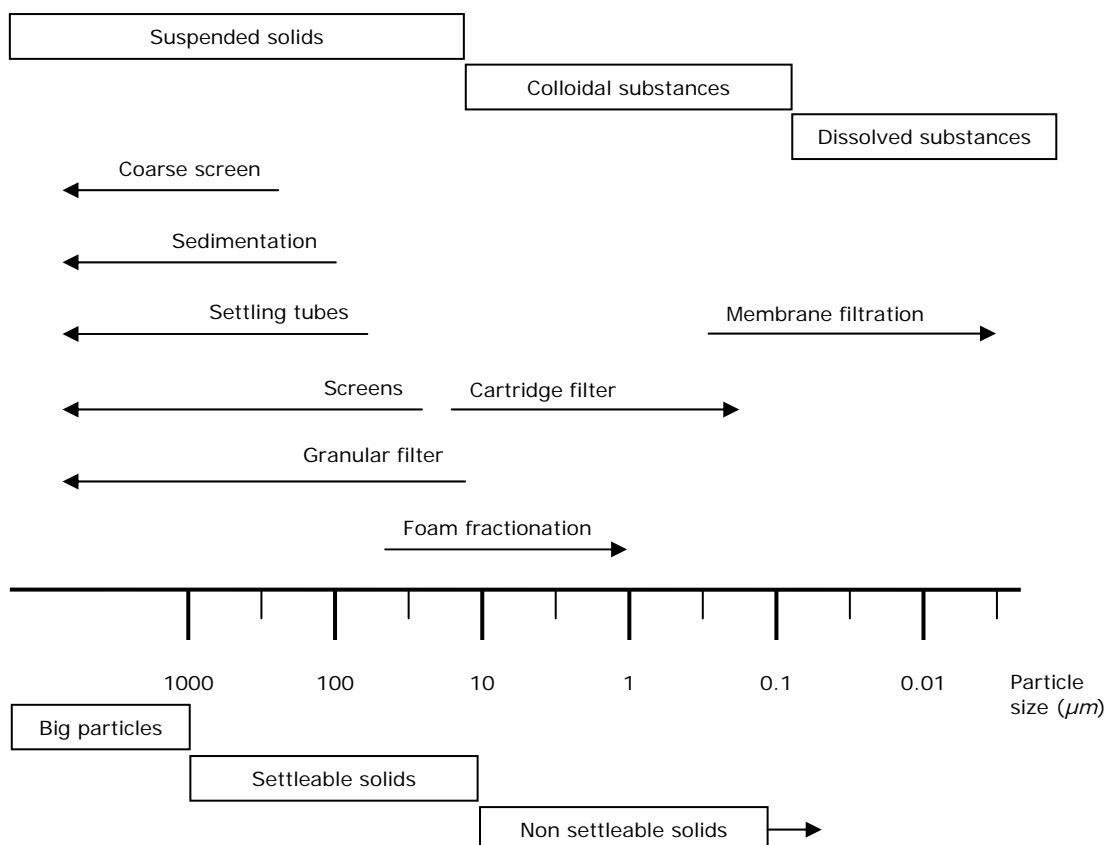


Fig. 1. Solid removal mechanisms available for operation in recirculation aquaculture systems (RAS) in relation to the particle size range over which the removal processes work (modified after Chen *et al.*, 1994, Rosenthal, 1997, and Timmons *et al.*, 2001).

New problems with particles are arising as feed formulations evolve and feed conversion efficiencies improve. Changing feed composition may alter the physical properties of feed pellets and subsequently faecal wastes that, in turn, will affect their removal from the culture medium. The development of high energy fish feeds based on extruded diets move towards increased fat content (around 30% and more; Rosenthal, 1997). Unfortunately, not all the fat will be consumed by the fish. Fat will leach out and react with fine solids at low temperatures, clogging fine filter mesh (Rosenthal, 1997). Excessive fat released into the water will also alter the surface tension and thereby negatively impact on flotation processes and on foam fractionation. At the end, more expenditure will be required to eliminate suspended solids from the culture water. High energy feeds contain also less phosphorous and nitrogen which reduces nutrient loads for the biofilter, however, the resulting faecal matter have different physical properties which need to be addressed by engineers when re-designing existing solid removal methods.

One approach to reduce suspended solids loads uses highly digestible feeds while minimizing feed losses (Brinker *et al.*, 2003).

1.5 Particle characteristics and size distribution

The two most important properties of suspended solids in RAS are specific gravity and particle size (Chen *et al.*, 1994). The specific gravity will be determined by the compactness and composition of the material. Particle size distribution depends also on the source of material (feed composition), as well as fish species and size. Shear forces as well as other mechanical forces will determine their breakdown into fines.

How particles will behave in the water column depends largely on their specific gravity. Additionally, not all particles in a given size spectrum will have the same specific gravity, which depends also largely on their organic or inorganic nature (Chen *et al.*, 1994) while their settling characteristics are also influenced by surface structure.

Particle characteristics were studied by Patterson and Watts (2003) for a smoltification site for *Salmo salar*. On an attempt to produce comparable data, this study considered the optical (macro- and microscopically) characteristics by examining particles from samples of different size classes (sieves) in relation to the growth of *Dicentrarchus labrax* in a marine environment. Binocular and digital scanning microscope images were used to indicate the ability of these techniques to describe the characteristics of particles and the associated bacterial flora.

Particle size distribution in fish culture water have been investigated by several authors (Chen *et al.*, 1993; Langer *et al.*, 1996; McMillan *et al.*, 2003; Brinker *et al.*, 2006). Although different methods, fish species and water characteristics were involved, these studies consistently reported that fine particles were the dominant problem in recirculation systems. Table 1 shows an overall view of particle size distributions found in RAS.

Tab. 1. Over-view of study results on particle size distribution (PSD) found in recirculating aquaculture systems using different determination methods; RPC = Resistance pulse counters (*e.g.* Coulter Counter, Elzone, and Fritsch; LLS = Laser light-scattering particle sizer; * = Binding substances were used in feeds (apparently affecting particle size distribution in fines and faeces); ** = Flow-through culture system.

Particle counter	Environment	Species	Weight (g)	PSD (μm)	% of fine solids (<20 μm)	Reference
RPC ^a	Fresh water	<i>Oncorhynchus mykiss</i>	500	7-50	95	Chen <i>et al.</i> (1993a)
RPC	Fresh water	<i>Oncorhynchus mykiss</i>	500	7-50	95	Chen <i>et al.</i> (1993b)
RPC	Fresh water	<i>Salvelinus fontinalis</i>	50	7-50	95	Chen <i>et al.</i> (1993b)
Sieves	Brackish water	<i>Anguilla anguilla</i>	15-20	0.45->100	56-68	Langer <i>et al.</i> (1996)
RPC		<i>Morone saxatilis</i>	270-560	0.4-100	50	Krumins <i>et al.</i> (2001)
LLS ^b	Fresh water	<i>Oncorhynchus mykiss</i>		4->500	15	Brinker <i>et al.</i> (2003)*
RPC		<i>Morone saxatilis</i>	400	0.4-900	70	McMillan <i>et al.</i> (2003)
LLS	Fresh water	<i>Salmo salar</i>		2-60	>90	Patterson & Watts (2003)
LLS	Fresh water	<i>Oncorhynchus mykiss</i>	63-700	0.2->600		Brinker & Rösch (2005)
LLS	Fresh water	<i>Oncorhynchus mykiss</i>	250-320	0.2->600	>60	Brinker <i>et al.</i> (2005)**
RPC	Sea water	<i>Dicentrarchus labrax</i>	320-350	2.8-710	95	Orellana <i>et al.</i> (2005)

All studies shown in Table 1 indicate that the efficiency of solid removal techniques were limited by their inability to capture fine solids (<20 μm). Certainly, the mass of small particles in relation to that of larger ones is almost negligible. However, their number is much higher, providing a huge surface area relative to the mass, thereby offering excessive space for attachment of free-floating bacteria. This is determinant since fine

solids will offer a high active surface not only to heterotrophic bacteria (Rosenthal, 1997) affecting considerably the water quality in the system as elucidated before, but also to facultative pathogens who opportunistically may hitchhike to find their hosts (the fish). Moreover, as particle size decreases, leaching processes become more important due to an exponential increase in diffusion distance from the inner part to the surface and because of the large contact area with the surrounding medium (surface-volume ratio).

While most of these facts attracted already great attention (Tab. 1) there is still a fundamental lack of knowledge concerning particle size distribution and proper elimination of fine solids in marine recirculation systems. The suspended solid removal techniques and the configuration of the recirculation system in this study consider a two-step suspended solid removal: (a) sedimentation (swirl separator), followed by (b) flotation (foam fractionation). This design configuration allowed separately to remove larger (sedimentation) and fine (flotation) particles from the culture water. Additionally, the use of ozone enhanced particle aggregation and subsequently flotation (foam formation) process while also chemically conditioning the water for biological filtration (oxidation of organics, and partly nutrients as well as partial inactivation of microorganisms).

1.6 Objectives

Based on the present state of the art of our knowledge on the biological effects of suspended solids and based on the system configuration designed for this study, the following objectives were formulated on which the detailed investigations have been designed:

- Do fish conventionally grown in intensive aquaculture systems perform comparatively well under the given experimental conditions?

Justification: If the results of the study are being useful in practice, this will only be possible when fish growth and conversion efficiency are not impaired.

- Can nutrient levels in water under the given system configuration be maintained at levels comparable to other culture systems?

Justification: The achievement of an optimal biological elimination of toxic excretory products should be possible to allow optimum growth and fish welfare.

- How does feed composition and system configuration affect total suspended solids being removed by the treatments?

Justification: Diet composition will affect faeces characteristics. The solid removal mechanisms have to ensure to maintain safe water quality and capture a critical mass of solids, preferably equal to the amount of input.

- Is removal efficiency of the swirl separator and foam fractionator related to particle size?

Justification: The combination of two a two-step solid separation will allow the elimination of larger particles (swirl separator) and fine solids (foam fractionation).

- Can the free bacterial load in the system water be effectively reduced by foam stripping?

Justification: High bacterial loads will deteriorate water quality and affect fish health while also consuming oxygen in system components designed to serve other purposes than bacterial cultures. Therefore free bacteria have to be eliminated efficiently and continuously from the culture water.

- Which effect does ozonation have on particle size, nutrient composition and bacterial load within the culture system?

Justification: The application of ozone will enhanced the removal of fine solids and the formation of larger aggregates, oxidize nutrients and inactivate free bacteria.

2 Materials and Methods

2.1 Origin and characterisation of the fish material used in this study

European sea bass (*Dicentrarchus labrax* L.) was selected as experimental species because of its importance in aquaculture, mainly in Europe. The fish (tank 1, $n_1=206$, average weight 4.7 g; tank 2, $n_2=206$, average weight 4.5 g) came originally from a hatchery facility in northern France (Ecloserie Marine de Gravelines).

2.1.1 Chronology of the scientific experiments and relevant events related to this study

Table 3 presents an overall resumé of the experiments realized and events of importance during the study period, in chronological order. The denomination of days (t_n) will be used further in the next chapters. The text, tables, and figures refer always to days from start (*e.g.* t_{142}). Table 3 shows also the dates related to each relevant event.

2.2 The recirculating aquaculture system (RAS)

The experiments were conducted in a closed marine recirculating aquaculture system (RAS) that was operated at the Leibniz Institute for Marine Science in Kiel (IFM-GEOMAR), Germany (Fig. 2). The system was designed in cooperation with the company Erwin Sander Elektroapparatebau GmbH (Uetze-Eltze, Germany), following the initial design of a recirculation prototype (Waller *et al.*, 2001) used for experimental purposes in marine aquaculture. This modified prototype included a different system configuration and operational combination of the components that have been used before, and some technical improvements. The experimental RAS consisted basically of two fish tanks and the water treatment units. The water treatment units combined the following methods: swirl separator; ozone enhanced foam fractionator; and biofiltration (mainly nitrification). The system had a water volume of 3.34 m³ (Tab. 2). The initial test operation was done in the middle of June 2001. During the following two weeks the system was operated in order to check the performance of the single components and to allow the biofilter unit to develop the necessary bacterial biomass for the heterotrophic and nitrifying processes.

The system was initially filled with seawater from the Baltic Sea recirculation system (16 psu) of the aquarium facilities at the institute. The same water was used to renew the losses (evaporation, samples). The salinity was gradually raised to 23 psu (t_{99}), mixing

seawater from the Baltic Sea recirculation system (16 psu) and the North Sea recirculation system (32 psu) of the public aquarium of the institute.

Figure 3 shows a schematic side view of the RAS. Arrows indicate the flow (water, air, ozone, CaO (Ca(OH)₂), and discharge water). The system was constructed as a low-head (low energy consumption) system, in order to minimize energy consumption and heat inputs by avoiding the use of conventional water pumps, taking advantage of gravity and air-lift systems.



Fig. 2. The closed marine recirculating aquaculture system (RAS) consisting of the following essential components: (1) fish tanks, (2) swirl separator, (3) biofilter and, (4) foam fractionator.

Tab. 2. Water volume (m³) of each component of the marine recirculating aquaculture system (RAS).

Components	Water volume (m ³)
Fish tanks, each 1.23 m ³	2.46
Swirl separator	0.24
Biological filtration	0.24
Foam Fractionator	0.30
Pipes	0.10
Total volume	3.34

Materials and Methods

Tab. 3. Time table for all relevant events related to this study. The events are expressed as days from start (t_0). Additional information is detailed for each event during the study period from t_0 to t_{902} .

Date	Days	Event	Information
12.7.2001	t_0	- Determination of initial biomass - Water sampling for solid waste: subsamples every 14 days - Determination of biomass: subsamples every 14 days	Anaesthetic MS-222, 35 mg*L ⁻¹
18.10.2001	t_{98}	- Determination of biomass	Anaesthetic MS-222, 35 mg*L ⁻¹
29.11.2001	t_{140}	- Determination of biomass - End of water sampling every day for dissolved nutrients determination	Anaesthetic MS-222, 35 mg*L ⁻¹
1.12.2001	t_{142}	- Air diffusers in both tanks	
5.2.2002	t_{208}	- CaO dosage by hand	200 g*d ⁻¹
22.2.2002	t_{225}	- Increase of anaesthetic doses	Anaesthetic MS-222 45 mg*L ⁻¹
28.2.2002	t_{231}	- CaO dosage automatically	Membrane pump, 200 g*d ⁻¹ Control over pH probe
8.3.2002	t_{239}	- Installation of additional biofilters	One for each tank
2.5.2002	t_{294}	- Change anaesthetic to Benzocaine	Anaesthetic Benzocaine 45 mg* L ⁻¹ .
30.5.2002	t_{322}	- Grading of the fish in Tank 2	Tank 2 >250 g
5.6.2002	t_{328}	- Grading of the fish in Tank 1	Tank 1 <250 g
1.7.2002	t_{354}	- Increase of CaO amount	300 g*d ⁻¹
22.7.2002	t_{375}	- Determination of biomass - Increase of anaesthetic dose	Anaesthetic Benzocaine 50 mg*L ⁻¹
13.9.2002	t_{428}	- End of water sampling every 3 days for dissolved nutrients determination	
17.9.2002	t_{432}	- Installation of the second type of biofilter (moving bed)	Trickling biofilter from fish tanks removed
19.9.2002	t_{434}	- End of the sampling for growth and solid waste	
22.9.2002	t_{435}	- Grading of the fish in both tanks	Tank 1 <300 g; Tank 2 >300 g
26.9.2002	t_{441}	- Samples for nutrient composition and sensory assessment	Fish quality analysis
10.10.2002	$t_{455} - t_{465}$	- Sampling for bacteria analysis	Total bacteria counts and colony forming units
21.10.2002	$t_{466} - t_{562}$	- Sampling for determination of particle size distribution	Swirl separator and foam collector tank
11.5.2003	$t_{668} - t_{679}$	- Sampling for dissolved nutrients and solid waste quantification. - Determination of particle size distribution	With ozone
29.5.2003	$t_{686} - t_{690}$	- Sampling for dissolved nutrients and solid waste quantification. - Determination of particle size distribution	Without ozone
5.6.2003	t_{693}	- CaO dosage with hose pump	
24.6.2003	t_{712}	- Installation of an air back-wash system inside the biofilter	
31.12.2003	t_{902}	- End of the operation of the RAS	

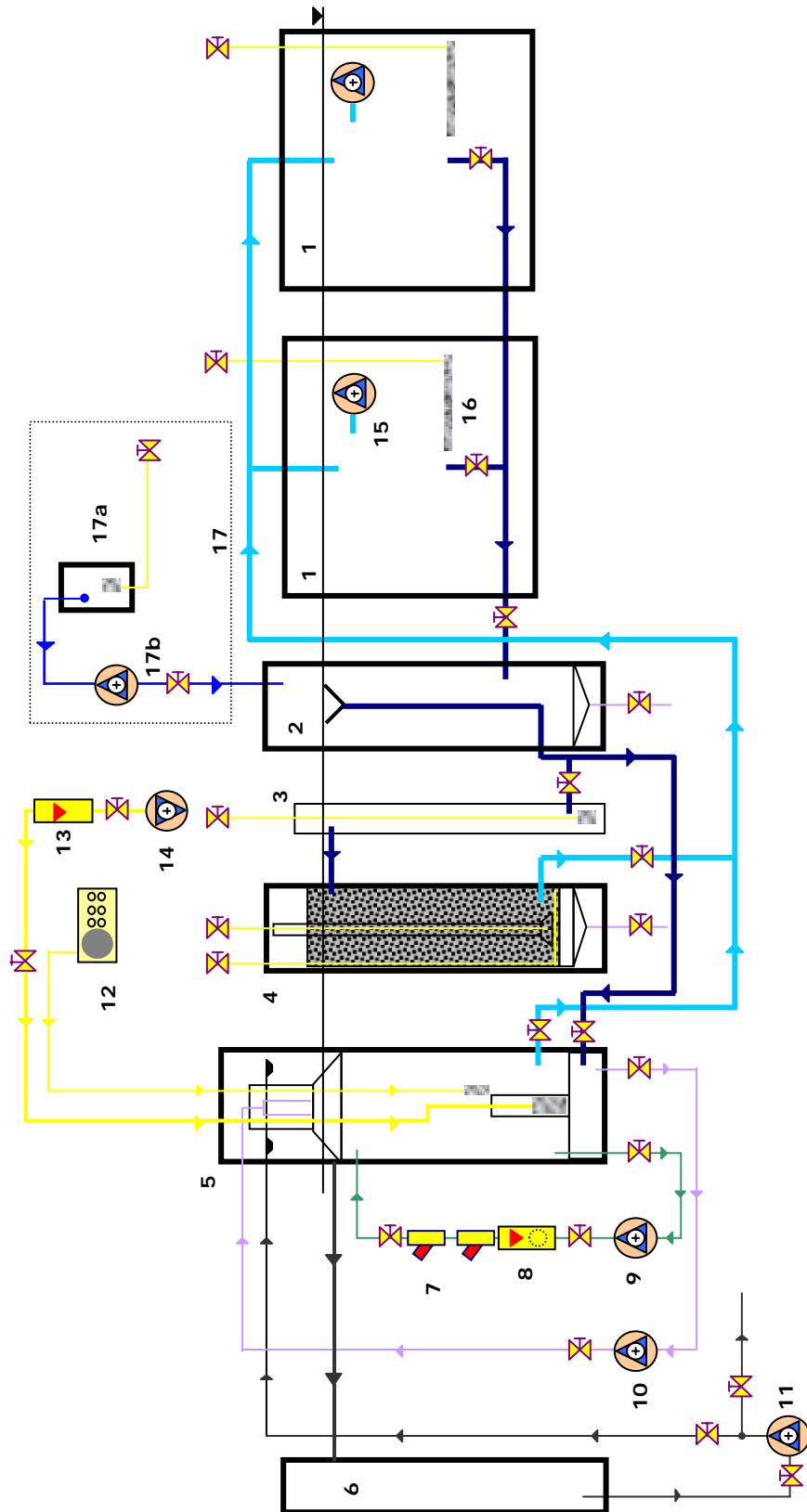


Fig. 3. Schematic side view of the RAS layout. Single components are explained in Table 4 and Figure 4.

Tab. 4. Legend for system components of the RAS numbered in Figure 3.

1	Fish holding tanks	13	Air flowmeter
2	Swirl separator	14	Compressor
3	Air-lift	15	Underwater pump for internal tank circulation
4	Biofilter (nitrification)	16	Ceramic air diffuser
5	Foam fractionator	17	CaO dosing system
6	Foam collector tank	17a	CaO canister with internal circulation
7	pH – ORP measuring probes	17b	CaO dosing pump
8	Water flowmeter		
9	Water pump for pH – ORP probes		
10	Water pump for inner foam flushing		
11	Water pump for outer foam flushing		
12	Ozone generator		

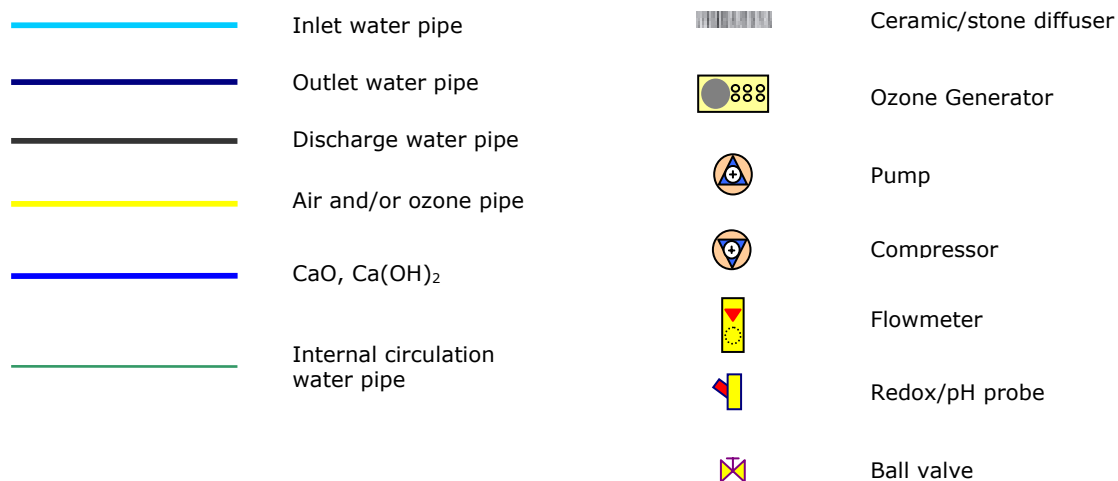


Fig. 4. Legend for pipes and system components of the RAS presented in Figure 3.

The water circulates as follows: The outflow water passed a square shaped (450 x 450 mm), pyramid cone (angle 30°) at the bottom of the fish tanks, through a PVC pipe (75 mm diameter) into the swirl separator. From the swirl separator the water flow splits into two pipes. One (75 mm diameter) serves the foam fractionation and the other (75 mm diameter) the air-lift (1.35 m height, 90 mm diameter). The air-lift brings the water up to the inlet of the biofilter. Inside the foam fractionator the water is moved upwards by an internal air-lift. The outflow pipe of the biofilter (63 mm diameter) and the outflow pipe

of the foam fractionator (75 mm diameter) join into one pipe that flows back into the fish tanks. The water flow was initially adjusted to approximately $3.5 \pm 0.2 \text{ m}^3 \cdot \text{h}^{-1}$.

The bypass from the swirl separator to the biofilter and to the foam fractionator in a parallel way was assembled in order to allow an increase of the amount of ozone that was injected to the foam fractionator. In the precedent prototype, the water flow was from the tanks through the swirl separator, into the foam fractionator and then into the biofilter. It was suspected that the rest ozone coming out of the foam fractionator could be harmful to the biofilm of nitrification bacteria. This new set up with the two components in question (biofilter and foam fractionator) assembled in parallel was used to improve the holding conditions of the fish in the tanks.

2.2.1 Swirl separator: first step of suspended solids separation

The first stage of the water treatment system was the swirl separator. Swirl separators are cylindrical structures with a conical base (Veerapen *et al.*, 2002). Water, laden with particulate matter (*e.g.* faeces, uneaten pellets, and bacterial flocks) from the culture tanks, enter the swirl separator tangentially and create a spiral flow, which induce to a circular (or vortex) flow pattern. A combination of gravitational and hydrodynamic drag forces is achieved. The particles that enter the swirl tank have to flow upwards to the outlet of the chamber. On its way upwards, bigger particles loose velocity, are drop out of the spiral flow and migrate to the centre of the swirl chamber, where velocities are lower. Particles in the centre of the chamber fall because of weight. The remaining fractions, consisting of water and fines, exits at top (Fig. 5a). Swirl separators required significantly less space than other conventional settling chambers or basins used in fresh water or other marine systems. The conical bottom of the swirl separator allowed the settling of the solids. The sampling can be done by piping out the solid matter. The discharging of the solids can be done by opening the ball valve installed at the base of the cylindrical tank (Fig. 5b).

Scott and Allard (1983, 1984) described and used two parallel hydrocyclones prefilters to remove heavy organic material such as faeces, uneaten fish feed and other particulate material. Although the performance of such a device revealed a high efficiency in the solid separation issue, there is no sign in the literature reviewed, to move from conventional drum filters commonly used in commercial aquaculture, to such a system. Langer *et al.* (1996) showed a high degree of clogging in the drum filter mesh and

indicated a partial breakdown of larger particles into smaller ones, during the filtration process. The energy consumption and additional fresh water costs for flushing the filter cloth are normally not considered. For this study, the use of a swirl separator was considered as appropriate and innovative, in conjunction with the whole water treatment engineering.

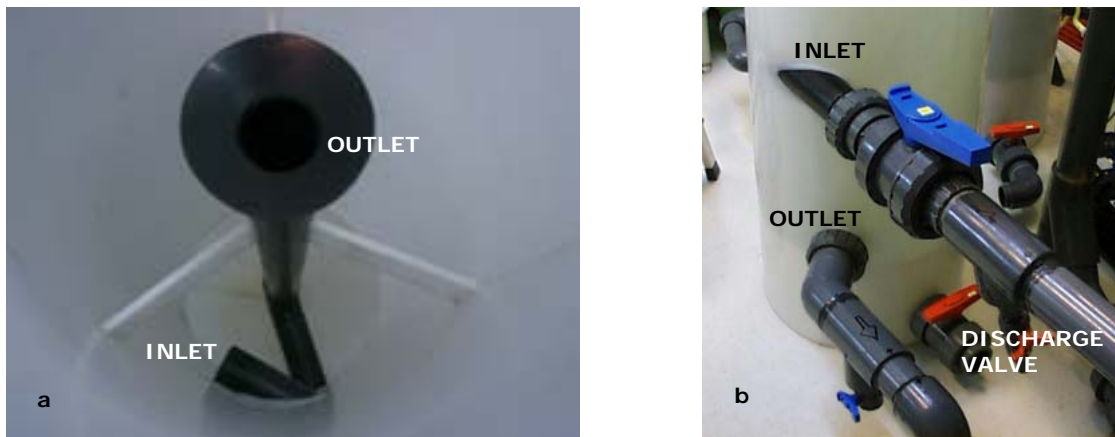


Fig. 5. Internal (a) and external (b) view from the swirl separator. Inlet, outlet and discharge valve are indicated.

2.2.2 Foam fractionator: second step of suspended solid separation

To remove the suspended solid fraction that is too small to settle and too fine to be removed by conventional methods, a foam fractionator was used. Figure 6 shows the foam fractionation device with the foam collector tank (a) and its foam tower with foam flushing nozzles (b) used in this study (company Sander Elektroapparatebau GmbH, model Aero Skim 500). The reaction chamber of the foam fractionator has a volume of 0.27 m^3 . The water inflow is at the bottom of the tank (Fig. 7). From there, an air-lift system transported the water into the reaction chamber. In the first one third of the chamber is a plexi glass tube, 45 cm height and 10 cm in diameter, in which six Teflon diffusers are installed and connected with an air compressor (Fig. 7). The plexi glass tube improves the performance of the air-lift and avoids turbulences in the lower third of the chamber. The air compressor delivered $120 \text{ L}\cdot\text{h}^{-1}$.

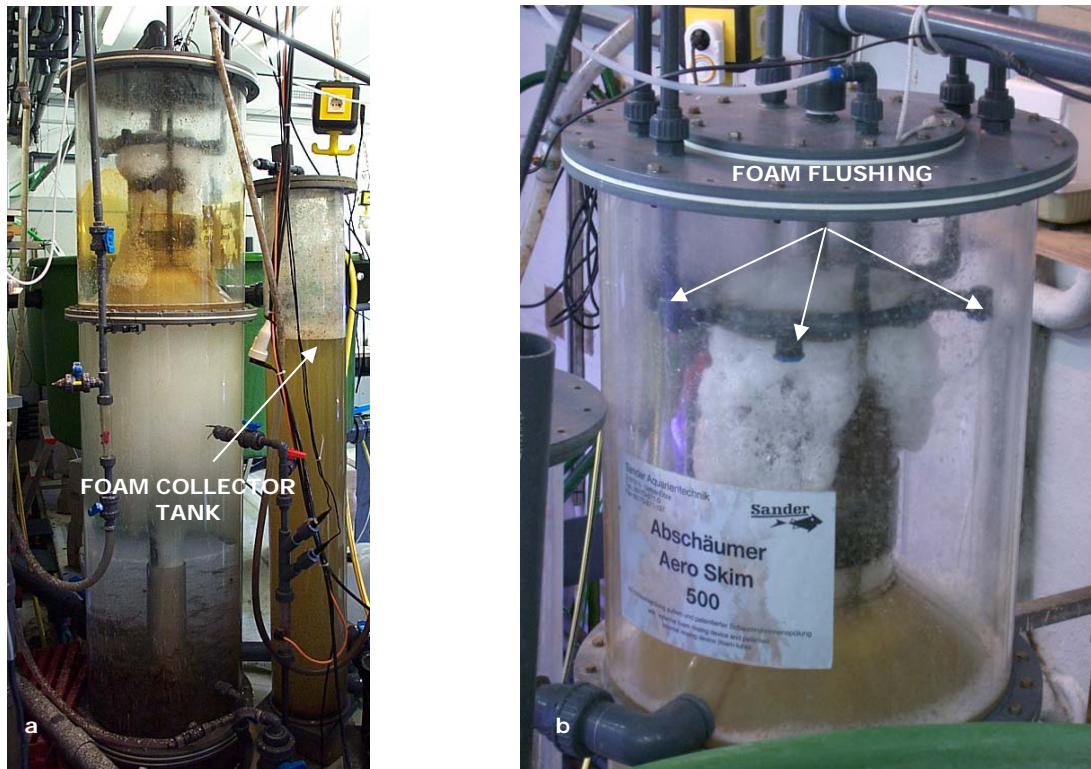


Fig. 6. Foam fractionator Aero Skim 500 with foam collector tank (a), foam flushing system and foam tower (b) in detail.

The inner foam tower allows accumulating the foam and transporting it upwards from layer to layer, while it is losing water (also called transport zone) (Sander, 1998). Up here the foam is getting more concentrated and dryer. The last layer has very dry foam, which is going to collapse into the outer foam tower (Fig. 8). The collapsed solution (foam) is much more concentrated in the condensate than in the initial water medium (Boonyasuwat, 2003). The foam in the outer foam tower is not in contact with the culture water anymore. A separate closed system pumps water from the foam collector tank into the outer foam tower through four sprinklers (Fig. 6b and Fig. 9) and flushes out the foam concentrate into the foam collector tank. The flushing interval was set at 30 sec flushing time every 30 min.

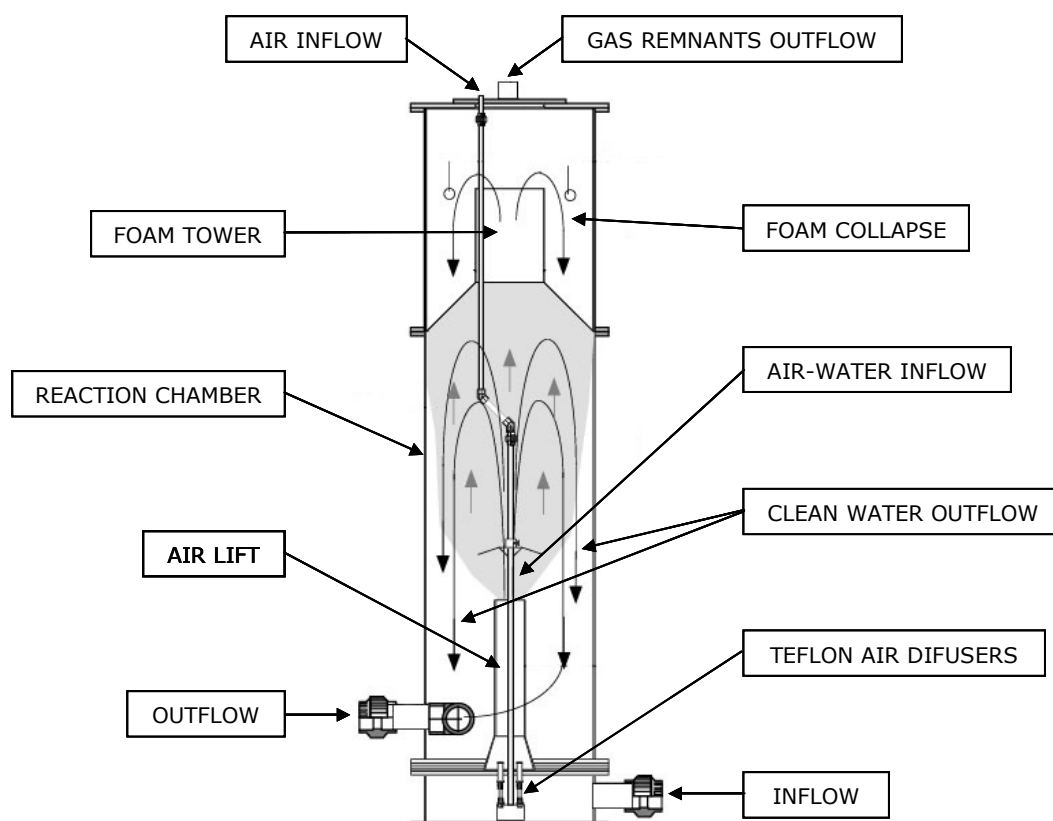


Fig. 7. Side view drawing of the foam fractionator unit in this study. Single components are detailed.

The inner foam tower is also equipped with a flushing device. It consists of a U-shaped 12 mm diameter PVC tube, having 1 mm orifices every 20 mm, attached to a PVC ball bearing and connected with an external water pump. The water is pumped from the skimmer inlet, through a plastic hose into the flushing device (Fig. 9). Because of the water pressure and the distribution of the fine orifices, the ball bearing rotate and move the U-shape device inside the inner foam tower in 360°. This allows cleaning the foam transport zone to avoid the sticking of particulate material on the inner wall of the foam tower, which can cause a decrease in the foam formation process. The flushing/cleaning interval was set at 15 sec every 30 min.

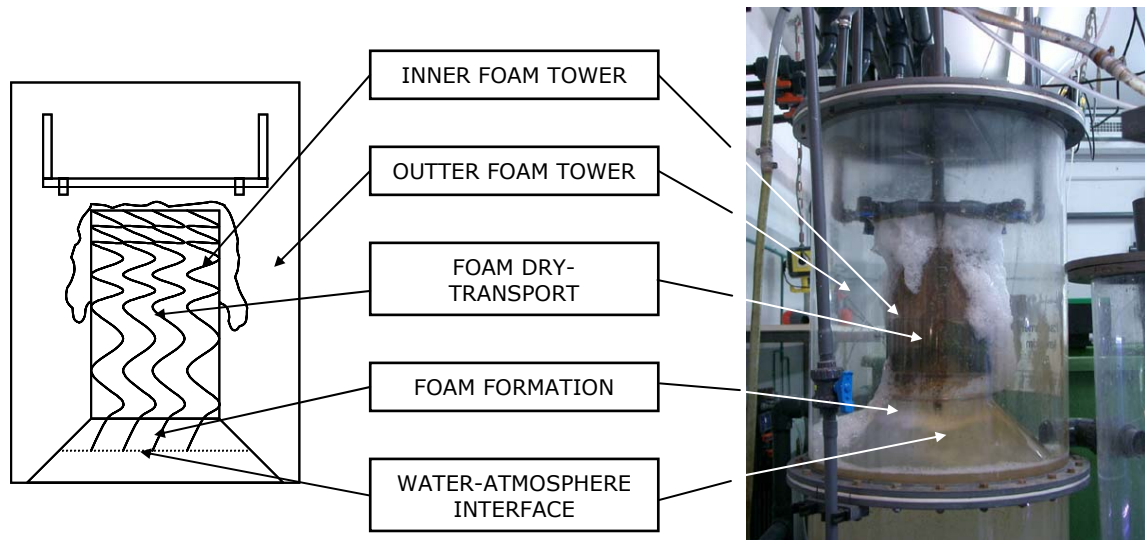


Fig. 8. Outer and inner foam tower from the Aero Skim 500. Water-atmosphere interface, foam formation, foam dry-transport, outer foam tower, and inner foam tower are detailed (adapted from Sander, 1998).

As described before, inside the reaction chamber a gas-water interface is achieved. The fine air bubbles coming from the air-lift diffusers are moved to the top of the chamber where the foam collecting funnel is positioned (Fig. 8). In the funnel the water-atmosphere interface is obtained, where the foam production takes place (Sander, 1998).

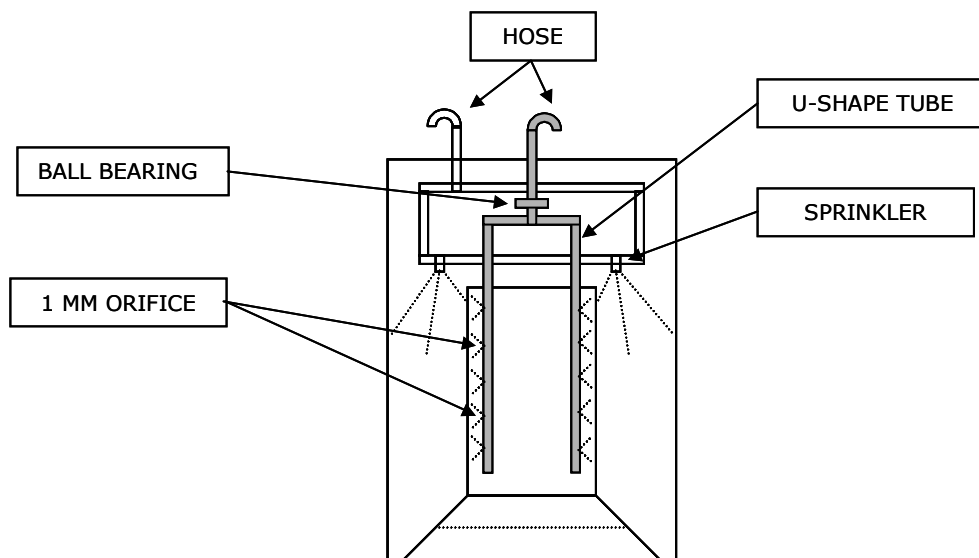


Fig. 9. Foam fractionator tower. Detailed drawing of the foam flushing system with sprinklers for the outer foam tower, and the U-shaped tube equipped with a ball bearing for flushing/cleaning the inner foam tower (patented by Erwin Sander Elektroapparatebau GmbH). The U-shape tube rotates in 360°.

2.2.2.1 Enhanced foam fractionation with ozone

Ozone has been used for the disinfection of water supplies since the beginning of the 20th century, when it was first applied to the treatment of the drinking water for the city of Paris, France (Diaper, 1972). Its application in this field has many advantages over chlorine because it neither increases the organic salt content nor produces pollutants after reaction, does not impart taste or colour to the treated water, is much more powerful disinfectant than chlorine, does not have any harmful influence to aquatic life and does not have undesirable residual effects, as it rapidly decomposes into O₂. Burleson and Pollard (1976) used ozone and sonication (*i.e.* the use of ultrasound to disrupt cells) to inactivate vegetative cells and spores in phosphate buffered saline water. Hamelin and Chung (1976) showed how ozone induces mutations in a great variety of genes in *E. coli* and affects the cell division capacity of the mutants. Ozone can react very fast with many organic and inorganic matters. The *ozonolysis* *i.e.* the cleavage by ozone will be the attack of gaseous ozone diluted with oxygen or air upon an unsaturated substance in the liquid phase (Bailey, 1958). This "attack" can be a one-step, C=C double bond attack, or a two-step attack, the first step being electrophilic, to produce aldehyde or ketone. The complete ozonolysis of triple bond substances produce carboxylic acid (Bailey, 1958).

In the last decades, ozone has been increasingly used in aquacultural operations (Rosenthal, 1981), *e.g.* to disinfect hatchery intake and effluent water streams, and to control pathogens (Blogoslawski and Stewart, 1977; Bullock *et al.*, 1997), oxidise ammonia and nitrite (Brazil, 1998), remove colour (Otte *et al.*, 1977) and odour, and reduce organic loading in recirculating hatchery and commercial aquarium water supplies. In shellfish aquaculture, ozone has also been used for the depuration of coliform-contaminated oysters and to inactivate the toxins produced by red tide dinoflagellates (Blogoslawski and Stewart, 1977; Rosenthal and Wilson, 1987).

For the present study, two units of ozone generators with different capacity were subsequently used. In the beginning of this study one ozone generator was installed (500 mg*h⁻¹ Co. Sander, Mod. S500, Fig. 10b). It was used for 130 days. After that a 1 to 4 g*h⁻¹ adjustable laboratory ozone generator was used (Co. Sander, prototype) (Fig. 10a). Both generators worked under the corona discharge principle, where dried air containing oxygen passed through an electrical field. The electrical current causes the "split" of the oxygen molecules. The resulting oxygen atoms, seeking for stability, attach to free oxygen molecules forming ozone. The laboratory ozone generator was equipped with two drying soils for the inlet air and one pressure reservoir chamber, to have a

constant dry air delivery to the electrical field. It was also equipped with two air cooling ventilators. The ozone gas was conducted through a Teflon[®] hose to the foam fractionator.

Figure 10c shows the rest-ozone-killer that was connected with the top of the foam fractionator to remove possible ozone in the air coming out of the foam fractionation tower. The grey PVC column was filled with 2 kg of granular active carbon (GAC) to adsorb the ozone present in the air. The U-shape tube on top avoided the entrance from water/moisture to the GAC filter. The U-shape acryl tube on the left was used to collect the excess entering water/moisture. GAC was used to achieve a big internal surface and because it gives a stable ozone removal under high moisture conditions. The GAC was renewed approximately every 6 months.



Fig. 10. Ozone generators used in this study: (a) laboratory 1 to 4 g*h⁻¹ ozone generator (prototype); (b) 500 mg*h⁻¹ ozone generator model S 500; and (c) air rest-ozone-killer.

The amount of ozone injected to the foam fractionator was controlled by the ORP value. The term ORP comes from oxidation/reduction potential and is measured in millivolts (mV). The ORP measures the tendency for a solution to either gain or lose electrons when it is subject to change by introduction of a new species. A solution with a higher ORP will have the tendency to gain electrons from new species (*i.e.* oxidize them) and a solution with a lower ORP will have the tendency to lose electrons to new species (*i.e.* reduce them). Reduction species are organic matter, proteins, faeces, and feed rests. The ORP value was measured inside the reaction chamber with a platinum electrode (Co. Sander, mod. PFGK-GEL). The ORP electrode was installed together with a pH electrode (Co. Sander, mod. HGK-GEL) in a by-pass closed water cycle (see Fig. 3, number 7). The ORP electrode was connected to the ORP display panel and through the main control system to the ozone generator. The threshold in the display panel was set to 350 (\pm 10) mV. Once the ORP value reached over 350 mV the control system turned the ozone generator automatically off.

2.2.3 Biological filtration: nitrification

The biological filtration (BOD removal and nitrification) is a fundamental water treatment process in every recycling method for the cultivation of aquatic animals. It mainly digests dissolved organic material (heterotrophic bacteria) and oxidizes ammonium-ions via nitrite to nitrate (two-step nitrification) by bacteria like *Nitrosomona sp.* and *Nitrobacter sp.* A solid medium is used as substrate for the attachment of the micro flora. Conventional biofilters employ sand or coral gravel as filter media. Modern filters make use of various plastic structures as grids, corrugated sheets, balls, honeycomb-shaped or wide-open blocks. The main goal is to provide a big active surface area for the micro flora settlement.

In the present study two types of biofilter and biofilter media were used (Tab. 5). The first type was a submerged packed bed filter media, downflow biofilter with a total available surface of 36.5 m². This biofilter was used from the beginning of the experiments until day t₄₃₁. The second type was a submerged moving bed filter media, downflow biofilter with a total available surface of 181.5 m². The filter media in this biofilter was moved and circulated by an internal air-lift system. The media were washed and cleaned due to the internal up flow circulation. By doing so no clogging happened. This type of biofilter features several advantages and flexibility against the fixed bed biofilters. Moving bed biofilters allow to have a bigger specific surface area in the same volume, they need low maintenance due to self-cleaning (no back wash needed), the water column is well supplied with oxygen, and the filter media does not act like a suspended solids trap. Figure 11 shows the two types of plastic filter media used. The size of the biofilter tank was the same for both media types. The biofilter tank had two ball valves, one at the outlet and one at the bottom for water discharge (Fig. 12).

Tab. 5. Characteristics of the biofilters and filter media used in this study.

Biofilter	Type	Filter media	Specific surface area	Biofilter active surface	Water volume
First	Fixed bed	PP	180 m ² *m ⁻³	36.5 m ²	0.24 m ³
Second	Moving bed	PE	963 m ² *m ⁻³	181.5 m ²	0.24 m ³
Additional (2)	Fixed bed	PP	180 m ² *m ⁻³	63.6 m ²	0.34 m ³

The air supply for the external air-lift that delivered water to the biofilter was through the main air supply system for the laboratory installations at the institute. The system delivers 1 bar pressure and the flow was set at approximately 900 L*h⁻¹. The air supply needed by the internal air-lift moving bed biofilter was also through the main air supply

system. In this case the flow was set at $150 \text{ L}\cdot\text{h}^{-1}$. Both filter media and filter design were delivered by the company Erwin Sander Elektroapparatebau GmbH.

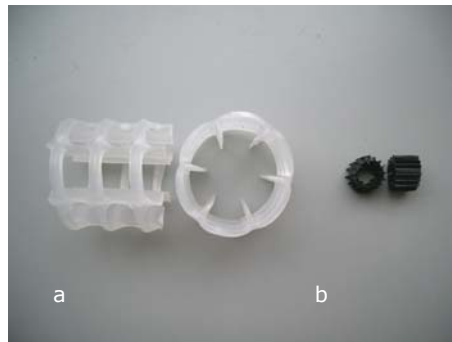


Fig. 11. Filter media used for biofiltration (nitrification). Polypropylene media (a), diameter 26 mm, specific surface of $180 \text{ m}^2 \text{ m}^{-3}$. Polypropylene media (b), diameter 10 mm, specific surface of $963 \text{ m}^2 \text{ m}^{-3}$.

Two separate additional biofilters units were installed at day t_{239} (Fig. 13), one for every fish tank. This was done because the main biofilter was incapable to work properly due to a high fish load in the tanks and because of excessive solids and bacteria inside the biofilter tank. These two additional biofilters were filled with the same media as type one (Tab. 5), with a total available surface of $31,8 \text{ m}^2$ each. The water was pumped (Eheim 1250, $20 \text{ L}\cdot\text{min}^{-1}$) from each tank through a plastic hose into the biofilter basin (Fig. 13). A PVC pipe square (40×40) was installed inside each biofilter and on top of the filter media to distribute the water properly. The outflow of the biofilter delivered the water directly in the tanks. This temporary solution was running during the design and installation of the second biofilter type.

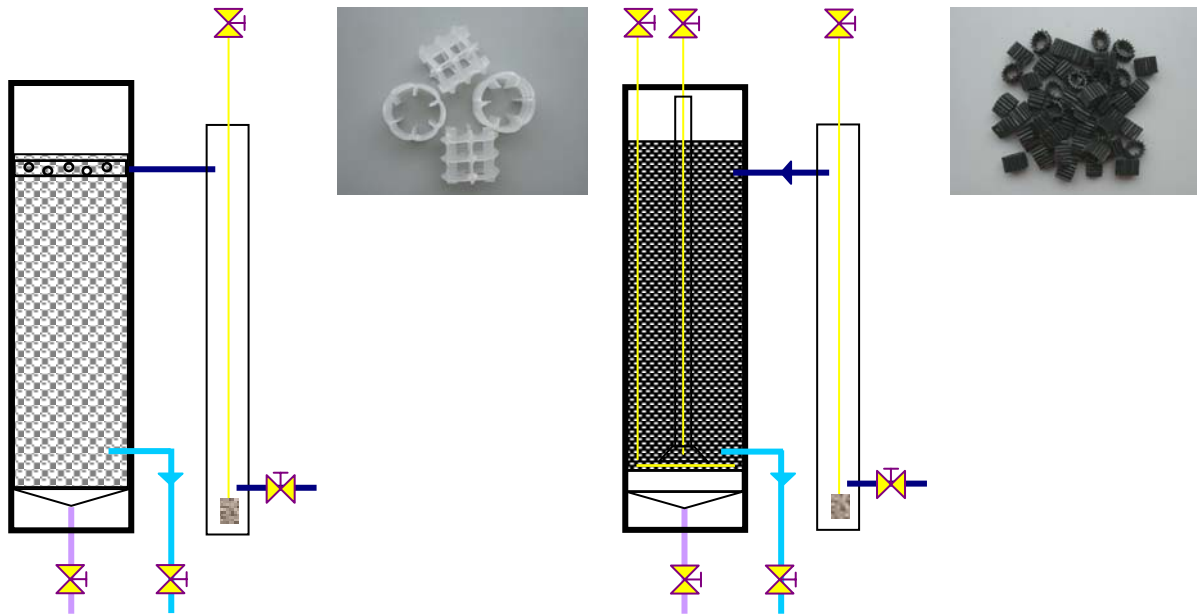


Fig. 12. Schematic drawing of the two main biofilter types used in the recirculation system during the study period.

The start-up phase of the biofilter lasted approximately 14 days. This was principally done to get a proper micro flora growth on the biofilter media. The two additional biofilters installed at day t_{239} were first inoculated with filter media and water coming from the main biofilter to achieve a short start up period.



Fig. 13. Side view of the two additional external trickling biofilter (one for each tank), installed during days t_{239} and t_{431} of the study period.

2.2.4 Rearing tanks

Circular tanks were employed throughout the study. Several authors have reviewed and reported the characteristics of different holding tanks for aquaculture, specially the advantages of circular tanks like Wheaton (1977), Rosenthal (1981b), and Timmons *et al.* (1998). In this type of tanks the inlet is usually at the water surface and the distribution of the water is tangentially to develop a circular flow pattern. This can play an important role in the collection and discharge of particulate matter from the holding unit. The self-cleaning properties described by Timmons *et al.* (1998) are present as well. In a circular tank there are also no dead corner areas and the water volume can be fully used by the fish.

For the rearing of sea bass in this experiment, two glass fibre reinforced plastic round tanks were installed. Glass fibre is a solid material, having a smooth surface (Waller, 2001). The tank shape and dimensions are presented in Figure 14. On the inner side of the water inlet a 90° PVC elbow was installed in each tank to produce an internal circular water flow pattern. On the opposite side and at the same height of the inlet, an underwater pump (Eheim 1250, 20 L*min⁻¹) was installed to achieve the same purpose, to ease the transport and collecting of the suspended solids in the middle of the tanks and to make the fish to swim in its normal school behaviour against the water flow (rheotaxis). To avoid the fish to escape through the inlet, special PVC fitting with a red PVC net nose was glued to the 90° inlet elbow. To avoid the fish to escape through the outlet pipe, a round plate of PVC (64 mm diameter) with holes (7 mm diameter) was installed inside the pipe (Fig. 14a). The tanks were flat-bottomed with a 0.45 x 0.45 m pyramid cone shape to the outer side (Fig. 14b). The two fish tanks were operated in parallel and placed on top of nine (3 x 3) cement bricks to support each tank bottom leg. The bottom of the tank was situated at 1.07 m height. The inlet was at 1.52 m height. Each tank had two ball valves, one in the main outlet pipe (63 mm diameter) and one smaller (32 mm diameter) for sampling and discharge (Fig. 14c).

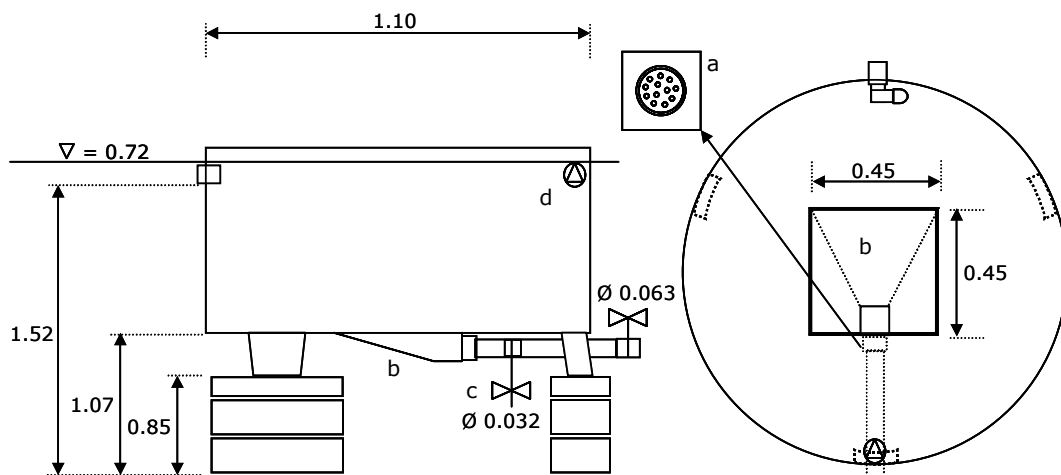


Fig. 14. Schematic presentation of the rearing tanks for *D. labrax*. Dimensions of arrows and levels are expressed in meters; (a) detail of a sieve plate inserted into the outlet pipe; (b) tank bottom outlet with a slope towards outlet pipe; (c) symbol for ball valves; (d) pump to generate internal circular water flow.

2.3 Secondary unit

2.3.1 Control of pH

The pH was controlled by adding calcium oxide (CaO) dissolved in distilled water to the culture water. During day t_0 and t_{208} no solution was added. From day t_{208} until t_{231} , 250 g of CaO was diluted in 10 L distilled water and the solution was added into the swirl separator, 5 L in the morning (around 10:30 hours) and 5 L in the afternoon (around 16:30 hours) to maintain a pH value above 7.0. From day t_{231} until t_{693} , the same amount of solution was automatically pumped from a canister into the swirl separator with a membrane motor pump (ProMinent, Mod. alpha ALPb, max $2.9 \text{ L}\cdot\text{h}^{-1}$). The pump was exchanged to a one channel hose pump (Fischer, max. $4.2 \text{ L}\cdot\text{h}^{-1}$) on day t_{693} and worked until day t_{902} . The solution dosage was automatically controlled by a pH measuring instrument. The power cable of the pump was connected to the relay switch inside the measuring instrument. It was capable to switch on *i.e.* off the dosage once the given pH set point value was reached (± 0.2). The relay switched the pump on when the pH value reaches 7.2. The dosage stopped when the pH value reached 7.8. To avoid the solution to precipitation inside the canister, air was bubbled inside the canister for agitation to keep the solution well mixed. The CaO amount was raised at day t_{354} up to 300 g per 10 L of distilled water.

The use of CaO buffer solution was satisfactory, but with some safety problems. When CaO was diluted in distilled water, lots of heat was produced. This made the preparation

and handling of the solution dangerous and immediately application impossible. Therefore, $\text{Ca}(\text{OH})_2$ was found to be a better solution. CaO was available at gravel grain size (5 – 10 mm) while $\text{Ca}(\text{OH})_2$ was in very fine dust form requiring a nose and mouth mask.

2.4 Data recording of water physics in the RAS

The determination of the following physical characteristics of the water took place daily from t_0 until t_{550} of the study period.

2.4.1 Temperature and salinity in the system

The measurement of water temperature and salinity was done with a TetraCon[®] 325 cell (company WTW) connected to the Universal Pocket Meter MultiLine P4 (company WTW). The reading of salinity was expressed as practical salinity units (psu). The cell was calibrated once a week using a calibration and control standard solution of $0.01 \text{ mol}\cdot\text{L}^{-1}$ KCl. For the temperature compensation, the MultiLine P4 instrument is equipped with a special non-linear function for sea water.

2.4.2 Dissolved oxygen concentration

The dissolved oxygen concentration in the culture water was measured using a Cellox[®] 325 probe (company WTW). The cell use the membrane covered galvanic probe measuring principle with a range of $0 \text{ mg}\cdot\text{L}^{-1}$ to $50 \text{ mg}\cdot\text{L}^{-1}$ and 0°C to 50°C . For the necessary incident flow to the cell the BR 325 battery stirrer was used (company WTW). The stirrer produced a flow of $18 \text{ cm}\cdot\text{s}^{-1}$. The calibration of the cell was done once a week using the OxiCal[®] - PE/OXI chamber. The galvanic head was checked every month, and the probe was regenerated if necessary.

2.4.3 Measurement of pH values

The pH value in the water was measured using the pH 340 Hand-Held Meter instrument and the SenTix[®] 41 pH combined electrode with integrated temperature probe (company WTW). The pH probe ranged from 0 to 14, and the temperature probe from 0°C up to 80°C . The probe was calibrated once a week using the standard solutions PL7 (pH 6,865 at 25°C) and PL9 (pH 9,180 at 25°C) (company WTW). Since the SenTix[®] 41 was

equipped with an integrated temperature probe no compensation was necessary to consider.

2.4.4 Measuring points

The measurement of the physical water quality characteristics took place daily at 09:00 and at 15:00 hours inside both rearing tanks. The ORP and pH values in the display of the probes inside the foam fractionator tower were also noted.

2.5 Feed composition and feeding amount

The feed used for the whole experimental period was manufactured by the company Biomar AS in Denmark. Since it was not cost efficient to get a special sea bass diet, rainbow trout (*Oncorhynchus mykiss*) feed was used. Table 6 shows the feed declaration for Biomar Ecostart 17 and Aqualife 17 diets for the different pellet sizes used.

The daily feeding ration was calculated based on feeding tables. Table 7 shows the feeding table used, in which the percent body weight (%BW) is given for different fish sizes and water temperatures. The feed quantity was calculated every day based on the biomass of each tank and after the morning temperature was measured. The percent body weight to feed rose with an increase in temperature and decline with the fish size.

Tab. 6. Declaration of the composition of the Biomar[®] extruded feed pellets for the different diets and feed sizes used. Data according to the information received from the manufacturer.

Diet Size (mm)	ECOSTART 17 1.2 Granular	ECOSTART 17 1.5	AQUALIFE 17 3	AQUALIFE 17 4.5	AQUALIFE 17 6
Crude protein (%)	50.0	47.0	42.0	42.0	42.0
Crude fat (%)	16.0	20.0	22.0	22.0	22.0
NFE (%)	14.0	14.0	16.0	16.0	16.0
Fibre (%)	1.0	0.8	3.0	3.0	3.0
Ash (%)	9.5	9.0	8.5	8.5	8.5
P total (%)	1.4	1.3	1.3	1.3	1.3
Met + Cys (%)	1.9	1.7	1.5	1.5	1.5
Gross energy (kcal)	4,946	5,157	5,235	5,235	5,235
Gross energy (J/g)	20,708	21,591	21,918	21,919	21,919

The feed was delivered into each tank using belt feeder (company Fiap). The feeders had a maximum capacity of 5 kg and a dispense period of 12 hours using a pull-back belt powered by a spring-wound clock mechanism. The feed was weight and loaded every morning around 9 o'clock.

Tab. 7. Feeding table used in this study. The percent body weight (%BW) of feed for different temperatures (°C), fish weight (g) and feed size (mm) are shown. Crumble feed are marked with a G (Granular).

Mean weight (g)	Size of feed (mm)	Temperature (°C)												
		14	15	16	17	18	19	20	21	22	23	24	25	26
		%BW												
1-5	1.2 G	2.2	2.3	2.6	2.8	3.0	3.3	3.5	3.9	4.2	4.5	4.8	5.1	5.4
6-14	1.2 G	1.7	1.9	2.1	2.4	2.6	2.9	3.2	3.4	3.6	4.1	4.5	4.9	5.2
15-20	1.5	1.2	1.5	1.8	2.1	2.4	2.7	2.9	3.2	3.4	3.7	4.2	4.6	5.0
21-40	1.5	0.8	0.9	1.1	1.4	1.6	1.8	2.0	2.2	2.3	2.6	2.8	3.4	4.0
41-60	3.0	0.6	0.8	1.0	1.2	1.4	1.6	1.8	2.0	2.1	2.3	2.5	2.9	3.2
61-100	3.0	0.5	0.7	0.8	1.0	1.2	1.4	1.6	1.8	1.9	2.1	2.3	2.7	3.0
101-200	4.5	0.6	0.7	0.7	0.9	1.0	1.2	1.4	1.6	1.7	1.9	2.0	2.3	2.5
201-300	4.5	0.4	0.5	0.6	0.8	0.9	1.0	1.1	1.3	1.4	1.5	1.6	1.8	2.0
301-500	6.0	0.3	0.4	0.4	0.5	0.6	0.8	1.0	1.1	1.2	1.3	1.4	1.6	1.7
501+	6.0	0.3	0.4	0.4	0.5	0.6	0.7	0.8	0.9	1.0	1.0	1.0	1.2	1.4

2.6 Determination of growth, mortality, feed conversion ratio and condition factor

2.6.1 Growth

The experimental phase in which the morphometrical parameters to determine the growth increase in the fish population were taken lasted from t_0 until t_{434} . In this period a sample of 20 fish (approximately 10%) of the total fish number in each tank was took out every 14 days. Total fish biomass in both tanks was determined in day's t_0 , t_{98} , t_{140} , t_{322} , t_{375} , and t_{435} . The fish were starved for 24 hours *i.e.* the day before the sampling no feeding took place. To avoid any injuries and for a better handling of the fish anaesthetic was applied. During t_0 and t_{294} tricaine (MS-222, company Sigma Aldrich) was utilized. From t_{294} until t_{435} and because of a better application of the drug (dilution) and response of the fish (recovery time) benzocaine powder (company Merck) was used to subdue the fish. The tricaine powder was directly added to the water. The benzocaine solution was prepared by dissolving the chemical in 3 mL of 100% ethanol. Between t_0 and t_{225} the doses used was $35 \text{ mg} \cdot \text{L}^{-1}$. The doses was raised up to $45 \text{ mg} \cdot \text{L}^{-1}$ after t_{294} and to $50 \text{ mg} \cdot \text{L}^{-1}$ after t_{375} . At the beginning two 10 L buckets were utilized, one for the anaesthetics and one for recovery. After t_{225} three 50 L buckets, one for the anaesthetic bath and two for recovery were prepared. A fine 5 mm mesh size knotless net catcher was utilized to avoid any damage to the fish skin. The fish were randomly caught out of the tank and put into the anaesthetic bath bucket. Total length was determined using an

ichthyometer with 0.1 cm accuracy. Total wet weight was determined using a digital scale with 0.1 gram accuracy.

2.6.2 Specific growth rate

The specific growth rate (SGR) is the percent of body weight gained per day. This was determined for every 14-days time interval, and was calculated using the Equation (1) explained by Ricker (1979):

$$\text{SGR} = \frac{\ln W_f - \ln W_i}{t} \quad \text{Equation (1)}$$

Where:

Wi: initial average weight (g)

Wf: final average weight (g)

t: time interval between weighing in days

2.6.3 Mortality

In the present study the status of the fish was observed daily. Dead fish were removed from the tank, measured, and weighted. External and internal features (abnormalities) were examined and recorded. Dead fish were not preserved.

2.6.4 Food conversion ratio

The food conversion ratio (FCR) (Equation (2)) is the ratio between the weight of food fed and the weight gain. FCR is the sum of the amount of food offered (kg) over a number of days (t) divided by the increase of wet fish weight (kg) over the time period (t).

$$\text{FCR} = \frac{\sum_{i=0}^t \text{Feed}_i}{\Delta \text{Biomass}} \quad \text{Equation (2)}$$

Where:

$\sum_{i=0}^t \text{Feed}_i$: feed consumed between i=0 until t

$\Delta \text{Biomass}$: biomass gained between i=0 and t

2.6.5 Condition factor

The relationship of weight to length is commonly termed condition factor (CF) (Equation (3)) (Donaldson *et al.*, 1979) and it is expressed as:

$$CF = \frac{W}{L^a} * 100 \quad \text{Equation (3)}$$

Where:

W: weight (g)

L: length (cm)

a: constant =3

The constant a is equal 3 according to the review presented by Froese (2006), based on the linear-volumetric relationship between weight and length, known also as the cube law.

2.6.6 Grading

In commercial aquaculture operations there are different management strategies regarding the splitting of fish into different size classes; this is commonly known as grading. The frequency depends on the cultivated species, the time of the year, size of the fish and the effort involved in the operation, the location of the site, the target market and others factors. Some farm managers work under the all-in/all-out principle to avoid unnecessary handling, some do grading only once during the grow-out period. Grading is also used to count and reduce the biomass in the cultivation unit (*e.g.* pen, tank, raceway or pond) and to adjust the daily feed ration to fish size.

In this study grading was done two times during the entire experimental period. This was necessary to start experimentations with a fairly and uniform size distribution, as well as reducing the load in the tanks after an extended growth period. The operation was done in the same way as described in 3.6.1 and took place on day t_{322} , where the fish were split in bigger and smaller than 250 g, and on day t_{437} separating the fish bigger and smaller than 300 g.

2.6.7 Fish quality

Fish being reared under an aquaculture program are expected to meet certain production criteria, many of which are associated with survival, growth, reproduction, and flesh quality (Schreck and Li, 1991). Certainly, farmers goals differ widely depending on species being reared, intensity of the fish husbandry, type of the final product (*e.g.* aggregated value) and market. The consumption of aquatic products is elected in most developed countries and disagreeable flavours in the product, and resulting consumer dissatisfaction may adversely affect the market demand (Ticker and Martin, 1991). Off-flavours, flesh firmness, smell, external appearance as well as microbiology indicators and nutrient analysis are conducted for every aquatic species that wants to be sold for human consumption. To evaluate the quality of sea bass reared in this study a fish sample (n=17) was taken on day t_{441} and transported on ice to an international fish wholesaler (company Frozen Fish International, Bremerhaven, Germany). The fish were analysed using a non-standard sensory assessment for fish products in which appearance, odour, taste and texture is evaluated (Tab. 8). Body weight and fillet yield was measured. Smell, taste, appearance and softness of the flesh were also tested, raw and cooked (steamed at 70°C for 15 min). Fillets samples were taken to determine fatty acids, protein and phosphate content. Total number of bacteria, enteric bacteria, and *E. coli* amounts were also determined. An analysis for listeria was done.

Tab. 8. Non-standard sensory assessment for fish products.

	Excellent to good		
	Excellent 9	Very good 8	Good 7
Appearance (colour)	Exceptionally appealing, bright, natural colour, typical for the sample	Bright natural colour, single slightly discoloured specimen allowed	Natural colour, a little too pale or dark, a few slightly discoloured specimen allowed
Appearance (shape)	Perfect preservation of shape, firm, undamaged shape	Very well preserved shape, single changed specimen	Well preserved shape, a few slightly or single strongly changed specimen
Cooked odour	Exceptional delicate, distinct, characteristic odour	Rich, strong characteristic odour	Good characteristic odour
Taste	Exceptional delicate, distinct, characteristic taste	Rich, strong characteristic taste	Good characteristic taste
Texture	Exceptional good, characteristic texture (tough, succulent tissue, very tender)	Very good, characteristic texture (tough tissue, tender)	Good characteristic texture (still tender)
	Satisfactory to borderline		
	Satisfactory 6	Mediocre 5	Borderline 4
Appearance (colour)	Slight reduction of typical colour (not uniformly light or dark)	Impairment of typical colour (slightly bleached, unbalanced)	Discolouration of sample surface (with tendency to other colourations)
Appearance (shape)	Good preserved shape, a few slightly or occasional strongly damaged specimen	Impairment of natural shape (slight loss of shape, shrunken)	General loss of shape, shrunken, still not unpleasant
Cooked odour	Normal slightly reduced odour (slightly flat, not rounded)	Impairment in natural odour, still acceptable (quite flat, sharp, perfumed)	Clearly reduced odour (stale, perfumed, slightly musty)
Taste	Normal slightly reduced taste (slightly flat, not rounded)	Impairment in natural taste, still acceptable (quite flat, sharp, perfumed)	Clearly reduced taste (stale, perfumed, slightly musty)
Texture	Normal slightly reduced texture, slight deviation	Impairment in natural texture, still acceptable (partly not uniform, slightly soft or hard)	Clearly reduced texture (not uniform, too soft, too hard, slightly watery)
	Poor to very bad		
	Poor 3	Bad 2	Very bad 1
Appearance (colour)	Strong discolouration of sample	Complete discolouration of sample surface, original colour no longer perceptible	Complete discolouration of sample surface towards repulsive colours
Appearance (shape)	Generally severe loss of shape	Severely changed shape, still not repulsive, advanced disintegration	shape of sample has fully disintegrated
Cooked odour	Altered odour (completely stale, slightly rancid or fermented, no longer appealing)	Unpleasantly changed odour, still not repulsive (rancid or fishy)	Repulsive, strange odour (foul, fermented, spoiled)
Taste	Altered taste (completely stale, slightly rancid or fermented, no longer appealing)	Unpleasantly changed taste, still not repulsive (rancid or fishy)	Repulsive, strange taste (foul, fermented, spoiled)
Texture	Altered texture (not uniform, too soft, too hard, slightly like leather, slightly tough)	Unpleasantly changed texture, fully paste-like, extremely hard	Repulsive texture

2.7 Determination of dissolved nutrients

Dissolved nitrogen based compounds and phosphorus were determined in the culture water. Total ammonia nitrogen (TAN), nitrite-nitrogen (NO_2^- -N), nitrate-nitrogen (NO_3^- -N) and orthophosphate (PO_4^{3-}) were determined daily from t_0 until t_{140} and regularly thereafter (every third day) between days t_{141} and t_{428} . The HACH® test kits were used (test kit number 8038 for NH_3^- -N, number 8507 for NO_2^- -N, number 8039 for NO_3^- -N and number 8178 for PO_4^{3-}). The tests are applicable for sea water and a high accuracy can be achieved. The test kits were initially tested against the standard procedures explained by Hansen and Koroleff (1999).

During the trials between day t_{668} and t_{690} , the total ammonia nitrogen concentration (TAN) was determined by the indophenols blue method according to Hansen and Koroleff (1999).

All determinations on concentrations in the culture water were done using a spectrophotometer (company Hach®, model DR/2010). The spectrophotometer uses a 25 mL, 1 inch, quartz glass sample cell.

2.7.1 Water sampling

Table 9 shows in detail the sampling points in the recirculation system during the different trial periods.

To avoid the presence of suspended material in the water sample all sampling points, with the exception of the additional biofilter, were equipped with a special constructed sampling-pipe and ball valve (Fig. 15). The pipe inside the plain tee has a diameter of 20 mm and allows taking water out in the same direction of the flow.

Tab. 9. Sampling point and nutrient analysis for the different trial periods. The cell marked with (♦) shows in the analysis performed.

Day interval	Sampling point	Dissolved nutrients			
		TAN	NO ₂ ⁻ -N	NO ₃ ⁻ -N	PO ₄ ⁻³
t ₀ – t ₁₄₀	Outlet swirl separator	♦	♦	♦	♦
	Inlet tanks	♦	♦	♦	♦
t ₁₄₁ – t ₄₂₈	Outlet swirl separator	♦	♦	♦	♦
	Outlet biofilter	♦	♦	♦	♦
	Outlet foam fractionator	♦	♦	♦	♦
	Inlet tanks	♦	♦	♦	♦
t ₂₃₉ – t ₄₂₈	Outlet additional biofilter	♦	♦	♦	♦
t ₆₆₈ – t ₆₉₀	Outlet swirl separator	♦	♦	♦	♦
	Outlet biofilter	♦	♦	♦	♦
	Inlet foam fractionator	♦	♦	♦	♦
	Outlet foam fractionator	♦	♦	♦	♦
	Inlet tanks	♦	♦	♦	♦

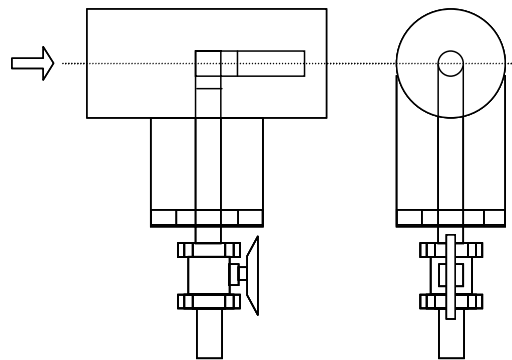


Fig. 15. Side and front view of the sampling-pipe and ball valve set constructed for diameter 75 mm and diameter 63 mm plain tees. The pipe inside is diameter 20 mm. The arrow shows the direction of the water flow.

For every determination a 25 mL probe was needed. The water samples were taken at the same time of the day and before feeding. In every case the glass receptacles were gently rinse with the same water coming from the respectively sampling-pipe. After measuring all receptacles, instruments and apparatus were washed and rinse twice with pure water. The glass sample cell for the spectrophotometer was cleaned with technical hydrochloric acid (30%) and rinse with pure water.

The samples were taken out in a 500 mL beaker. After 30 min settling time, a 25 mL measuring cylinder was used to measure each 25 mL sample and put it into the wide neck reagent bottle made of soda-lime glass for the final nutrient determination. The settling time was applied in order to avoid the presence of solids in the probe. For the measurements between day t_{668} and day t_{690} the water samples were taken out in 1000 mL laboratory bottles. The water sample was filtrated using a vacuum Witt type filter apparatus through a 47 mm diameter, GF/F filter (glass micro fibre filter, company Whatman®). For the TAN determinations the water samples were pressure filtrated using a 50 mL syringe and a 25 mm diameter, cellulose nitrate, 0.45 μm pore filter (company Sartorius®).

2.7.2 Calibration of the analytical methods

Calibration in the context of spectrophotometer analysis means comparison of the sample absorption after chemical reaction with the absorption of a standard (*i.e.* an artificial sample of known concentration), which has been treated in exactly the same manner (Hansen and Koroleff, 1999).

In this study, a calibration procedure was done for every nutrient determination method before every measuring schedule listed in Table 8 started.

2.7.3 Determination of total ammonia-nitrogen (TAN) concentrations

2.7.3.1 Determination methods

The total ammonia nitrogen determination (TAN) between t_0 and t_{428} was done using the Nessler method (Hach® method 8038). The practical steps were done as follows:

- Mineral stabilizer was first added to the sample in order to complexes the hardness (Mg^+ and Ca^+ ions), equivalent to 1 mL per sample.
- Polyvinyl alcohol (3 drops) was than added to the sample to aid the colour formation of the Nessler reagent with ammonium ions.
- Nessler reagent (1 mL) was finally added.
- The bottle was softly turned one time to mix the reagents.
- The reaction time lasted 5 min.
- The sample was spilled in the sample cell and red at 425 nm wave length.
- A yellow colour is formed proportional to the ammonia concentration in the water.

Between day's t_{668} and t_{690} the indophenols blue method described by Hansen and Koroleff (1999) was used. In this method the sum of ammonium (NH_4^+) and ammonia (NH_3) is measured. Ammonia reacts in moderately alkaline solution with hypochlorite to give monochloramine which, in the presence of phenol, catalytic amounts of nitroprusside ions and excess of hypochlorite, gives indophenol blue (Hansen and Koroleff, 1999). The intensity of the blue colouring in the sample is direct proportional to the TAN concentration. The absorbance of the blue colouring complex was measured using a wave length of 630 nm. For the manual method, the following reagents were prepared according to Hansen and Koroleff (1999). The hypochlorite reagent and the citrate buffer were prepared using one simplified step described by Nolting (2000):

Phenol reagent: 80.0 g phenol ($\text{C}_6\text{H}_5\text{OH}$) was dissolved in 300 mL ethanol. 600 mL pure water was added. 600 mg of disodium nitroprusside dihydrate [$\text{Na}_2\text{Fe}(\text{CN})_5\text{NO} \cdot 2\text{H}_2\text{O}$] were dissolved in 100 mL pure water. The solution was stored in an amber glass bottle at $<8^\circ\text{C}$.

Hypochlorite reagent: 3.6 g of solid sodium hydroxide (NaOH) were dissolved in pure water up to 100 mL. 0.5 mg of dichloro-s-triazine-2,4,6-(1H,3H,5H)-trione sodium salt (DTT) were dissolved in the NaOH prepared solution. The resulted solution was stored in an amber glass bottle at $<8^\circ\text{C}$.

Citrate buffer: 240 g of trisodium citrate dihydrate ($\text{C}_6\text{H}_5\text{Na}_3\text{O}_7 \cdot 2\text{H}_2\text{O}$) and 20 g of EDTA (disodium salt) were dissolved in 600 mL of pure water. 10 mL of NaOH 1.0 M solution was added. The resulted solution was boiled until the volume was less than 0.5 L, cooled, dissolved up to 500 mL with pure water and stored in a polyethylene bottle at room temperature.

For this method the practical steps were done as follows:

- 1 mL of phenol reagent was added.
- 0.5 mL of citrate buffer was than added on.
- 1 mL of hypochlorite reagent was finally added to.
- The reaction time lasted between minimum 12 h and maximum 24 hours.
- The samples were storage in darkness and at room temperature (20°C).
- The next day the reading took place at 630 nm wave length.
- A blue colour is formed in proportional amount to the ammonia concentration in the sample.

2.7.3.2 Calibration of the measuring methods

The calibration of the Nessler method was done for the trials between t_0 and t_{140} and between t_{141} and t_{428} . The calibration of the indophenols blue method was done for the trial between t_{668} and t_{690} . The salinity effect was considered and calibrated as well.

The calibration consists first in the preparation of a standard solution according to Hansen and Koroleff (1999). 53.5 g of dried (100°C) ammonium chloride (NH_4Cl) were dissolved in pure water and dilute to 100 mL. A drop of chloroform was added as preservative. The solution was kept in a glass bottle at $<8^\circ\text{C}$ and contained $10 \text{ mmol}\cdot\text{L}^{-1}$ ($18.04 \text{ mg}\cdot\text{L}^{-1}$) ammonium. Seawater was prepared for the salinity present in the culture water. The standard solution was stepwise diluted with seawater and mixed with the reagents according to the steps listed in 2.7.3.1. The turbidity (absorbance) caused by the reagents was also measured. Finally a regression of the absorbance versus the concentration was calculated. The absorbance values measured can be transformed to concentration values using the regression Equation. The calibration plots and regressions used are shown in Figure 16 and Figure 17.

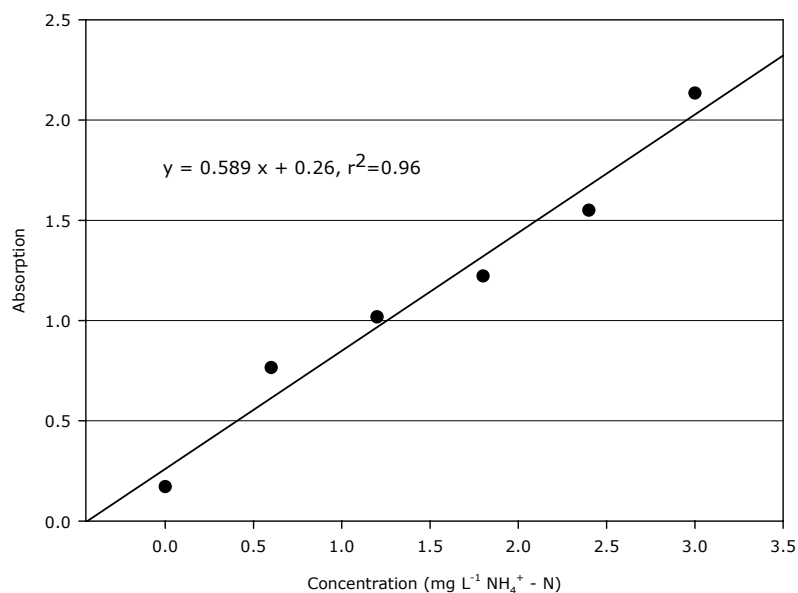


Fig. 16. Calibration regression ($p < 0.05$) for the determination of the total ammonia concentration (TAN) in the culture water during t_0 and t_{140} of the study period.

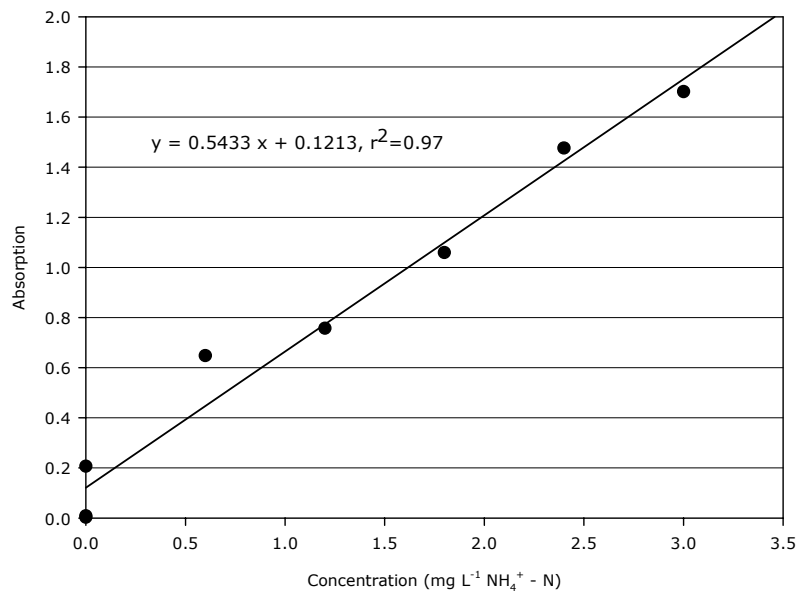


Fig. 17. Calibration regression ($p < 0.05$) for the determination of the total ammonia concentration (TAN) in the culture water during t_{141} and t_{428} of the study period.

For the indophenols blue method applied during t_{668} and t_{690} , the linear salinity correction described by Hansen and Koroleff (1999) was used. The TAN concentration was calculated using the Equation (4):

$$\text{TAN} = [1 + 0.0073 * (\text{PSU} * d^{-1})] * 0.319 * (A - 0.048) * d \quad \text{Equation (4)}$$

Where:

TAN: $\text{mg} * \text{L}^{-1}$

Linear salinity correction: $[1 + 0.0073 * (\text{PSU} * d^{-1})]$

Calibration factor: 0.319

Reagent blank: 0.048

Dilution factor: d

2.7.4 Determination of nitrite-nitrogen (NO_2^- -N) concentrations

2.7.4.1 Determination method

The nitrite-nitrogen concentration (NO_2^- -N) was determined using the Hach[®] method number 8507 with powder pillows. In this method nitrite present in the sample reacts with sulfanilic acid to form an intermediate diazonium salt. This couples with chromotropic acid to produce a pink coloured complex which is in direct proportion with the amount of nitrite present in the sample. The measurement was done stepwise as follows:

- The content inside the powder pillow was carefully added to the reagent bottle.
- The bottle was shortly shaken to dissolve the powder.

- A reaction time of 15 min was applied.
- The sample was spilled into the sample cell and read at 507 nm wave length.

2.7.4.2 Calibration of the measuring method

The calibration of the diazonium method was also done for every measuring interval. The nitrite standard solution was prepared according to Hansen and Koroleff (1999) by first drying anhydrous sodium (NaNO_2) at 100°C for 1 h. 0.69 g were dissolved in 1 L of pure water and stored cool inside the refrigerator ($<8^\circ\text{C}$). The solution contained $10 \text{ mmol}\cdot\text{L}^{-1}$ of nitrite. Sea water with the needed salinity was prepared. Before starting the stepwise dilution and absorption measures the standard was diluted by 100, which means 1 mL standard and 99 mL of sea water. The turbidity (absorbance) caused by the reagents was also measured. Finally a regression of the absorbance versus the concentration was calculated. The absorbance values measured can be transformed to concentration values using the regression Equation. The calibration plots regressions used in the experiments between t_0 to t_{140} , and t_{141} to t_{428} are shown in Figure 18 and Figure 19 respectively.

For the trial between t_{668} and t_{690} the calibration factor and the reagent blank were calculated averaging three regressions for salinities 10, 20 and 30 psu. The nitrite-nitrogen concentration was then determined using the Equation (5):

$$\text{NO}_2^- \text{-N} = 0.177 * (\text{A}-0.021) * d \quad \text{Equation (5)}$$

Where:

$\text{NO}_2^- \text{-N}$: $\text{mg}\cdot\text{L}^{-1}$

Calibration factor: 0.177

Reagent blank: 0.021

Dilution factor: d

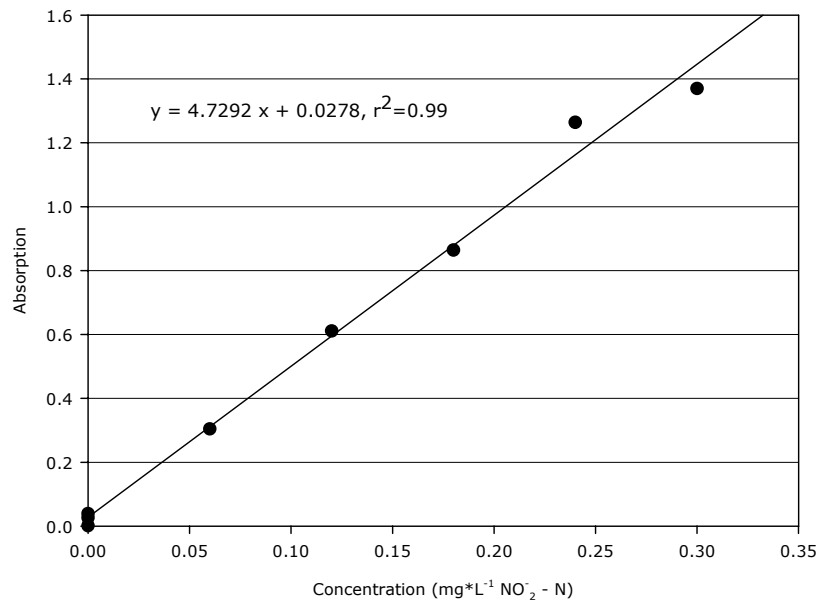


Fig. 18. Calibration regression ($p < 0.05$) for the determination of the nitrite-nitrogen concentration (NO_2^- -N) in the culture water during t_0 and t_{140} of the study period.

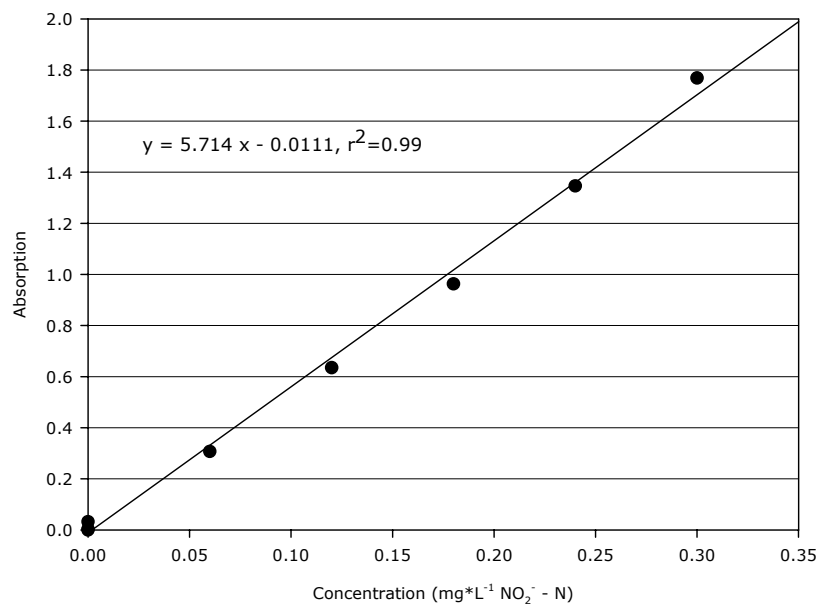


Fig. 19. Calibration regression ($p < 0.05$) for the determination of the nitrite-nitrogen concentration (NO_2^- -N) in the culture water during t_{141} and t_{428} of the study period.

2.7.5 Determination of nitrate-nitrogen (NO_3^- -N) concentrations

2.7.5.1 Determination method

The concentration of dissolved nitrate-nitrogen (NO_3^- -N) was determined using the powder pillow cadmium reduction method Hach[®] number 8039. The cadmium metal present in the powder reduces nitrate to nitrite. The nitrite ions reacts in an acidic medium with sulfanilic acid to form an intermediate diazonium salt. This salt couples to

gentisic acid to form an amber-coloured product. The coloured solution is directly proportional to the amount of nitrate present in the sample. The determination of the nutrient concentration was done in the following way:

- The content in the powder pillow was carefully added to the reagent bottle.
- The bottle was gently shaken for exactly 1 min to dissolve the powder.
- A reaction time of 5 min was applied.
- The sample was spilled into the sample cell and read at 500 nm wave length.

2.7.5.2 Calibration of the measuring method

To prepare the standard solution, 1.011 g of dry potassium nitrate (KNO₃) was dissolved and made up to 1 L of pure water. The solution contained 10 mmol L⁻¹ nitrate and is stable (Hansen and Koroleff, 1999).

The standard solution was diluted stepwise and absorption was measured. The turbidity (absorbance) caused by the reagents was also measured. Finally a regression of the absorbance versus the concentration was calculated. The absorbance values measured can be transformed to concentration values using the regression Equation. The calibration plots and regressions used are shown in Figure 20 and Figure 21.

For the trial between t_{668} and t_{690} the calibration factor was determined considering the correlation of the calibration factors calculated for four different salinity values (0, 10, 20, and 30 psu). The reagent blank was determined using pure water, since the nitrate concentration in artificial sea water contained too much background noise. The nitrate-nitrogen concentration was then determined using the Equation (6):

$$\text{NO}_3^- \text{-N} = [(0.3424 * \text{PSU}) + 30.654] * (A - 0.021) * d \quad \text{Equation (6)}$$

Where:

NO₃⁻-N : mg*L⁻¹

Calibration factor: [(0.3424 * PSU) + 30.654]

Reagent blank: 0.021

Dilution factor: d

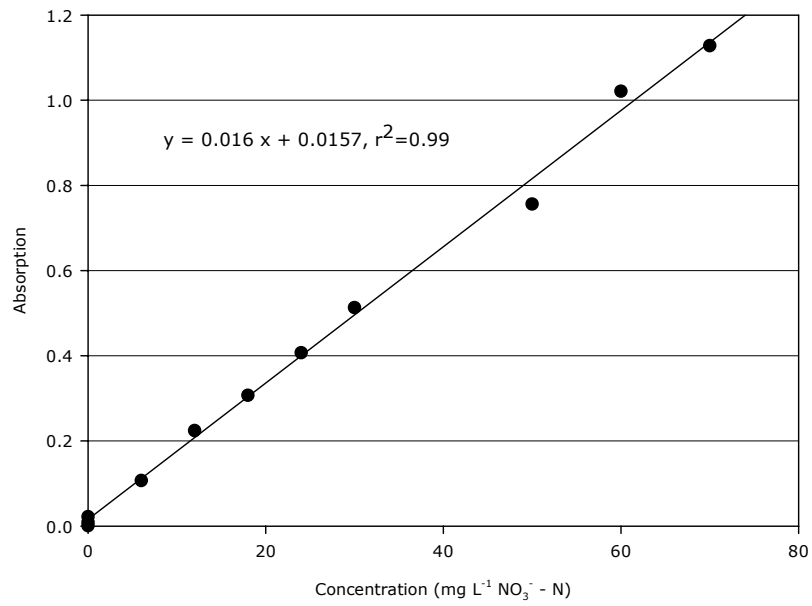


Fig. 20. Calibration regression ($p < 0.05$) for the determination of the nitrate- nitrogen concentration (NO_3^- -N) in the culture water during t_0 and t_{140} of the study period.

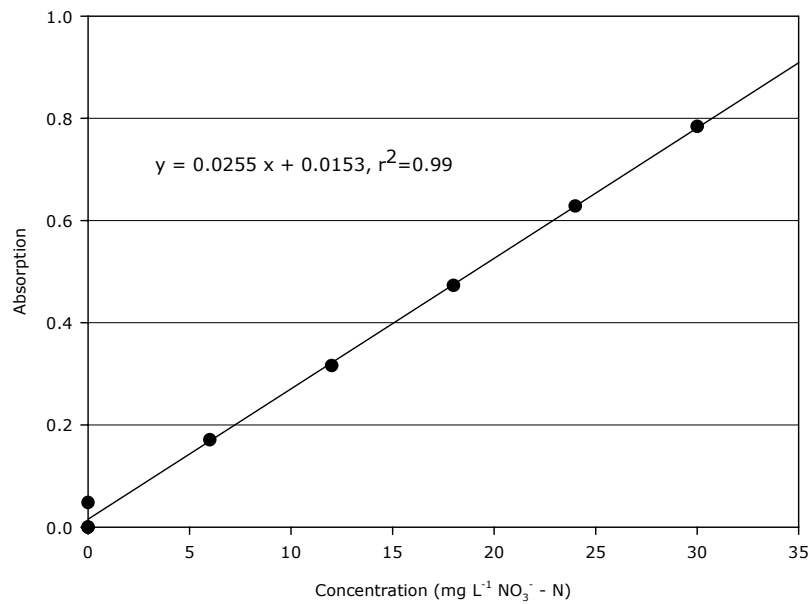


Fig. 21. Calibration regression ($p < 0.05$) for the determination of the nitrate-nitrogen concentration (NO_3^- -N) in the culture water during t_{141} and t_{428} of the study period.

2.7.6 Determination of the phosphorus (PO_4^{-3}) concentrations

2.7.6.1 Determination method

All the methods for the determination of inorganic phosphate in seawater are based on the reaction of the ions with an acidified molybdate reagent to yield a phosphomolybdate heteropoly acid, which is then reduced to a highly coloured blue compound (Hansen and Koroleff, 1999). The Hach[®] method used (number 8178) works under this principle. The determination of the phosphorous concentration (also called orthophosphate) was done as follows:

- 1 mL of the molybdate reagent was added to the reagent bottle.
- Then, 1 mL of the amino acid solution was added.
- The bottle was softly inverted several times to mix the reagents.
- A 10 min interval was applied.
- The solution was spilled into the sample cell a red at 530 nm wave length.

2.7.6.2 Calibration of the measuring method

The phosphate standard solution and the sulphuric acid were prepared according to Hansen and Koroleff (1999). Concentrated sulphuric acid ($\sigma=1.84 \text{ g}\cdot\text{mL}^{-1}$) was added to pure water in relation 1:3 up to 1 L. After cooling the volume was checked. The volume lost was refill with pure water up to 1 L. The solution was stored in a polyethylene bottle. Potassium di-hydrogen phosphate (KH_2PO_4 , relative molecular mass 136.09) was dried at 110°C and then placed in a desiccator. Exactly 136.09 mg were dissolved in pure water which has been added 0.2 mL of sulphuric acid (prepared) and made up to 100 mL. The solution contained $10 \text{ mmol}\cdot\text{L}^{-1}$ phosphate and was stored in a glass bottle.

The standard solution of phosphate was stepwise diluted and absorbance was measured. The turbidity (absorbance) caused by the reagents was also measured. Finally a regression of the absorbance versus the concentration was calculated. The absorbance values measured can be transformed to concentration values using the regression Equation. The calibration plots and regressions used are shown in Figure 22 and Figure 23.

For the trial between t_{668} and t_{690} the calibration factor and the reagent blank were calculated averaging three regressions for salinities 0, 10, 20, and 30 psu. The phosphate concentration was then determined using the Equation (7):

$$PO_4^{-3} = 21.16 * (A-0.013) * d$$

Equation (7)

Where:
 PO_4^{-3} : $mg \cdot L^{-1}$
 Calibration factor: 21.16
 Reagent blank: 0.013
 Dilution factor: d

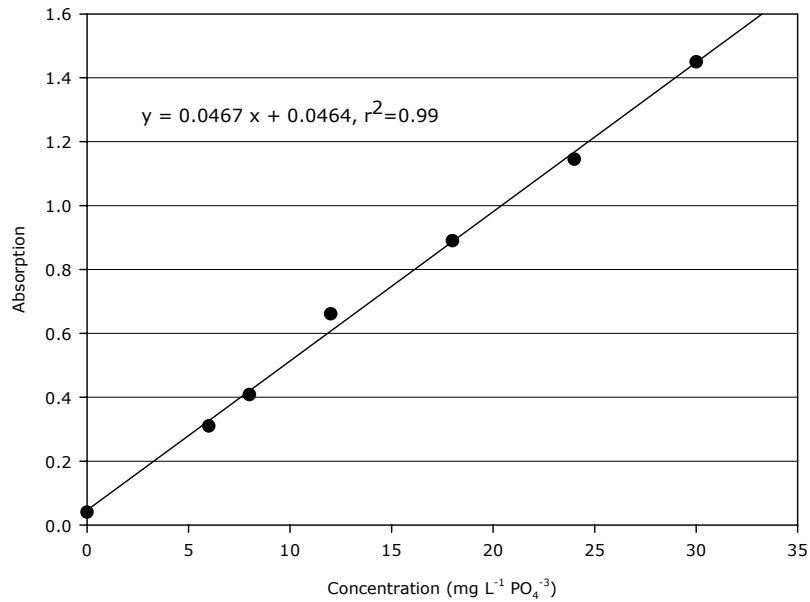


Fig. 22. Calibration regression ($p < 0.05$) for the determination of the phosphate concentration (PO_4^{-3}) in the culture water during t_0 and t_{140} of the study period.

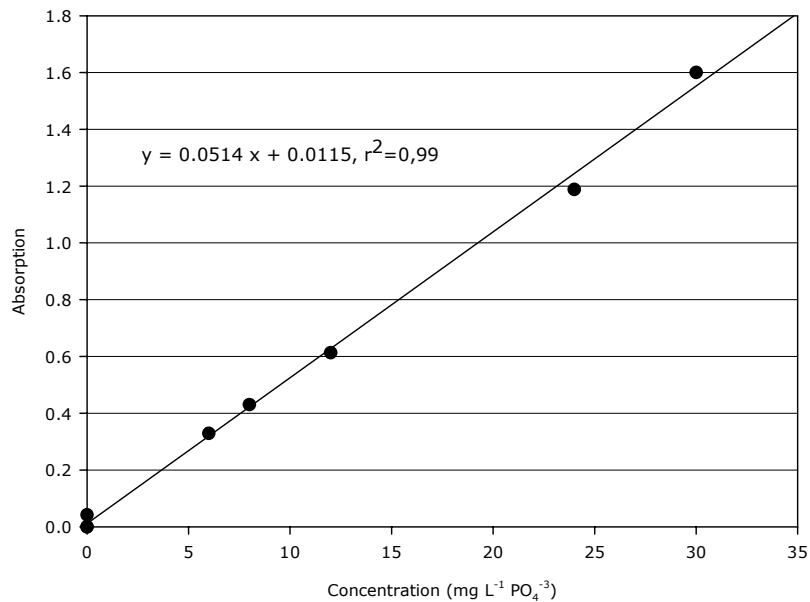


Fig. 23. Calibration regression ($p < 0.05$) for the determination of the phosphate concentration (PO_4^{-3}) in the culture water during t_{141} and t_{428} of the study period.

2.8 Analysis of the solid waste

Suspended solids adversely impact all aspects of recirculating aquaculture systems, so the first objective of any recirculating treatment scheme is the removal of solid wastes (Timmons *et al.*, 2001). The solid waste removal performance in the RAS was studied for solid the removal units swirl separator and foam fractionator.

Total suspended solids (TSS) in the swirl separator were determined in regular every 14 days between t_0 and t_{434} . Additionally measurements were done between t_{668} and t_{690} . The amount of fine solids coming from the foam fractionator was studied in the experiments conducted in the period between t_{668} and t_{690} .

2.8.1 Solid waste in the swirl separator: sampling and preparation for analysis

Solid waste in the funnel bottom of the swirl separator was collected by piping out the water-solids mixture into a bucket. The bucket content was carefully poured into sedimentation cones. After 60 min the settled solids were collected in low form beakers. The solid sample was passed sequentially through a series of stainless steel analytical sieves, with square openings; first through the 1600, 800 and 400 μm sieves, and then through the 200, 100 and 50 μm sieves. The amount of solids retained in each sieve was carefully flushed with distilled water into a beaker. Finally, seven size classes were obtained, one for each sieve pore size and one for the fine solids coming after the 50 μm sieves. This size class was assessed as $<50 \mu m$. Each of the seven size classes were vacuum filtered using a Erlenmeyer form, filtering flask, with a side-arm socket, a 500 mL filtration beaker and glass micro fibre filter (GF/C, company Whatman[®]), 90 mm diameter, with a nominal pore size of about 1.58 μm . The vacuum filtration was done using a vacuum pressure between -200 and -500 mbar.

For the period between t_0 and t_{434} and depending on the amount of solids gathered for each size class, either the total amount of solids or three subsamples were filtrated. For the filtration of a subsample, the beaker containing the size class sample was stirred using a 60 mm magnetic stirrer stick (company Ika[®]), to achieve homogeneity. From this homogeneous solution a 22 mL subsample was taken and filtrated as explained. During the trials between t_{668} and t_{690} , the solid waste was determinate using only three subsamples for every size class.

The glass micro fibre filters were initially ignited at 500°C for 12 h, stored in Petri dishes and cooled inside a desiccation chamber down to room temperature (25°C) and weighted. During the filtration process, the filtrate was flushed (rinsed) three times with gently distilled water to avoid any salt effect. After filtering, the filters were dried at 60°C for at least 12 h and until the weight was constant. Once the weight was determined, the filters were again ignited this time at 540°C for 8 h for the determination of ashfree organic content. For this purposes aluminium dishes were used.

Additional solid sample were taken for the carbon, nitrogen and phosphorus analysis and for the determination of energy content (calorimeter). For this purposes, solid material was carefully scratched from the glass micro fibre filters with a fine spatula and put into aluminium dish. The solid sample was dried at 60°C, weighted and stored in glass tubes with plastic lids, inside a desiccation chamber at 25°C.

Figure 24 shows a schematic explanation of the analysis done with the solid material collected from the RAS.

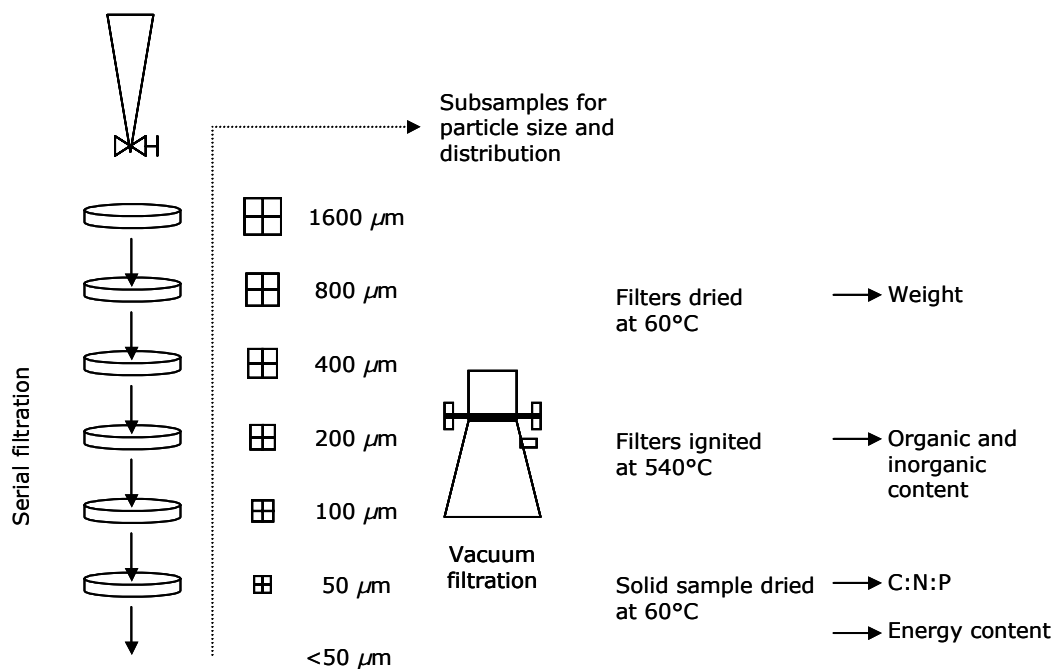


Fig. 24. Schematic explanation for the analysis of the solid material in this study.

2.8.2 Solid waste in the foam fractionator: sampling and preparation for analysis

The fine solids coming from the foam fractionator were studied in detail between t_{668} and t_{690} . Foam flushing water samples were taken for carbon, nitrogen and phosphorus analysis. These samples were filtered using 25 mm diameter glass micro fibre filters (GF/F, company Whatman®). 10 mL subsamples were taken for the Multisizer I analysis. Additional 25 mL subsamples (three parallels) were filtered using 47 mm diameter glass micro fibre filters (GF/F, company Whatman®) for the determination of solid weight and ashfree organic content. In this case the initial water level of the foam flushing tank was also measured to determine water volumes produced by foam.

2.8.3 Analysis for the determination of carbon and nitrogen content in the solids

For the determination of the carbon and nitrogen (C,N) content in the solid samples, an elemental analyser (company Euro Vector®, model EA) was used. After drying the samples at 60°C for 6 hours, the material was weighted (approximately 1.0 – 1.5 mg), wrapped in tin foil and burned at 1020°C in the combustion column. As carrier gas for the combustion products, highly purified helium was utilised. The heat released during the combustion of the tin guarantees the complete burning, even of very stable substances. The gaseous combustion products are led through a catalyst pipe. The resulting gas mixture consists of nitrogen oxides, carbon dioxide, water, and not consumed oxygen. The gas flow passes through a reduction pipe, which is a quartz tube filled with small bits of copper wire. At approximately 680°C the oxygen is bound at the copper and the nitrogen oxides are converted to molecular nitrogen. Then, the gas flows through a water trap and is separated in a temperature controlled gas chromatography furnace at approximately 95°C. This furnace consists in a gas chromatography separation column and a thermal conductivity detector. The quantity of carbon and nitrogen is determined by calculating the integrated surface under the curve peaks of the chromatogram. The calibration of the equipment was done by burning acetanilide, which has a known carbon and nitrogen relationship of 7:1.

2.8.4 Analysis for the determination of phosphorus content in the solids

For the determination of the total phosphorus in the solid matter, the same oxidizing proceeding as describes in 2.7.7.1 was used. Solid samples were weight (1-2 mg) on ¼ of a glass fibre filters (GF/C, diameter 90 mm) and put into clean glass bottles. The

oxidizing agent Oxisolv (Merck®) was added and heat was applied (115°C for 30 min). The final phosphorus content determination was done using an auto analyzer.

2.8.5 Analysis for the determination of energy content in the solids

For the determination of the energy content in the solid samples an adiabatic calorimeter (company Ika®, model C 4000A) was used. The calorimeter was connected to a computer where the Ika® CalWin® software was installed. These allowed controlling the equipment, safe, and evaluate the data.

The samples were prepared using the tablet method, in which around 0.1 g of a dried sample was pressed to a tablet form. Inside the calorimetric bomb, the tablet was put into the quartz crucible with the cotton string winded to the ignition filament. The bomb was filled with 30 bar oxygen to ensure a complete combustion of the substance. The bomb was then placed in the calorimeter inner vessel filled with water. The ignited sample passed its heat to the bomb and to the water. The heat of combustion produced increases the temperature of the calorimeter system. About 10 to 15 min after ignition the heat exchange between the calorimetric bomb and the water surrounding it in the inner vessel is completed. The temperature rise is then measured and serves to calculate the gross calorific value (H_0). This calculation is possible because the heat capacity (C) of the adiabatic system was previously determined burning a reference substance, in this case benzoic acid.

The heat capacity (C) is the amount of heat which is required to raise the temperature of the measuring system by 1 degree Kelvin, and can be calculated using the following Equation (8):

$$C = \frac{H_{OB} * m_B + Q_F}{\Delta T} \quad \text{Equation (8)}$$

Where:

C: $J * K^{-1}$

H_{OB} : gross calorific value of the standard substance ($J * g^{-1}$)

m_B : weight (g)

Q_F : sum of all extraneous heat (J)

ΔT : temperature increase measured (K)

The gross calorific value (H_0) of the samples was calculated using the Equation (9):

$$H_0 = \frac{C * \Delta T - Q_F}{m_p} \quad \text{Equation (9)}$$

Where:

H_0 : $J \cdot g^{-1}$

C : heat capacity of the calorimeter system ($J \cdot K^{-1}$)

ΔT : temperature increase measured (K)

Q_F : sum of all extraneous heat (J)

m_p : weight of substance to be determined (g)

2.8.6 Analysis for the determination of ashfree organic content

The ashfree organic content of the solid material was determined by incineration of the sample in a muffle furnace at 540°C for 8 hours. After incineration samples were cooled down at room temperature (20°C) inside a desiccation chamber to avoid the absorption of moisture. Samples were weighted before and after incineration. Percentages of ashfree organic content (%OC) were calculated from the weight difference before and after incineration, in relation to the original sample weight.

2.9 Particle size analysis

Particle size determination was conducted using a resistance pulse counter (Multisizer I, Coulter Counter®). This method determined the size of particles suspended in an isotonic solution (electrolyte). The suspension passes through an aperture (orifice tube) with an electric field. The displacement of electrolyte due to a particle induces a change in the resistance across the aperture in the orifice tube. This difference in the resistance is measured and correlated to the particle volume. The orifice tubes used had an aperture of 140 μm and 1000 μm . According to the manufacturer, the orifice tubes can measure only between approximately 2% and 60% of the given aperture, *i.e.* the orifice tube with an 1000 μm aperture did only measured particles in the range from 22.5 – 714.7 μm . The orifice tube with a nominal 140 μm aperture measured particles between 2.8 μm and 87.8 μm .

Finally, from the solids studied between t_{466} and t_{562} and during the trials between t_{668} and t_{690} , a size class subsample (10 mL) was taken for the analysis of the particles size and distribution with the Multisizer I (company Coulter Counter®) and for the image analysis.

2.10 Optical examination of particulate matter in the RAS

In order to know more about the size, structure and shape of solid matter, subsamples collected from each size class fraction retained by the sieves were taken in small Petri dishes (\varnothing 55 mm) with 20 mL distilled water. Subsamples were taken for periods 2 (t_{28}), 4 (t_{56}), 8 (t_{113}), 12 (t_{176}), 16 (t_{239}), 20 (t_{294}), 24 (t_{361}) and 28 (t_{437}).

The size classes $<50 \mu m$, $50-100 \mu m$, $100-200 \mu m$ and $200-400 \mu m$ were analyzed using a digital scanning microscope (company Zeiss[®] model DSM 940). Samples were first filtrated through a 13 mm diameter, cellulose-acetate filter (company Sartorius[®]) and dried at 60°C for 24 hours. Filters were than sputter coated using gold-palladium as target material (sputter coating device company Balzers model SCD 004). Black and white pictures were taken.

Size classes $400-800 \mu m$, $800-1600 \mu m$ and $>1600 \mu m$ were analyzed using a Leica[®] MZ95 binocular equipped with a black and white video camera (company Hitachi[®] model CCD) and connected to a computer. The camera allowed taking pictures of the samples using the software PC-TV.

Pictures obtained with the binocular were analyzed using the image processing software Adobe[®] Photoshop 5.0 and Image-J. Image-J is a public domain Java image processing program. Adobe[®] Photoshop 5.0 was used to clean the raw picture from objects of no interest and to convert it to an 8-bit binary image. Image-J was used to analyze the picture with the "Analyze Particles" feature that can count and size particles.

2.11 Bacteria in the RAS

Another source of particulate matter in an aquaculture system is the micro fauna (Chen *et al.*, 1994). A closed recirculation system offers sufficient organics for bacteria growth in the water column and on tanks, walls, and pipes.

2.11.1 Bacteria number, biomass and survival percentage

For the investigations on bacterial population in the culture water (number, biomass and survival percentage), samples of the foam fractionator and the foam collector tank were taken. Two methods for bacteria number determination were used.

2.11.1.1 Method I: Total bacteria number and bacteria biomass

For the quantification of the total number of bacteria an epi-fluorescence microscopy was used (company Zeiss[®], model Axiophot-Axioplan, with a HBO 50 W mercury vapour lamp). The epi-fluorescence microscope irradiates a stained sample with light of a specific wave length. The sample (*i.e.* the dye) absorbs the light in that given wavelength, emits light with less energy at another, longer wavelength. This light emission is called fluorescence. The fluorescing cells can be observed in the microscope and shine out against a dark background with high contrast. As fluorescence dye (fluorochrome) acridine orange was utilized. Acridine orange is a very simple stain for DNA and RNA. Acridine orange interacts with DNA by intercalation of the acridine nucleus between successive DNA base pairs. The absorption of acridine orange is in between 440 and 480 nm (blue), the emission is in between 520 nm (green for DNA) and 650 nm (orange for RNA). Acridine orange stain living as well as dead cell.

Water samples were taken in 100 mL amber glass bottles. The bottles were previously washed with particle free (filtered through cellulose nitrate filter, 0.2 μm pore, company Sartorius[®]), bi-distilled water and dried at 70°C. The samples were fixed immediately after sampling by adding particle free, 37% formol (filtered through cellulose nitrate filter, 0.2 μm pore, company Sartorius[®]), 1 mL for 50 mL sample, and stored in the dark at room temperature (20°C). For the final filtration and staining of the sample, 25 mm diameter polycarbonate filters (company Sartorius[®], pre-stained with irgalan black to avoid auto fluorescence and to provide a black contrasting background) were used. The filters were put in a vacuum filtration set (Witt type). Samples (1 to 3 mL) were filtrated at -150 mbar. After that, 1 mL acridine orange was added, and left on for 5 min. The rest of solution on the filter was eliminated by vacuum through. The filter was dried at room temperature (20°C). Finally, the filter was put on a microscope slide, fixed with one drop of Cargille[®] immersion oil, and covered with a cover slip. The fixed samples were stored at -8°C.

For counting and sizing the bacteria a New Porton G12 grid (company Graticules LTD., UK) was used (Fig. 25). Since the bacteria on the filter have a Poisson distribution, the counting has to be by chance in relation to the filter surface. The edges and the centre of the filter have to be taken into account. Figure 26 shows two different ways of covering the whole filter, while counting. If particles are present, they should not cover more than 50% of the field of view. In total, 400 bacteria have to be counted for a reliable result. The total number of cells is calculated using the Equation (10):

$$B_n = \frac{M * mf * df}{V} \quad \text{Equation (10)}$$

Where:

B_n : bacteria number ($N * mL^{-1}$)

M: mean number of bacteria counted (N)

mf: microscope factor (367455.41)

df: dilution factor

V: volume of filtrated sample (mL)

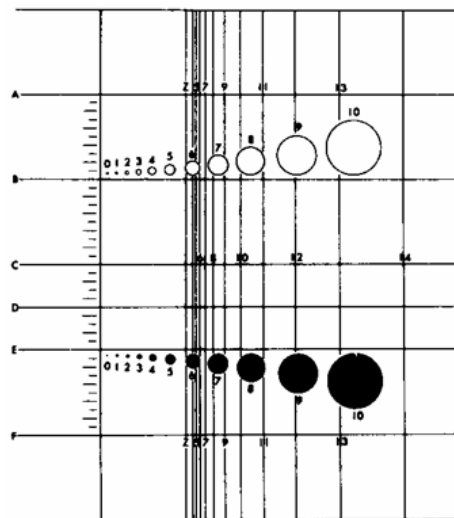


Fig. 25. New Porton microscopy grid G12 used for counting and seizing of bacteria.

The New Porton grid (Fig. 25) has 11 circles with different diameters, from circle number 0 ($0.2 \mu m$ diameter) up to circle number 10 ($7.6 \mu m$ diameter). These ones are used to measure the cells for the determination of the bacteria biomass. The form of the cell as to be identified and ordered in one of three shapes: rods (bacilli), spheres (cocci) or spiral (spirilla). The objective is to assign one or a combination of two circles to explain the length and width dimensions of the cell. With these two dimensions (descriptions) the volume of the cell can be calculated using the Equation 11.

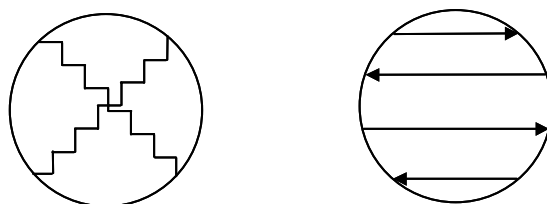


Fig. 26. Counting directions across the filter.

The cell volume was calculated using Equation (11), that is:

$$B_V = \frac{\pi}{4} * (B_{\emptyset})^2 * \left(B_L - \frac{B_{\emptyset}}{3} \right) \quad \text{Equation (11)}$$

Where:

B_V : bacteria volume (μm^3)

B_{\emptyset} : bacteria diameter (μm)

B_L : bacteria length (μm)

Once the cell volume was determined, the carbon content of each bacteria cell can be estimated using the Equation (12) of Simon and Azam (1989):

$$C_{cont} = 1.04878 * (88.6 * B_V^{0.59}) \quad \text{Equation (12)}$$

Where:

C_{cont} : carbon content (fg)

B_V : bacteria volume

Finally, the mean bacterial biomass can be calculated using the Equation (13):

$$B_{BIO} = B_n * C_{cont} * 10^{-6} \quad \text{Equation (13)}$$

Where:

B_{BIO} : mean bacterial biomass ($\mu g C * L^{-1}$)

B_n : bacteria number ($n * mL^{-1}$)

C_{cont} : carbon content (fg)

2.11.1.2 Method II: Heterotrophic plate count

The heterotrophic plate (HPC) count is a procedure for estimating the number of live heterotrophic bacteria. Petri dishes with a standard cultivation media are inoculated with water samples, in different dilutions. Bacteria colonies arise from single cell, pairs, or chains, all of which are included in the term colony forming unit (CFU). The colonies can be counted after incubation.

The cultivation media, marine agar (Zobell 2216), was previously prepared and cooked with autoclaved water from the recirculation system. 20-30 mL of agar was poured in a Petri dish (plate), cooled and stored in the dark at room temperature (20°C). The water sample was took out and put into a 100 mL glass bottle. The glass bottles were

previously sterilized using the same procedure as for method I. After the sample was took, the time until the inoculating was kept as short as possible to minimize an error in the measurement because of an extra bacterial growth between sampling and inoculating, and to avoid any external contamination. Seven dilutions rows for the water sample were done, starting with dilution zero (pure sample) down to dilution -6 that is, 1 mL sample diluted with autoclaved water down to 1 million. The samples coming directly out of the foam tower were diluted down to -8 that is, 1 mL sample diluted with autoclaved water down to 100 million. A volume of 100 μL of each dilution was inoculated on the agar plates. Three parallel plates were inoculated for each dilution. After inoculating, the plates were put into plastic bags and stored in the dark at room temperature (20°C) for 7 and 14 days respectively. The first counting took after 7 days place. The second counting 7 days after. The total number of CFU per plate has to be between 30 and 300 for a reliable determination.

Finally, the total number of CFU per mL was calculated using the Equation (14):

$$\text{CFU} = B_{\text{count}} * \text{df} * \text{vf} \quad \text{Equation (14)}$$

Where:

CFU : colony forming units ($\text{CFU} \cdot \text{mL}^{-1}$)

B_{count} : mean bacteria number counted on the plate

df : dilution factor

vf : volume factor

2.11.2 Microscopic examination of bacteria

Bacteria samples were microscopically examined using a digital scanning microscope (see 2.9). In this case, samples were first treated with an ethanol solution chain, using 30%, 50%, 70%, 90% and finally three times 100% ethanol baths, to replace the water. After this, the samples were dried using the critical point drying method. This method allows avoiding the collapsing or deforming of the wet structure of the sample, by never allowing a liquid/gas interface to develop; in this way the bacteria are not exposed to surface tension forces. Samples were than prepared for the scanning microscope by sputter coating the filters as described in 2.9. Black and white photography sets were taken for posterior analysis.

2.12 Water flow in the RAS

As explained in chapter 2.2 the RAS was built as a low-head (low energy consumption) system and the water flow was achieved only through the water height difference caused by the air-lift systems. For this reason it was impossible to incorporate flow meter devices, since the water pressure in the pipe was not enough to move the cone inside the flow meter.

For measuring the water flow an ultrasonic flow measuring system was used (company Prosonic®, model Flow DMU 93). The equipment operates on the principle of transit time differences. An acoustic signal (ultrasonic) is transmitted from one sensor to the other. The time (transit) that the signal requires to arrive at the receiver sensor is then measured. The difference in the transit time is directly proportional to the velocity of the flow. The flow is finally calculated using the equation $Q=v*A$ (Q =volumetric flow, v =flow velocity and A =pipe cross-sectional area). Figure 27 shows the Prosonic system principle and the sensors attached to the pipes of the RAS.

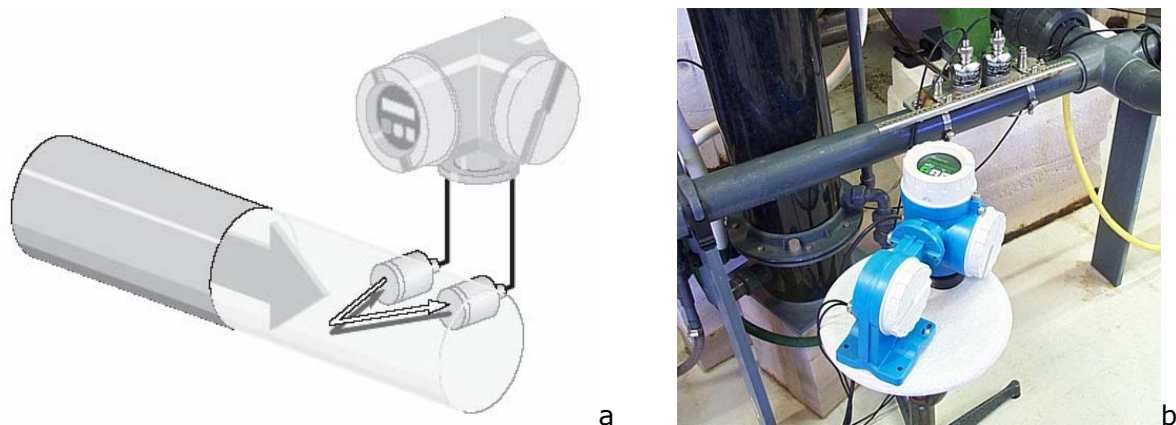


Fig. 27. Flow measuring principle (Panel (a)) of the ultrasonic flow meter (Prosonic® DMU 93; drawing by Prosonic®). The positions of the transmitting and receiving sensors attached to the PVC pipe varied and are dependant of the pipe material, pipe diameter and pipe wall thickness. Panel (b) shows the flow meter attached to the outlet pipe coming from the fish tanks during the measurement.

The flow measuring system was positioned at two points in the RAS: outlet fish tanks and outlet biofilter. The first point was choosing to know the flow velocity coming out of both fish tank. The second, because the air-lift system installed in the inlet of the biofilter was dependant from the air flow coming from the main air supply for the aquarium facilities, and was equipped with an air flow meter regulated by a valve. The air valve for the air-lift supply was adjusted for several air flows, from $100 \text{ L}\cdot\text{h}^{-1}$ up to $900 \text{ L}\cdot\text{h}^{-1}$ (in $50 \text{ L}\cdot\text{h}^{-1}$ steps) and the flow was read from the Prosonic display.

3 Results

The main experiment focussed on the qualitative and quantitative dynamics of total suspended solids (TSS) occurring in, and removed from a recirculating aquaculture system (RAS) under varying operational conditions (*e.g.* increasing biomass, two temperatures regimes and stepwise increasing salinity), while on growing juvenile European sea bass (*Dicentrarchus labrax* L., initial stock $n=206$ per tank, total initial biomass 2.6 kg). The dissolved and particulate organic and inorganic wastes were quantified. The investigations on TSS were undertaken with and without the application of ozone.

In the first part of the results, growth and fish health are detailed. In the second part, the abiotic parameters of the RAS are presented. The third part of the results presents the particulate matter analysis and its relation to fish biomass and to system efficiency in terms of safe water quality conditions for fish growth. This part considers also the intermitted use of ozone. Also, microbiological analyses of the system process water are presented. Finally, the RAS was analyzed from an engineering point of view focussing mainly on determining total flow rates through the system and biofilter (by pass) thereby providing the basis to calculate retention times.

Table 10 presents the various study periods numbered delineating a biweekly interval between day t_0 and day t_{437} . Notice that for tank 2 period 22 lasted somewhat longer until day t_{322} .

Tab. 10. Period number denomination for each day interval from start.

Period 1	t_0-t_{14}	Period 8	$t_{99}-t_{113}$	Period 15	$t_{204}-t_{225}$	Period 22	$t_{309}-t_{328}$ (322)
Period 2	$t_{15}-t_{28}$	Period 9	$t_{114}-t_{126}$	Period 16	$t_{226}-t_{239}$	Period 23	t_{329} (323)- t_{347}
Period 3	$t_{29}-t_{42}$	Period 10	$t_{127}-t_{140}$	Period 17	$t_{240}-t_{252}$	Period 24	$t_{348}-t_{361}$
Period 4	$t_{43}-t_{56}$	Period 11	$t_{141}-t_{154}$	Period 18	$t_{253}-t_{266}$	Period 25	$t_{362}-t_{375}$
Period 5	$t_{57}-t_{70}$	Period 12	$t_{155}-t_{176}$	Period 19	$t_{267}-t_{280}$	Period 26	$t_{376}-t_{389}$
Period 6	$t_{71}-t_{84}$	Period 13	$t_{177}-t_{189}$	Period 20	$t_{281}-t_{294}$	Period 27	$t_{390}-t_{403}$
Period 7	$t_{85}-t_{98}$	Period 14	$t_{190}-t_{203}$	Period 21	$t_{295}-t_{308}$	Period 28	$t_{404}-t_{437}$

3.1 Growth performance of *Dicentrarchus labrax*

3.1.1 Weight and length increment over time

Mean total length (TL) and mean wet weight (W) for each tank and period are shown in Figure 36 and Figure 37. The fish were sorted twice, on day t_{322} and day t_{328} for tank 1 and 2 respectively, and on day t_{437} both tanks simultaneously. The first grading split fish in those smaller than 250 g (tank 1), and larger than 250 g (tank 2). At the end of this trial (t_{437}) the fish were sorted again into smaller (tank 1) and larger fish (tank 2) with the splitting weight of 300 g (second grading, not reported). The first grading is indicated in all graphs by a vertical dashed line. In the following we consider growth in weight and length, comparing in both tanks the development prior and after the first grading. Data after the second grading were not further considered for periodically growth determination.

Before the first grading took place the fish in tank 1 were reared from 4.7 ± 0.7 g to 241.8 ± 40.5 g, and from 7.6 ± 0.4 cm up to 26.5 ± 1.9 cm (Fig. 28 A, B). In tank 2 the fish grew from 4.5 ± 0.8 g to 247.2 ± 40.5 g, and from 7.5 ± 0.4 cm up to 26.7 ± 1.6 cm (Fig. 29 A, B). As we can see from the data, growth in both tanks was fairly comparable until sorting. The equations fitted the data well.

After first grading the system was re stocked as follows: Tank 1, 194 sea bass, mean weight of 215.1 ± 27.8 g and a mean total length of 25.6 ± 1.4 cm; Tank 2, 167 fish, mean weight 279.1 ± 21.4 g, mean total length of 27.8 ± 1.2 cm. It is of interest to note that after sorting, fish grew faster as expected (calculated, dotted red curve), following the function $f(x)=a/(1+(\exp(-(x-x_0)/b)))$ (dashed bold black line) (Fig. 28 and 29). Presumably this phase of accelerated growth happen due to favourable culture conditions in terms of food availability. The variability observed in fish size can be explained because of a very inefficient feed delivery into the tank. Small feed amounts largely separated in time and delivered in one side of the circular tank (band feeder) led to an active feeding by larger and stronger fish. Comparable smaller fish were unable to get the %BW of feed calculated for the daily meal, resulting in a reduced growth. This earlier food depression (partial food deprivation) well known in aquaculture was compensated after sorting.

It is often recommended not to sort the fish very often if the growth curve takes the normal course, to avoid the sensible reaction to behavioural and subsequent effects on

the condition factor (CF). The social behaviour and the metabolism of the fish are definitely responsible of the lower turnover (in body weight) partially observed in this trial.

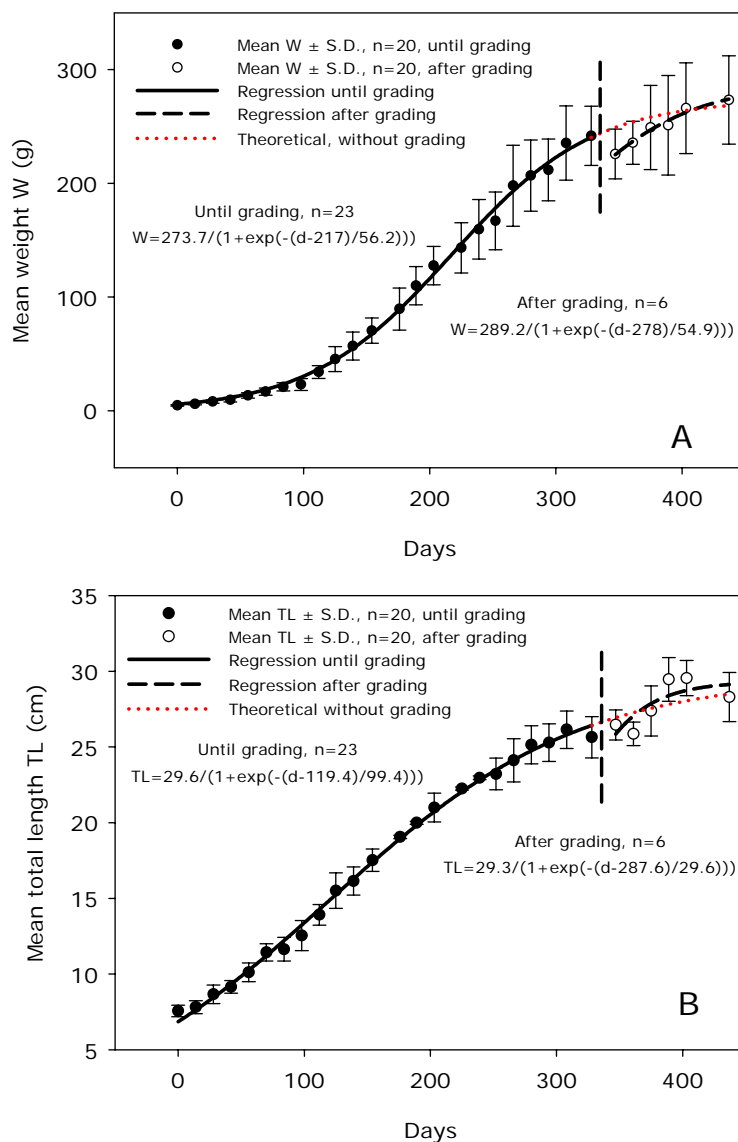


Fig. 28. Growth performance of *Dicentrarchus labrax* reared in tank 1. Panel A depicts the increment of weight ($W \pm S.D.$) over time before grading; bold black line shows the regression line fitted by the function $f(x) = a / (1 + (\exp(-(x-x_0)/b)))$ with: $a=273.7$; $b=56.2$; $x_0=217$; $R^2=0.99$; dotted red line shows the theoretical curve assuming no grading; dashed bold black line shows the regression line after grading fitted by the same equation with coefficients $a=289.2$; $b=54.9$; and $x_0=278$; $R^2=0.97$. Panel B shows the increment of total length ($TL \pm S.D.$) over time; bold black line shows the regression line fitted by the function $f(x) = a / (1 + (\exp(-(x-x_0)/b)))$ with: $a=29.6$; $b=99.4$; $x_0=119.4$; dotted red line shows the theoretical development of the curve assuming no grading; dashed bold black line shows the regression line after grading fitted by the same equation with coefficients $a=29.3$; $b=29.6$; and $x_0=287.6$. The vertical dashed line shows grading day (t_{328}).

At the end of period 28 (t_{437}), the system had a stock of: 141 fish in tank 1 (mean weight 273.3 ± 34.5 g; mean total length 28.1 ± 1.2 cm) and 124 fish in tank 2 (weight averaged 347.8 ± 23.5 g and total length averaged 30.1 ± 0.9 cm).

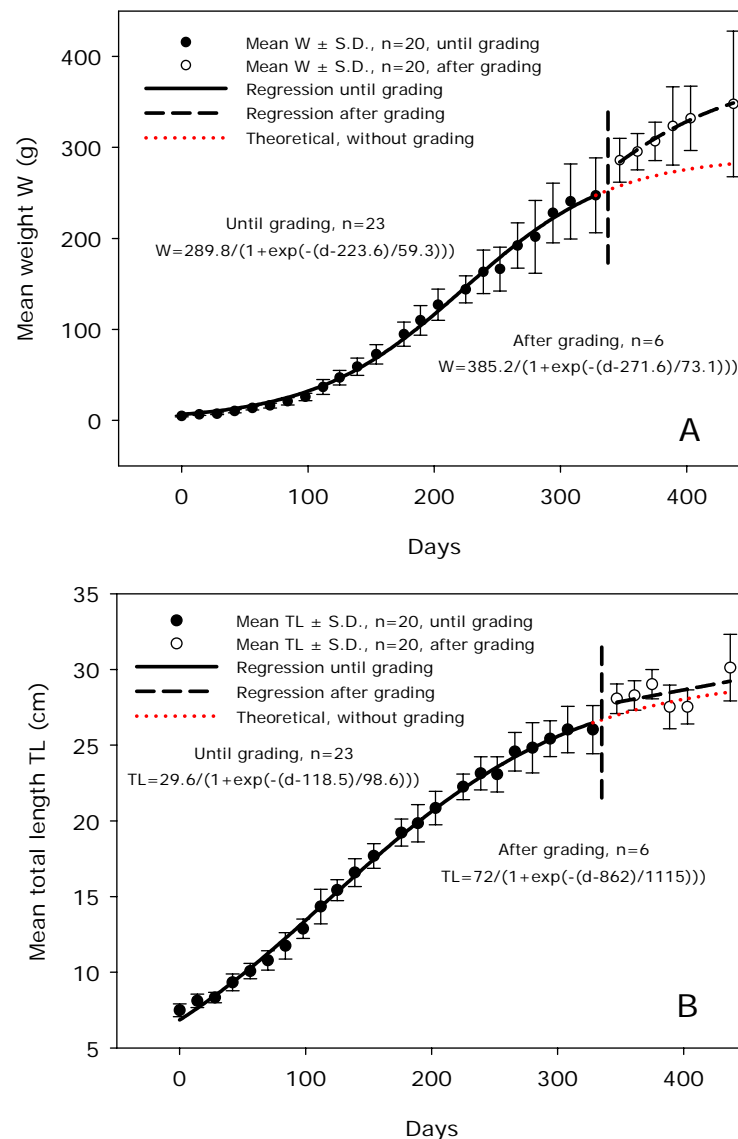


Fig. 29. Growth performance of *Dicentrarchus labrax* reared in tank 2. Panel A depicts the increment of weight ($W \pm S.D.$) over time before grading; bold black line shows the regression line fitted by the function $f(x) = a / (1 + (\exp(-(x - x_0) / b)))$ with: $a = 289.8$; $b = 59.3$; $x_0 = 223.6$; $R^2 = 0.99$; dotted red line shows the theoretical curve assuming no grading; dashed bold black line shows the regression line after grading fitted by the same equation with coefficients $a = 385.2$; $b = 73.1$; and $x_0 = 271.6$; $R^2 = 0.97$. Panel B shows the increment of total length ($TL \pm S.D.$) over time; bold black line shows the regression line fitted by the function $f(x) = a / (1 + (\exp(-(x - x_0) / b)))$ with: $a = 29.6$; $b = 98.6$; $x_0 = 118.5$; dotted red line shows the theoretical development of the curve assuming no grading; dashed bold black line shows the regression line after grading fitted by the same equation with coefficients $a = 72$; $b = 1115$; and $x_0 = 862$. The vertical dashed line shows grading day (t_{328}).

The relationship between mean total length (TL) and mean wet weight (W) is graphically presented in Figure 30 A and B, for tank 1 and 2 respectively. The exponential function presented in the graphic is explained by the equation $W = a \cdot TL^b$. In both cases, the coefficient of determination of the correlation (R^2) was 0.97. The parameters b for tank 1 and 2 are 2.5 and 3.0 respectively, explaining an isometric growth.

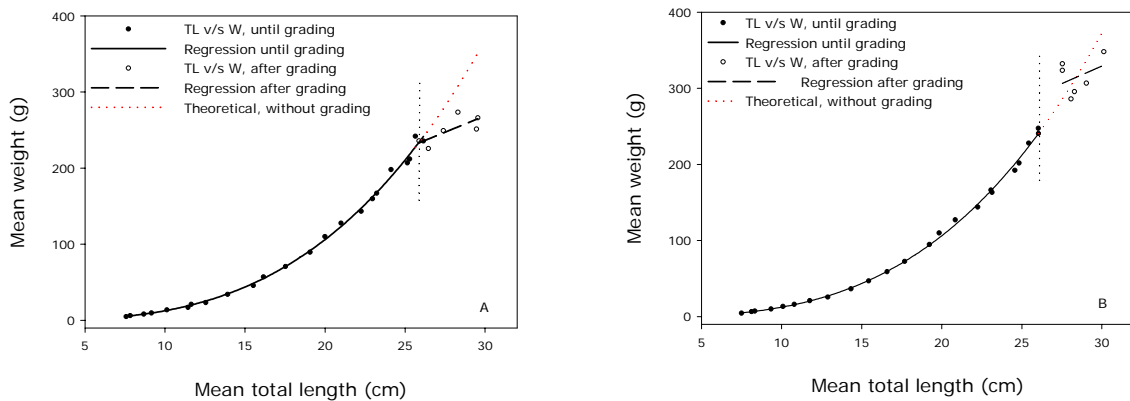


Fig. 30. Length-weight relationship for European sea bass grown in the RAS, fitted for tank 1 (A) and 2 (B). Graph A: Bold black line shows the regression line for the length/weight relationship, explained by the function $f(x)=a*x^b$ with $a=0.012$; $b=3.1$; $R^2=0.99$. Dotted red line shows the theoretical curve assuming no grading. Dashed bold black line shows the regression line after grading fitted by the same equation with coefficients $a=10.3$; $b=0.96$; $R^2=0.55$. Graph B: Bold black line shows the regression line for tank 2 fitted by the function $f(x)=a*x^b$ with $a=0.01$; $b=3.1$; $R^2=0.99$. Dotted red line shows the theoretical development of the curve assuming no grading. Dashed bold black line shows the regression line after grading fitted by the same equation with coefficients $a=19.2$; $b=0.84$; $R^2=0.11$. The vertical dashed line shows the first grading (day t_{328}).

3.1.2 Specific growth rate

Specific growth rate (SGR) was determined for each tank and period and results are presented in Figures 31 and 32 for tank 1 and 2, respectively. The data points for both tanks were very scattered, and therefore, no statistically differences between the tanks were found ($p>0.05$). SGR values declined with weight increase. The function $f(x)=a*x+b$ explained the data with 73.1% accuracy for tank 1, and 70.2% for tank 2. As mentioned before, the fish grew faster after the first grading (data points after the dashed line). The mean feed intake expressed in %BW (percent body weight) for tank 1 and 2 amounted to 1.4% (min 0.6%, max 1.9%).

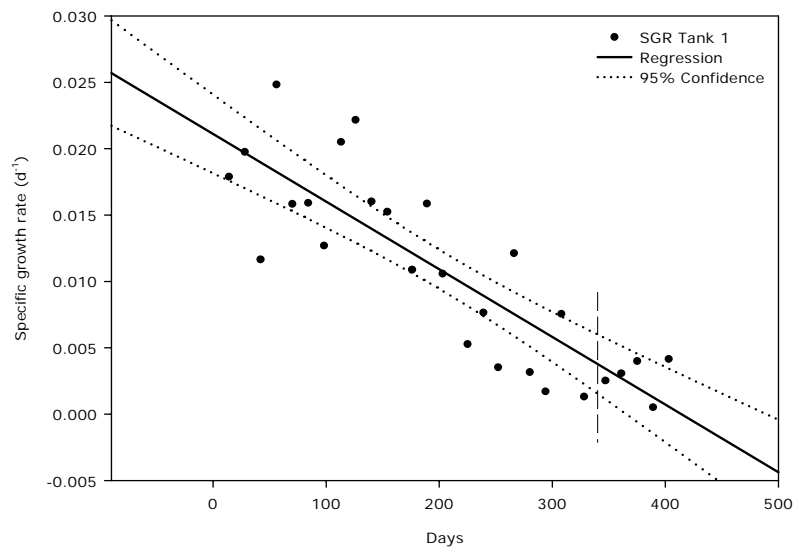


Fig. 31. Specific growth rate (SGR) per day for tank 1. The dashed vertical line shows the first grading (t_{328}). The function (bold line) is expressed by the curve following $f(x)=a*x+b$ ($a=-5.1 \times 10^{-5}$; $b=0.0211$; $R^2=0.73$). Dotted lines show the 95% confidence interval.

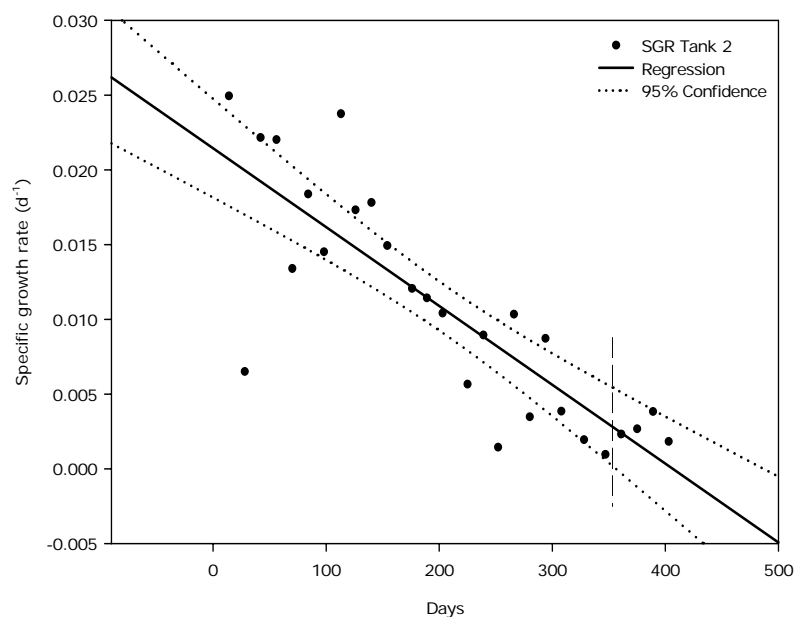


Fig. 32. Specific growth rate (SGR) per day for tank 2. The dashed vertical line shows the first grading (t_{328}). The function (bold line) is expressed by the curve following $f(x)=a*x+b$ ($a=-5.3 \times 10^{-5}$; $b=0.0214$; $R^2=0.70$). Dotted lines show the 95% confidence interval.

Figure 33 shows the increment of fish biomass and density in the system. Density expressed in $\text{kg}\cdot\text{m}^{-3}$ was calculated for the total water volume in the system in contrary to standard density determination, in which only tank volume is considered. The lowest density in the system was at the beginning of the experiment and amounted to $0.6 \text{ kg}\cdot\text{m}^{-3}$. The maximum density of $27.9 \text{ kg}\cdot\text{m}^{-3}$ was reached on day t_{308} with a total biomass of 93.3 kg fish. During the last 130 days of the experiments (from day t_{309} until

day t_{437}), density decreased because of mortalities and fish harvested for laboratory analysis.

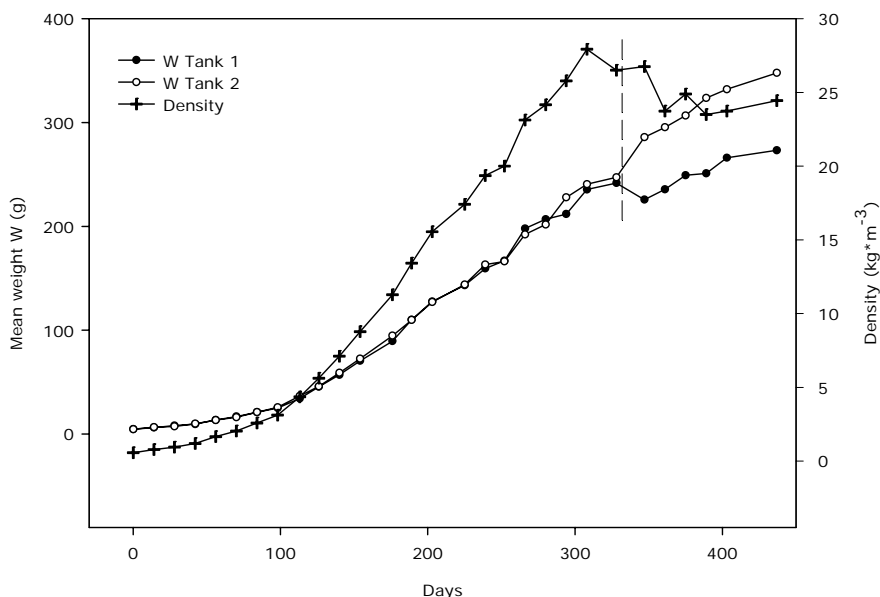


Fig. 33. Increment of fish biomass as mean weight (g) for tank 1 and 2 (primary y-axis) and density expressed in $\text{kg}\cdot\text{m}^{-3}$ (secondary y-axis) in the system from t_0 until t_{437} . Density was calculated for the whole water volume in the system (3.34 m^3). The dashed vertical line represents the first grading (t_{328}).

3.1.3 Feeding and feed amount

The feeding of the fish was carried under a commercial aquacultural scenario *i.e.* maximum feeding amount for accelerated growth. The amount of feed offered was calculated for every test period, according to fish biomass in each tank and water temperature, following the feeding table (Tab. 6) presented in chapter 3.5. For several days the feeding was cancelled or aborted because of inappropriate farming conditions (technical problems, water quality), some other interruptions occurred because of the planned experiments. Figure 35 shows the increment in total amount of delivered feed for the entire study period

The amount of feed was distributed evenly on the moving feeder belt to have a constant delivery to the tank over 8-10 hours a day. Technical problems were occasionally encountered because of a malfunctioning of the mechanism that moves the belt (no feed fed at all) or because of water dampness between belt and feeder, not allowing the belt to deliver the feed as planned. Water splashed by fish during the feeding frenzy close to the feeders wetted the feed. This problem was later solved by using a synthetic sponge

(pore size approximately 0.5 mm) between feeder bottom and feeder belt, capturing the splash water.

Since high energy, extruded rainbow trout diets were used (fat content 22%), changes in the formation and quality of the foam in the foam fractionator was observed. The reduction of foaming occurred mainly after the daily morning meal and disappeared during the day. The effect was not observed every day but became more often with the increase in feed amount. Unfortunately it was impossible to have access to special formulated diets for sea bass, with less fat content.

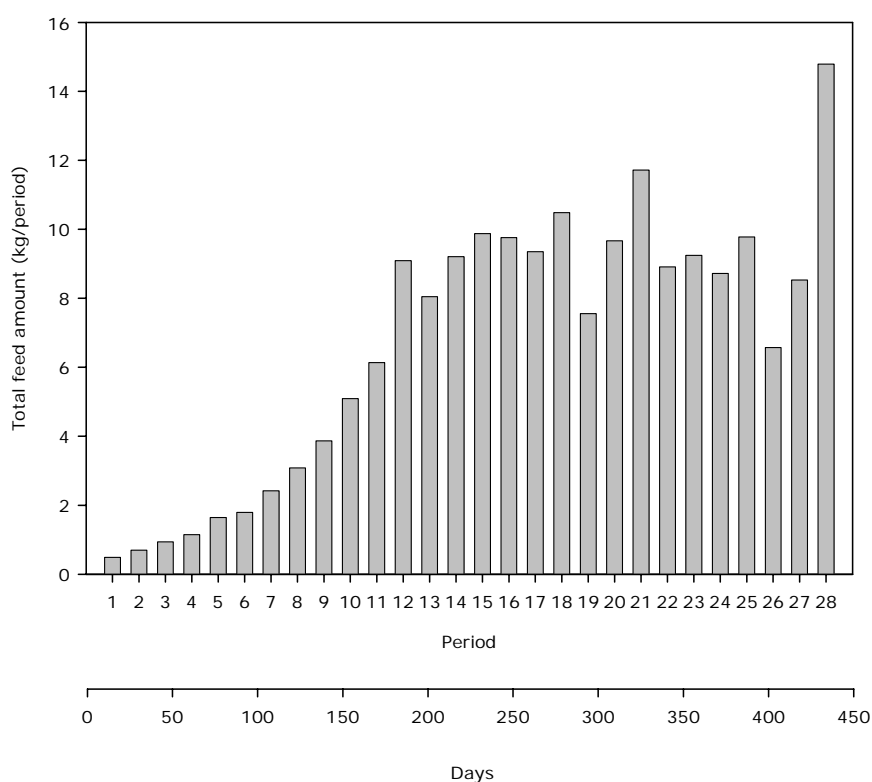


Fig. 34. Amount of feed (kg) offered per period to both fish tanks during the experiment. X-axis shows the time intervals in periods (28) and days (437). The periods lasted between 13 - 15 days with the exception of periods 12 and 20 (22 days), period 22 (20 days), period 23 (19 days), and period 28 (34 days).

Feed pellet size was changed four times during the course of the trial, based on increasing fish weight. The size change was done gradually. Table 11 shows the percentage of the two feed sizes offered during the transitional period in a stepwise manner (each step usually lasting for two days).

Tab. 11. Percent composition of the feed fed during a feed size change. Each feed amount was given for two days *i.e.* it took 6 days for a complete feed size change (G=granulated feed).

Days	Feed size (mm)				
	1.2G	1.5	3	4.5	6
t ₇₇ -t ₇₈	75	25			
t ₇₉ -t ₈₀	50	50			
t ₈₁ -t ₈₂	25	75			
t ₁₃₃ -t ₁₃₄		75	25		
t ₁₃₅ -t ₁₃₆		50	50		
t ₁₃₇ -t ₁₃₈		25	75		
t ₂₇₄ -t ₂₇₅			75	25	
t ₂₇₆ -t ₂₇₇			50	50	
t ₂₇₈ -t ₂₇₉			25	75	
t ₄₀₅ -t ₄₀₆				75	25
t ₄₀₇ -t ₄₀₈				50	50
t ₄₀₉ -t ₄₁₀				25	75

3.1.4 Feed conversion ratio

Feed conversion ratio (FCR) was found to be comparable between tank 1 (mean 1.4 ± 0.5 , min 0.8, max 2.9) and tank 2 (mean 1.3 ± 0.6 , min 0.8, max 3.0). The scattering of the data were considerable though. The FCR at the beginning of the experiments amounted to values around and even below 1, which was found to be a good result but unusual for fingerlings. Normally, it is expected to obtain higher FCR's (1.3 – 1.5) with small fish. Feed intake should increase with fish size and FCR's should decline to values around 1 to 1.2. After fish reached a mean weight of about 140 g (t₂₃₉) feeding didn't take place every day. FCR's rose up to values greater than 1.5. High mortalities did also influence the conversion index, however, adjustments in feeding rate due to mortality loss were not made at that time. Commercial fish farmers normally correct to feeding rates for the common FCR.

3.1.5 Condition factor

The results on the condition factor are presented in Table 12 for both tank 1 and 2. The first initial low value can be attributed to fish fingerlings still recovering from the transportation stress before stocking, while also being gradually adjusted to appropriate feeding levels. The subsequent low extreme values remain unexplained. However, the potential of having a biased sample cannot be excluded. The data varied little and are not statistically significant between periods and between tank 1 and 2 though ($p > 0.05$).

Comparing the data between periods with low water temperature (16°C, periods 1-5) and the period with water temperature at 23°C (periods 6-28) no significant difference in

Results

condition factor was found. Before sorting the fish, the condition factor in both tanks amounted to values between 1.3 and 1.4. After grading the condition factors declined slightly to values between 1.2 and 1.3. Statistically, however, re-conditioned tanks did not differ significantly with values before grading ($p>0.05$). It seems that grading the fish did not affect the condition factor as much as was expected.

Tab. 12. Condition factors determined for tank 1 and 2, for the periods before (study periods 1 to 22, day's t_{14} until t_{322}) and after grading (study periods 23 to 28, day's t_{347} until t_{437}). Averaged values \pm S.D. were calculated for each bi-weekly study period. The number of determinations for each period amounted to 20 individuals.

Sampling day	Study period	Condition factor Tank 1	Condition factor Tank 2
t_{14}	1	1.1 ± 0.1	1.1 ± 0.1
t_{28}	2	1.3 ± 0.1	1.2 ± 0.1
t_{42}	3	1.2 ± 0.1	1.3 ± 0.1
t_{56}	4	1.2 ± 0.1	1.2 ± 0.1
t_{70}	5	1.3 ± 0.2	1.3 ± 0.1
t_{84}	6	1.1 ± 0.1	1.3 ± 0.1
t_{98}	7	1.3 ± 0.1	1.3 ± 0.1
t_{113}	8	1.2 ± 0.1	1.2 ± 0.1
t_{126}	9	1.3 ± 0.1	1.2 ± 0.1
t_{140}	10	1.3 ± 0.1	1.3 ± 0.1
t_{154}	11	1.3 ± 0.1	1.2 ± 0.1
t_{176}	12	1.3 ± 0.1	1.3 ± 0.1
t_{189}	13	1.3 ± 0.1	1.3 ± 0.1
t_{203}	14	1.4 ± 0.1	1.4 ± 0.1
t_{225}	15	1.4 ± 0.1	1.4 ± 0.1
t_{239}	16	1.3 ± 0.1	1.3 ± 0.1
t_{252}	17	1.3 ± 0.1	1.3 ± 0.1
t_{266}	18	1.3 ± 0.2	1.4 ± 0.1
t_{280}	19	1.4 ± 0.2	1.3 ± 0.1
t_{294}	20	1.3 ± 0.1	1.3 ± 0.1
t_{308}	21	1.3 ± 0.1	1.4 ± 0.1
t_{322}	22	1.3 ± 0.3	1.4 ± 0.1
After grading		Tank 1 fish <300 g	Tank 2 fish >300 g
t_{347}	23	1.3 ± 0.1	1.3 ± 0.1
t_{361}	24	1.2 ± 0.1	1.3 ± 0.1
t_{375}	25	1.2 ± 0.1	1.3 ± 0.1
t_{389}	26	1.2 ± 0.2	1.3 ± 0.1
t_{403}	27	1.3 ± 0.1	1.2 ± 0.2
t_{437}	28	1.3 ± 0.1	1.2 ± 0.1

3.1.6 Mortality

Mortalities in the system are reported in Table 13. The number of dead fish removed from the system was low during the first 330 days of cultivation. Some dead individuals were normally found a few hours (4-12 h) after handling the fish for biomass determination. The mortalities in tank 1 assigned to period 22 (n=27) was due to an over dosage of anaesthetic given for weighing purposes. In tank 2 on day t_{376} mortality was higher (n=52). The reasons for this mortality remain largely uncertain. Fish were examined for external and internal pathological features. Skin and gill smears were taken. Scales were found to be intact. Spotted bleeding was found in some areas of the belly and the caudal fin of all specimens. The rays of the pelvic and anal fins were reddish (assuming internal bleeding). All fish had vaulted opercula (indicating asphyxia). No macroscopically gill damages were found. Around the liver, dense fat clusters were observed. The mucous membrane inside the body cavity appeared moist and shiny. No sign of peritonitis and no sticking organs were seen. The smears taken from the skin tissue showed damaged cells suggesting various stages of dermatitis. The smears from the gills showed reddish lamellae with light bleeding spots. Disruptions of cells from the mucous membrane were also observed. The true cause is unknown. Certainly their may be cumulative stress factors involved over a longer time horizon not investigated here.

Tab. 13. Mortalities during the experimentation, indicating number of fish, day of occurrence, and percentage of the total, for tank 1 and 2.

Tank 1			Tank 2		
Day	Number	% of the total	Day	Number	% of the total
t_{85}	1	0.5	t_{114}	1	0.5
t_{127}	1	0.5	t_{177}	1	0.5
t_{155}	1	0.5	t_{204}	2	1.0
t_{204}	1	0.5	t_{226}	3	1.5
t_{226}	1	0.5	t_{253}	5	2.5
t_{281}	3	1.5	t_{267}	1	0.5
t_{309}	27	13.6	t_{309}	3	1.6
t_{329}	2	1.0	t_{323}	8	4.8
t_{348}	6	3.1	t_{376}	52	32.3
t_{376}	17	9.1	t_{390}	21	17.5
t_{390}	2	1.3	t_{404}	1	0.8
t_{404}	1	0.7			

3.1.7 Fish yield and quality

Culturing sea bass in conventional recirculation systems may affect product quality. The present laboratory analyses to evaluate the fish quality, covers very basic non-standard criteria and are presented in Table 14.

Total number of bacteria cultivated expressed as colony forming unit per gram (CFU*g⁻¹) found in the fish flesh was 71,000*g⁻¹, 29 % less than the lower acceptable limit (100,000*g⁻¹). *Enterobacteriaceae* and *Escherichia coli* were found a concentrations less than 10 cells per gram (n*g⁻¹). The analysis for *Listeria monocytogenes* was negative.

Tab. 14. Results of non-standard laboratory analysis for: fat and protein content, total volatile basic nitrogen (TVB-N), salt content, total bacteria counts expressed in colony forming units (CFU n*g⁻¹), *Enterobacteriaceae*, and *Escherichia coli* expressed in number per gram (n*g⁻¹), and *Listeria monocytogenes* presence in sea bass fillet cultivated in the RAS.

Fat (%)	Protein (%)	Phosphate (mg*100g ⁻¹)	TVB-N (mg*100g ⁻¹)	Salt (%)
4.0	20.7	528.0	22.0	0.14
CFU (n*g ⁻¹)			<i>Listeria monocytogenes</i>	
Total	<i>Enterobacteriaceae</i>	<i>E. coli</i>	Presence	
71,000	<10	<10	negative	

Weights of fish and fillet were determined (Tab. 15). Fillet yield in percentage of the total body weight was determined. The belly flaps were cut-off and not included in the fillets. Nearly 35% of the body was obtained as flesh for consumption. Unfortunately, the "V" cut of the fillet (Fig. 34) was incomparable with other standard fish processing procedures known from other aquaculture and fish processing activities, particularly since European sea-bass from aquacultural production is sold as whole fish on international markets.

The results of the sensory assessment are detailed in Table 16. According to the criteria used, the maximum rating (at a scale from 0 to 9) was achieved for every category: raw appearance (colour and shape), raw odour and texture, and taste (steamed at 70°C for 15 min).

Tab. 15. Total fish weight (g), fillet weight (both sides, (g)), and fillet yield (%) for European sea bass (n=17). The fish were handled using the so called "V" cut (see Figure 42).

Sample number	Fish weight (g)	Fillet weight (g)	Yield (%)
1	448	159	35.5
2	411	129	33.4
3	430	155	36.0
4	460	144	31.3
5	409	152	37.2
6	390	134	34.4
7	413	139	33.7
8	401	128	31.9
9	478	163	34.1
10	420	131	31.2
11	410	144	35.1
12	458	162	35.4
13	377	126	33.4
14	505	184	36.4
15	422	142	33.6
16	461	158	34.3
17	410	152	37.1
Mean \pm S.D.	429.6 \pm 33.7	147.2 \pm 15.6	34.4 \pm 1.8

Tab. 16. Results from the sensory assessment for fish products using the Karlsruher Schema. The grade 9 corresponds to an excellent quality.

	Appearance (colour)	Appearance (shape)	Odour	Texture	Taste
Raw	9	9	9	9	-
Steamed	9	9	9	9	9
Remarks	Exceptional appealing, bright, natural colour, typical for the flesh.	Perfect preservation of shape, firm, and undamaged shape.	Exceptional delicate, distinct, and characteristic odour.	Exceptional good, characteristically texture, tough, succulent tissue and very tender.	Exceptional delicate, distinct, and characteristic taste.



Fig. 34. European sea bass *Dicentrarchus labrax* "V" fillets, with skin. The fish were not eviscerated.

3.2 Water physical characteristics in the culture system

The physical characteristics of the water in the fish tanks (temperature ($^{\circ}\text{C}$), salinity (psu: practical salinity units), oxygen concentration ($\text{mg}\cdot\text{L}^{-1}$), and pH) were measured twice a day in both tanks, approximately at 9:00 and 18:00 hours, between t_0 and t_{431} . From t_{437} until t_{537} the parameters were measured only once a day at 9:00 o'clock.

Make-up water was added to the RAS to renew losses due to system's maintenance and samples for dissolved and particulate nutrient determinations, and to maintain flow. The particular low head design of the RAS demand a minimum water level inside the fish tanks. This level was given by the distance from the ground level to the inlet of the tanks (~ 1.58 m). In average a rate of $0.04 \text{ m}^3\cdot\text{d}^{-1}$ was added to the system, representing $1.2 \text{ \%}\cdot\text{d}^{-1}$.

3.2.1 Temperature and salinity

The system was run in a cold water and low salinity state between day's t_0 and t_{98} . The temperature averaged 17.2°C and 17.1°C in tank 1 and 2, respectively. Average salinity between t_0 and t_{84} was 15.8 psu in both tanks. After this initial period, temperature was raised to levels varying between 22.3°C and 22.2°C , and salinity between 22.6 psu and 22.7 psu for tank 1 and tank 2, respectively.

Daily average temperature (Fig. 35) and salinities (Fig. 36) are graphically presented for tank 1 and 2.

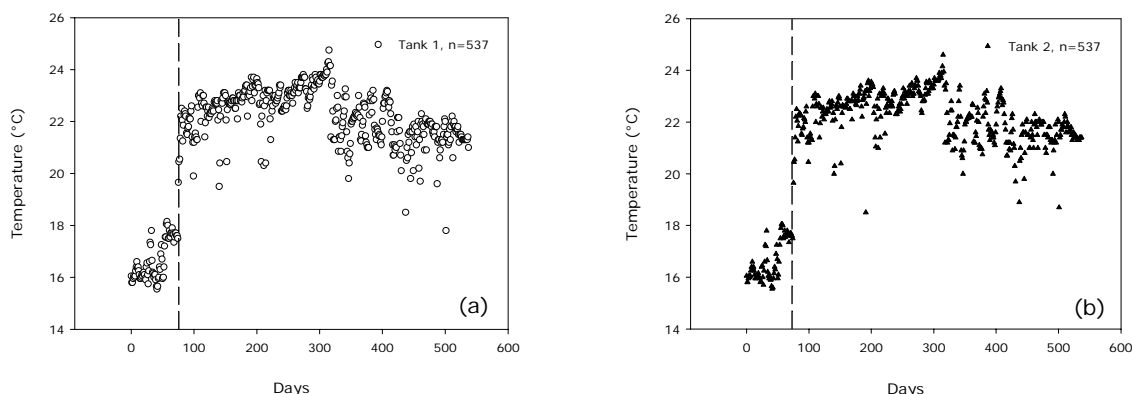


Fig. 35. Daily averaged temperature ($^{\circ}\text{C}$) determined at 9:00 and 18:00 h, for tank 1 (a) and 2 (b). Dashed line represents the designed change in temperature level (n =total number of determinations).

Temperature fluctuations differed minimally between the two tanks but were noticeable during winter time (between day t_{415} and t_{550}). Room temperature was conditioned (20°C) but somewhat dependant on external weather conditions. Figure 35 depicts the daily temperature values for the entire study period indicating a gradual but continuous and subtle increase in temperature (about 1°C) until day t_{300} , reflecting the influence of additional heaters to cope with winter conditions on temperature control. Therefore, these additional heat sources were removed, leading to somewhat larger daily fluctuations of temperature, despite operating in a so-called temperature controlled room.

As can be seen in Figure 36, it is obviously difficult to keep salinity constant, despite the relative comparability of the mean values. Fluctuations were observed because of evaporation and the frequent but partial renewal of water due to: (a) maintenance needs, (b) unexpected events requiring larger volumes of exchange than usual, and (c) fish handling procedures requiring extra water transfer during sorting and growth determinations.

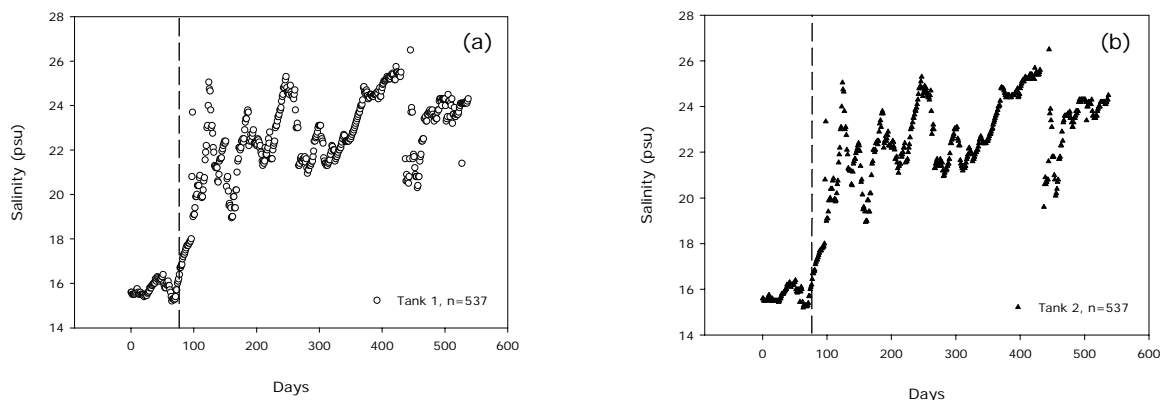


Fig. 36. Daily average salinity determined at 9:00 and 18:00 h, in psu for tank 1 (a) and 2 (b). Dashed line represents the designed change in temperature levels (n =total number of determinations).

3.2.2 Dissolved oxygen concentration

Dissolved oxygen concentrations were determined and are presented in Figure 37, for both tanks. Maximal values were observed between t_0 and t_{84} (dashed line) due to the lower water temperature. The mean concentration over this initial experimental period was $9.1 \text{ mg}\cdot\text{L}^{-1}$ for tank 1 and $9.3 \text{ mg}\cdot\text{L}^{-1}$ for tank 2. From t_{85} onwards until t_{537} , the dissolved oxygen concentration averaged $7.2 \text{ mg}\cdot\text{L}^{-1}$ for tank 1 and $7.4 \text{ mg}\cdot\text{L}^{-1}$ for tank 2.

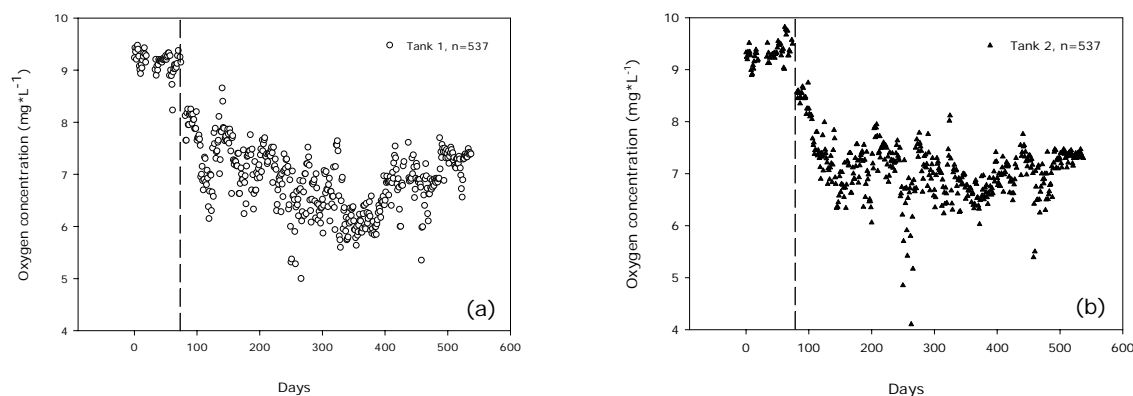


Fig. 37. Daily average dissolved oxygen concentration ($\text{mg}\cdot\text{L}^{-1}$) determined at 9:00 and 18:00 h in tank 1 (a) and 2 (b). Dashed line represents the gradually change in temperature (n =total number of determinations).

Figure 37 shows the daily oxygen concentration for the study period indicating the gradual decrease in oxygen concentration (about $2 \text{ mg}\cdot\text{L}^{-1}$) until day t_{400} , reflecting the influence of the temperature fluctuations described before, affecting the solubility of oxygen in the water but also due to increased oxygen consumption by the growing fish. Continuous aeration was by ceramic diffusers, one inside each tank.

3.2.3 pH in the culture system

Daily averages of pH values are presented in Figure 33, for tank 1 and 2. Mean pH for both tanks was about 7.2, however, the data have to be assessed on the time scale as the effect of the pH value on other water quality parameters is crucial. Maximum and minimum values reached in tank 1 up to 8.6 and 5.9, and in tank 2 around 9.0 and 5.9, respectively. After the change to a higher operational temperature, the pH dropped considerably until the adjustments of the buffer additions were made. Because of the continues daily addition, pH values were maintained above 7.0 at all times with little daily fluctuations but a slight general upward trend towards the end of the study period.

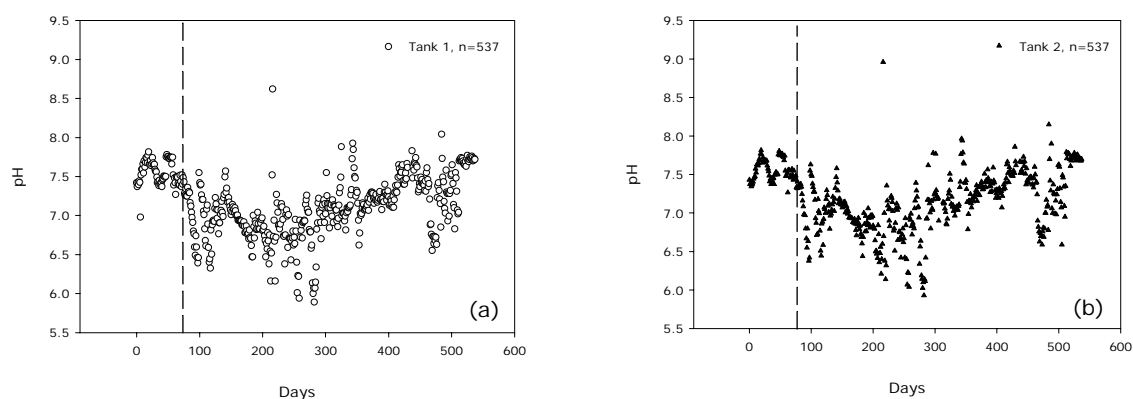


Fig. 38. Daily average pH value in tank 1 (a) and 2 (b), determined at 9:00 and 18:00 h. Dashed line represents the gradually change in temperature (n =total number of determinations).

Oxidation reduction potential (ORP in mV, or Redox-potential) and pH were separately measured inside the foam fractionator. Figure 39 shows the daily mean values for both parameters, from t_0 until t_{537} . On average, the ORP was around 270 mV and the pH was about 7.3. Dotted lines in Figure 39 show the set-point values for the automatic turn-off-turn-on system for the ozone generator (ORP=350 mV) and the set-point values for the automatic turn-off-turn-on system for the CaO *i.e.* Ca(OH)₂ dosage (pH=7.2).

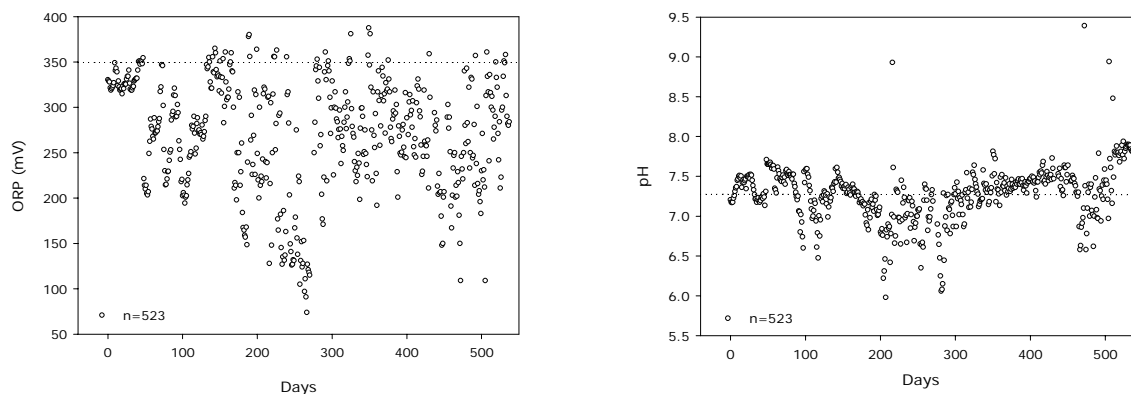


Fig. 39. Daily average (9:00 and 18:00 h) oxidation reduction potential (ORP) in mV, and pH value in the foam fractionator, from t_0 until t_{537} . Dotted lines show the turn-off-on set-point of the ozone generator (ORP=350 mV) and the set-point value of pH=7.2 for the CaO (Ca(OH)₂) dosage.

3.3 Dissolved nutrients concentrations in the culture system

The trend of dissolved nutrient concentrations in the culture water during the study period between t_0 and t_{428} was monitored for total ammonia-nitrogen (TAN), nitrite-nitrogen (NO₂⁻-N), nitrate nitrogen (NO₃⁻-N), and phosphate (PO₄⁻³). Results are graphically presented for the experimental period between days t_0 and t_{428} .

3.3.1 Water renewal (exchange)

No system can operate without any water exchange (renewal). The needs for replacement originates from evaporation loss to accidental spills as well as regular splash water losses during fish feeding and handling, and finally cleaning and sampling for water chemistry. Table 17 shows the dates and the volumes that were periodically renewed. This information on time and volume exchange (renewed) was crucial for the calculations and interpretations of the sometimes abrupt changes occurring in nutrient concentrations, especially for TAN, NO₂⁻-N, and NO₃⁻-N in the effluent of the biofilter, and NO₃⁻-N and PO₄⁻³ concentrations in the entire system. The time interval for partial renew of system's water volumes are irregular and mostly determined by unnecessary events,

while also occasionally demanded by the investigational protocol (e.g. weighing and sorting of the fish and frequent sampling for water quality and suspended solids during intensive measuring periods). For common routine procedures, water renewal volumes averaged around 400 L, equivalent to 11.8 % of the total system volume.

As can be seen from Table 17, the routine water renewal of the system was roughly on a weekly basis. Some events with higher exchange volumes reflect accidental broken pipes (water loss) or the need of extra release of accumulated solids from the biofilter. In total there were eight such non-routine occasions with some immediate short-term influences on the system water quality. Overall, during the entire study period, the total volume renewed accounts for 17.3 m³ which is equivalent to about 5-6 total system volumes. Considering the duration of the experiment, however, this accounted for only 1.2 % of the system volume per day, including replacement of evaporation losses which usually account for 0.2% to 0.3% (based on experiments with in indoor systems at high air humidity). The percentage variability of renewal per operational interval is also indicated in Table 17.

Tab. 17. Time and volume of water exchange (renewal) during the experimental period for suspended solids load in a high-density fish culture recirculating system. The experiment lasted for 437 days. Time is indicated as days from start (t=0) to the end (t=437) of the study. Water volumes are expressed in litres (L) and in percent of system volume.

Day	Vol. (L)	(%)	Day	Vol. (L)	(%)	Day	Vol. (L)	(%)	Day	Vol. (L)	(%)
t ₆₁	700	21.0	t ₁₅₃	240	7.2	t ₂₂₃	480	14.4	t ₂₈₁	500	14.9
t ₈₂	800	24.0	t ₁₅₉	12	0.4	t ₂₂₈	240	7.2	t ₂₈₇	240	7.2
t ₉₄	240	7.2	t ₁₆₇	480	14.4	t ₂₃₇	240	7.2	t ₂₉₀	240	7.2
t ₁₀₁	800	24.0	t ₁₇₀	80	2.4	t ₂₄₆	240	7.2	t ₂₉₃	240	7.2
t ₁₀₈	240	7.2	t ₁₈₀	300	9.0	t ₂₄₈	500	14.9	t ₃₀₅	1000	29.6
t ₁₂₂	240	7.2	t ₁₈₄	240	7.2	t ₂₅₀	240	7.2	t ₃₀₈	240	7.2
t ₁₂₄	600	18.0	t ₁₈₈	240	7.2	t ₂₆₀	240	7.2	t ₃₃₈	240	7.2
t ₁₂₈	40	1.2	t ₁₉₁	240	7.2	t ₂₆₄	240	7.2	t ₃₅₇	240	7.2
t ₁₃₅	480	14.4	t ₁₉₈	480	14.4	t ₂₆₉	300	9.0	t ₃₅₉	240	7.2
t ₁₄₆	240	7.2	t ₂₀₆	240	7.2	t ₂₇₄	240	7.2	t ₃₆₄	1500	44.8
t ₁₅₁	40	1.2	t ₂₁₂	240	7.2	t ₂₇₉	240	7.2	t ₄₀₀	240	7.2

3.3.2 Water quality in the outlet of the swirl separator

Total ammonia-nitrogen (TAN) and nitrite-nitrogen (NO₂⁻-N) concentrations in the outlet of the swirl separator are presented in Figure 40. The swirl separator receives the mixed water effluent from both fish tanks. TAN concentration over 428 days averaged 1.0 mg*L⁻¹ (max. 3.6 mg*L⁻¹ and min. 0.04 mg*L⁻¹). Nitrite-nitrogen concentration averaged 0.2 mg*L⁻¹ (max. 0.7 mg*L⁻¹ and min. 0.01 mg*L⁻¹).

Relative high TAN concentrations around $1.5 \text{ mg}\cdot\text{L}^{-1}$ were found at the beginning of the trial due to the natural mineralization process in the biofilter and the instabilities during start-up phase. During the two preparatory weeks before day zero (t_0) the system was running without fish load and no feed was added. When fish were stocked into the tanks an immediate high peak of total ammonia concentration (Fig. 40, days t_0 to t_{25}) appeared with large daily fluctuations. After that period, the biofilter apparently gained efficiency in ammonia oxidation, leading to a subsequent minimum concentration which tended to increase slowly with time as fish biomass was growing. Nitrite-nitrogen peaks were found to appear about 14 days after the TAN highest concentrations were measured during the start-up phase, but remained comparatively low (around $0.6 \text{ mg}\cdot\text{L}^{-1}$).

The oxidation efficiency of the biofilter was considered poor during this initial phase, although there seems to be from time to time a high change in concentrations and with time also a slight upward trend in the overall ammonia level. The results confirm that biofiltration needs a long start-up period to new levels of nutrient and biomass loads.

High total ammonia peaks were also occasionally observed after this initial start-up phase. These were always found related to extraordinary events. On day t_{94} for example, two 50 cm air stones were installed inside the biofilter (between the filter media) to improve oxygen concentration near and around the bacterial biofilm. This caused the release of clogged particulate matter layers firmly attached to the fixed biofilter media. This matter partly leads to reduced flow and occasionally clogging the space between biofilter substrates walls. Aeration mechanically released these thick plaques which were then distributed throughout the system, broken into small fractions and then contributing temporarily to high turbidity in the fish tanks causing temporarily very low water quality. As a result, water pH and oxygen concentrations dropped rapidly. Feeding was cancelled. It was necessary to clean the biofilter media and the biofilter basin with the subsequent refill of 0.24 m^3 of seawater to maintain system hydraulic. By washing and rinsing several times the filter media, the bacteria colonies on the plastic surface were apparently affected. The consequences of this impasse were observed a few days later. TAN concentrations rose to levels between 1.8 and $3.1 \text{ mg}\cdot\text{L}^{-1}$ (Fig. 40, t_{100}), indicating a decline in the efficiency of the biofilter to oxidise ammonia. The removal of NO_2^- -N was kept in normal levels. The measured concentrations stayed around 0.2 and $0.3 \text{ mg}\cdot\text{L}^{-1}$.

Continued analysis of these events revealed that ammonia concentrations between days t_{274} and t_{281} rose up to values above $3.0 \text{ mg}\cdot\text{L}^{-1}$. This extraordinary increase was related to the change in the feeding regime. From day t_0 until day t_{266} the feed was delivered

continuously by the belt feeder over 12 h per day. After determining the fish biomass on day t_{268} , the fish were in good condition (average weight above 250 g), and for this size class the feeding regime was changed to two rations a day each spreading over four hours (09:00 to 13:00 hrs; and 17:00 to 21:00 hrs) using the belt feeder; By changing the feeding regime, the fish metabolism as well as excretory products and their daily rhythm changed. The immediate consequences of this change in feed management was clearly observed and reflected by the subsequently poor performance of the nitrification process in the biofilter.

Following the interpretation of TAN and NO_2^- -N concentrations presented in Figure 40, on day t_{282} the fish biomass was determined again resulting in unusual water consumption (0.5 m^3). The subsequent water replacement explains the decline in the TAN and NO_2^- -N concentrations on day t_{283} .

Towards the end of this part of the experiments, TAN and NO_2^- -N concentrations increased again from day t_{334} to levels above $2.0 \text{ mg} \cdot \text{L}^{-1}$, and dropped around day t_{378} to levels below $2.0 \text{ mg} \cdot \text{L}^{-1}$ and stayed above $1.5 \text{ mg} \cdot \text{L}^{-1}$ until the end of this experiment (t_{428}). On day t_{334} the fish biomass was determined. This exercise was a regular event (every 14 days), the system became more sensible in time and minimal changes in the water parameters caused by external influence were reflected as causing higher variations in the overall data on systems performance, with marked fluctuations of nutrient concentrations over the next few days. This period of instability was taken as signal that the system may approach carrying capacity limits. Also during this period the $\text{Ca}(\text{OH})_2$ dosing system showed some operational inconsistencies.

Overdosing occurred a few times (*e.g.* day t_{345}); while dose delivery failed at other times (*e.g.* day t_{352}). Low pH values (below 7.2) were noted over a period of about 18 days. During the same period the TAN concentration increased to values above $2.0 \text{ mg} \cdot \text{L}^{-1}$. Once lower pH values (no $\text{Ca}(\text{OH})_2$ dosage) occurred, the recovery periods lasted for a longer time despite proper dosing than the time during which slight overdosing when comparatively high pH values were reached. This is not surprising because of fish respiration and continued other demands on the bio-carbonate system. During the last 17 days of this experiment, the pH value increased and stayed above 7.4 while the TAN concentration maintained values between 1.5 and $2.0 \text{ mg} \cdot \text{L}^{-1}$.

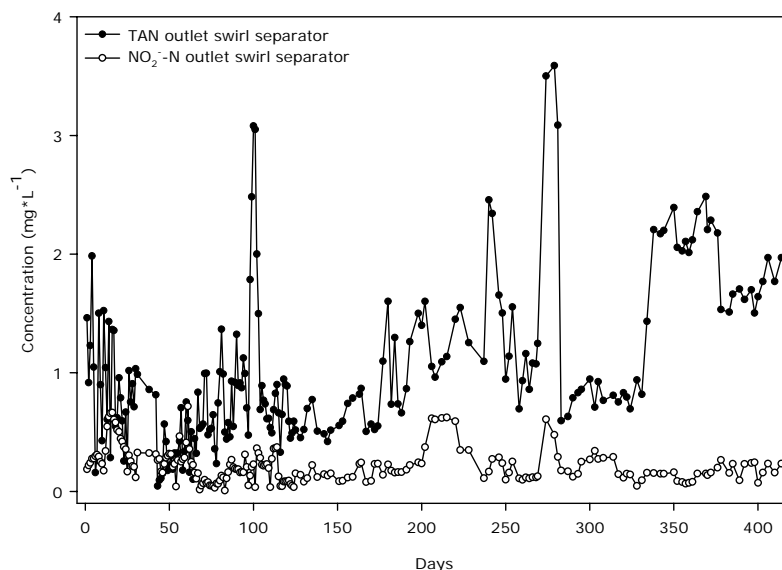


Fig. 40. Total ammonia-nitrogen (TAN) and nitrite-nitrogen (NO_2^- -N) concentrations ($\text{mg}\cdot\text{L}^{-1}$) in the outlet water of the swirl separator from day t_0 until day t_{428} ($n=213$). The swirl separator received the mixed effluent water from both fish tanks.

Figure 41 presents the nitrate-nitrogen (NO_3^- -N) and phosphate (PO_4^{-3}) concentrations in the outlet of the swirl separator for the entire study period. The trend on the nitrate-nitrogen accumulation in the system is obvious and can easily be explained. No denitrification unit was running during this part of the experiments and because of the system design, little areas with anoxic conditions existed to provide conditions for denitrifiers. The accumulation trend was counter-acted most effectively when a substantial amount of water was renewed (see Tab. 17). The same trends were observed for the phosphate concentration.

As previously reported for other parameters, NO_3^- -N and PO_4^{-3} concentrations also rose after the events explained for day t_{268} (feed regime change), but decreased after the renewal of water done on day t_{305} . The increment observed after day t_{268} is of uncertain origin but could be explained in retrospect by a high NO_3^- -N content in the water supply source. Although unlikely, a partial denitrification process cannot completely be excluded. So called "unintended denitrification" may occur in every small spot in the system that became temporarily anaerobic.

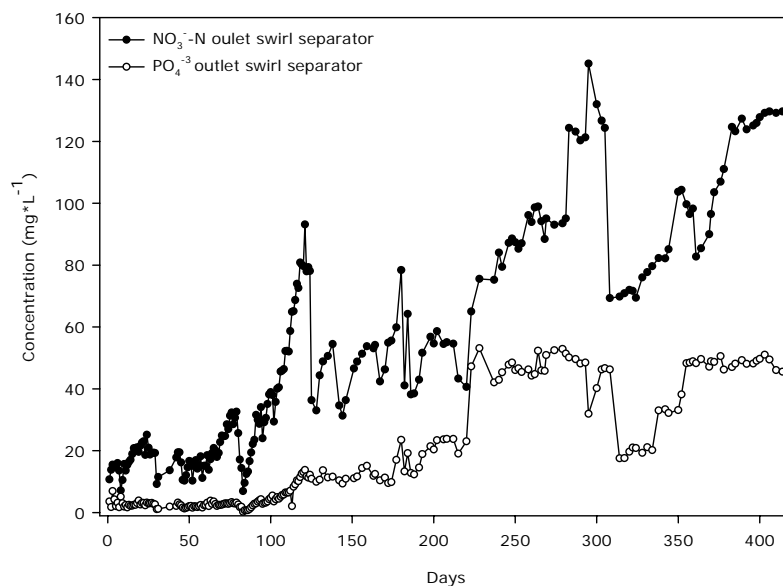


Fig. 41. Nitrate-nitrogen (NO_3^- -N) and phosphate (PO_4^{3-}) concentration ($\text{mg}\cdot\text{L}^{-1}$) in the outlet water of the swirl separator receiving the effluent of two fish tanks, from day t_0 until day t_{428} ($n=213$).

3.3.3 Water quality in the inlet and outlet of the biofilter (nitrification)

As described in chapter 2.2, the water leaving the swirl separator is supplied to the biofilter. Figure 45 shows the TAN concentrations in the inlet and outlet of the biofilter. Figure 42 compares inlet and outlet TAN concentrations, indicating the oxidation performance of that unit for TAN.

TAN concentrations in the outlet of the biofilter were on average $1.2 \text{ mg}\cdot\text{L}^{-1}$, with a maximum value of $2.9 \text{ mg}\cdot\text{L}^{-1}$ and a minimum of $0.4 \text{ mg}\cdot\text{L}^{-1}$. As described in 3.3.1 the peaks observed between days t_{274} and t_{281} were unexpected, but can be explained as a consequence of the maintenance work on the foam fractionators. Feeding was cancelled at that time to reduce metabolic excretion. However, fish were constantly disturbed during repair and high swimming activity and spontaneous disruption of the schooling behaviour observed increased the metabolism, thereby partially cancelling the no-feeding effect.

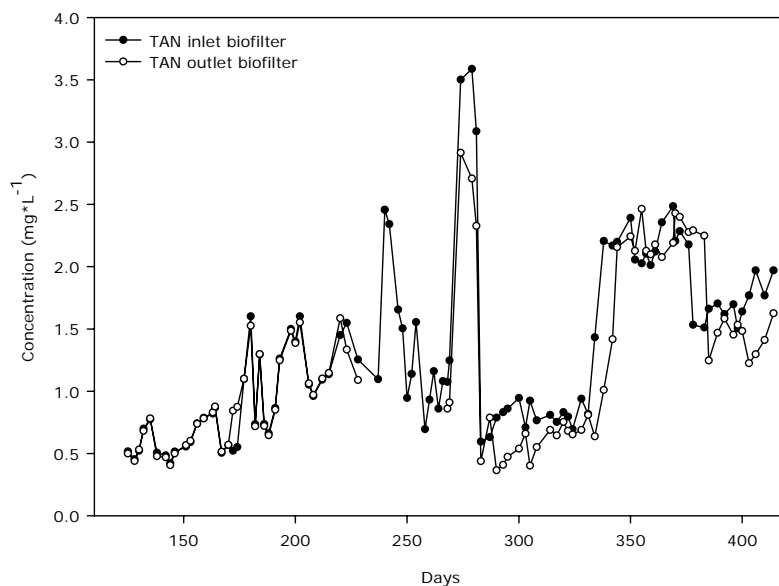


Fig. 42. Total ammonia nitrogen (TAN) concentrations ($\text{mg}\cdot\text{L}^{-1}$) in the outlet and inlet water of the biofilter water (by-pass), receiving approximately 2/5 of the fish tank effluent. Data plotted considered between day t_{125} and day t_{428} ($n=98$) from the study period.

Comparing the TAN concentrations measured in the in and outlet of the biofilter (Fig. 43), there was a long phase during which no quantifiable differences were noted between day t_{125} and day t_{228} . From day t_{268} onward until t_{428} , TAN concentrations leaving the biofilter were on average $0.24 \text{ mg}\cdot\text{L}^{-1}$ lower than the inlet concentrations. Extreme values observed represent maximum oxidation levels of $+1.2 \text{ mg}\cdot\text{L}^{-1}$ and accumulation levels of $-0.76 \text{ mg}\cdot\text{L}^{-1}$ TAN during a single pass through the unit.

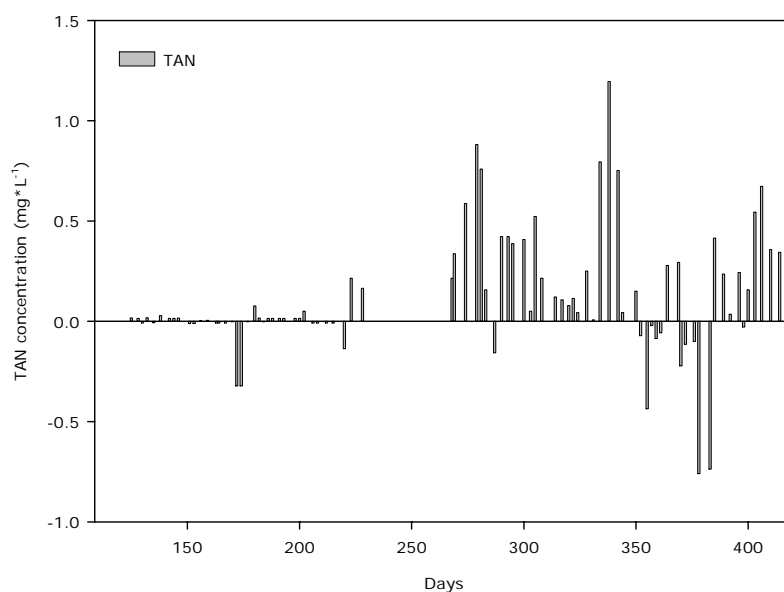


Fig. 43. Difference in the total ammonia nitrogen (TAN) concentrations ($\text{mg}\cdot\text{L}^{-1}$) between in and outlet of the biofilter water (by-pass) receiving approximately 2/5 of the fish tank effluent, from day t_{125} until day t_{428} of the study period. Positive values indicate a removal and negative values an increase in the TAN concentration in the water passing the biofilter.

The relationship between in and outlet TAN concentrations (Fig. 44) followed a linear regression. The oxidation efficiency for TAN by the bacterial flora in the biofilter was 15% (slope <1). It was noted that lower concentrations showed more linearity than concentrations above 2.0 mg*L⁻¹.

The ratio of TAN to NO₂⁻-N in the outlet of the swirl separator was on average 8.2 ± 6.2 during the time interval from day t₁₂₅ until day t₄₂₈. The data showed a very high variability between single data pairs compared. It was observed that high TAN concentrations were in association with low NO₂⁻-N concentrations thou. It has to be taking into account that, NO₂⁻-N is an intermediate component, coming as a product from the oxidation of TAN, but also disappearing after the synthesis of NO₃⁻-N. A nitrification dependant relation couldn't be therefore established.

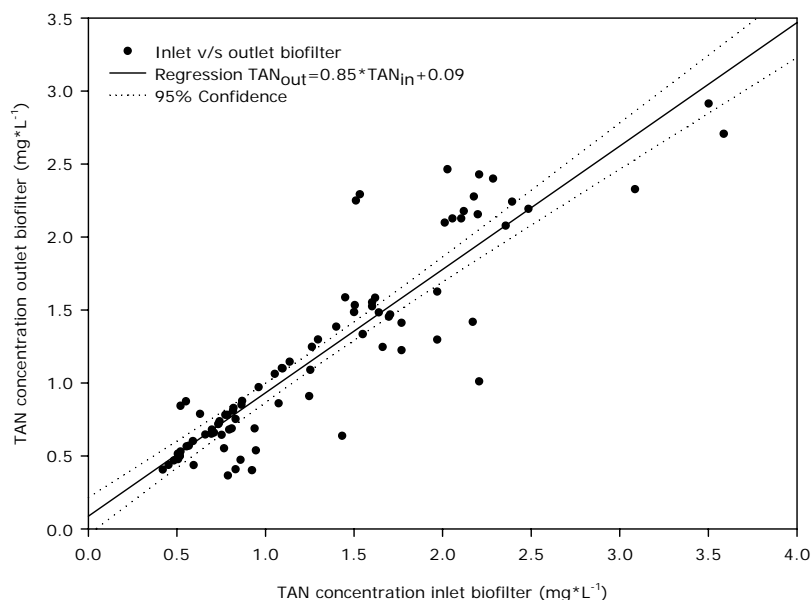


Fig. 44. Relationship between total ammonia nitrogen (TAN) concentration (mg*L⁻¹) in the inlet and outlet of the biofilter water (by-pass) receiving approximately 2/5 of the fish tank effluent, for the study period between day t₁₂₅ and t₄₂₈ (n=98). Plotted data are explained by the regression (bold black line) $f(x)=a*x+b$ with $a=0.85$, $b=0.09$, $R^2=0.82$. Dotted lines show the 95% confidence interval.

NO₂⁻-N concentration in the outlet of the biofilter was unstable (Fig. 45), but stayed at levels below 0.7 mg*L⁻¹ for the period between days t₁₂₅ and t₄₂₈. The average concentration was 0.2 mg*L⁻¹. Maximum and minimum values determined were 0.6 mg*L⁻¹ and 0.1 mg*L⁻¹ respectively. NO₂⁻-N peaks observed did not lead to an increase of the nitrification performance. These high concentrations were presumably causing an inhibition of the second step of the nitrification process. TAN to NO₂⁻-N ratios were highly variable, in average 10.2 ± 8.8 mg*L⁻¹, and no relation could be established.

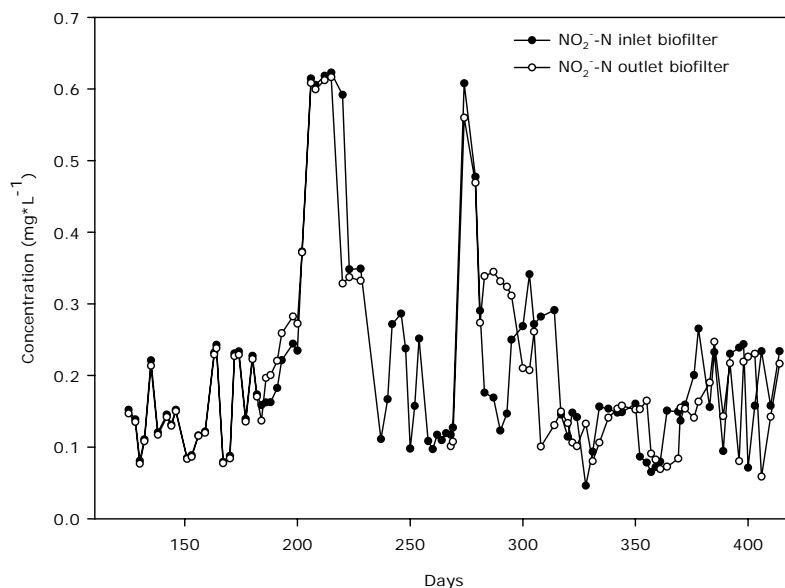


Fig. 45. Nitrite-nitrogen (NO_2^- -N) concentrations ($\text{mg}\cdot\text{L}^{-1}$) in the inlet and outlet water of the biofilter water (by-pass) receiving approximately 2/5 of the fish tank effluent, from day t_{125} until day t_{428} ($n=98$) of the study period.

Comparing the NO_2^- -N concentration in the water going in and out from the biofilter, it was noticed that the difference was very low, ranging between a maximum of $+0.26 \text{ mg}\cdot\text{L}^{-1}$ (removal) and $-0.21 \text{ mg}\cdot\text{L}^{-1}$ (increase) (Fig. 46). The removal efficiency was satisfactory (Fig. 47). The NO_2^- -N concentration in the outlet of the biofilter was 19% lower than in the inlet.

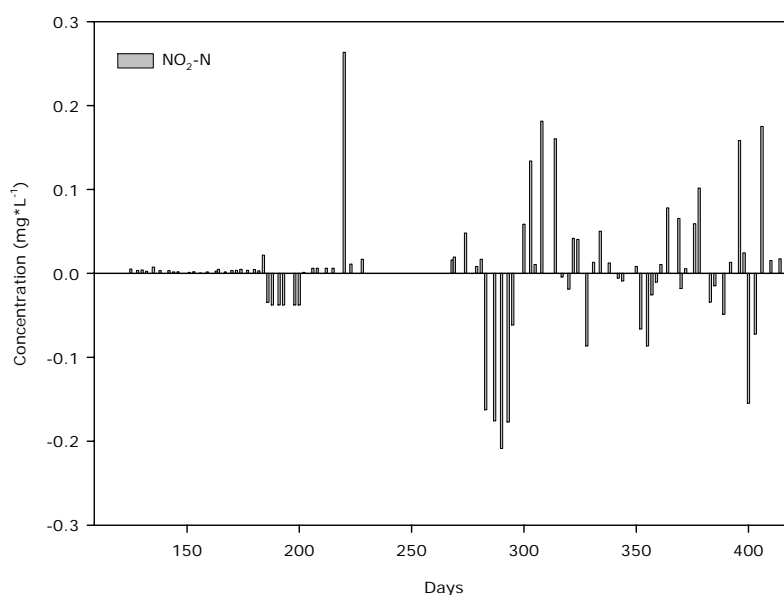


Fig. 46. Difference in the nitrite-nitrogen (NO_2^- -N) concentrations ($\text{mg}\cdot\text{L}^{-1}$) between the inlet and outlet of the biofilter water (by-pass) receiving approximately 2/5 of the fish tank effluent, from day t_{125} until day t_{428} of the study period. Positive values indicate a removal and negative values an increase in the NO_2^- -N concentration in the water passing the biofilter.

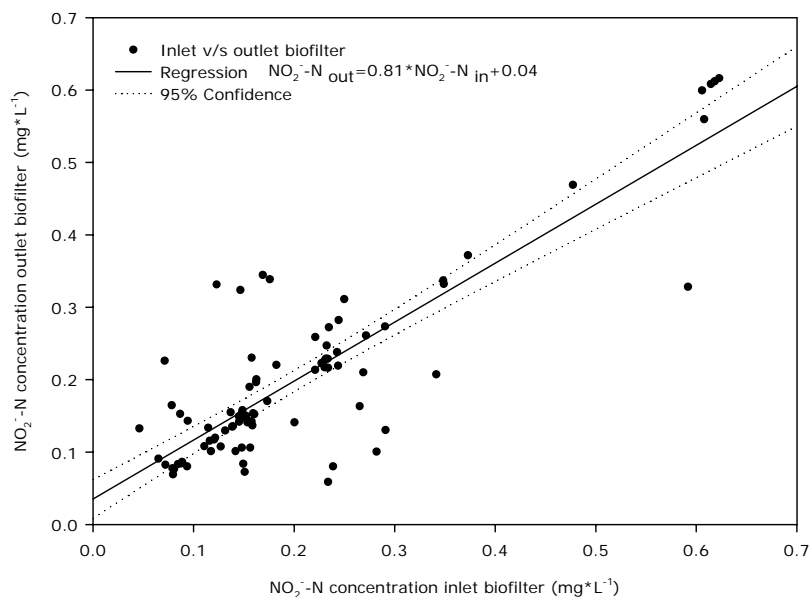


Fig. 47. Relationship between nitrite-nitrogen (NO_2^- -N) concentration ($\text{mg}\cdot\text{L}^{-1}$) in the inlet and outlet of the biofilter water (by-pass) receiving approximately 2/5 of the fish tank effluent, for the study period between day t_{125} and t_{428} ($n=98$). Plotted data are explained by the regression (bold black line) $f(x)=a*x+b$ with $a=0.81$, $b=0.04$, $R^2=0.73$. Dotted lines show the 95% confidence interval.

NO_3^- -N concentration in the outlet of the biofilter rose continuously, on average at a rate of $2.2 \text{ mg}\cdot\text{L}^{-1}\cdot\text{d}^{-1}$. The maximum concentration occurred on day t_{300} and amounted to $145.6 \text{ mg}\cdot\text{L}^{-1}$ (Fig. 48). NO_3^- -N concentration raised in 9 occasions. For every increment in the concentrations of NO_3^- -N a regression line was calculated. The covariance analysis showed a non parallel relationship between at least two regression lines. The regression coefficients were significantly different from each other ($p<0.05$).

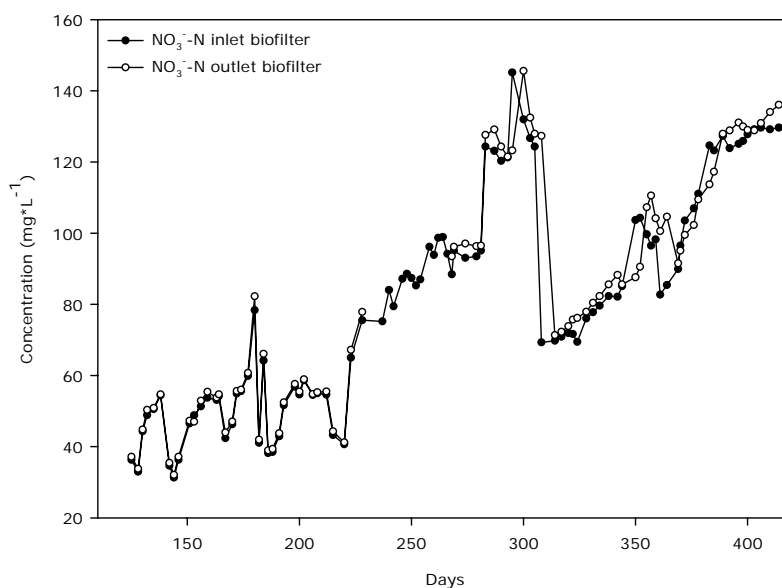


Fig. 48. Nitrate-nitrogen (NO_3^- -N) concentrations ($\text{mg}\cdot\text{L}^{-1}$) in the inlet and outlet of the biofilter water (by-pass) receiving approximately 2/5 of the fish tank effluent, for the study period between day t_{125} and day t_{428} ($n=98$).

The difference between the NO_3^- -N concentrations in the out- and inlet of the biofilter was mainly negative, indicating a slight increase that most likely reflects the incomplete second step nitrification (Fig. 49). There were exceptions: Relatively high positive peaks at days t_{295} , t_{350} and between t_{370} and t_{385} can partly be explained by volumes of water renewed (see Tab. 17) in association of the events detailed at the beginning of this chapter.

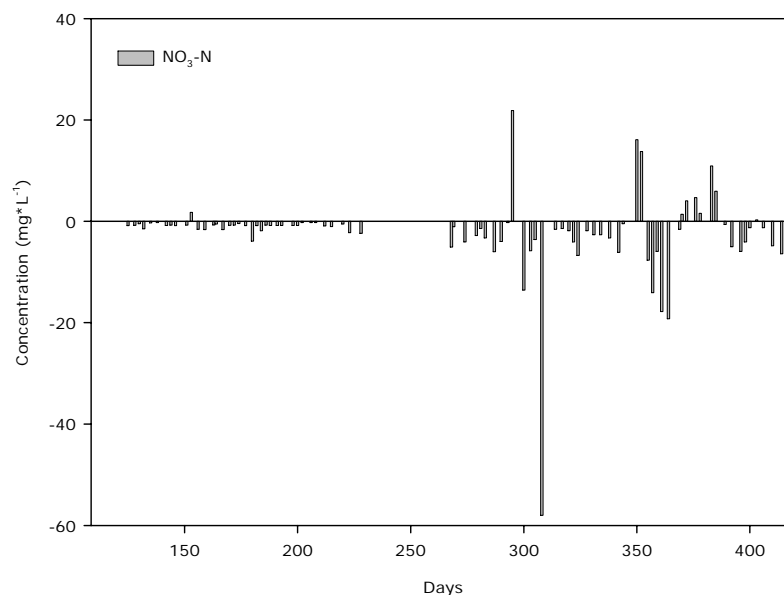


Fig. 49. Difference in the nitrate-nitrogen (NO_3^- -N) concentrations ($\text{mg}\cdot\text{L}^{-1}$) between the inlet and outlet of the biofilter water (by-pass) receiving approximately 2/5 of the fish tank effluent, for the study period between day t_{125} until day t_{428} . Positive values indicate a removal and negative values an increase in the NO_3^- -N concentration in the water passing the biofilter.

3.3.4 Water quality in the outlet of the foam fractionator

The water leaving the swirl separator can also be considered as the water entering the foam fractionator. Figure 50 shows the course of the TAN concentration in the inlet and outlet water of the reaction tower. TAN concentrations determined in the outlet during days t_{125} and t_{428} fluctuated between a minimum of $0.4 \text{ mg}\cdot\text{L}^{-1}$ and a maximum value of $3.5 \text{ mg}\cdot\text{L}^{-1}$, indicating from time to time the high variation of excretion and biofiltration processes within the entire system. The average value was $1.2 \text{ mg}\cdot\text{L}^{-1}$.

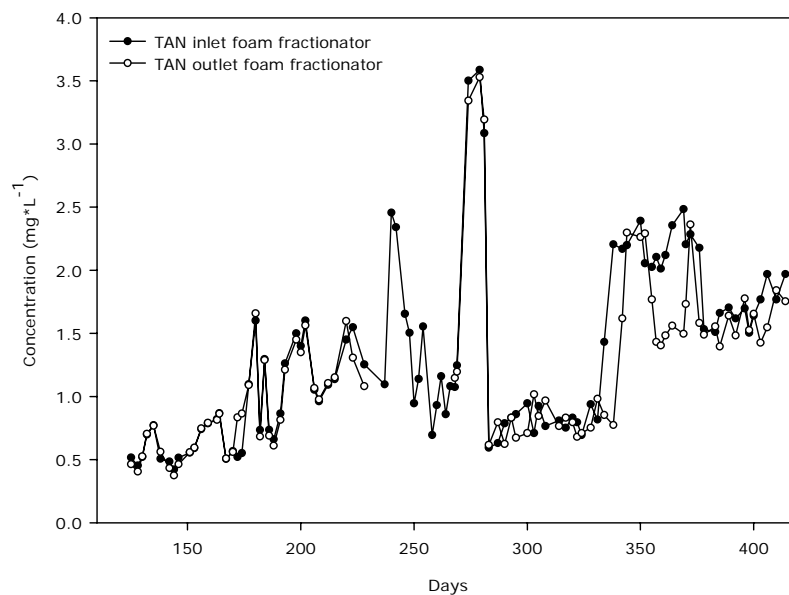


Fig. 50. Total ammonia nitrogen (TAN) concentrations ($\text{mg}\cdot\text{L}^{-1}$) in the inlet and outlet water of the foam fractionator (by-pass) receiving approximately 3/5 of the tank effluent, for the study period between day t_{125} until day t_{428} ($n=98$).

Taking into account that the ozone dosage was controlled by the ORP set-point value, with an upper threshold of 350 mV, the removal of TAN measured in the foam fractionator was unexpected and remained unclear. Differences of the outlet-inlet concentrations (Fig. 51) were maintained below $0.2 \text{ mg}\cdot\text{L}^{-1}$ until day t_{331} , with a few exceptions. Afterwards and until day t_{428} the removal values were between 0.2 and a maximum of $1.4 \text{ mg}\cdot\text{L}^{-1}$. Removals above $0.5 \text{ mg}\cdot\text{L}^{-1}$ were found to be exceptional.

The removal efficiency of TAN in the foam fractionator amounted to 18% (Fig. 52). It is certainly possible that un-ionized ammonia/ammoniac was stripped out in the reaction chamber, because of the constant upwards water transport by air bubbles. No measurements, however, were conducted to evaluate this pathway of elimination.

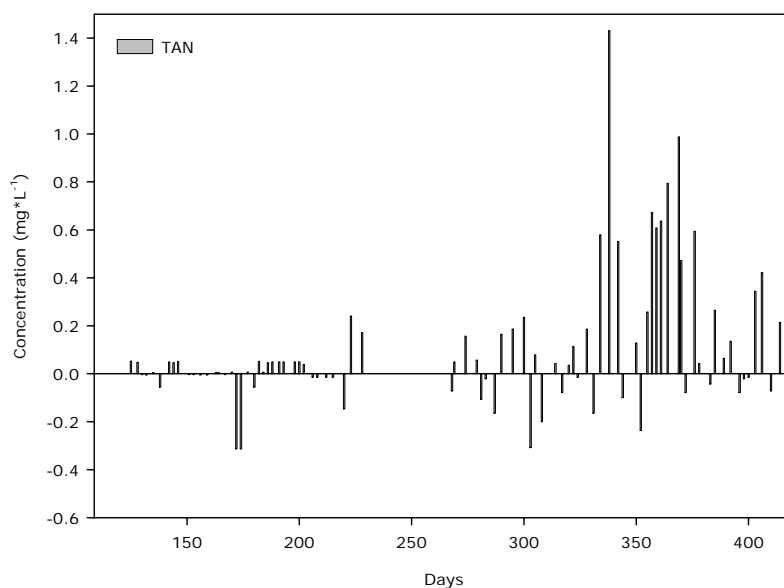


Fig. 51. Difference in the total ammonia nitrogen (TAN) concentrations ($\text{mg}\cdot\text{L}^{-1}$) between the inlet and the outlet of the foam fractionator (by-pass) receiving approximately 3/5 of the tank effluent, from day t_{125} until day t_{428} of the study period. Positive values indicate a removal and negative values an increase in the TAN concentration in the water passing the foam fractionator.

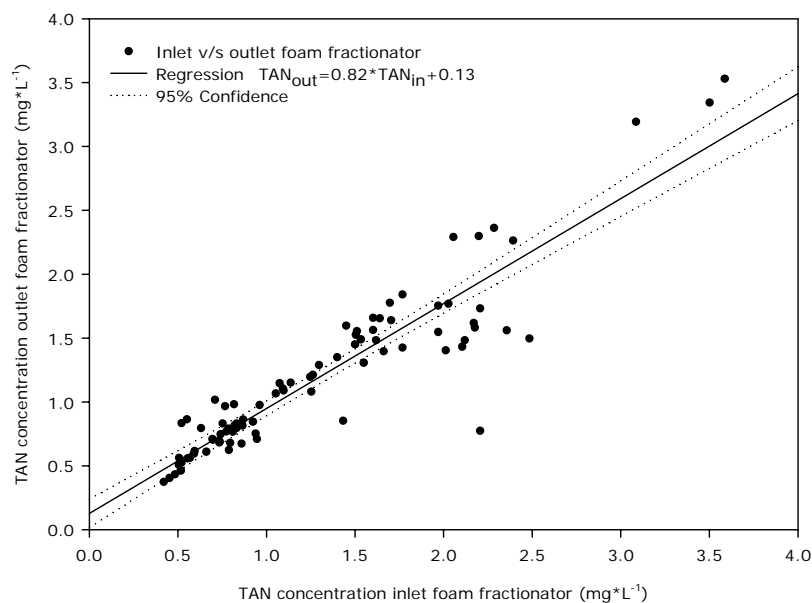


Fig. 52. Relationship between total ammonia nitrogen (TAN) concentration ($\text{mg}\cdot\text{L}^{-1}$) in the inlet and outlet water of the foam fractionator (by-pass) receiving approximately 3/5 of the tank effluent, for the study period between day t_{125} and t_{428} ($n=98$). Plotted data are explained by the regression (bold black line) $f(x)=a*x+b$ with $a=0.82$, $b=0.13$, $R^2=0.85$. Dotted lines show the 95% confidence interval.

The average NO_2^- -N concentration found in the water leaving the foam fractionator was $0.2 \text{ mg}\cdot\text{L}^{-1}$. A maximum value of $0.6 \text{ mg}\cdot\text{L}^{-1}$ was observed during days t_{206} and t_{215} (Fig. 53), indicating an overall high system concentration. During these days the outlet concentration was actually higher than the inlet concentration. These observations were

linked to a temporary system failure during which on day t_{205} the outlet pipe of the biofilter broke. This required to stop temporarily the system flow (several hours) while also a significant amount of water was lost. Subsequent cleaning of (a) the swirl separator tower, (b) the air-lift device and (c) the biofilter basin on day t_{207} , affected the bacteria colonies on the biofilter media and on other surfaces, thereby causing a shift in the nitrification process. The observations of this study show that unexpected extremes in water quality changes, in particular nutrients, are an indicator of unusual events or direct system failures that secondarily affect the performance of biofilters and subsequently the entire system, including other treatment units.

Although the retention time in the foam fractionator was relatively high (4.7 min), in contrast to the values recommended by the manufacturer (between 1 and 1.5 min), the average amount of NO_2^- -N removed from the system during a single pass of the water through the column was $0.2 \text{ mg}\cdot\text{L}^{-1}$. Despite of some few observations where nitrite-nitrogen increased in the outlet (Fig. 54), this compound was generally and continuously oxidized.

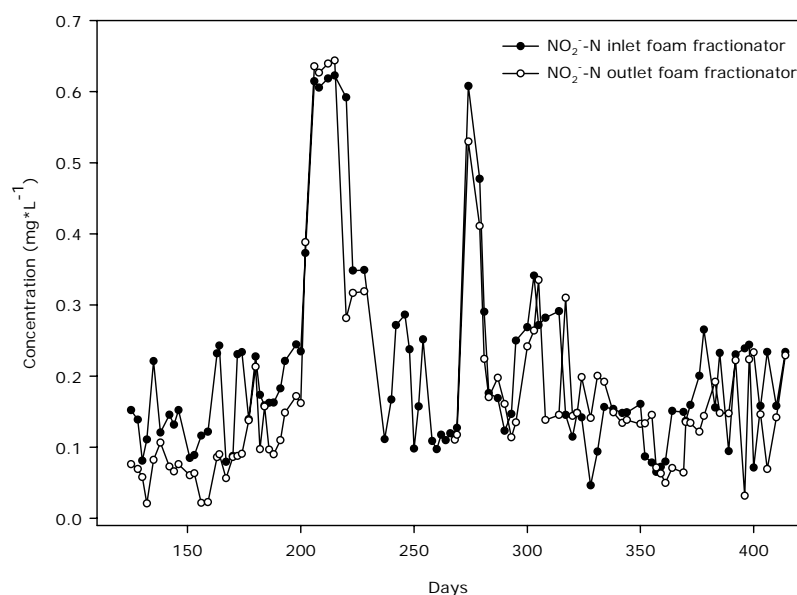


Fig. 53. Nitrite-nitrogen (NO_2^- -N) concentrations ($\text{mg}\cdot\text{L}^{-1}$) in the inlet and outlet water of the foam fractionator (by-pass) receiving approximately 3/5 of the tank effluent, between day t_{125} until day t_{428} ($n=98$) of the study period.

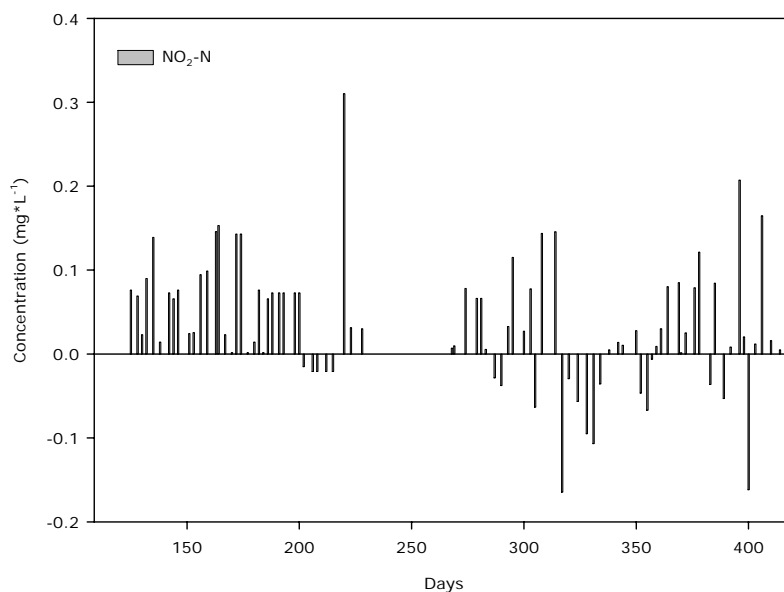


Fig. 54. Difference in the nitrite-nitrogen (NO_2^- -N) concentrations ($\text{mg}\cdot\text{L}^{-1}$) between inlet and outlet water of the foam fractionator (by-pass) receiving approximately 3/5 of the tank effluent, between day t_{125} until day t_{428} of the study period ($n=98$). Positive values indicate a removal and negative values an increase in the NO_2^- -N concentration in the water passing the foam fractionator tower.

Figure 55 shows the linear course of the relationship between in and outlet NO_2^- -N concentrations ($R^2=0.73$). It was found that the NO_2^- -N outlet concentration from the foam fractionator was on average 19% lower than the inlet concentration, indicating a reasonable oxidation was taking place mainly by the ozonation process.

NO_3^- -N concentrations in the reactor tower were not measured because it was considered that the oxidation of NO_2^- -N takes place through the chemical oxidation properties of ozone, and not because of bacterial activity. It was assumed that the bacteria settled in the system were responsible for the production *i.e.* accumulation of NO_3^- -N in the culture water.

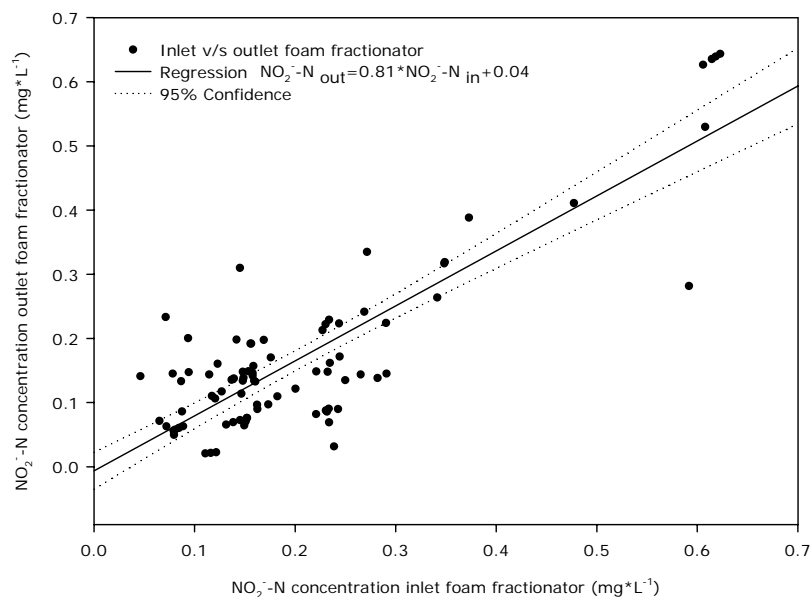


Fig. 55. Relationship between nitrite-nitrogen (NO_2^- -N) concentration ($\text{mg}\cdot\text{L}^{-1}$) in the outlet of the swirl separator and the outlet of the biofilter (nitrification) for the period between day t_{125} and t_{428} ($n=98$). Plotted data are explained by the regression (bold black line) $f(x)=a*x+b$ with $a=0.81$, $b=0.04$, $R^2=0.73$. Dotted lines show the 95% confidence interval.

Although no rational relationship was established between oxidation reduction potential (ORP) and NO_2^- -N concentration in the foam fractionator, Figure 56 shows the cloud of data that can associate high ORP values (above 250 mV) with low NO_2^- -N concentrations ($< 0.4 \text{ mg}\cdot\text{L}^{-1}$). It is unlikely that a relationship exists, however, the NO_2^- -N concentrations were too low ($< 1 \text{ mg}\cdot\text{L}^{-1}$) to obtain a window of enough data to find a mathematical relationship.

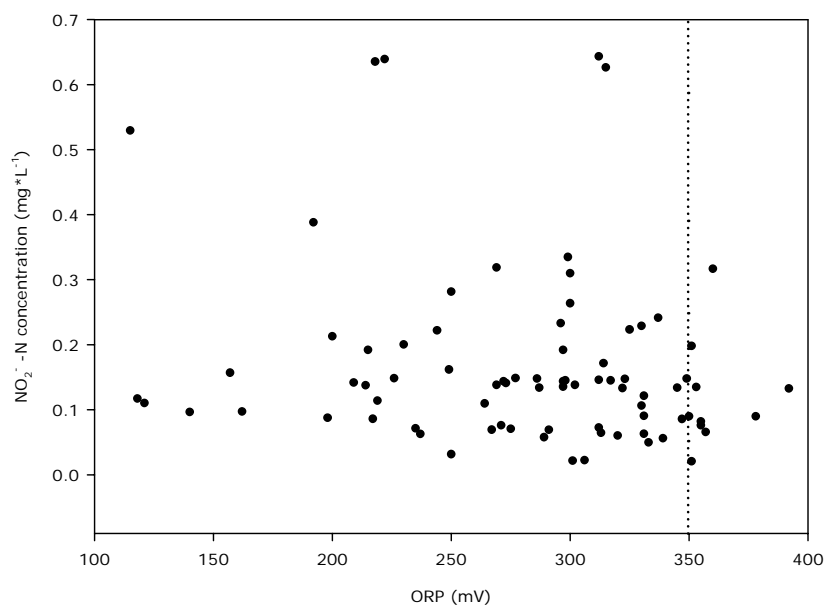


Fig. 56. Oxidation reduction potential (ORP) and nitrite-nitrogen (NO_2^- -N) concentration in the water of the foam fractionator tower, for the study period between day t_{125} and t_{414} ($n=80$). Dotted line shows the mV value used for the automatic switch to turn off the ozone generator (set point=350 mV).

3.3.5 Water quality in the outlet of the additional biofilter

As described in section 3.2.3, two separate trickling biofilter, one for each fish tank, were additionally installed between day t_{239} and day t_{428} . Figures 57 and 63 show the course of development of the TAN and the NO_2^- -N concentrations respectively, in the outlet of the biofilter installed for tank 1. Values are compared with the concentrations in the fish tank.

Average TAN concentrations in the outlet of the additional biofilters was $1.5 \text{ mg} \cdot \text{L}^{-1}$. Minimum and maximum values were $0.6 \text{ mg} \cdot \text{L}^{-1}$ and $3.5 \text{ mg} \cdot \text{L}^{-1}$, respectively. Maximum values were found at the start-up of these two filters and are partly explained by the breakdown of organic matter and release of inorganic nitrogen components, although the filter material was previously submerged in water coming from the recirculation system for about 10 days so that the start-up phase should have been completed. Between day t_{281} and day t_{283} , fish were sampled for weight and this involves water replacement, causing a decrease in the TAN and NO_2^- -N concentrations (Fig. 57).

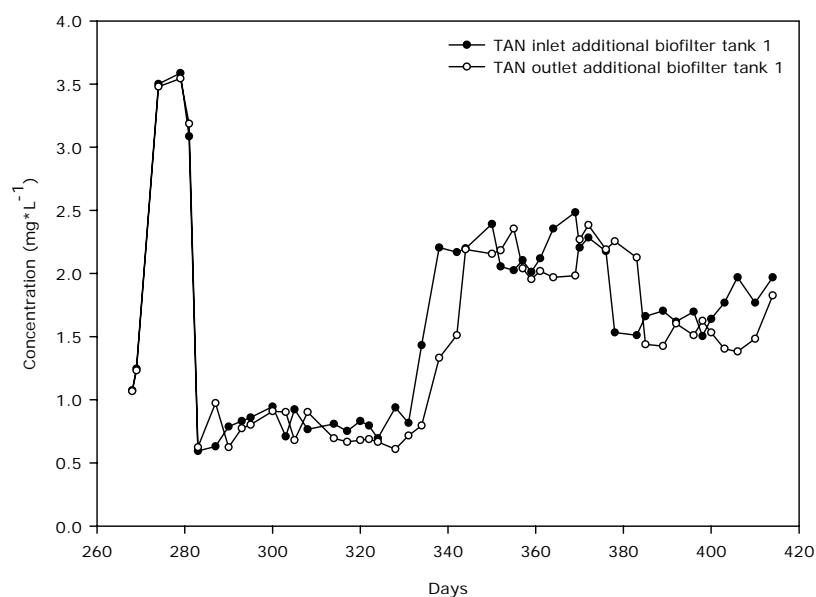


Fig. 57. Total ammonia nitrogen (TAN) concentrations ($\text{mg} \cdot \text{L}^{-1}$) in the inlet and outlet water of the additional biofilter installed in tank 1, for the period between day t_{268} until day t_{428} ($n=48$).

After a period of relatively constant TAN concentrations in the system levels raised up to around $2.0 \text{ mg} \cdot \text{L}^{-1}$ between days t_{284} and t_{331} and remained at this level for more than 40 days. On day t_{332} the automatic pH control unit failed, causing first a drop in the pH value (<7) for several days (until t_{336}), and after repair stabilizing at 7.1 for a week, and finally

raising to values between 7.9 and 8 (on day t_{343}). This period of pH instability affected the entire system.

Differences in the TAN concentrations between inlet and outlet water of the additional biofilters (Fig. 58) were found to be positive (oxidation) in 73% of the collected data. The removal efficiency, however, was lower than the biofilter. The linearity of the relationship in the TAN concentration in the inlet and outlet water of the additional biofilter is presented in Figure 59. The TAN concentration in the outlet water was in general 6% lower than the inlet water.

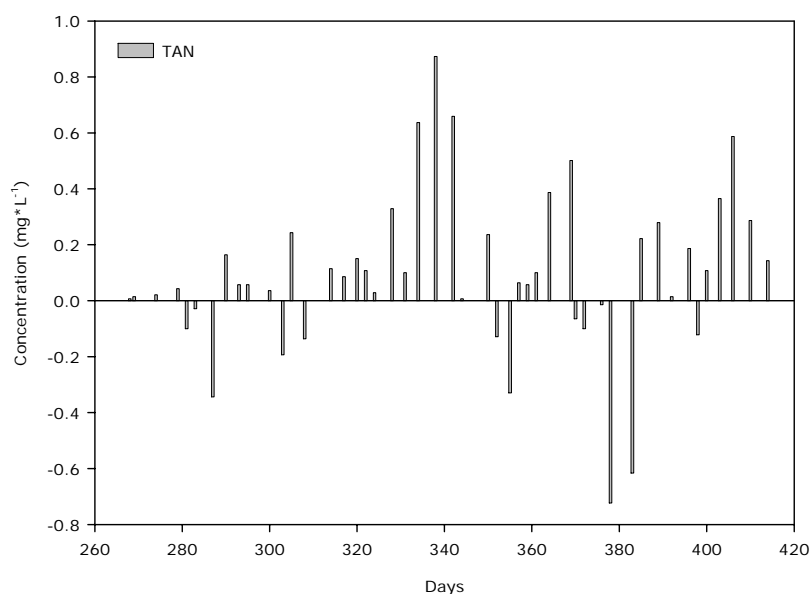


Fig. 58. Difference in the total ammonia nitrogen (TAN) concentrations ($\text{mg}\cdot\text{L}^{-1}$) between inlet and outlet water of the additional biofilter installed in tank 1, for the study period between day t_{125} until day t_{428} . Positive values indicate a removal and negative values an increase in the TAN concentration in the water passing the additional biofilter.

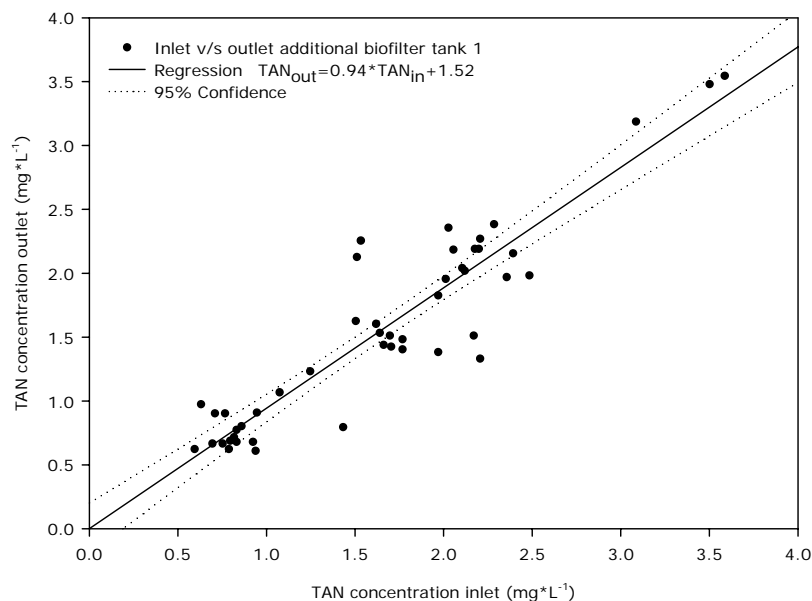


Fig. 59. Relationship between total ammonia nitrogen (TAN) concentration ($\text{mg}\cdot\text{L}^{-1}$) in the inlet and outlet of the water of the additional biofilter installed for in tank 1, for the study period between day t_{125} and t_{428} ($n=48$). Plotted data are explained by the regression (bold black line) $f(x)=a*x+b$ with $a=0.94$, $b=1.52$, $r^2=0.86$. Dotted lines show the 95% confidence interval.

NO_2^- -N concentrations in the outlet of the additional biofilters (Fig. 60) fluctuated between values below $0.1 \text{ mg}\cdot\text{L}^{-1}$ and $0.6 \text{ mg}\cdot\text{L}^{-1}$. The average concentration was $0.2 \text{ mg}\cdot\text{L}^{-1}$. As described above, the initial phase of the nitrification in the biofilter was clearly distinguished by high NO_2^- -N values. The problems associated with the malfunction of the pH dosage system were also found to have their effect on the NO_2^- -N concentration, but fluctuations were found to follow a zigzag course, in contrast to the changes in TAN. These observations can be partially explained by NO_2^- -N produced and removed at the same time. Low TAN concentrations were found to be associated to relatively high NO_2^- -N concentrations between day's t_{284} and t_{331} .

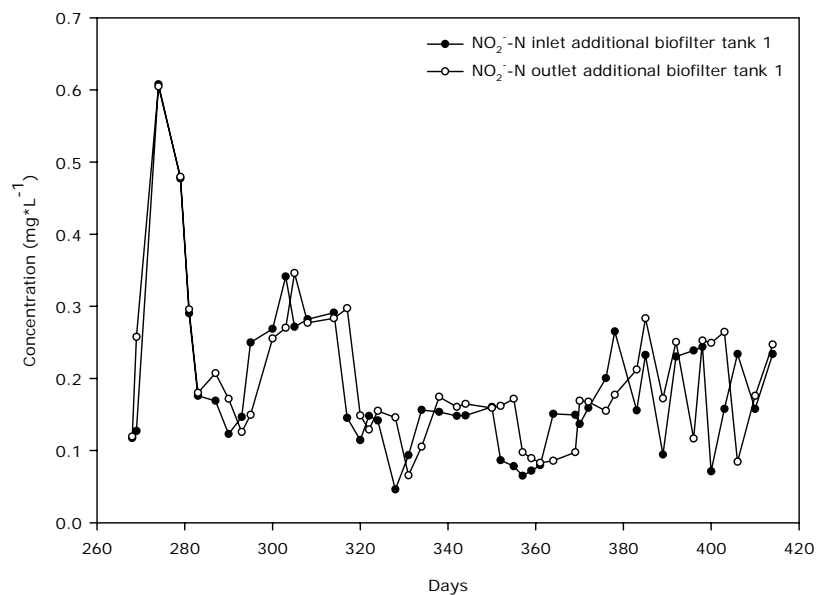


Fig. 60. Nitrite-nitrogen (NO_2^- -N) concentrations ($\text{mg}\cdot\text{L}^{-1}$) in the inlet and outlet water of the additional biofilter installed in tank 1, for the study period between day t_{268} until day t_{428} ($n=48$).

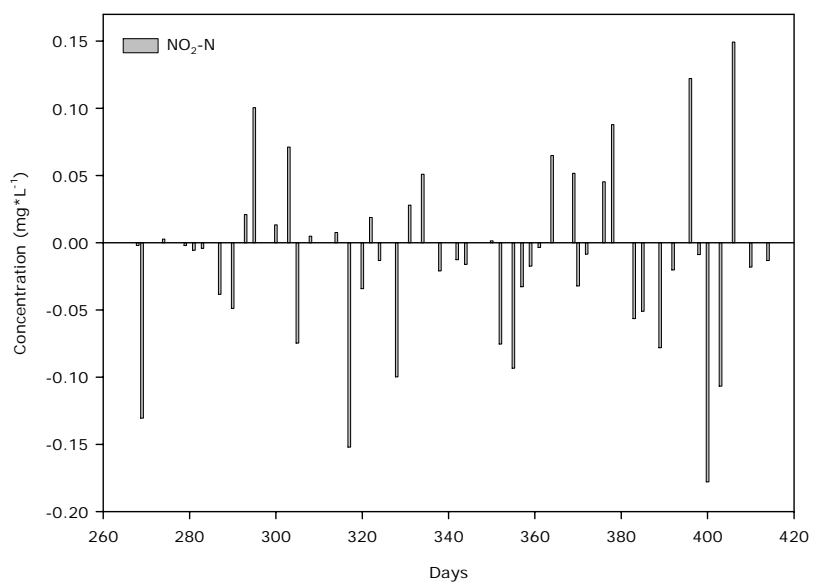


Fig. 61. Difference in the nitrite-nitrogen (NO_2^- -N) concentrations ($\text{mg}\cdot\text{L}^{-1}$) between inlet and outlet water of the additional biofilters installed in tank 1, for the study period between day t_{268} until day t_{428} ($n=48$). Positive values indicate a removal and negative values an increase in the NO_2^- -N concentration in the water passing the additional biofilter.

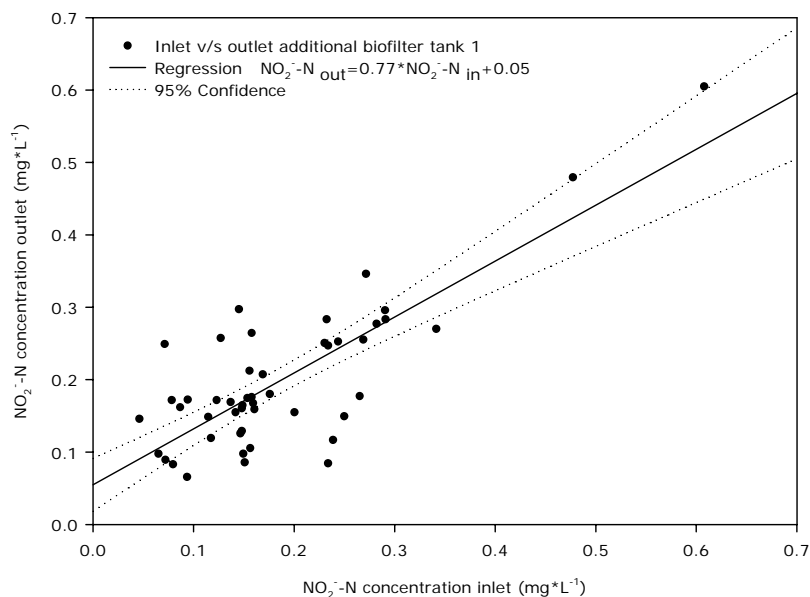


Fig. 62. Relationship between nitrite-nitrogen (NO_2^- -N) concentration ($\text{mg}\cdot\text{L}^{-1}$) in the inlet and outlet water of the additional biofilters installed in tank 1, for the study period between day t_{268} until day t_{428} ($n=48$). Plotted data are explained by the regression (bold black line) $f(x)=a*x+b$ with $a=0.77$, $b=0.05$, $R^2=0.63$. Dotted lines show the 95% confidence interval.

Comparing the inlet and outlet NO_2^- -N concentrations over time (Fig. 61), the days during which a measurable oxidation of nitrite occurred in the additional biofilter were only 30% of the total observation days. An increase of the NO_2^- -N concentration was observed in 50% of the sampling dates (negative values). Despite of these variations on overall oxidation of NO_2^- -N took place, that outlet concentration was 23% lower than the inlet concentration. The linearity of the relationship established is presented in Figure 62. This removal efficiency was found to be 4 percent point higher than the biofilter operating in the main water stream.

3.3.6 Water quality in the inlet of the fish tanks

The trend in water quality was also monitored at the inlet pipes of the fish tanks. These pipes received the mixing water coming from the biofilter and foam fractionator. Figure 63 shows the results of the TAN and NO_2^- -N concentrations determined between day t_0 and t_{428} . No data were available for this sampling point in the period between day t_{237} and t_{268} .

The course of the TAN and NO_2^- -N concentrations did not vary significantly from the fluctuations found in the biofilter (nitrification) and the foam fractionator, presented earlier in this chapter. Relatively high TAN concentrations and daily fluctuation between 0.5 and 2 $\text{mg}\cdot\text{L}^{-1}$ were found at the beginning of the experiment, after the fish were

stocked. After the first 20 days of the trial the average concentration was $1.0 \text{ mg} \cdot \text{L}^{-1}$. Relatively high $\text{NO}_2^- \text{-N}$ concentrations were measured during the same period, but staying below $0.7 \text{ mg} \cdot \text{L}^{-1}$. Total ammonia peaks were also observed after this initial phase. Around day t_{100} the TAN concentration raised up to $2.9 \text{ mg} \cdot \text{L}^{-1}$, probably as result of the two air stones installed between the biofilter media (see 3.3.1). $\text{NO}_2^- \text{-N}$ concentrations around day t_{100} stayed below $0.4 \text{ mg} \cdot \text{L}^{-1}$. The TAN peak in Figure 63 around day t_{279} ($3.5 \text{ mg} \cdot \text{L}^{-1}$) can be associated to the change in the feeding strategy after sorting the fish as previously outlined. The abrupt decrease in the TAN and $\text{NO}_2^- \text{-N}$ concentrations on day t_{283} was a consequence of fish handling (weighing), involving water exchange. From day t_{334} until the end of this part of the experiment TAN concentration rose again to values around $2.0 \text{ mg} \cdot \text{L}^{-1}$ and declined again during the last 15 days to values around $1.5 \text{ mg} \cdot \text{L}^{-1}$. As explained before, this fluctuation is partly explained by the impasses with the pH control system detailed in 3.3.1.

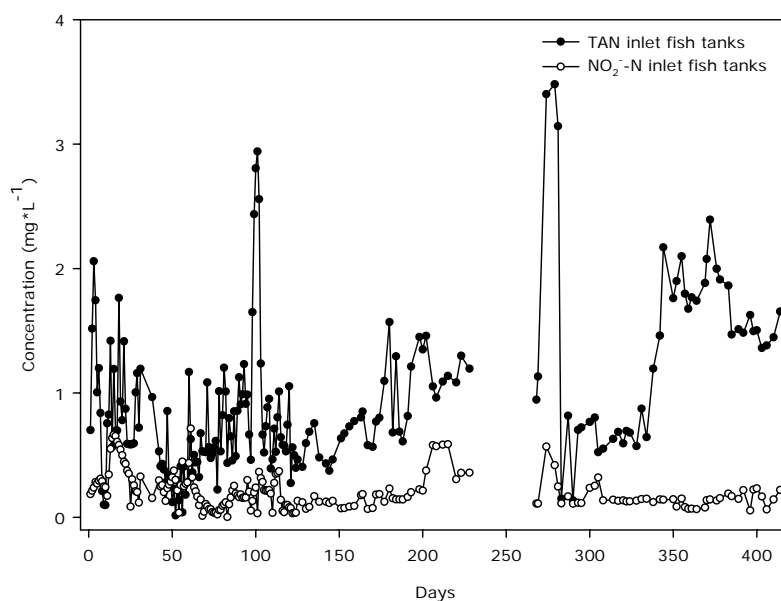


Fig. 63. Total ammonia nitrogen (TAN) and nitrite-nitrogen ($\text{NO}_2^- \text{-N}$) concentration ($\text{mg} \cdot \text{L}^{-1}$) in the inlet of the fish tanks, from day t_0 until day t_{428} ($n=200$).

The accumulation of $\text{NO}_3^- \text{-N}$ and PO_4^{-3} in the system (Figure 64) was observed and followed during the 428 days of experimentation. This trend was interrupted *i.e.* the concentration dropped when significant amounts of water were exchanged or renewed. A definitely remarkable event is the increment in the $\text{NO}_3^- \text{-N}$ concentration after changing the feeding regime (day t_{268}).

The maximum $\text{NO}_3^- \text{-N}$ concentration was measured on day t_{355} and amounted $168.7 \text{ mg} \cdot \text{L}^{-1}$. The highest PO_4^{-3} concentration of $59.9 \text{ mg} \cdot \text{L}^{-1}$ was determined on day t_{228} .

It was observed that the systems equilibrium was affected by external factors, such as fish weighing causing water loss/renewal or by short-term malfunction of the pH control system. The system was capable to re-establish its equilibrium, but this took from a few hours at the beginning of the experiment, up to 72 hours during the last months of the study period. This was acknowledged as a signal that the system was reaching carry capacity limits.

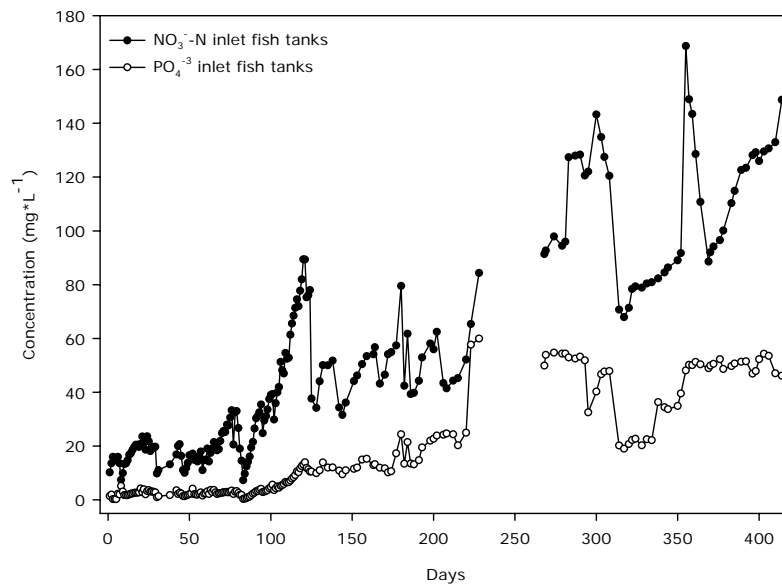


Fig. 64. Nitrate-nitrogen (NO_3^- -N) and phosphate (PO_4^{3-}) concentration ($\text{mg}\cdot\text{L}^{-1}$) in the inlet of the fish tanks, between days t_0 until day t_{428} ($n=200$).

Looking at results, and considering the turn over rate (system water volume per hour), the conditions in the RAS were maintained within but close to safe limits throughout the 428 days of the experiments described above. The events mentioned in this chapter, however, had definitely an effect on all other system components (fish tanks, swirl separator, biofilter, foam fractionator, and the additional biofilters hooked up to the fish tanks). Water treatment units (chemical and biological) responded positively to all events under the given conditions so that total system failure was prevented. Nevertheless some water quality parameters, for example such as high NO_2^- -N concentrations, reached critical values over a short time span that would be otherwise lethal if maintained over an extended time period. Coping with these water quality fluctuations, the system configuration within a RAS has an important bearing on how extreme fluctuations of water quality parameters are levelled. Sometimes by-pass solutions where the mass flow from one component to the next was diluted was decisive for the success on growing fish.

3.4 Particulate matter in the culture system

3.4.1. Nutrients, organic and energy composition of the solid matter in the RAS

Particulate waste in the culture system was collected from the swirl separators basin and analyzed during the entire experimental period between days t_0 and t_{437} ($n=28$ samples). The sludge was classified in seven size classes. For each size class, total suspended solids (TSS) were determined and sub samples were monitored for carbon (C), nitrogen (N), phosphate (P), organic content (OC) and energy (E). Nitrogen-phosphate (N:P) as well as carbon-nitrogen (C:N) ratios were calculated.

Figure 65 shows the percentage composition of the particle size distribution by weight, for the TSS samples collected from the swirl separator between days t_{14} and t_{203} (Fig. 65a) and between days t_{225} and t_{437} (Fig. 65b)

As can be seen from Figure 65, during the first four samples (days t_{14} to t_{56}) the percentage composition was similar for particles in the upper size classes 400-800 μm and 800-1600 μm . Below 400 μm the TSS shifted its composition between 50 μm and >400 μm . Small particles below 50 μm were found in day t_{42} to be almost 15%, stayed below 10% in day's t_{14} , t_{28} , and t_{56} thou. The sample took on day t_{70} showed a substantial portion of particles below 50 μm (19.1%) and a major increase in particles of the size class 800-1600 μm , from 4.3% up to 23.1%. This phenomenon remains unclear since the feed quality and size were the same as in the precedent samples.

Particle in the size >1600 μm appeared significantly for the first time on day t_{84} with 5.7% of the TSS amount. This event was explained by the change in the pellet size from 1.2 mm granulated to 1.5 mm pelletized feed. In this sample the particles in the size class 400-800 μm increased its meaning from 20.6% to 35.3%, and the particles between 50 μm and 200 μm were not fairly present from around 10% down to 5%. It was observed that the TSS amount declined from 9.4 g to 5.9 g DW (equivalent to a reduction from 7.3% to 4.2% of the total feed fed respectively) (Tab. 18). It was also observed that the 400-200 μm size class raised its portion from 20.6% to 35.3%. On the other hand, the 50-100 μm size class decline from 11.7% to 4.3% and the 100-200 μm size class from 10.0% down to 5.4%.

From day t_{98} and until day t_{140} the weight distribution was marked by the relative increase of the size class 400-800 μm from 28.9 up to 44.9 after the second pellet size

change (from 1.5 mm to 3 mm). Size classes below 200 μm were observed to tend to decrease its relative proportion. This became importance after the pellet size changed, were particles below 200 μm were only 14.7% of the total. In this case the total amount of suspended solids increased from 15.3 g to 19.8 g, and the percentage from the total feed decline from 5.3% to 5.0% (Tab. 18). A noteworthy difference was observed in the <50 μm size class with a decrease in its portion from 12.7% down to 7.9%.

Between day t_{140} and day t_{266} there couldn't be established a significant trend in the composition by size class of the TSS. The portion of particles below 200 μm was very small at the beginning but became more importance and was found around 30% on day t_{266} (Fig. 65). Nevertheless the main proportion of solids was always situated for particles between 200 μm and 1600 μm .

After the third change in pellet size, from 3 mm to 4.5 mm, the sample of day t_{380} didn't show any significant change in the weight distribution of particles in the size classes. In samples taken between day t_{328} and day t_{347} very few particles were found between 200-400 μm . Unclear remain the 20% of particles bigger than 1600 μm found in the sample of day t_{328} , and the 53.7% of particles of the size class 400-800 μm found in sample on day t_{347} . Between the samples taken on days t_{403} and t_{437} TSS and the total feed amount declined from 51.7 g (4.6%) to 45.7 (4.0%), respectively (Tab. 18). The relative decrease of the fine solids (<50 μm) from 11.2% to 6.63, and the increase of solids filtered between 800-400 μm was from 3.3 g (6.3%) up to 6.8 g (14.8%).

No significant changes in the composition of TSS by size class was found after the fourth change of the pellet size from 4.5 mm to 6 mm, (days t_{403} and t_{437}). The relative distribution of particles for each filter size class remained at the same level, with the exception of the 200-400 μm particle size class (increase from 16.3% to 25.0% TSS), and a decrease from 45.4% down to 37.1% in the 400-800 μm size class.

It is noteworthy that particles below 200 μm loose importance in its relative portion from day t_{239} until t_{437} .

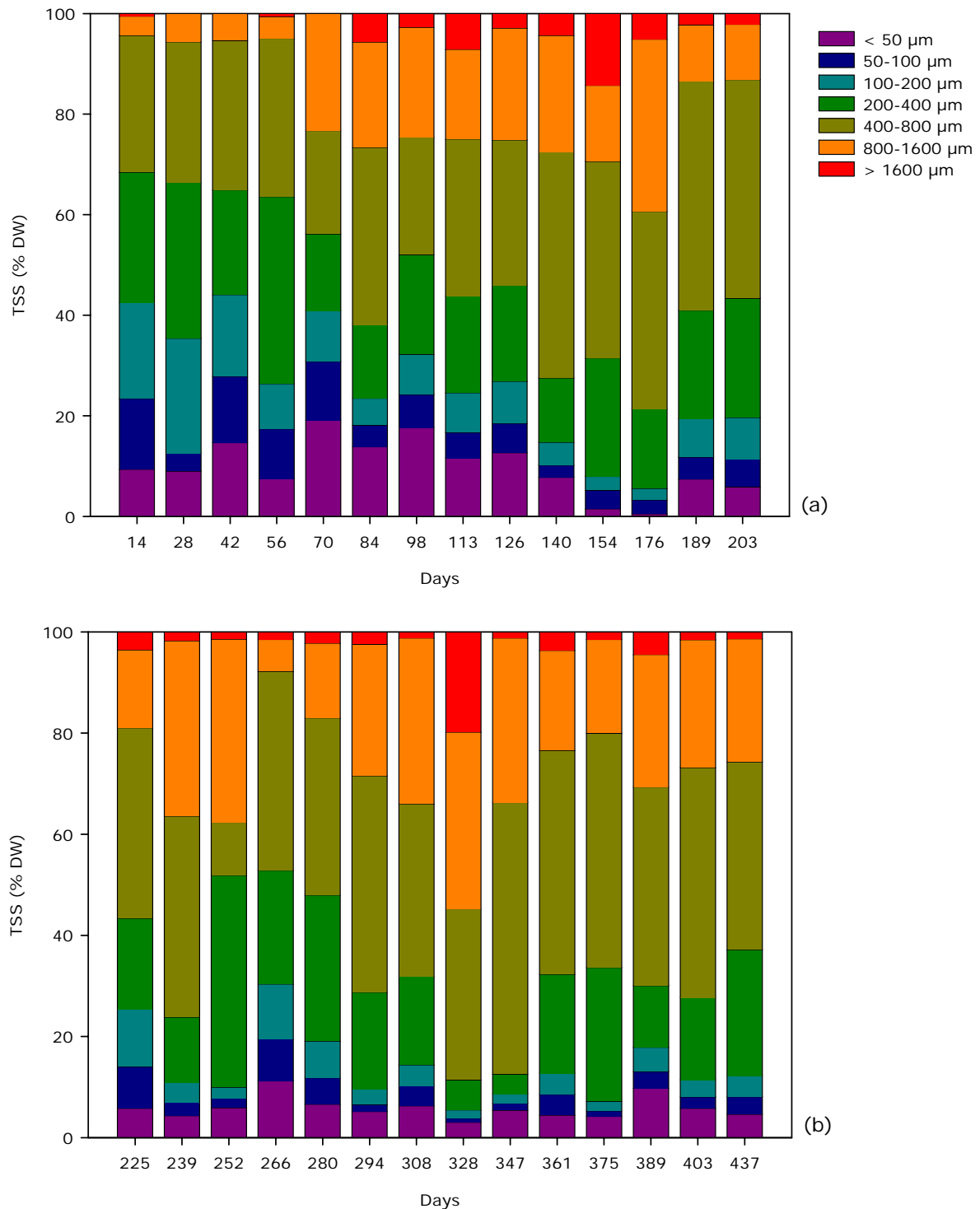


Fig. 65. Composition of the total suspended solids (TSS) in percentage of dry weight (% DW) for every size class category ($n=7$), collected from the swirl separator basin. Figure (a) shows the results obtained during day's t_{14} and t_{203} and figure (b) during day's t_{225} and t_{437} of the experimental period. Particle size categories see colour scale at top right hand corner.

Tab. 18. Total suspended solids dry weight (TSS g DW) as percentage (%) of the feed, collected from the swirl separator in relation to the feed amount fed the day before sampling, and the biomass in the RAS determined for each sample day pooled for both tanks. The different feed sizes used are detailed. Feeding periods where one of diet composition and one feed size were used are marked with grey and white areas. The particulate wastes were collected 24 hours after feeding. The data represent the sum of average values of three subsamples for every size class, from the 24-hour collected sludge; ¹ Feed amount fed the day before; ² G=granulated feed; ³ Malfunction of one belt feeder, only tank 2 was fed.

Sampling Day	Total Biomass (kg)	¹ Feed (g)	Pellet size (mm)	TSS (g DW)	% of feed
t ₁₄	2.6	38.4	² 1.2G	1.0	2.7
t ₂₈	3.2	54.4	1.2G	1.1	2.1
t ₄₂	4.0	58.8	1.2G	1.3	2.2
t ₅₆	5.5	92.3	1.2G	3.2	3.5
t ₇₀	6.8	128.8	1.2G	9.4	7.3
t ₈₄	8.6	140.0	1.5	5.9	4.2
t ₉₈	10.4	200.0	1.5	8.5	4.3
t ₁₁₃	14.5	241.0	1.5	12.8	5.3
t ₁₂₆	18.8	291.4	1.5	15.3	5.3
t ₁₄₀	23.7	391.8	3.0	19.8	5.0
t ₁₅₄	29.3	498.5	3.0	25.3	5.1
t ₁₇₆	37.7	587.2	3.0	27.8	4.7
t ₁₈₉	44.8	788.9	3.0	32.7	4.2
t ₂₀₃	51.9	788.5	3.0	35.2	4.5
t ₂₂₅	58.2	³ 474.3	3.0	20.0	4.2
t ₂₃₉	64.7	1065.2	3.0	41.1	3.9
t ₂₅₂	66.8	1099.6	3.0	45.4	4.1
t ₂₆₆	77.2	1135.7	3.0	51.7	4.6
t ₂₈₀	80.7	1156.5	4.5	45.7	4.0
t ₂₉₄	86.2	1202.8	4.5	60.4	5.0
t ₃₀₈	93.3	1292.2	4.5	62.4	4.8
t ₃₂₈	88.6	1399.4	4.5	62.6	4.5
t ₃₄₇	89.4	1399.4	4.5	65.3	4.7
t ₃₆₁	79.3	990.0	4.5	46.8	4.7
t ₃₇₅	83.1	1265.2	4.5	64.7	5.1
t ₃₈₉	78.5	1137.1	4.5	59.7	5.3
t ₄₀₃	79.3	916.5	4.5	61.0	6.7
t ₄₃₇	81.7	1112.7	6.0	66.1	5.9

The data presented in Table 18 show that the TSS collected from the swirl separator amounted to less than 10% of the total feed quantity fed the day before. This value is lower than the theoretical calculated waste production of 15%. The theoretical calculation was done based on the digestibility of protein (91%), fat (92%), carbohydrates NFE (nitrogen free extract) (88%), fibres (0%), and ash (40%). The data reflect the sum of the average weights obtained from three subsamples for each particle size class. The sludge was collected from the swirl separator conic bottom after 24 hours, which probably induced the leaching process during this time interval.

Table 19 shows the carbon content in the suspended solids classified to be smaller than 50 μm which ranges between 22.1% and 26.5% until day t₂₀₃. After that, carbon

contents were found to be greater than 30% with an unexplained peak at day t_{225} with a value above 30%.

Tab. 19. Composition of the total suspended solids in the swirl separator receiving the effluent of two fish tanks, collected between day t_{14} and day t_{437} of the study period, for the particle size class $<50 \mu m$. Carbon (C), nitrogen (N), phosphorus (P), and organic contents (OC) are presented as percentage of dry weight (%DW); Energy contents (E) are expressed in Joules per gram (J/g). Different feed compositions and sizes are marked with grey and white areas. The carbon-nitrogen (C:N) and nitrogen-phosphorus (N:P) ratios are detailed for each sampling day. Cells with no available data are marked with (-); G = Granulated feed.

Sampling Day	Pellet size (mm)	C	N	P	OC	E	C:N	N:P
t_{14}	1.2G	-	-	-	41.8	-	-	-
t_{28}	1.2G	-	-	-	46.8	-	-	-
t_{42}	1.2G	-	-	-	53.6	-	-	-
t_{56}	1.2G	-	-	-	66.3	-	-	-
t_{70}	1.2G	23.4	4.1	1.7	65.6	19,742	6:1	2:1
t_{84}	1.5	25.5	4.1	3.2	65.6	19,588	6:1	1:1
t_{98}	1.5	25.6	4.2	3.2	65.5	18,245	6:1	1:1
t_{113}	1.5	24.6	4.1	4.3	42.3	18,891	6:1	1:1
t_{126}	1.5	22.1	3.9	5.6	53.2	18,182	6:1	1:1
t_{140}	3.0	24.1	3.9	4.2	54.0	16,589	6:1	1:1
t_{154}	3.0	24.7	3.1	4.8	58.2	18,722	8:1	1:1
t_{176}	3.0	24.6	3.2	5.3	46.0	19,272	8:1	1:1
t_{189}	3.0	26.5	3.6	4.1	45.8	19,302	7:1	1:1
t_{203}	3.0	24.0	4.5	5.5	46.3	15,273	5:1	1:1
t_{225}	3.0	30.9	4.6	6.0	49.3	12,678	7:1	1:1
t_{239}	3.0	32.5	4.5	4.4	43.5	16,403	7:1	1:1
t_{252}	3.0	31.1	4.0	3.9	53.7	19,437	8:1	1:1
t_{266}	3.0	30.4	4.2	3.3	49.9	15,321	7:1	1:1
t_{280}	4.5	32.5	4.7	3.5	39.8	16,683	7:1	1:1
t_{294}	4.5	30.4	4.1	2.6	47.3	19,293	7:1	2:1
t_{308}	4.5	30.7	4.2	3.2	47.6	11,525	7:1	1:1
t_{328}	4.5	30.4	4.0	3.5	43.9	16,812	8:1	1:1
t_{347}	4.5	31.8	3.9	3.4	44.1	18,289	8:1	1:1
t_{361}	4.5	30.2	3.8	3.4	57.7	18,179	8:1	1:1
t_{375}	4.5	31.3	4.1	3.3	51.6	19,554	8:1	1:1
t_{389}	4.5	30.8	4.1	3.5	46.2	17,337	8:1	1:1
t_{403}	4.5	31.1	4.2	3.2	48.5	18,361	7:1	1:1
t_{437}	6.0	31.1	4.0	2.7	46.1	18,526	8:1	1:1

Nitrogen content amounted in average 4.0%. Low values between 3.1% and 3.6% were observed subsequently between day's t_{154} and t_{189} . The phosphorus content in the solid matter was relatively constant around 3.2% and 3.5%, with the exception of the time interval between t_{126} and t_{225} where values raised over 4.0% with a peak on day t_{225} of 6.0%. An extraordinary low value of 1.7% was found on day t_{70} . Organic content remain relatively constant around 50%. Between day's t_{70} and t_{98} the organic matter found in this size class raised to values around 65.5%. The energy content in the solid size class $<50 \mu m$ was in average $17,592 \pm 2,146$ J/g. High and low energy contents were found disperse over the whole experimental period. Low values were found concentrated in the period between day's t_{203} and t_{308} .

Analyzing the data for the particle size class between 50 μm and 100 μm (Tab. 20), the carbon content averaged 20.3%. Exceptional values were found in samples t_{56} with 29.0%, t_{70} with 39.3%, and t_{140} with 38.1% of carbon content. It was observed that the carbon content was lower in this particle size class through all the period in which 1.5 mm pellet was fed (t_{84} until t_{126}). Nitrogen content was found around 2% in average with only one extreme value of 5.7% found in the sample took on day t_{70} . In the same period a very low phosphorous content was found, leading to a highest N:P ratio of 4:1 in the whole experimental period. It is thoroughly possible that small amounts of not ingested feed were present in this size class due to the high carbon and nitrogen content. Sometimes when too small pellets are offered to relatively big size fish there is a high probability that the feed stays in the water without being eaten. The organic content in this particle size averaged 60.6%. The amount of non digested organics was fairly stable through the whole period. The energy content found in this size class was 18,034 J/g in average. Carbon to nitrogen ratios were found to be relatively high compared to the results observed in the smaller size class (<50 μm). Higher C:N ratios during the use of 3 mm pellets were observed.

Tab. 20. Composition of the total suspended solids in the swirl separator receiving the effluent of two fish tanks, collected between day t_{14} and day t_{437} of the study period, for the particle size class between $50 \mu\text{m}$ and $100 \mu\text{m}$. Carbon (C), nitrogen (N), phosphorus (P), and organic contents (OC) are presented as percentage of dry weight (%DW); Energy contents (E) are expressed in Joules per gram (J/g). Different feed compositions and sizes are marked with grey and white areas. The carbon-nitrogen (C:N) and nitrogen-phosphorus (N:P) ratios are detailed for each sampling day. Cells with no available data and ratios below 1:1 are marked with (-); G = Granulated feed.

Sampling Day	Pellet size (mm)	C	N	P	OC	E	C:N	N:P
t_{14}	² 1.2G	20.3	1.9	2.9	63.2	20,827	11:1	1:1
t_{28}	1.2G	-	-	-	67.9	-	-	-
t_{42}	1.2G	-	-	-	70.8	-	-	-
t_{56}	1.2G	29.0	3.1	1.7	63.2	19,922	9:1	2:1
t_{70}	1.2G	39.3	5.7	1.6	51.1	20,430	7:1	4:1
t_{84}	1.5	17.2	1.8	1.9	64.4	20,228	9:1	1:1
t_{98}	1.5	19.0	2.0	2.5	72.8	18,641	9:1	1:1
t_{113}	1.5	23.6	2.5	3.6	63.2	18,553	10:1	1:1
t_{126}	1.5	13.9	1.6	4.7	59.8	16,599	9:1	-
t_{140}	3.0	38.1	2.3	3.1	52.6	15,137	17:1	1:1
t_{154}	3.0	17.1	1.6	4.3	62.5	20,079	11:1	-
t_{176}	3.0	12.1	0.9	4.4	51.1	20,401	13:1	-
t_{189}	3.0	20.3	1.4	3.5	68.4	19,591	15:1	-
t_{203}	3.0	20.4	1.5	4.5	61.7	14,759	13:1	-
t_{225}	3.0	20.8	1.6	5.2	59.6	11,358	13:1	-
t_{239}	3.0	23.9	1.6	4.1	63.4	15,226	15:1	-
t_{252}	3.0	22.0	3.0	5.7	64.6	19,420	7:1	1:1
t_{266}	3.0	19.6	2.4	6.6	58.2	16,370	8:1	-
t_{280}	4.5	13.4	1.2	7.0	49.7	16,214	11:1	-
t_{294}	4.5	15.0	1.2	7.3	53.9	19,730	13:1	-
t_{308}	4.5	14.9	1.0	7.1	50.2	18,669	14:1	-
t_{328}	4.5	15.9	1.2	9.0	49.5	16,829	13:1	-
t_{347}	4.5	18.2	2.0	3.4	62.5	20,475	9:1	1:1
t_{361}	4.5	16.4	1.3	3.6	62.8	18,711	13:1	-
t_{375}	4.5	21.6	2.0	4.1	70.7	19,825	11:1	-
t_{389}	4.5	24.1	2.0	5.1	61.1	17,327	12:1	-
t_{403}	4.5	15.2	1.8	3.9	58.4	19,035	9:1	-
t_{437}	6.0	16.1	2.3	3.9	62.4	17,325	7:1	1:1

The particles from the $100 \mu\text{m}$ to $200 \mu\text{m}$ filter fraction (Tab. 21) showed a relatively constant carbon content during the whole experimental phase (average 19.8%). Comparable high values were subsequently found in samples taken at days t_{28} , t_{42} and t_{70} (Tab. 21), which correspond to the time interval where 1.2 mm granulated pellets were fed. The nitrogen content for this size class showed also relatively high values, between 3.1% and 5.9% for the same time period. With the exception of the sample taken on day t_{252} (3.2%), the rest of the samples showed an average content of 1.4% when the smallest pellet size was fed with the highest protein content (50%) compared to the other diets. The phosphorous content found in the solid matter tended to rise over time with the different diets and pellet sizes, but was highly variable between samples. Average values of 2% were found when 1.2 mm granulated pellet were fed, 3.5% when 1.5 mm feed was used, 3.6% when 3 mm pellet were fed, and 5.8% during the time

where 4.5 mm pellet size was given to the fish. The last sample on day t_{437} (6 mm pellets fed) showed a phosphorous content of 2.9%.

Tab. 21. Composition of the total suspended solids in the swirl separator receiving the effluent of two fish tanks, collected between day t_{14} and day t_{437} of the study period, for the particle size class between $100 \mu\text{m}$ and $200 \mu\text{m}$. Carbon (C), nitrogen (N), phosphorus (P), and organic contents (OC) are presented as percentage of dry weight (%DW); Energy contents (E) are expressed in Joules per gram (J/g). Different feed compositions and sizes are marked with grey and white areas. The carbon-nitrogen (C:N) and nitrogen-phosphorus (N:P) ratios are detailed for each sampling day. Cells with no available data and ratios below 1:1 are marked with (-); G = Granulated feed.

Samplin g Day	Pellet size (mm)	C	N	P	OC	E	C:N	N:P
t_{14}	² 1.2G	15.0	1.4	3.1	60.7	20,356	11:1	-
t_{28}	1.2G	29.1	3.4	1.6	64.0	20,143	9:1	2:1
t_{42}	1.2G	26.7	3.1	1.8	65.9	20,247	9:1	2:1
t_{56}	1.2G	-	-	-	63.3	-	-	-
t_{70}	1.2G	29.7	5.9	1.8	61.5	20,936	5:1	3:1
t_{84}	1.5	17.6	1.7	2.6	67.4	20,437	10:1	1:1
t_{98}	1.5	19.5	1.8	3.4	70.0	17,132	11:1	1:1
t_{113}	1.5	19.3	1.9	3.8	65.5	17,461	10:1	-
t_{126}	1.5	17.6	1.6	4.1	57.9	12,318	11:1	-
t_{140}	3.0	22.0	1.0	2.9	73.2	17,450	21:1	-
t_{154}	3.0	17.9	1.4	3.3	60.5	17,503	13:1	-
t_{176}	3.0	16.0	1.0	3.3	47.3	14,725	15:1	-
t_{189}	3.0	25.9	1.5	1.9	69.8	17,876	18:1	1:1
t_{203}	3.0	20.6	1.3	3.9	61.5	12,959	16:1	-
t_{225}	3.0	19.7	1.2	4.7	63.3	12708	16:1	-
t_{239}	3.0	18.1	1.0	3.0	71.4	16,435	19:1	-
t_{252}	3.0	24.3	3.2	3.5	61.5	18,162	8:1	1:1
t_{266}	3.0	15.5	1.5	5.9	63.3	10,726	10:1	-
t_{280}	4.5	18.5	1.4	6.5	54.9	17,929	13:1	-
t_{294}	4.5	21.2	1.5	6.4	56.1	14,248	15:1	-
t_{308}	4.5	17.9	1.1	6.5	52.1	18,198	16:1	-
t_{328}	4.5	12.0	0.8	5.2	43.8	14,123	15:1	-
t_{347}	4.5	17.0	1.6	7.0	64.6	20,256	10:1	-
t_{361}	4.5	21.1	1.7	3.8	62.7	19,715	13:1	-
t_{375}	4.5	18.5	1.8	6.5	56.6	19,930	10:1	-
t_{389}	4.5	16.6	1.4	7.4	63.1	10,558	12:1	-
t_{403}	4.5	15.3	1.6	3.2	56.3	19,634	10:1	-
t_{437}	6.0	17.1	1.4	2.9	55.8	16,512	12:1	-

The organic content in the suspended solids sampled with mesh size between $100 \mu\text{m}$ and $200 \mu\text{m}$ (Tab. 21) was relatively constant and amounted on average to 61.2%. The energy content found in the solid matter of this size class was found to be over 20,000 J/g when 1.2 mm granulated feed was administrated to the fish. These values can be associated to the high carbon content found in the same period, compared to the rest of the samples. In the samples from day t_{84} until day t_{437} the energy content averaged 16,391 J/g. Carbon to nitrogen ratios varied from 8:1 to 21:1. No correlation was found between the single results and the high variability of the values remained unclear. Due to the high phosphorous content found in the solid matter and the comparable low nitrogen

content, only a few N:P ratios could be established. N:P ratios of 2:1 and 3:1 were found only in the samples of days t_{28} , t_{42} and t_{70} , corresponding to the time where small 1.2 granulated feed was used.

Tab. 22. Composition of the total suspended solids in the swirl separator receiving the effluent of two fish tanks, collected between day t_{14} and day t_{437} of the study period, for the particle size class between 200 μm and 400 μm . Carbon (C), nitrogen (N), phosphorus (P), and organic contents (OC) are presented as percentage of dry weight (%DW); Energy contents (E) are expressed in Joules per gram (J/g). Different feed compositions and sizes are marked with grey and white areas. The carbon-nitrogen (C:N) and nitrogen-phosphorus (N:P) ratios are detailed for each sampling day. Cells with no available data and ratios below 1:1 are marked with (-); G = Granulated feed.

Sampling Day	Pellet size (mm)	C	N	P	OC	E	C:N	N:P
t_{14}	² 1.2G	22.9	1.7	2.2	69.7	20,669	14:1	1:1
t_{28}	1.2G	31.0	2.7	1.2	61.6	20,534	12:1	2:1
t_{42}	1.2G	27.5	2.2	1.1	63.9	20,458	12:1	2:1
t_{56}	1.2G	24.7	2.7	2.1	63.3	20,391	9:1	1:1
t_{70}	1.2G	24.5	3.3	0.8	65.8	20,728	7:1	4:1
t_{84}	1.5	22.3	1.8	2.0	71.2	19,202	12:1	1:1
t_{98}	1.5	22.9	1.7	4.7	67.0	19,171	14:1	
t_{113}	1.5	25.6	1.7	2.3	64.3	14,339	15:1	1:1
t_{126}	1.5	29.4	2.0	3.1	64.3	14,030	15:1	1:1
t_{140}	3.0	25.4	0.7	1.9	70.7	15,234	35:1	
t_{154}	3.0	30.6	1.7	2.0	62.8	16,376	18:1	1:1
t_{176}	3.0	15.9	0.7	2.7	70.2	12,177	22:1	
t_{189}	3.0	20.7	0.8	1.7	73.6	14,909	26:1	
t_{203}	3.0	25.8	1.2	2.7	68.3	13,907	22:1	
t_{225}	3.0	30.6	1.2	2.5	62.5	14,220	25:1	
t_{239}	3.0	31.9	1.0	1.3	62.9	14,325	32:1	1:1
t_{252}	3.0	28.2	2.1	3.0	64.5	19,287	13:1	1:1
t_{266}	3.0	21.8	2.1	3.5	64.2	17,071	10:1	1:1
t_{280}	4.5	21.7	1.0	3.7	70.0	16,930	22:1	
t_{294}	4.5	20.4	1.1	6.7	69.4	12,396	18:1	
t_{308}	4.5	20.5	0.9	5.6	63.4	17,084	23:1	
t_{328}	4.5	30.6	1.7	2.4	57.8	13,788	18:1	1:1
t_{347}	4.5	21.6	1.5	3.9	62.8	20,086	15:1	
t_{361}	4.5	21.8	1.0	3.6	65.7	18,557	22:1	
t_{375}	4.5	26.7	1.5	1.6	66.9	15,669	18:1	1:1
t_{389}	4.5	29.0	1.4	3.1	62.8	15,478	21:1	
t_{403}	4.5	15.0	1.4	5.7	69.5	19,903	10:1	
t_{437}	6.0	17.6	1.4	1.9	73.1	14,488	13:1	1:1

In the size class of particles between 200 μm and 400 μm (Tab. 22) the carbon content found in the solid matter averaged 25%. Values below 20% were found distributed along the time axis, without any relation to the diet composition. Nitrogen content thou were found relatively high in the first months of experimentations, reaching the highest value of 3.3% on day t_{70} . In the samples where extremely low values were measured, like on day t_{140} and t_{176} both with only 0.7%, it was not possible to establish any relationship with neither nutrient nor energy contents. The phosphorous content measured in this particle size varied extremely over the time (minimum 0.8% on day t_{70} and maximum

6.7% on day t_{294}). Only the low values observed in the first 70 days of experimentations (between 0.8% and 2.2) can be associated to the relatively high values found in the nitrogen and energy content. These observations matched to the time during which 1.2 mm granulated pellets was used. The organic content measured in the solid samples averaged 66% and no significant extremely low or high values were observed during the sampling interval. The highest energy content values measured (greater than 20,000 J/g) were again found in the first 5 samples. After that, energy contents averaged only 16,223 J/g. Extraordinary high C:N ratios of 32:1 and 35:1 were found in two samples. The rest of the data showed a high variability over the time. The nitrogen to phosphorous ratio was found to be below one in almost 50% of the samples. N:P ratios of 2:1 and 4:1 were observed in the first months of trials.

Tab. 23. Composition of the total suspended solids in the swirl separator receiving the effluent of two fish tanks, collected between day t_{14} and day t_{437} of the study period, for the particle size class between 400 μm and 800 μm . Carbon (C), nitrogen (N), phosphorus (P), and organic contents (OC) are presented as percentage of dry weight (%DW); Energy contents (E) are expressed in Joules per gram (J/g). Different feed compositions and sizes are marked with grey and white areas. The carbon-nitrogen (C:N) and nitrogen-phosphorus (N:P) ratios are detailed for each sampling day. Cells with no available data and ratios below 1:1 are marked with (-); G = Granulated feed.

Day	Pellet size (mm)	C	N	P	OC	E	C:N	N:P
t_{14}	² 1.2G	22.9	0.9	0.9	71.2	20,147	25:1	1:1
t_{28}	1.2G	-	-	-	72.5	-	-	-
t_{42}	1.2G	32.8	2.1	1.3	61.5	20,273	15:1	2:1
t_{56}	1.2G	28.5	1.8	0.5	61.9	20,076	16:1	4:1
t_{70}	1.2G	26.8	2.8	0.7	64.9	19,705	9:1	4:1
t_{84}	1.5	19.9	1.3	2.5	74.0	19,014	16:1	1:1
t_{98}	1.5	20.0	1.0	1.8	72.8	19,859	20:1	1:1
t_{113}	1.5	25.1	1.2	1.7	69.4	16,970	21:1	1:1
t_{126}	1.5	25.1	1.1	2.8	68.5	15,086	22:1	-
t_{140}	3.0	31.5	1.1	2.4	62.2	16,232	29:1	-
t_{154}	3.0	24.8	1.3	1.6	63.6	18,081	19:1	1:1
t_{176}	3.0	28.1	1.4	3.2	63.5	13,551	20:1	-
t_{189}	3.0	21.5	1.0	2.1	73.6	17,810	21:1	-
t_{203}	3.0	21.9	0.9	2.8	71.7	18,760	23:1	-
t_{225}	3.0	20.9	0.9	1.9	72.2	15,078	23:1	-
t_{239}	3.0	20.4	0.8	1.6	71.8	16,158	25:1	1:1
t_{252}	3.0	22.7	1.4	1.2	72.8	17,469	16:1	1:1
t_{266}	3.0	24.2	1.5	2.8	70.0	19,548	16:1	1:1
t_{280}	4.5	20.8	1.0	5.1	67.9	13,362	21:1	-
t_{294}	4.5	24.2	0.7	4.3	69.1	14,138	37:1	-
t_{308}	4.5	21.6	0.8	2.5	71.8	13,746	27:1	-
t_{328}	4.5	24.8	1.1	1.3	69.7	15,287	23:1	1:1
t_{347}	4.5	25.6	1.6	3.4	68.1	17,584	16:1	-
t_{361}	4.5	22.5	0.7	1.4	73.1	18,662	34:1	-
t_{375}	4.5	23.3	0.7	0.8	71.6	18,025	33:1	1:1
t_{389}	4.5	30.3	0.7	1.6	65.1	17,997	43:1	-
t_{403}	4.5	46.7	2.3	1.8	47.7	15,383	20:1	1:1
t_{437}	6.0	17.0	0.8	1.2	59.7	17,122	22:1	1:1

Particles between 400 μm and 800 μm had an average carbon content of 25% (Tab. 23). Only three measurements were found to be comparably high, with 32.8% on day t_{42} , 31.5% on day t_{140} , and 46.7% on day t_{403} . Two of these samples were associated to a comparably high (greater than average) nitrogen content of 2.1% on day t_{42} and 2.3% on day t_{403} . The rest of the samples showed an average nitrogen content of 1.2%. Again the highest values were observed during the first two months of sampling. Similar results were obtained for the energy content, where the highest values were measured in the first three samples. The solid matter analyzed after these three initial samples averaged 16,859 J/g. The phosphorous content in this particle size class was very different between samples. The highest values were found in three subsequent samples taken between days t_{280} and t_{308} perhaps caused by incomplete feed intake during these days. The percentage of organic matter in the solid fraction collected with mesh sizes between 400 μm and 800 μm averaged 67.8% and remained relatively constant over time. The carbon to nitrogen ratios differed greatly between samples, ranging from 9:1 to 43:1. Nitrogen to phosphorous ratios were above 1:1 only and differed in the samples between days t_{42} (2:1) and t_{70} (4:1).

Tab. 24. Composition of the total suspended solids in the swirl separator receiving the effluent of two fish tanks, collected between day t_{14} and day t_{437} of the study period, for the particle size class between $800 \mu m$ and $1600 \mu m$. Carbon (C), nitrogen (N), phosphorus (P), and organic contents (OC) are presented as percentage of dry weight (%DW); Energy contents (E) are expressed in Joules per gram (J/g). Different feed compositions and sizes are marked with grey and white areas. The carbon-nitrogen (C:N) and nitrogen-phosphorus (N:P) ratios are detailed for each sampling day. Cells with no available data and ratios below 1:1 are marked with (-); G = Granulated feed.

Sampling Day	Pellet size (mm)	C	N	P	OC	E	C:N	N:P
t_{14}	² 1.2G	-	-	-	70.5	-	-	-
t_{28}	1.2G	-	-	-	74.8	-	-	-
t_{42}	1.2G	-	-	-	70.2	-	-	-
t_{56}	1.2G	26.6	1.8	0.6	69.2	20,888	15:1	3:1
t_{70}	1.2G	26.2	1.8	1.5	68.1	20,906	14:1	1:1
t_{84}	1.5	29.0	2.0	2.5	63.8	19,449	14:1	1:1
t_{98}	1.5	20.3	1.7	2.9	73.4	19,943	12:1	1:1
t_{113}	1.5	20.5	1.6	3.1	69.5	17,736	13:1	1:1
t_{126}	1.5	20.1	1.6	3.2	68.1	13,616	13:1	1:1
t_{140}	3.0	34.2	2.8	2.5	58.7	14,815	12:1	1:1
t_{154}	3.0	20.4	1.1	1.9	71.8	15,386	19:1	1:1
t_{176}	3.0	17.6	1.1	3.9	71.8	13,359	16:1	-
t_{189}	3.0	18.4	1.1	1.5	74.3	18,990	17:1	1:1
t_{203}	3.0	21.9	1.5	3.0	70.1	14,626	14:1	1:1
t_{225}	3.0	23.0	1.4	1.8	72.8	14,381	16:1	1:1
t_{239}	3.0	21.3	1.1	2.1	72.9	15,499	19:1	-
t_{252}	3.0	22.6	2.5	2.6	68.1	19,287	9:1	1:1
t_{266}	3.0	21.3	2.3	2.6	70.7	13,914	9:1	1:1
t_{280}	4.5	17.4	1.1	4.7	67.9	19,047	16:1	-
t_{294}	4.5	18.9	0.7	4.0	73.8	13,370	29:1	-
t_{308}	4.5	19.2	0.6	5.6	71.4	14,143	31:1	-
t_{328}	4.5	21.9	1.4	3.8	71.8	16,750	16:1	-
t_{347}	4.5	20.3	1.6	4.3	72.8	18,376	13:1	-
t_{361}	4.5	33.0	1.4	2.6	60.5	20,236	23:1	1:1
t_{375}	4.5	28.5	1.3	1.1	64.8	17,508	23:1	1:1
t_{389}	4.5	31.2	1.3	2.0	59.0	17,380	23:1	1:1
t_{403}	4.5	22.2	0.8	4.1	69.7	17,011	29:1	-
t_{437}	6.0	30.7	1.0	1.1	62.8	18,556	29:1	1:1

The data for nutrient, organic and energy content for the solid matter collected by filter mesh sizes between $800 \mu m$ and $1600 \mu m$ are presented in Table 24. During the first weeks of the experiments, the absence of solid material in the upper size classes was seen and samples for analysis could not be obtained. Carbon content in this size class was measured only after day t_{56} and averaged 23.5%. Relatively high values were observed when the feed composition (pellet size) was changed going from 1.2 mm granulated to 1.5 mm pelletized feed. Carbon content rose from 26.2% to 29%. Later, when 3 mm extruded pellets were used, 34.2 % of carbon content was measured on day t_{140} . Finally, when the feed size was changed again from 4.5 mm to 5 mm, carbon content varied from 22.2% to 30.7%. Taking into account that the same phenomenon was partially observed for the nitrogen and phosphorous content, it is concluded that even using a strategic feeding management regime changing the pellet size or diet

composition, a certain and similar amount of non-digested feed ends up in the suspended solid fraction. The energy content of the gathered solids did not increase considerably when the feed changes became effective, but again the highest energy values were found in the samples between days t_{56} and t_{70} , when 1.2 mm granulated feed was delivered to the fish tanks. The carbon to nitrogen ratio showed a very variable and non correlative distribution. The nitrogen to phosphorous ratio was relatively stable with 1:1 in all samples, with the exception of the sample of day t_{70} which showed a ratio of 3:1.

Tab. 25. Composition of the total suspended solids in the swirl separator receiving the effluent of two fish tanks, collected between day t_{14} and day t_{437} of the study period, for the particle size class $>1600 \mu m$. Carbon (C), nitrogen (N), phosphorus (P), and organic contents (OC) are presented as percentage of dry weight (%DW); Energy contents (E) are expressed in Joules per gram (J/g). Different feed compositions and sizes are marked with grey and white areas. The carbon-nitrogen (C:N) and nitrogen-phosphorus (N:P) ratios are detailed for each sampling day. Cells with no available data and ratios below 1:1 are marked with (-); G = Granulated feed.

Sampling Day	Pellet size (mm)	C	N	P	OC	E	C:N	N:P
t_{14}	² 1.2G	-	-	-	64.2	-	-	-
t_{28}	1.2G	-	-	-	-	-	-	-
t_{42}	1.2G	-	-	-	-	-	-	-
t_{56}	1.2G	-	-	-	95.5	-	-	-
t_{70}	1.2G	-	-	-	86.7	-	-	-
t_{84}	1.5	21.1	1.9	2.2	71.2	20,869	11:1	1:1
t_{98}	1.5	22.4	2.4	2.5	70.6	17,709	9:1	1:1
t_{113}	1.5	21.0	2.4	3.3	67.8	17,280	9:1	1:1
t_{126}	1.5	22.1	2.1	3.7	67.3	17,860	11:1	1:1
t_{140}	3.0	24.8	1.4	2.7	67.7	16,380	18:1	1:1
t_{154}	3.0	25.0	1.7	1.6	67.0	15,469	15:1	1:1
t_{176}	3.0	24.1	2.0	2.5	60.4	14,071	12:1	1:1
t_{189}	3.0	15.8	2.2	1.8	72.4	16,358	7:1	1:1
t_{203}	3.0	14.6	3.0	3.3	67.8	16,890	5:1	1:1
t_{225}	3.0	19.1	2.5	1.6	66.3	14,865	8:1	2:1
t_{239}	3.0	22.1	3.5	2.7	67.7	14,307	6:1	1:1
t_{252}	3.0	16.5	4.4	2.9	60.2	20,295	4:1	2:1
t_{266}	3.0	10.3	2.6	2.8	55.0	13,017	4:1	1:1
t_{280}	4.5	23.1	2.1	3.4	68.0	19,397	11:1	1:1
t_{294}	4.5	19.2	2.1	6.5	62.0	19,496	9:1	-
t_{308}	4.5	15.7	3.2	4.1	41.8	18,541	5:1	1:1
t_{328}	4.5	26.3	2.5	3.2	64.9	12,544	10:1	1:1
t_{347}	4.5	30.0	4.2	3.9	58.9	19,579	7:1	1:1
t_{361}	4.5	20.1	3.9	4.9	63.3	15,293	5:1	1:1
t_{375}	4.5	19.0	3.4	3.2	60.0	19,086	6:1	1:1
t_{389}	4.5	43.6	4.7	0.8	49.2	16,279	9:1	6:1
t_{403}	4.5	23.0	4.3	0.9	68.2	20,585	5:1	5:1
t_{437}	6.0	24.8	1.4	1.4	68.1	18,319	18:1	1:1

As mentioned before, the lack of solids for analysis of all nutrients was mainly particle sizes greater than $1600 \mu m$. These particles were not available during the period where 1.2 mm granulated feed was used (Tab. 25). Only a very small quantity was obtained from the sieve grid on days t_{14} , t_{56} and t_{70} . The particles filtrated allowed the determination of organic content only after burning the glass fibre filter. It was noticed

that particles that seemed to be greater than 1600 μm such as faeces or some fibrous material were mainly retained in the 1600 μm mesh squares of the sieve although they were longer than 1600 μm but definitely smaller in diameter. They simply slipped through the mesh. In some cases these solids were trapped through the sieve square grid but were flushed into the next sieve when more material from the glass beaker was added to the sieve during the collection procedure. This methodological source of possible error is unavoidable. Table 25 shows the results of the nutrient analysis of the solid material found in the size class $>1600 \mu\text{m}$. Carbon content fluctuated between 10.3% and 43.6%, and averaged 21.9%. Significant increments were obtained from samples taken right after the pellet size was changed. Nitrogen contents averaged 2.7%. Contents above 3% were observed during the last months of the experiment. After every pellet change, the nitrogen content in the solid material decreased. This difference was considerable with the last pellet size change, decreasing from 4.3% to 1.4%. This observation remains unexplained since it was expected that, when a pellet size change takes place, the nutrient contents in the upper particles size category should increase.

Figure 66 shows the quantitative comparison of total suspended solids collected in the swirl separator for each particle size class in relation to the three feed s used during this study. Carbon, nitrogen, phosphorous, ashfree organic, and energy content are presented. Data were averaged for the samples in which the same feed was used. As already reported in Materials and Methods feed 1 was fed from the beginning until t_{70} ; Feed 2 between t_{71} until t_{126} ; Feed 3 was utilized from t_{127} until t_{437} . Data are unfortunately lacking for the size class greater than 1600 μm in the feed 1 fed to small fish ($<17 \text{ g}$), due to insufficient collected material or absence of solid matter for analysis. The volume recovered was just sufficient to determine ashfree organic matter. Therefore no material was left for the analysis of nutrients and energy content. Carbon content in samples taken from the swirl separator was in general higher when the feed 1 was used, with exception of particles smaller than 50 μm (Fig. 66a). Relative high carbon contents was found in the particles between 50 and 200 μm . Differences in this range of collected particles in relation to the other feeds were significant ($p < 0.05$). No significant difference were found in the remaining size classes ($p > 0.05$). The carbon content in particles ranging between 200 and 1600 μm was around 25% higher when the feed 1 was fed compared to the other two feeds. Carbon content in particles ranging between 50 and 200 μm however, was only 2% to 5% lower when feed 1 was used compared to feed 2 and 3, respectively. Nitrogen content in the three feed types was significantly different for the particle size fraction between 50 and 800 μm ($p < 0.05$) (Fig. 66b). This was mainly because of the higher protein content in feed 1 (50%). However, it remained

unclear why in small particles ($<50 \mu\text{m}$) and particles larger than $800 \mu\text{m}$ no significant differences were found in terms of nitrogen content between the three feeds ($p>0.05$).

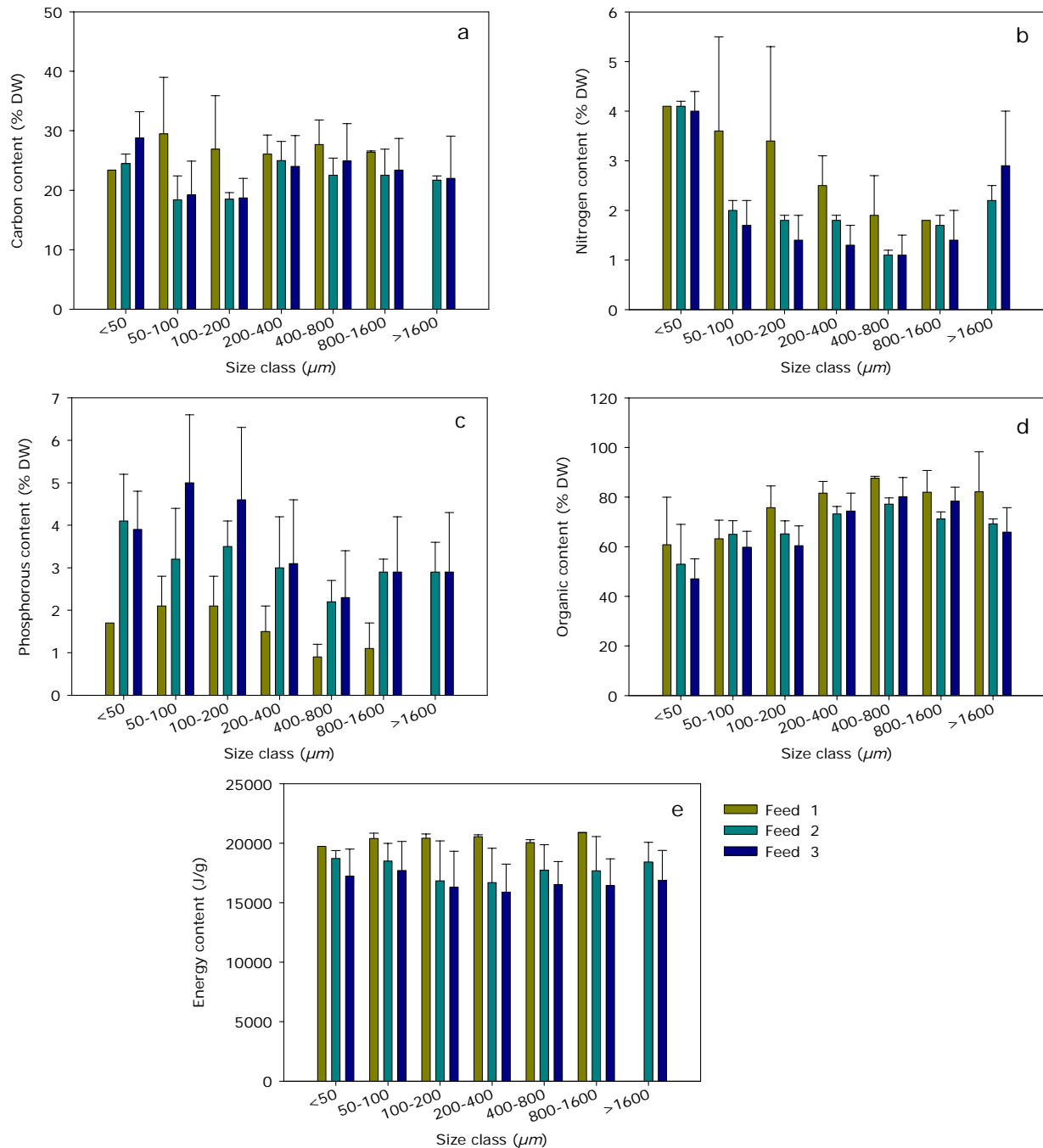


Fig. 66. Comparison of nutrients and energy of the total suspended solids collected from the swirl separator receiving the effluent of two fish tanks, between day's t_{14} and t_{437} , detailed for the three different feeds used (see chapter 3.5). Feed 1 was t_0 - t_{70} ; Feed 2 t_{71} - t_{126} ; Feed 3 t_{127} - t_{437} . Columns: mean \pm S.D., calculated for each size class and period ($n=5$ for Feed 1; $n=4$ for Feed 2; $n=19$ for Feed 3). Nitrogen (a), phosphorous (b), carbon (c), and ashfree organic content (d) are presented as percentage of dry weight (%DW) of the total amount of solids collected in the sample. Energy contents (e) are expressed in Joules per gram (J/g).

Even for particles smaller than 50 μm derived from feed 1 and 2, the highest nitrogen contents (around 4%) occurred. Additionally, solid matter in the size class $>1600 \mu\text{m}$ had relatively higher nitrogen contents when feed 1 and 2 was used only.

Phosphorous contents in various waste particle sizes derived from all three feeds are presented in Figure 66c. Data are fairly scattered shown high variability. However, significant differences were found between particles derived from feed 1 and the other two feeds in all particle size classes. Overall feed 1 yielded the lowest phosphorous content in system particles while feeds 2 and 3 provided much higher but fairly comparable results for particle size classes above 200 μm . In particle sizes between 50 and 200 μm , feeding diets 2 and 3 yielded significantly different but highest phosphorous contents in particles as determined during the entire experimental series.

The ashfree organic contents for all particle sizes are presented in Figure 66d, exhibiting a slight upward trend with particle size up to 800 μm regardless of the feed used. For all feeds types there was a slightly decline in the two highest particle classes ($> 800 \mu\text{m}$). Feed 1 yielded always the highest ashfree organic content in the particles collected in the swirl separator.

Energy contents expressed in J/g showed relative constant values in samples with each of feed types used (Fig. 66e). Highest energy contents were found in the solid matter when feed 1 was used, followed by feed 2 and finally feed 3. Feed 1 had a gross energy content of about 20,700 J/g on average $20,390 \pm 380 \text{ J/g}$ ($n=3$) were found present in the solid particles; Feed 2 gross energy was 21,590 J/g and $17,800 \pm 2,190 \text{ J/g}$ ($n=3$) were determined in the solids; Feed 3 had a gross energy content of 21,920 J/g according to the manufacturer and $16,700 \pm 2,430 \text{ J/g}$ ($n=3$) were found in the faeces and solids derived in the system with this feed. The energy found in the solid matter was about 98% of the energy content of the feed containing mainly non-digestible energy for the fish. Feed 1 had small pellet sizes (1.2 mm granulated) with low gross energy content. In contrast, when feed 3 was used (3, 4.5, and 6 mm pellets) only 76% of the gross energy content was found in the solids when compared to the feed.

The number of observations (values) for every determination differed between each type of feed utilized because the numbers of days sampled during which different feeds were used (diet composition and pellet size) increased with time.

3.4.2. Description of particle shape and size

To distinguish solids by size classes by fractionating the samples allowed collecting material from each size class and examining them microscopically using two different optical techniques.

Although described in Material and Methods, it is worthwhile noting some methodological specifics to understand the presentation of results more clearly.

The solid particles below $400\ \mu\text{m}$ were prepared for Digital scanning microscopy (DSM) and were collected via micro fibre filters, dried at 60°C and therefore resulted often in some fragmentation of particles. Additionally, particles that were originally agglomerates were often separated after drying and appeared as individual items. Fragile and apparently “soft” solid matter was seen to be partly attached to or stuck in the filter pore, as result of the vacuum filtration.

Normal microscopy (binocular) was used to study the solid material larger than $400\ \mu\text{m}$. To avoid the drying of the samples they were put into a small Petri dish with distilled water to obtain a much clear appearance of particle agglomerations. Photography with a white/greyish background allowed sufficient contrast at surfaces for the later isolation of particles and image analysis with the Image-J software. Here, the observations through the binocular corresponded well with photography that was taken by the video camera. The DSM technique provided images with a uniform pattern and it was impossible to generate pictures with sufficient contrast for image analysis. On the other hand, DSM pictures presented a realistic description of the three dimensional properties of the solid particles.

The following sets of pictures were selected as they are judged to be representative examples from the 28 samples taken between day t_0 and day t_{437} . Samples presented correspond to samples dates 2 (t_{28}), 4 (t_{56}), 8 (t_{113}), 12 (t_{176}), 16 (t_{239}), 20 (t_{294}), 24 (t_{361}), and 28 (t_{437}), reflecting an even distribution of samples along the time axis so that system particles derived from all feeds and feed size changes were considered. Photography obtained with the binocular are presented along with the image analysis.

The microscopic examination of particles below $400\ \mu\text{m}$ taken in the samples mesh on day t_{28} (Fig. 67) show fine solid material of unknown composition but presumably containing calcareous material because of its shape and appearance (unusual for organic

particles) (Fig. 67a, b, and d), as well as a single particle fractured into several smaller ones (Fig. 67c).

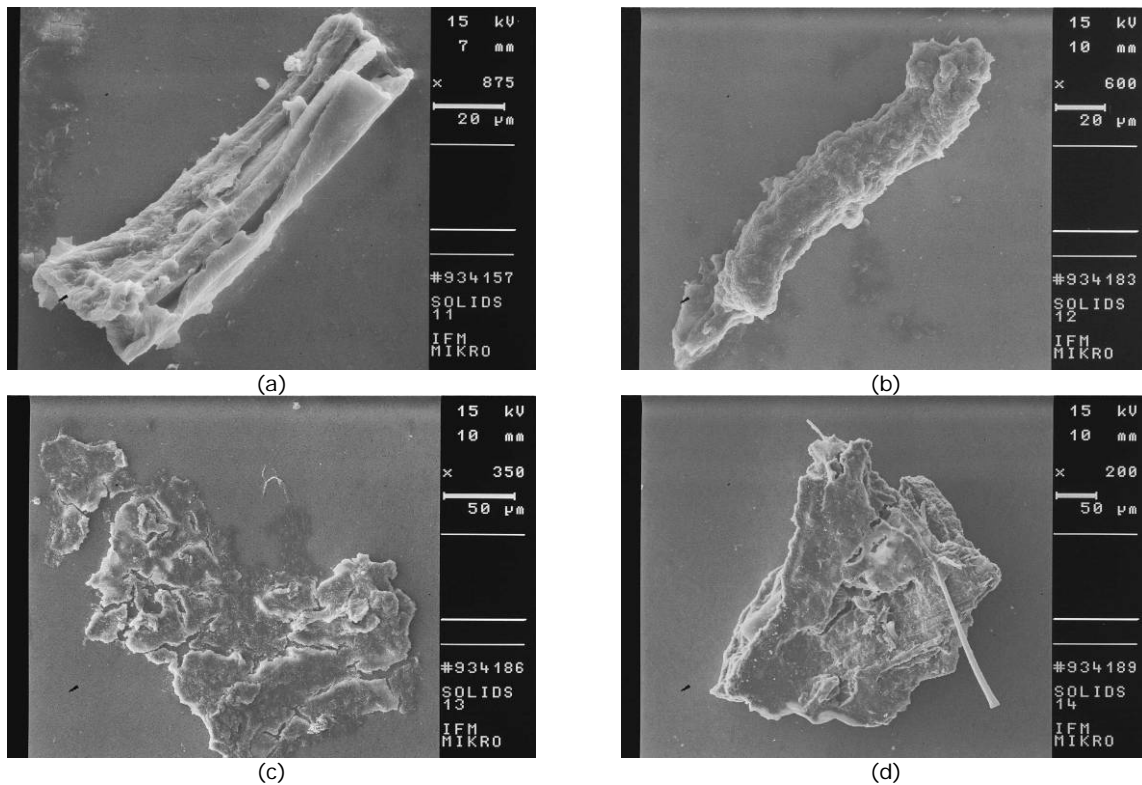


Fig. 67. Examples on particle size and shape of suspended solids (digital scanning microscope (DSM) photography) of the swirl separator on day t_{28} . (a) Particle sampled after filtering with a mesh size of $50\ \mu\text{m}$; (b) Particles sampled with mesh size range of $50\text{-}100\ \mu\text{m}$; (c) Particles sampled with mesh size range of $100\text{-}200\ \mu\text{m}$, and (d) Particles sampled with mesh size range of $200\text{-}400\ \mu\text{m}$. Scaling bars in each picture.

Particles belonging to larger size classes ($400\text{-}800\ \mu\text{m}$ and $800\text{-}1600\ \mu\text{m}$) exhibit a total calculated surface of around $2.0\ \text{mm}^2$ (surface area was calculated on the simplified assumption of a flat and not round form; all particles were considered to have even surface). This is because the Image-J software is incapable of three dimensional analyses.

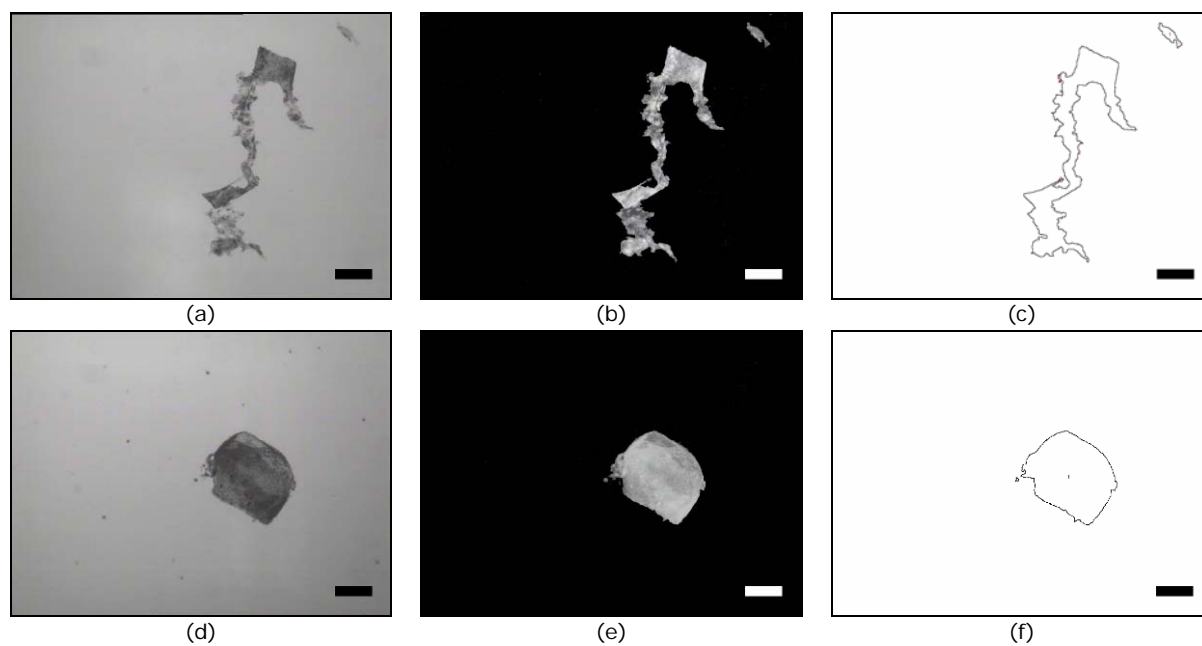


Fig. 68. Photography of suspended solids collected from the swirl separator on day t_{28} . The raw pictures (a,d) were transformed (b,e) and analyzed to determine particle surface area (c,f). Figures a,b,c showed an example of particles isolated from the 400-800 μm size fraction, and figures d,e,f showed an example of particles isolated from the 800-1600 μm size fraction. Scale bar = 500 μm .

The five particles counted by the software (Fig. 68c) of which only one was found to be greater than the 400 μm mesh size of the sieve indicates that also smaller particles sizes are captured by this filter. The particles displayed in Figure 68f had a surface area of 1.9 mm^2 .

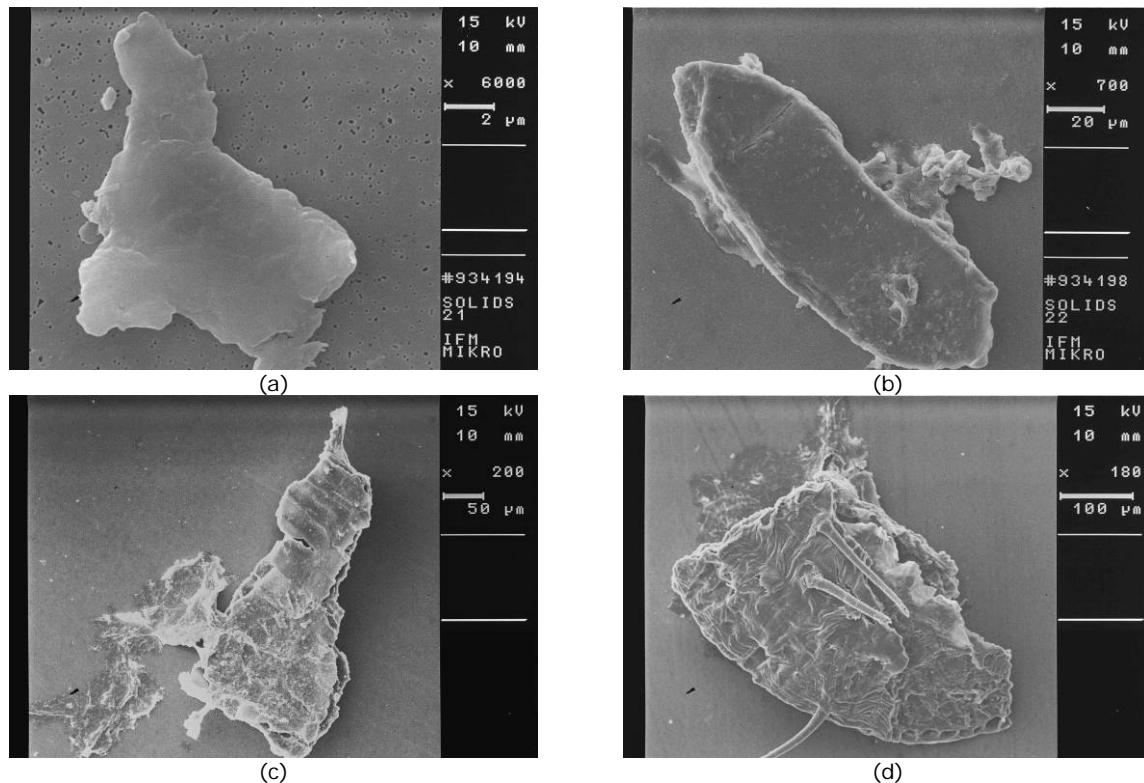


Fig. 69. Examples on particle size and shape of suspended solids (digital scanning microscope (DSM) photography) of the swirl separator on day t_{56} . (a) Particle sampled after filtering with a mesh size of $50 \mu\text{m}$; (b) Particles sampled with mesh size range of $50\text{-}100 \mu\text{m}$; (c) Particles sampled with mesh size range of $100\text{-}200 \mu\text{m}$, and (d) Particles sampled with mesh size range of $200\text{-}400 \mu\text{m}$. Scaling bars in each picture.

Figure 69 depicts particles of the minor size fractions analyzed by scanning microscopy. Figure 69a represents an example of the size class $<50 \mu\text{m}$. The figure includes a particle less than $1 \mu\text{m}$ (upper left corner of the figure), indicating that sometimes very small particles are trapped with larger ones (as one may expect). In Figure 69c and 69d firmly inorganic looking material form long and thin particles of various origins (*i.e.* fibre?) and seem to attach quite frequently, affecting the volume to surface ratio of the overall particle flow.

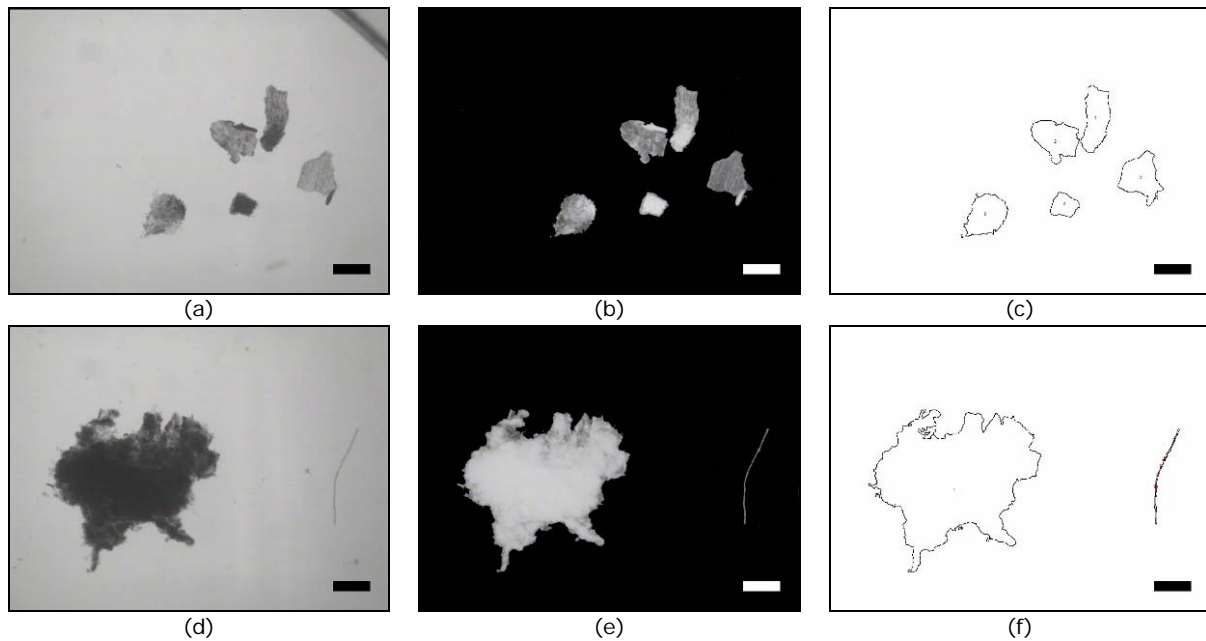


Fig. 70. Photography of suspended solids collected from the swirl separator on day t_{56} . The raw pictures (a,d) were transformed (b,e) and analyzed to determine particle surface area (c,f). Figures a,b,c showed an example of particles isolated from the 400-800 μm size fraction, and figures d,e,f showed an example of particles isolated from the 800-1600 μm size fraction. Scale bar = 500 μm .

Solids collected from the swirl separator and captured by mesh sizes between 400-800 μm are presented in Figure 70 (a, b, c) and they also represent a wide size range. Although optically all particles seem to be in a similar size category, only 50% of all particles counted ($n=7$) were greater than the sieve mesh size ($160,000 \mu^2$), indicating again that smaller particles are retained along with larger ones.

The image of the particle shown in Figure 70d, e, and f had a calculated total surface area of 2.7 mm^2 . It presented a very soft spherical particle. Considering the diameter of the particle, it should have been retained in the filter $>1600 \mu\text{m}$, which would be equivalent to a surface area of 2.6 mm^2 . Instead, it was found in the size sample fraction 800-1600 μm , probably passing through the 1600 sieve by the flushing pressure during the handling of the sample or by the flexibility to temporarily change its shape under external forces.

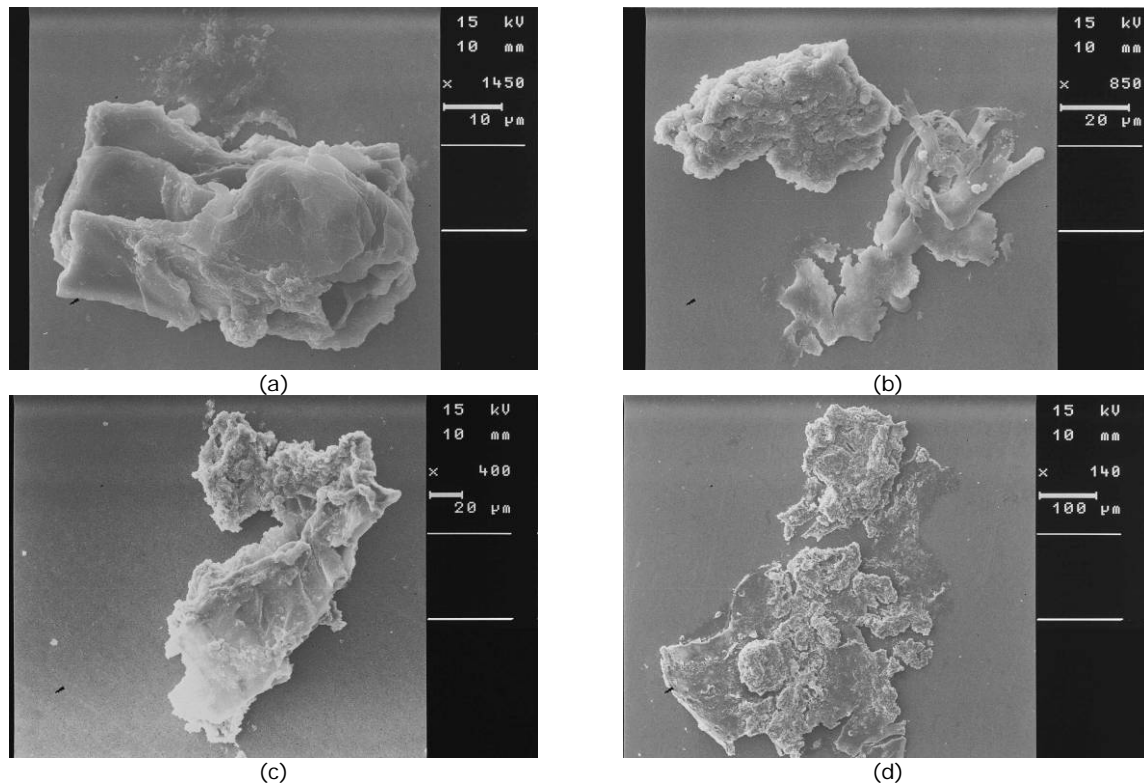


Fig. 71. Examples on particle size and shape of suspended solids (digital scanning microscope (DSM) photography) of the swirl separator on day t_{113} . (a) Particle sampled after filtering with a mesh size of $50 \mu\text{m}$; (b) Particles sampled with mesh size range of $50\text{-}100 \mu\text{m}$; (c) Particles sampled with mesh size range of $100\text{-}200 \mu\text{m}$, and (d) Particles sampled with mesh size range of $200\text{-}400 \mu\text{m}$. Scaling bars in each picture.

The particles depicted in Figure 71 represent sizes of various shapes being in the range of approximately $35 \mu\text{m}$ (smaller) to $500 \mu\text{m}$ (larger) sizes. They were all retained by various filtration mesh sizes as indicated in the figure caption.

All the samples taken were gently flushed with distilled water during the vacuum filtration. Looking at the samples in Figure 71 it seems that, reaching a certain point, a particle cannot break down more by simply flushing it with water. Instead, fragile particles of apparently soft material (Fig. 71b and 71d) seem to fracture because of drying. On the other hand, solid particles shown in Figure 71a, 71b (upper left hand particle) and 71c represented firm and strong particles not disintegrated during heating or drying.

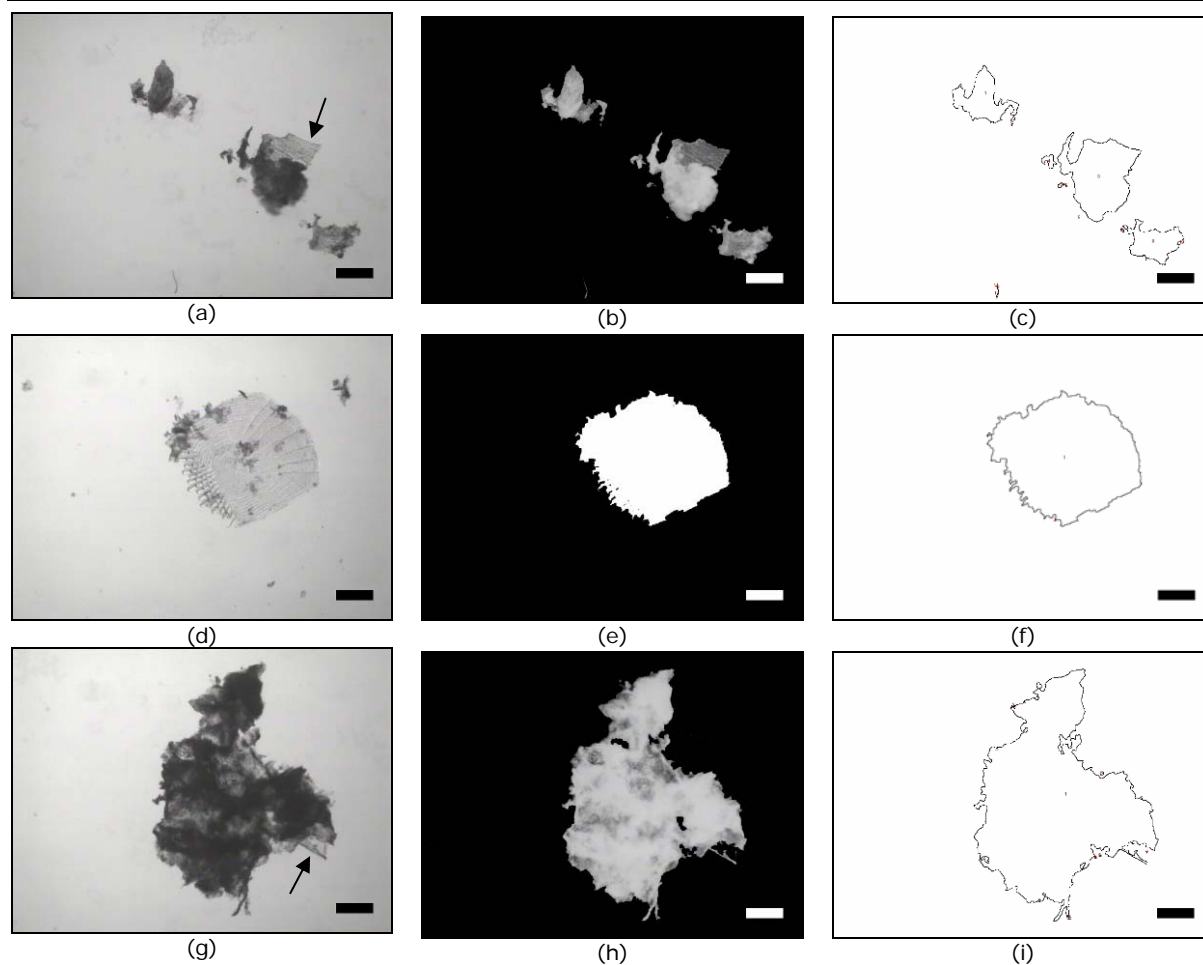


Fig. 72. Photography of suspended solids collected from the swirl separator on day t_{113} . The raw pictures (a,d,g) were transformed (b,e,h) and analyzed to determine particle surface area (c,f,i). Figures a,b,c showed an example of particles isolated from the 400-800 μm size fraction, and figures d,e,f showed an example of particles isolated from the 800-1600 μm size fraction, and figures g,h,i showed an example of particles isolated from the >1600 μm size fraction. Scale bar = 500 μm . Arrows indicate attached particles.

During the sampling and analysis of the solid material many fish scales were observed. They occurred in almost every sample taken during the entire experimental period. Several times it was observed that the fish behaved very aggressively during feeding. The spines dorsal fin in *Dicentrarchus labrax* is relative long and extends during feeding frenzy. This behaviour may cause mechanical stress among fish rubbing their skin leading to epidermis lesions with scale losses. Figure 72d shows a small firm ctenoid scale covering an area of about 2.3 mm^2 . Very small particles were found to be attached to this small scale the spines of the scale thereby acting as particle trap. Very soft laminar tissue seems also to attract other particles (Fig. 72a and 72g light areas indicated by arrows). The particle presented in Figure 72g had a total surface of 8.2 mm^2 . The group of particles that shows Figure 72a could thoroughly been one piece before handling.

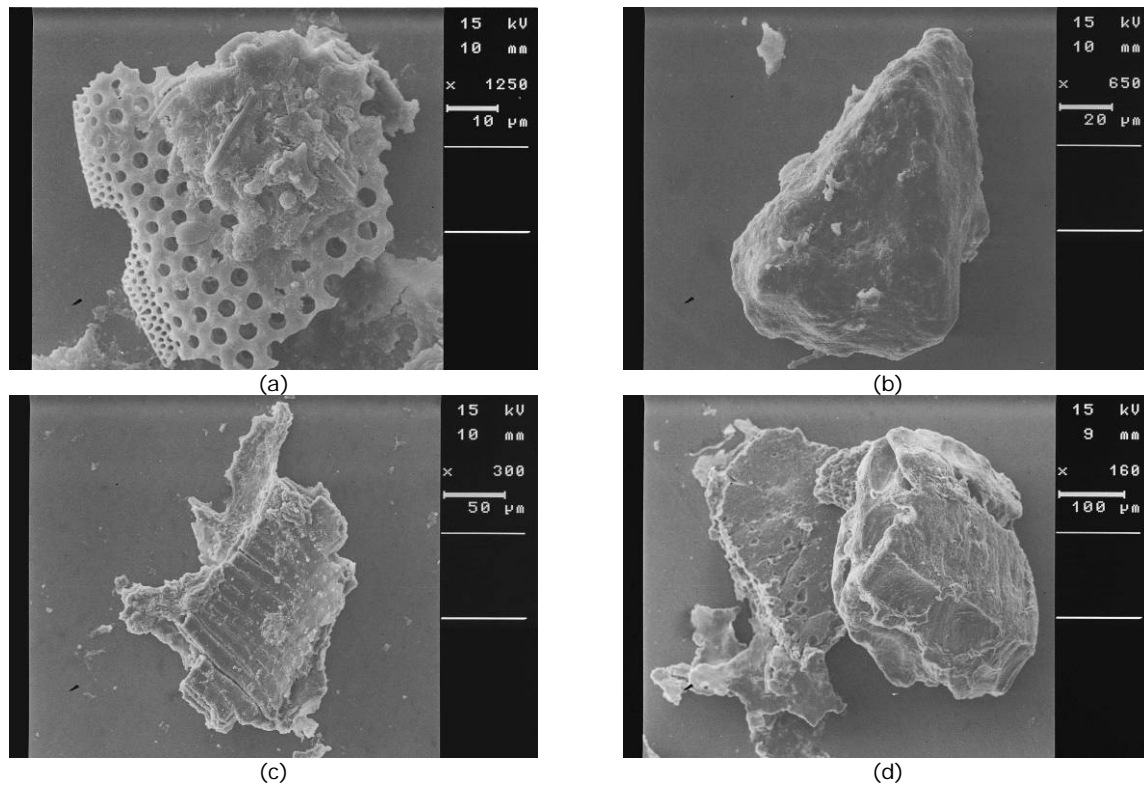


Fig. 73. Examples on particle size and shape of suspended solids (digital scanning microscope (DSM) photography) of the swirl separator on day t_{176} . (a) Particle sampled after filtering with a mesh size of $50 \mu\text{m}$; (b) Particles sampled with mesh size range of $50\text{-}100 \mu\text{m}$; (c) Particles sampled with mesh size range of $100\text{-}200 \mu\text{m}$, and (d) Particles sampled with mesh size range of $200\text{-}400 \mu\text{m}$. Scaling bars in each picture.

The DSM observations of filtered material showed also structures that were presumable broken pieces of a specimen of the diatom *Coscinodiscus radiatus* (Fig 73a). Additional particulate matter covers the surface of this diatom fraction. Figure 73b and 73d shows firm particles apparently representing grains of fine sand. Because of the preparatory method used it is uncertain but likely that these features represent attached bacteria.

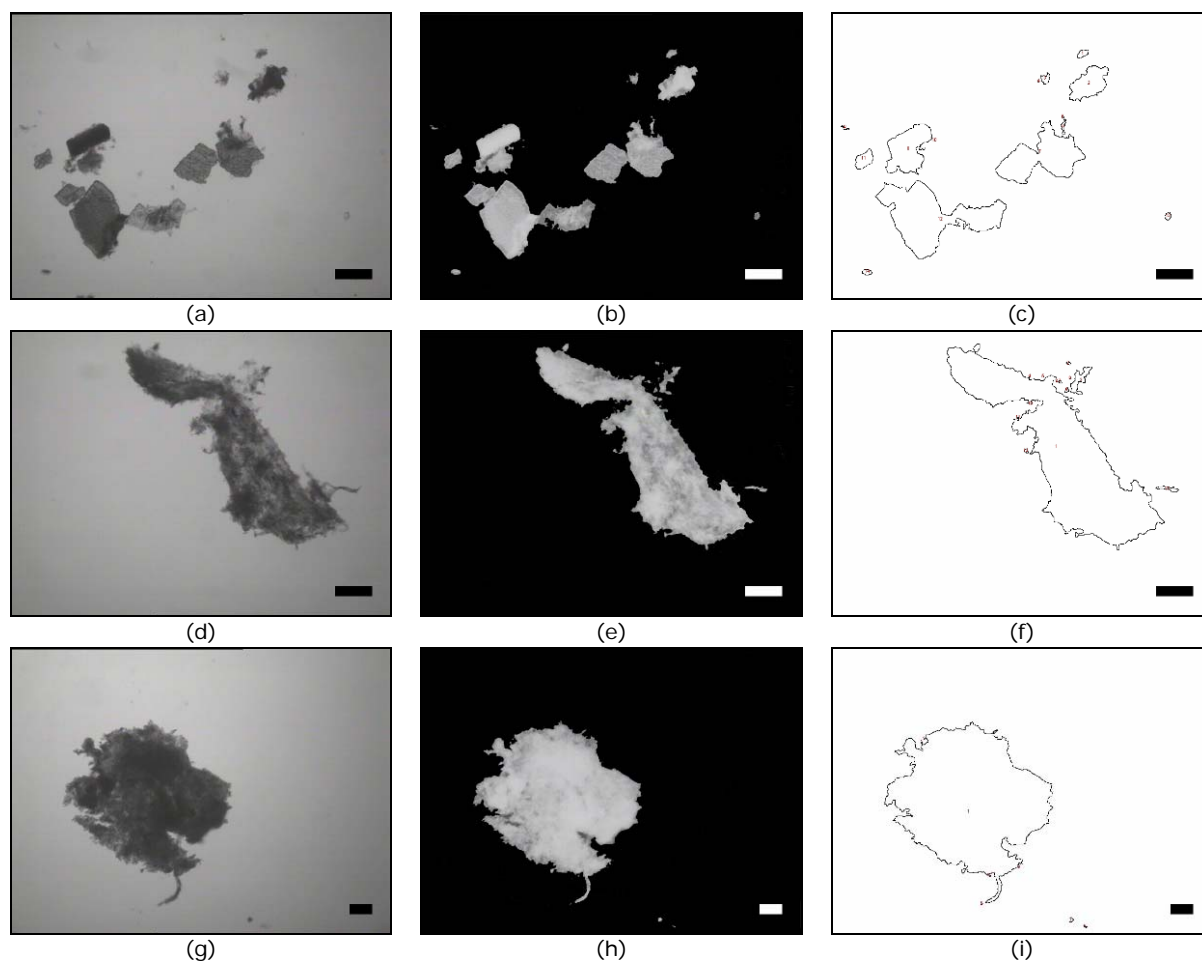


Fig. 74. Photography of suspended solids collected from the swirl separator on day t_{176} . The raw pictures (a,d,g) were transformed (b,e,h) and analyzed to determine particle surface area (c,f,i). Figures a,b,c showed an example of particles isolated from the 400-800 μm size fraction, and figures d,e,f showed an example of particles isolated from the 800-1600 μm size fraction, and figures g,h,i showed an example of particles isolated from the >1600 μm size fraction. Scale bar = 500 μm .

Normally, the solid matter collected from the RAS had a dark brown colour. After filtrating and during microscopic observations sometimes exhibited light brown colour and some were white and/or some slightly green. Figure 74a shows a group of light and dark brown particles. Single particles were found to be relatively thin and almost transparent. Similar particles were found to form conglomerates and therefore appeared as one single dark brown particle. Particles presented in Figure 74 (a-c) had an added total surface area of 3.5 mm^2 . Figure 74d and 74g shows two examples of particulate matter collected from the swirl separator with the same texture and colour, but different shape. Surface area coverage of both particles was slightly different (5.1 mm^2 , Fig. 74d, semi-transparent; 5.9 mm^2 in Fig. 74g, dark appearance).

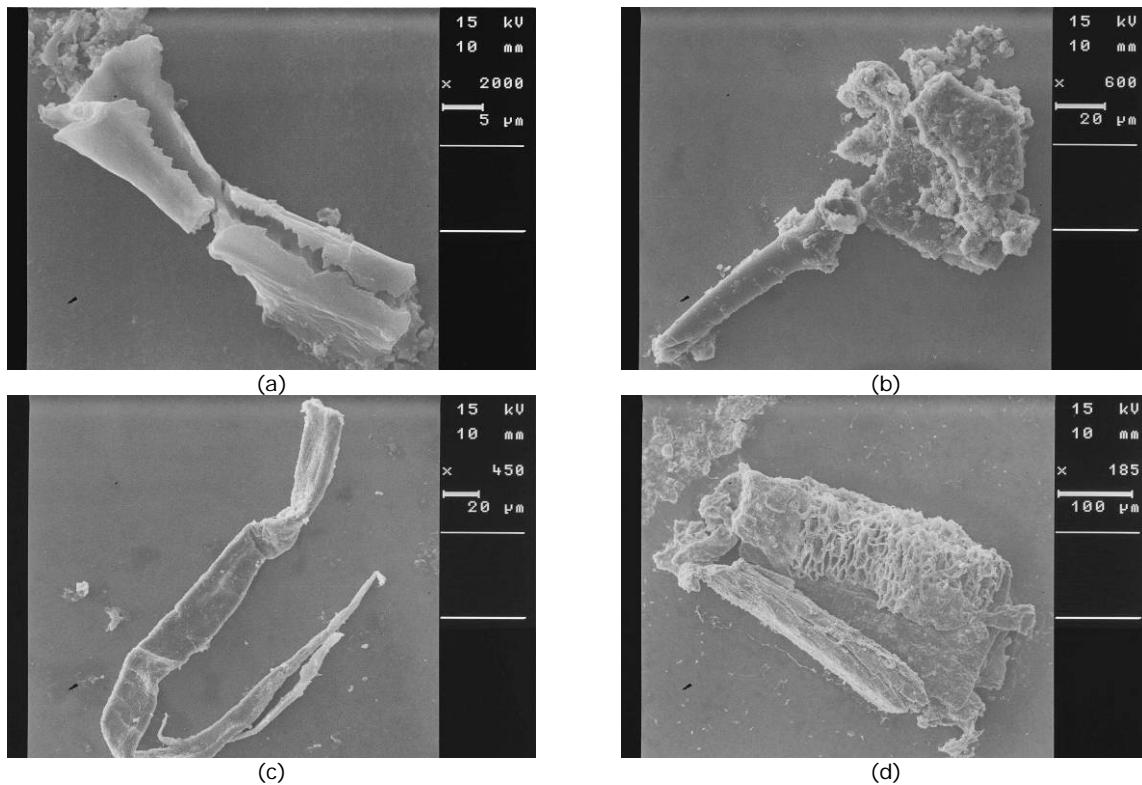


Fig. 75. Examples on particle size and shape of suspended solids (digital scanning microscope (DSM) photography) of the swirl separator on day t_{239} . (a) Particle sampled after filtering with a mesh size of $50 \mu\text{m}$; (b) Particles sampled with mesh size range of $50\text{-}100 \mu\text{m}$; (c) Particles sampled with mesh size range of $100\text{-}200 \mu\text{m}$, and (d) Particles sampled with mesh size range of $200\text{-}400 \mu\text{m}$. Scaling bars in each picture.

Particles collected from sample number 16 (t_{239}) presents Fig. 75. Showing another set of examples of commonly observed shapes tending to break into pieces (Fig. 75a) or attach to soft particles when having a rod-shaped form of relatively hard material. Figure 75c and d may represent long cells of algal or plant origin which often occurred in samples. However, identification was impossible after sample drying.

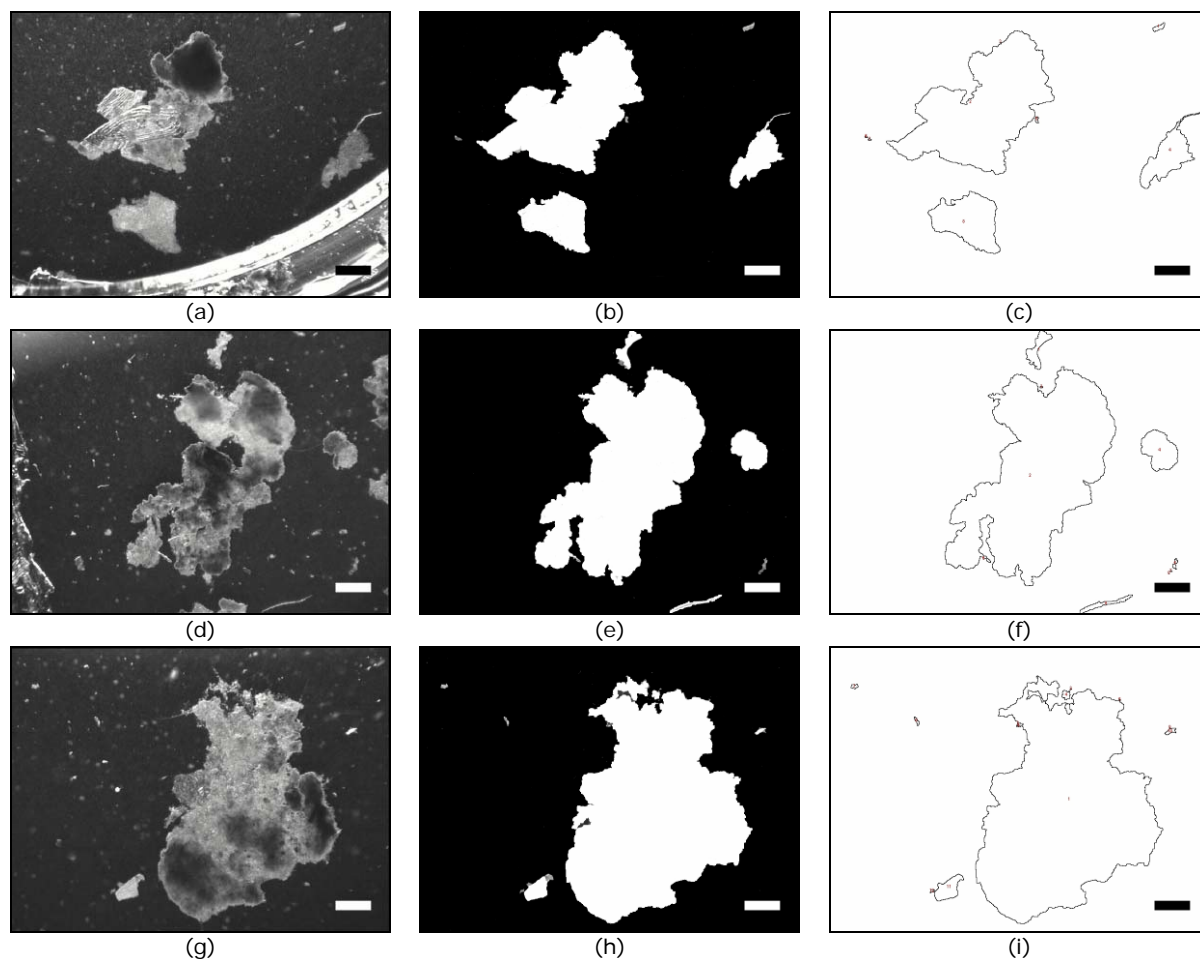


Fig. 76. Photography of suspended solids collected from the swirl separator on day t_{239} . The raw pictures (a,d,g) were transformed (b,e,h) and analyzed to determine particle surface area (c,f,i). Figures a,b,c showed an example of particles isolated from the 400-800 μm size fraction, and figures d,e,f showed an example of particles isolated from the 800-1600 μm size fraction, and figures g,h,i showed an example of particles isolated from the >1600 μm size fraction. Scale bar = 500 μm .

With the increase in fish body weight (*i.e.* biomass in the system), the relative portion of bigger particles increased and bigger agglomerates were identified. Figure 76a shows an aggregation of particles surrounding a piece of a fish scale. Figure 76d presents an example of one solid particle with several solid characterisations identified by its texture, colour and transparency. The same phenomenon can be seen in Figure 76g. It is assumed that these particles originate from fish faeces more than from undigested *i.e.* not consumed feed. The three particles depicted in Figure 76c had a total surface of 0.3, 0.5, and 2.2 mm^2 , respectively. The total surface for the main particles in Figure 76f and 76i amounts 8.4 mm^2 and 11.3 mm^2 , respectively.

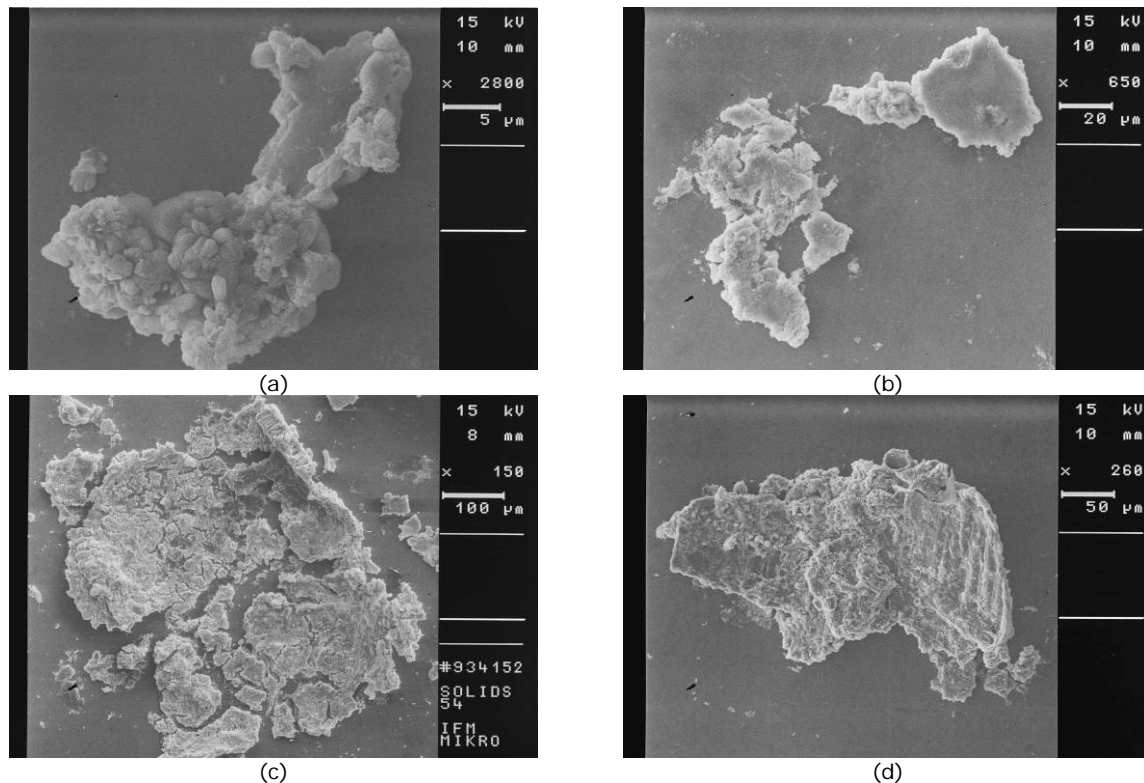


Fig. 77. Examples on particle size and shape of suspended solids (digital scanning microscope (DSM) photography) of the swirl separator on day t_{294} . (a) Particle sampled after filtering with a mesh size of $50 \mu\text{m}$; (b) Particles sampled with mesh size range of $50\text{-}100 \mu\text{m}$; (c) Particles sampled with mesh size range of $100\text{-}200 \mu\text{m}$, and (d) Particles sampled with mesh size range of $200\text{-}400 \mu\text{m}$. Scaling bars in each picture.

Some particles presented a strong wrinkled surface, making it impossible to determine accurately their true surface area coverage because of many edges (Fig. 77a). Fractured (Fig. 77b and 77c) and firm (Fig. 77d) particles were also present in this sample. It was presumed that these particles in depicted in Figure 80c were wrinkled and perhaps shrunk because of drying. Therefore, these figures provide some basic information about the characteristics of the particles more than precise information on their original size and shape. It was suspected that these fractured solids had their origin in soft organic tissue with high water content. The material that appeared inorganic (*i.e.* calcareous?), was clearly distinguishable and seemed often to be broken by mechanical forces.

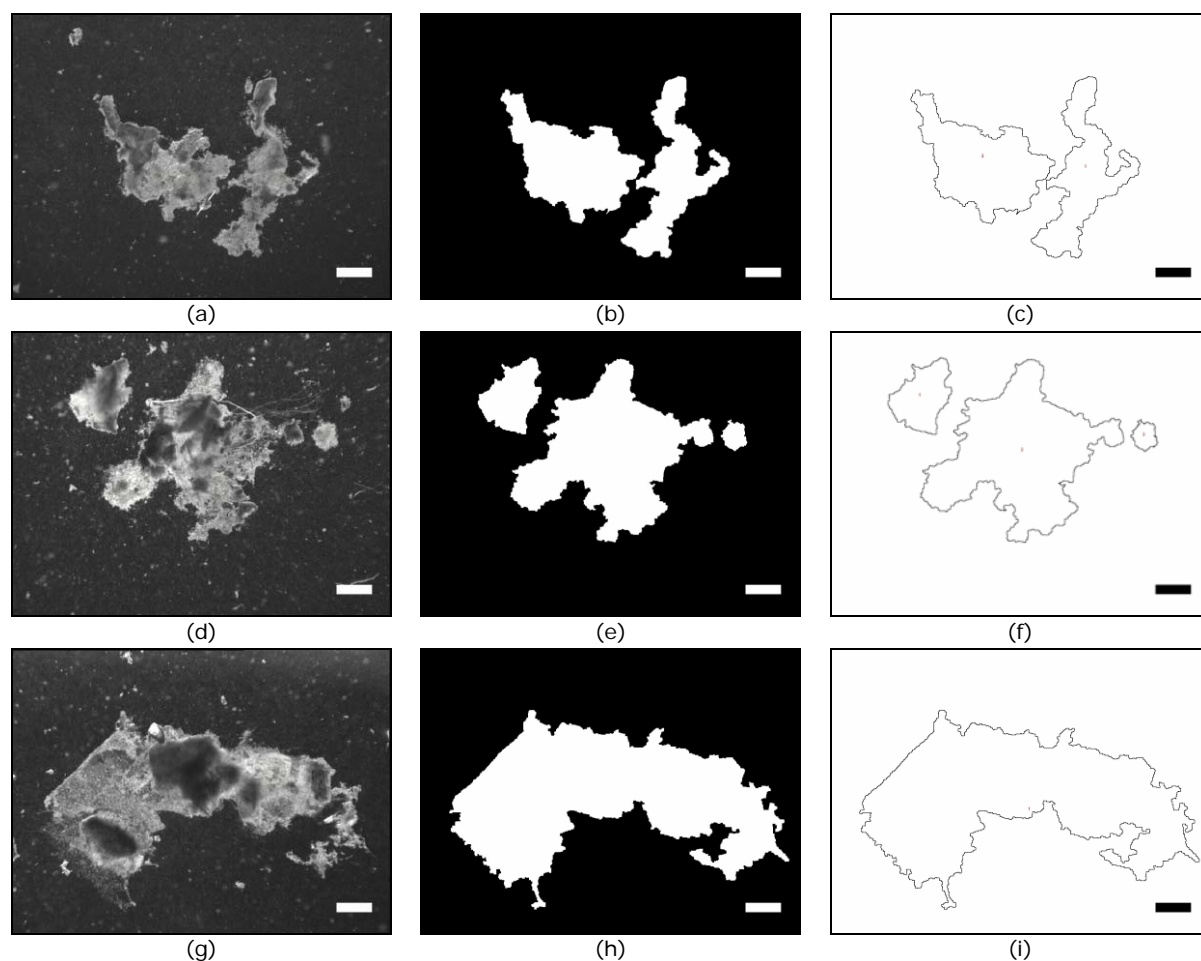


Fig. 78. Photography of suspended solids collected from the swirl separator on day t_{294} . The raw pictures (a,d,g) were transformed (b,e,h) and analyzed to determine particle surface area (c,f,i). Figures a,b,c showed an example of particles isolated from the 400-800 μm size fraction, and figures d,e,f showed an example of particles isolated from the 800-1600 μm size fraction, and figures g,h,i showed an example of particles isolated from the >1600 μm size fraction. Scale bar = 500 μm .

Figure 78 presents examples for particles from the samples taken on day t_{294} (sample 20) for the size classes between 400 and >1600 μm mesh size. Agglomerations were often observed at that time. Some fine thread-like material can be seen in Figure 78d but, unfortunately they were too diffused and fine and therefore, not recognized by the Image-J software. They are therefore not included in the surface analysis. Figure 78d and 78g shows different agglomerated materials characterising particles. Total surface of such particles have also been measured and those in Figure 78a represented a total surface area of 6.1 mm^2 , in Figure 78d they covered 6.7 mm^2 , and Figure 78g read 12.2 mm^2 .

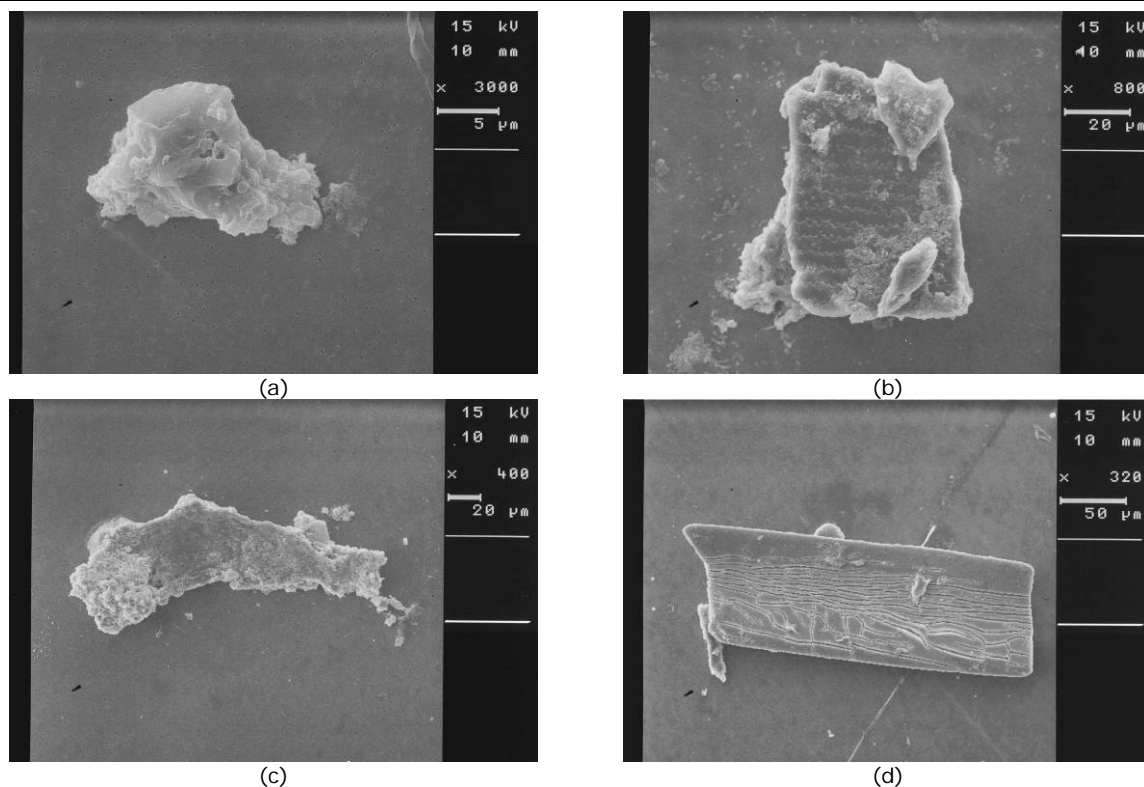


Fig. 79. Examples on particle size and shape of suspended solids (digital scanning microscope (DSM) photography) of the swirl separator on day t_{361} . (a) Particle sampled after filtering with a mesh size of $50 \mu\text{m}$; (b) Particles sampled with mesh size range of $50\text{-}100 \mu\text{m}$; (c) Particles sampled with mesh size range of $100\text{-}200 \mu\text{m}$, and (d) Particles sampled with mesh size range of $200\text{-}400 \mu\text{m}$. Scaling bars in each picture.

Particles of inorganic origin were not too abundant but found occasionally and the sample of day t_{361} is a good example to be presented here (Fig. 79b and 79d). Very small inorganic particles (Fig. 79a) were few and difficult to find. They appeared to be fractions from bigger particles more than belonging to solid matter that can be easily removed from the swirl separator but stayed in the collection chamber, moving around for a long time and thereby grinded down further. The percentage of solids belonging to this size class (below $50 \mu\text{m}$) was found to be less than 5% in these samples. Figure 79c shows a solid fragment to which smaller particles are apparently still attached and may be released soon by mechanical forces. Figure 79c and d depicts fairly intact inorganic particles with some attached material of unclear origin.

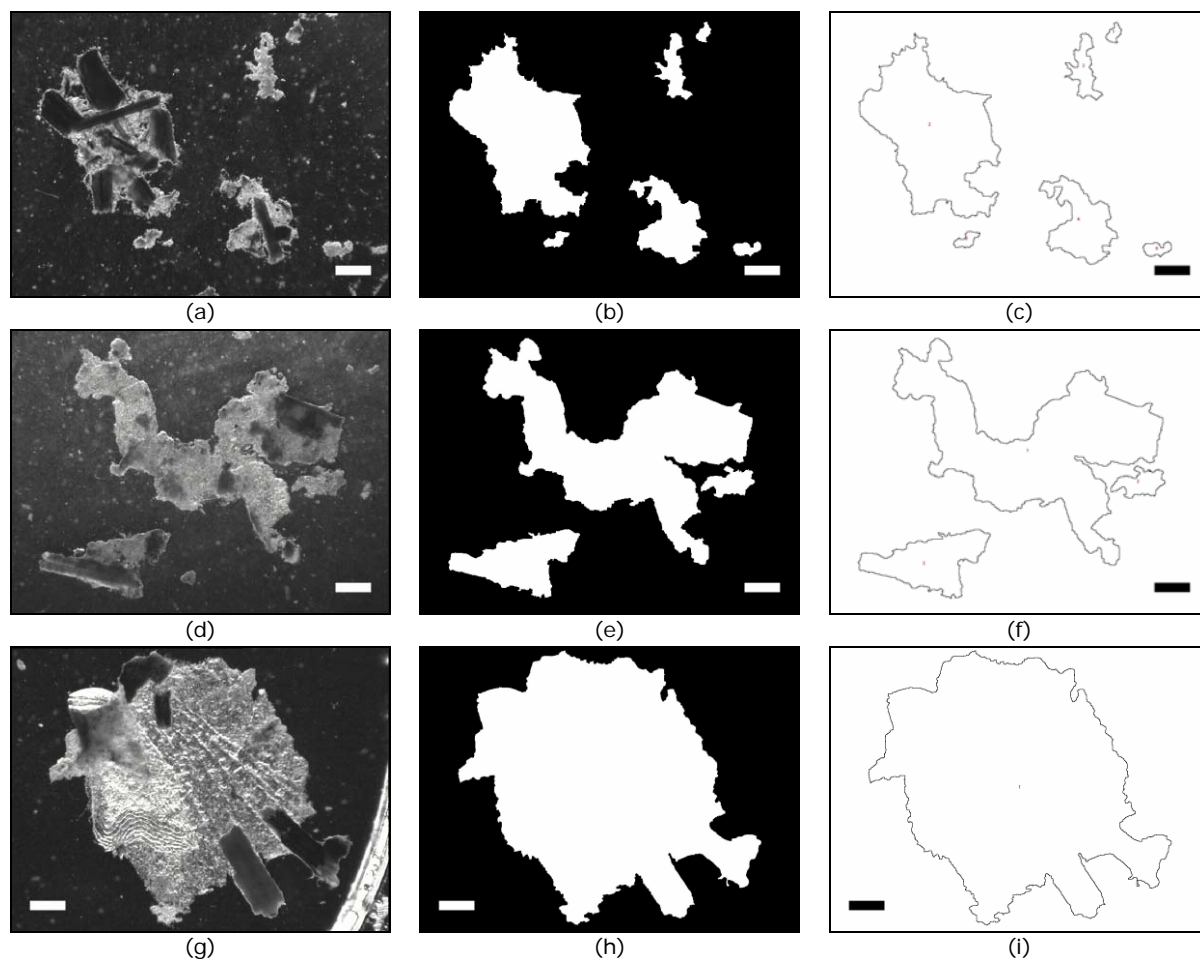


Fig. 80. Photography of suspended solids collected from the swirl separator on day t_{361} . The raw pictures (a,d,g) were transformed (b,e,h) and analyzed to determine particle surface area (c,f,i). Figures a,b,c showed an example of particles isolated from the 400-800 μm size fraction, and figures d,e,f showed an example of particles isolated from the 800-1600 μm size fraction, and figures g,h,i showed an example of particles isolated from the >1600 μm size fraction. Scale bar = 500 μm .

Agglomerations of solids (Fig. 80a) were found in the upper particle size classes (>400 μm). Firm (dark) material seemed to be strongly attached (“glued”) to each other by soft and lighter material. It has to be noted that both larger particles depicted in Figure 80a were attached to each other (or represented a single particle) when observed under the microscope but separated during observation just before the picture was taken. The big larger spectrum in particle sizes and shapes was also found in this sample and it is therefore considered to be representative. Interesting observation offered Figure 80g where a small fragment of a ctenoid scale was identified. This particle had a total surface area of 18.8 mm^2 . Particles shown in Figures 80a and 80d had a total surface of 7.4 and 10.9 mm^2 , respectively and an overall size of over 1600 μm .

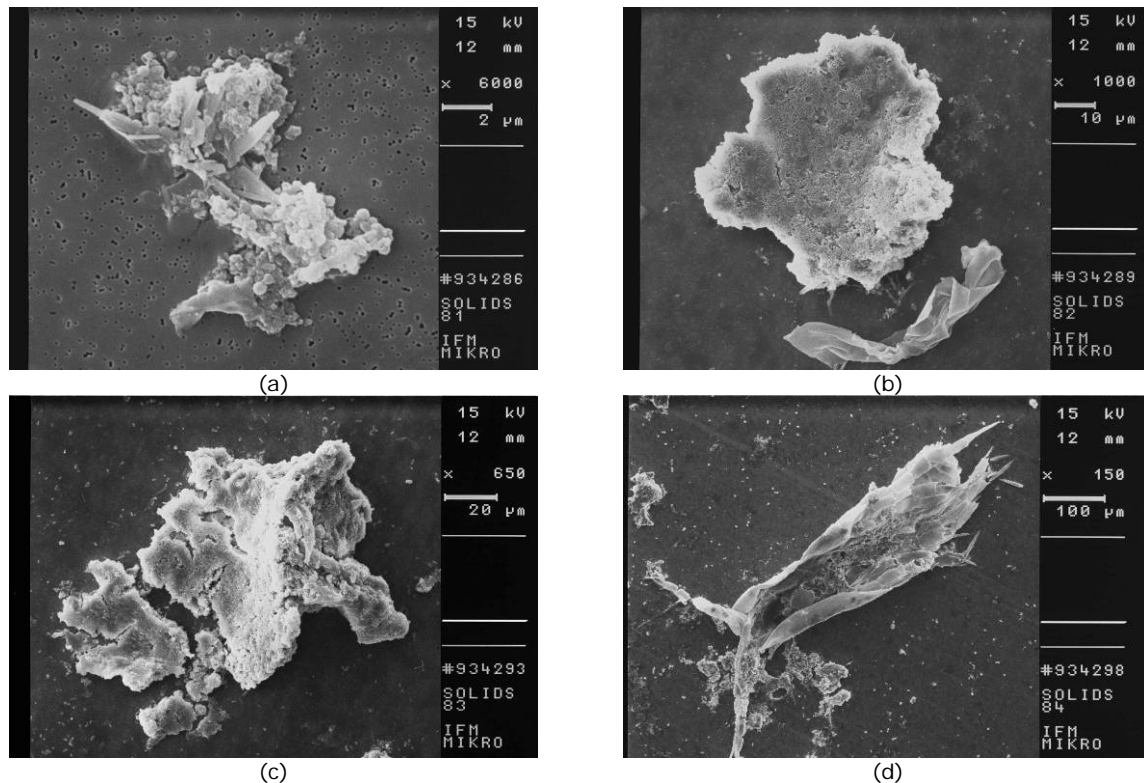


Fig. 81. Examples on particle size and shape of suspended solids (digital scanning microscope (DSM) photography) of the swirl separator on day t_{437} . (a) Particle sampled after filtering with a mesh size of $50 \mu\text{m}$; (b) Particles sampled with mesh size range of $50\text{-}100 \mu\text{m}$; (c) Particles sampled with mesh size range of $100\text{-}200 \mu\text{m}$, and (d) Particles sampled with mesh size range of $200\text{-}400 \mu\text{m}$. Scaling bars in each picture.

Particles of sample number 28 (day t_{437}) is presented in Figure 81a showing a small particle with a high surface roughness and little round to egg-shaped forms. Although the filtration was gently and done at only -150 mbar , the particles seemed to be reshaped by the filtration process while partly being pressed onto the filter pores. Some very soft and fragile tissue may not survive the filtration process unaffected and definitely changing their shape during drying. Fairly compact solids (Fig. 81a and 81b) were also observed in this sample. The particle depicted in Figure 81d belongs to the size fraction $200\text{-}400 \mu\text{m}$. It was rarely found but looked like the exoskeleton of a small crustacean, indicating their occurrence in the system which is not as uncommon feature, well known by RAS operators but seldom reported if prepared feeds are used.

Particles above $400 \mu\text{m}$ diameter collected in the swirl separator are presented in Figures 82a, 82d, and 82g. Long but thin solids were often observed and seen to serve as a bridging element to agglomerate particles of different material and size to larger units (Fig. 82a). The surface calculated for these particles has been slightly overestimated because of simplifications in the determination of circumferences and diameters. The Image-J software used is incapable to subtract spaces between particles when calculating surfaces.

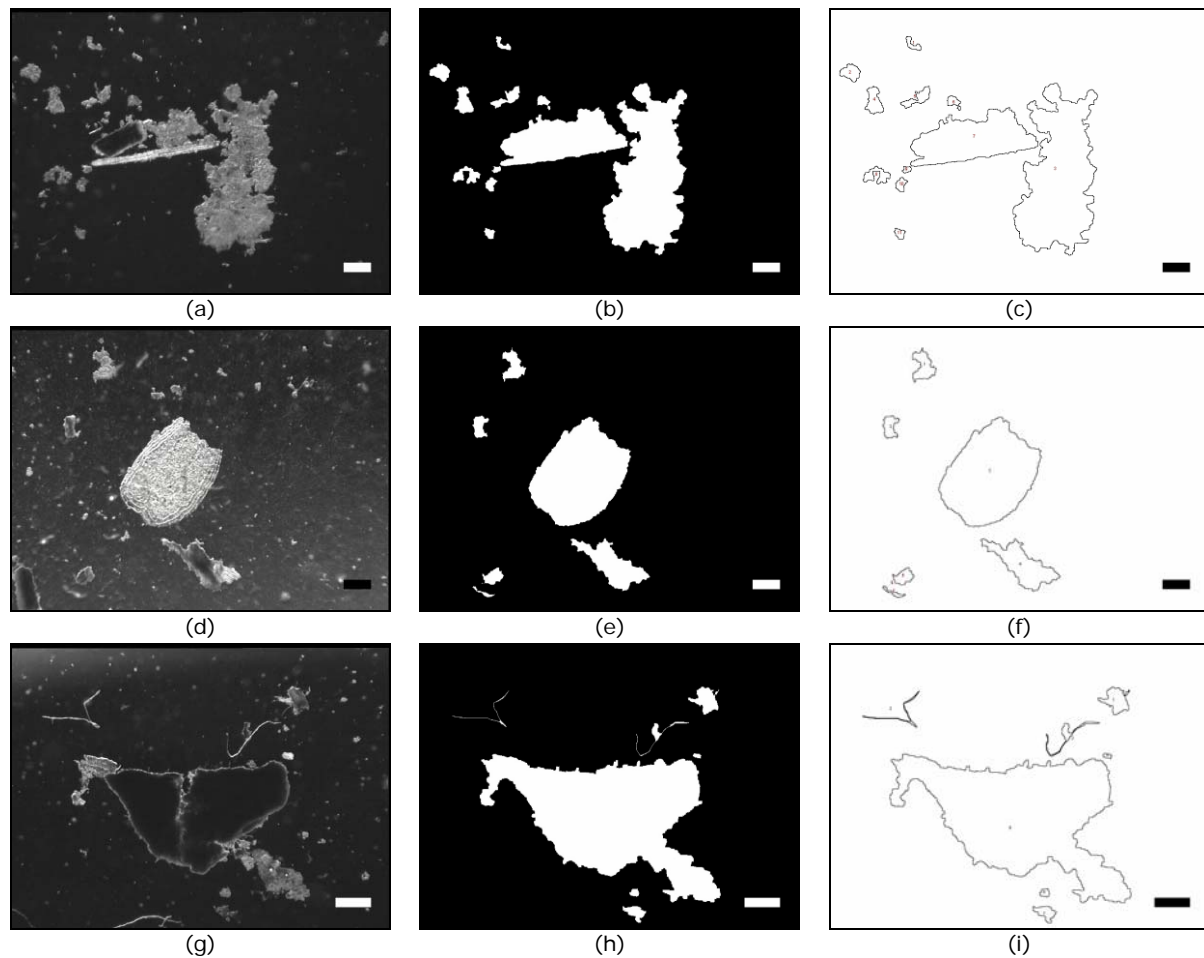


Fig. 82. Photography of suspended solids collected from the swirl separator on day t_{437} . The raw pictures (a,d,g) were transformed (b,e,h) and analyzed to determine particle surface area (c,f,i). Figures a,b,c showed an example of particles isolated from the 400-800 μm size fraction, and figures d,e,f showed an example of particles isolated from the 800-1600 μm size fraction, and figures g,h,i showed an example of particles isolated from the >1600 μm size fraction. Scale bar = 500 μm .

Nevertheless, total surface of the 11 particles identified in the agglomerate shown in Figure 82c accounted for 5.8 mm^2 . The scale shown in Figure 82f is 1.5 mm^2 from a total surface calculated of 4.8 mm^2 . Figure 82g presents a particle that seems almost divided into two pieces and may soon brake into two. This single solid, together with the surrounded material had a surface of 3.4 mm^2 . Fine articles with a diameter lower than the smallest mesh size (50 μm) but a long extension (Fig. 82i, long threads) appeared in all size classes. These fine solids seem not to pass through the filters openings because of being trapped. The two thread-like items shown in Figure 82i exhibited a total surface area of 0.13 and 0.11 mm^2 , respectively.

All of the above examples clearly indicate the difficulty to asses the total active surface area of particles in the recycling system because of the intrinsic variability in shape and size and their apparent rapidly occurring changes due to turbulence during transport with

the culture medium in pipes and other mechanical forces induced by equipment such as pumps and air-lifts. All estimates based on the determined particle size distribution have to be taken with caution until the dynamic of changes in fractionation and agglomeration of particles circulating in the system are better understood. The present study sheds some light of these processes affected by swirl separator techniques for suspended solid removal.

3.4.3 Particle size analysis

The data analysed here represent a separate experimental part outside the core study period. Particulate wastes in the RAS (faeces and uneaten feed) and collected by the swirl separator were analyzed to better quantify, the particle size distribution and their number in the collected sludge. However this was not possible to do on a continue basis but was done to gain supplemental information to the filtration analysis. Results obtained with the Coulter Counter® originate from 5 samples days t_{466} to t_{562} , indicating that small and fine particles dominated the particle distribution (Fig. 83). There was no significant difference ($p > 0.05$) in the counts *i.e.* distribution of particle sizes between measurements. Figure 83 illustrates plotted data for particle concentration (numbers per litre) in the separator sludge, obtained with the 1000 μm orifice tube. Particle size distributions approximated a hyperbolic curve showing a peak around 39 μm . The numbers rapidly decreased with increasing particle size. Particle numbers peaked between 67,000 and 98,000. Larger particles around 300 μm were between 6 and 30 per litre. Sizes around 400 μm diameter accounted for only 1 – 3 particles per litre. Figure 84 shows the particle size distribution for the same sample but using an orifice tube of 140 μm capturing in the range of 2.8 μm to 87.8 μm . These results were obtained using the 140 μm orifice tube. The magnitude of the peaks observed in these measurements was around 4.8 μm . The distribution of these fine particles followed the same pattern as small particles measured with the 1000 μm orifice tube, and the curve approximates a hyperbola. Particle numbers around 20 μm accounted between 5,000 and 12,000. Around 40 μm particle counts were found in the range between 200 and 600 particles. The counts obtained for particles around 60 μm were situated in the range of 50 to 100 particles per litre.

For the particles ranging in size between 22.5 μm and 714.7 μm there was a relatively high percentage (>50%) of particles between 35 μm and 45 μm . Distribution of particles sampled in the size ranged between 2.8 μm and 87.8 μm contained more than 50% of the fine solids that were situated between 4 μm and 7 μm in diameter.

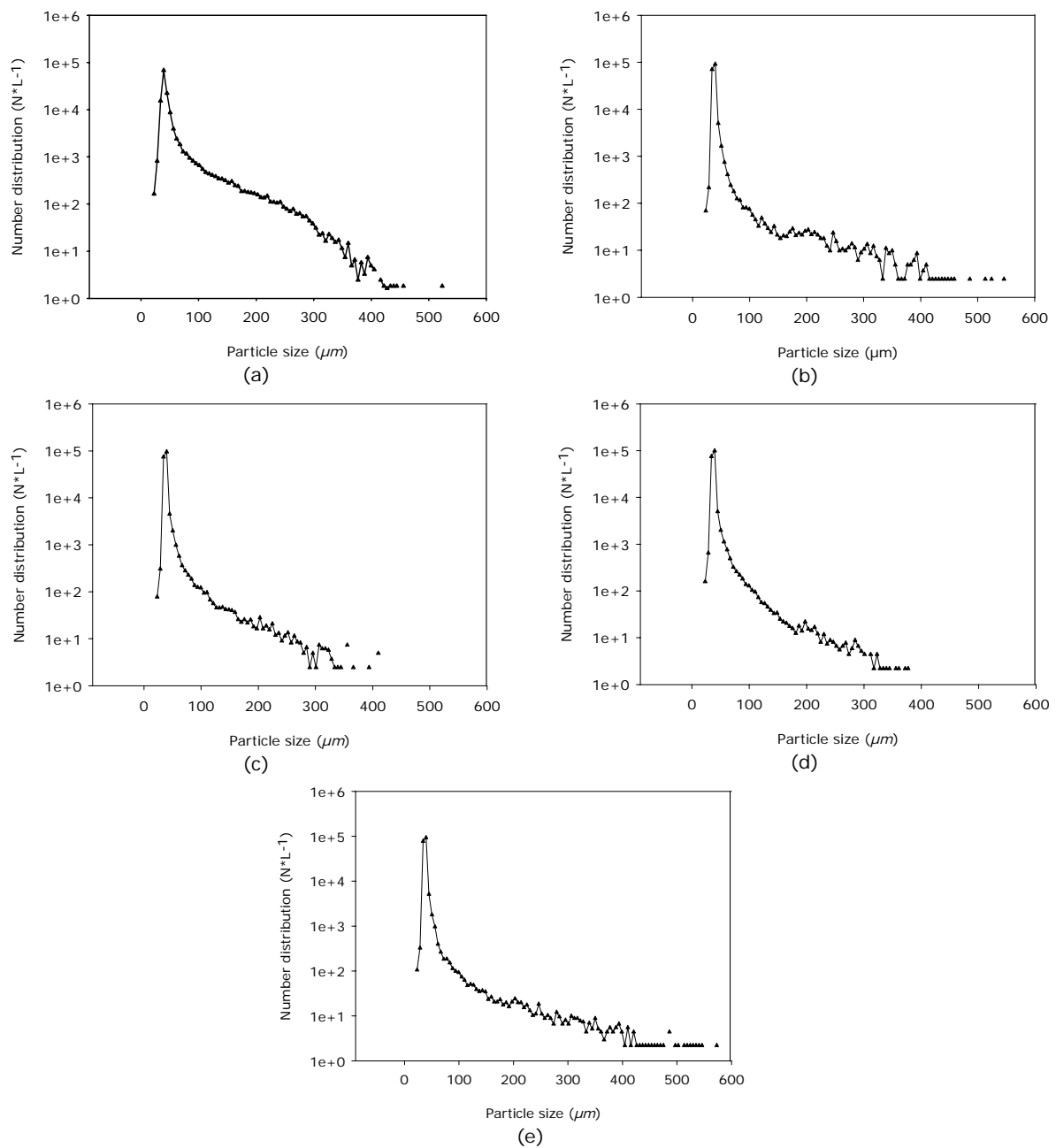


Fig. 83. Performance of the swirl separator receiving the effluents of two fish tanks (water flow $3.2 \text{ m}^3 \cdot \text{h}^{-1}$). Graphics shows the particle size distribution for 5 x 24-hour collection of sludge (a) to (e), between t_{466} and t_{562} of the study period. Particle number ($N \cdot L^{-1}$) distribution for particles ranging between $22.5 \mu m$ and $714.7 \mu m$ in diameter (Coulter Multisizer[®] 1000 μm orifice tube) are presented.

It has to be mentioned that the subsamples presented in Figure 83 and 84 came from the same sample *i.e.* were taken from the same glass beaker. This raises the questions whether this fraction of extremely fine solids in suspension (Fig. 84a to 84e) was just not recognized during in the first run measurement because of the size spectrum that can be covered by the 1000 μm orifice tube; or whether this fraction was generated by shear forces during the first run through the 1000 μm orifice tube?

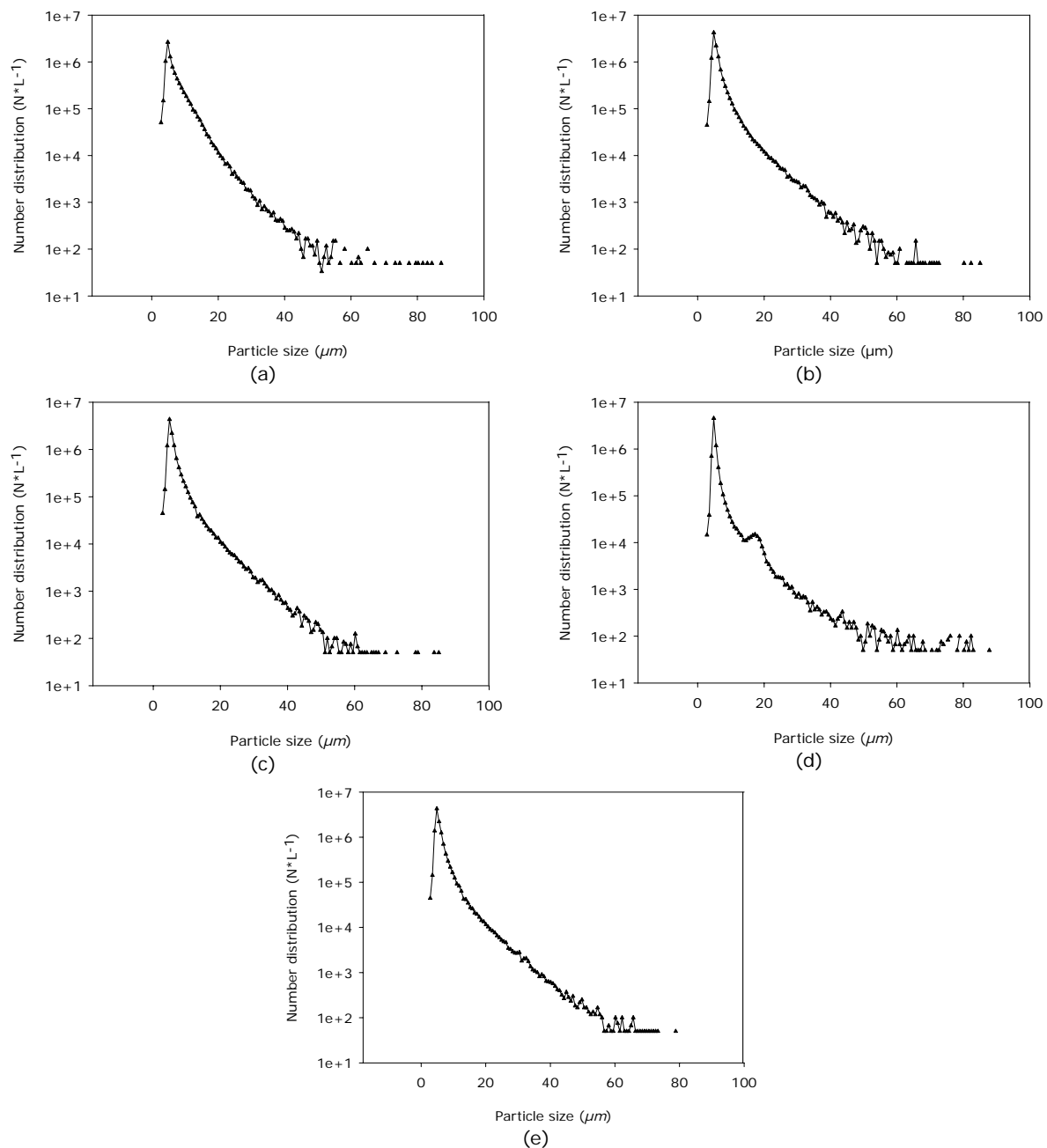


Fig. 84. Performance of the swirl separator receiving the effluents of two fish tanks (water flow $3.2 \text{ m}^3 \cdot \text{h}^{-1}$). Graphics shows the particle size distribution for 5 x 24-hour collection of sludge (a) to (e), between t_{466} and t_{562} of the study period. Particle number ($\text{N} \cdot \text{L}^{-1}$) distribution for particles ranging between $2.8 \text{ } \mu\text{m}$ and $87.8 \text{ } \mu\text{m}$ in diameter (Coulter Multisizer[®] 140 μm orifice tube) are presented.

All samples showed a reliable homogeneity prior to measurement. The stirrer inside the measuring beaker of the Coulter Counter[®] was set at position 4 and 1.5 for the $1000 \text{ } \mu\text{m}$ and the $140 \text{ } \mu\text{m}$ orifice tube, respectively. Unfortunately no rpm data can be obtained from these set ups. Different stirrer velocities were used because with the speed 1.5 it was impossible to get an appropriate homogeneity of the sample. Relatively big particles and/or particle aggregations stayed at the bottom of the measuring beaker. It was

therefore assumed that the stirring affected marginally the original size composition of the sample. Assuming this, Figure 84 expands mainly the lower part of the data set presented in Figure 83. Because of the uncertainty of overlap and proportion of artefact, these figures are still depicted separately.

3.4.4. Bacteria in the system

The solid matter produced in the recirculating aquaculture system (RAS) corresponded not only to the overall removal of solid particles. Bacteria did also rapidly grow in the system and were also partly accumulated and removed from the culture water via the employed treatment methods. In this study, bacteria were mainly removed by fine solids eliminated through the foam stripping process, where bacteria attached to these solids aggregating in the foam. Also bacteria at the air-water interface of ascending gas bubbles were attached and incorporated into the developing foam and were thus continuously eliminated.

The first experiment conducted in this study regarding this matter, was done between day t_{455} and t_{465} . Water samples were taken from the inlet and outlet of the foam fractionator, and directly from the foam that was produced inside the foam tube. Water samples were immediately fixed with formalin, than stained with acridine orange (AO) and counted with the epi-fluorescence microscope. Table 27 presents the results of these 8 days sampling exercise. The analysis of variance showed a significant difference ($p < 0.05$) between the eight samples. On the other hand, differences between inlet and outlet bacteria counts showed no significant differences ($p > 0.05$).

Tab. 27. Total bacteria count (TBC, $N \cdot mL^{-1}$) counted in water samples ($n=3$) taken from the inlet pipe, foam beaker, and outlet pipe of the foam fractionator basin ($n=8$ days). Samples stained with acridine orange.

Sample number	Inlet foam fractionator TBC, $N \cdot mL^{-1}$	Foam beaker TBC, $N \cdot mL^{-1}$	Factor	Outlet foam fractionator TBC, $N \cdot mL^{-1}$	Efficacy (%)	Feed (g) previous day	Foam characteristics
1	504,414,000	1,710,661,000	3.4	2,498,000	99.5	*no feed	normal, wet
2	2,809,000	404,639,000	144.0	2,709,000	3.6	766.5	normal, dry
3	6,201,000	800,975,000	129.2	5,080,000	18.1	847.3	normal, dry
4	8,429,000	2,130,816,000	252.8	6,673,000	20.8	766.5	normal, dry
5	2,851,000	249,397,000	87.5	2,737,000	4.0	766.5	no foam
6	2,627,000	1,031,218,000	392.5	1,694,000	35.6	no feed	no foam
7	4,277,000	647,980,000	151.5	4,740,000	- 10.8	847.3	normal, wet
8	15,277,000	2,636,167,000	172.6	16,278,000	- 6.6	no feed	normal, dry
Mean	68360,625	1,201,481,625		5,301,125			
S.D.	176,243,412	863,417,690		4,734,377			

* foam fractionator tower was cleaned before starting the experimentations

To obtain reliable results, the foam tower was cleaned the day before sampling started. This may have affected the system and caused the high quantity of bacteria found in the inlet water at the first sample date. Although the water flow through the system did not stop and the foam fractionator was totally uncoupled from the rest of the system, many bacteria flocks were released and ended in the total water flow after the foaming tower was assembled and re-connected back to the system. High turbidity in the water was observed. Feeding was cancelled. Bacteria counts found in the outlet water in relation to the counts in the inlet water showed a removal efficacy of 99.5% at day 1. Differences between in and outlet expressed as percentage of TBC removed during other days fluctuated between 3.6% and 35.5%. In the last two samples, 10.8% and 6.6% more bacteria counts were measured in the outlet water, indicating that despite a high concentration factor achieved in the foam there are a number of processes that do allow the counts to increase, leaving much room to study the causes and to improve the stability of the foaming process.

Bacterial counts in foam samples confirm their contribution to the high quantity of ashfree organic material found in the samples indicating the effective concentration during foam formation. It was observed that bacteria were more diluted in the water during days when the foaming process mainly collapsed. The bacteria removal process was continuous as long as foam stripping was in operation, although with variable efficiency. The results presented here should be taken as snapshot information because it was unfortunately impossible to collect samples more regularly to permit a removal rate over time.

To evaluate the inactivation properties of ozone along with the simultaneous removal of bacteria through foam stripping against the microbial community established in the fish culture water, an experiment was conducted between day t_{469} and t_{482} . Samples were taken from the same sampling points described above, and used for immediate inoculation on agar plates. Subsamples were also fixed and stained for counting under the microscope. A fourth water sample was taken from the outlet of the biofilter for comparison. The sampling was done at days without feeding the fish the day before sampling, and at a fully continuing feeding regime (880 g).

Figure 85 shows the percentage of colony forming units (CFU) against the percentage of total bacterial counts (expressed as non-colony forming units (nCFU)). This denomination of TBC was used because acridine orange stained living as well as dead bacteria having access to the complete bacterial species spectrum for counting. The growth of bacteria

on agar depended on the kind of agar that was used. Not every bacterial species is capable to grow on every agar media. A certain underestimation is obvious making data interpretation somewhat uncertain. None the less, the data presented showed no significant difference ($p>0.05$).

Bacterial counts in the inlet and outlet of the foam stripping tower, and in the outlet of the biofilter (nitrification) were at similar level than found in coastal waters (around 1.5 millions per mL)., This hold for samples taken when no feed was offered to the fish the day before.

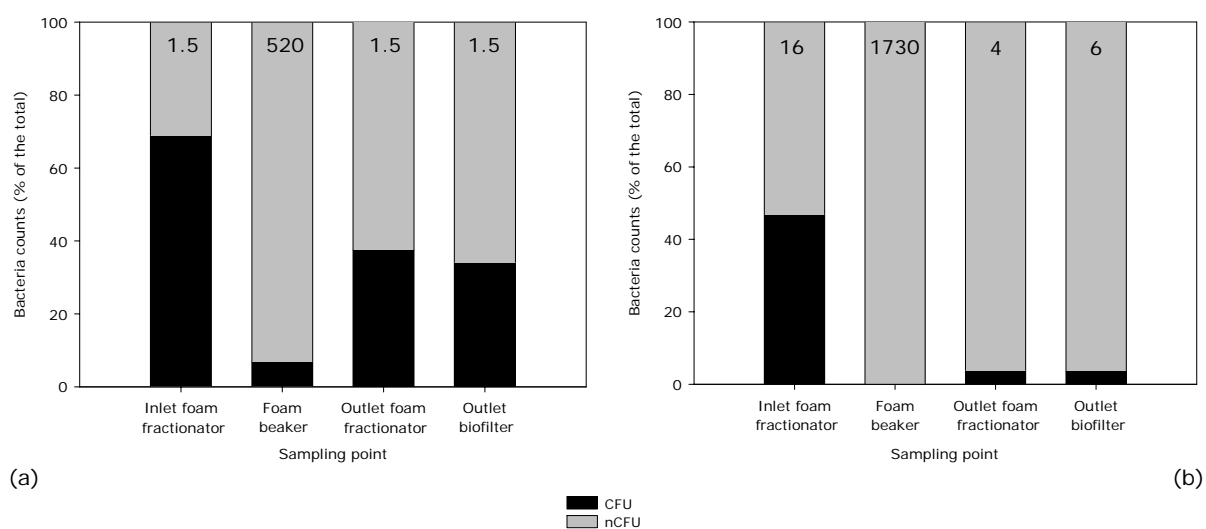


Fig. 85. Total bacteria counts (% of the total), categorized in colony and non-colony forming units (CFU and nCFU respectively), collected from the inlet water, foam beaker, and outlet water of the foam fractionator basin, and from the water in the biofilter tank (n=3 replicates); (a) presents the data collected when no feeding was given to the fish the day before; (b) shows the data obtained when the full daily meal was fed the day before (880 g). Number in the columns represent total counts in millions cells*L⁻¹.

The plate counts of bacteria found in the sample taken a day after 880 g feed was fed were much higher, reaching about 16 millions in the inlet of the foam fractionator, 4 million in the outlet, and 6 millions cells per mL in the outlet of the biofilter (nitrification). In the condensed foam, total counts amounted to 520 millions per mL and 1730 millions per mL at days without and with feeding. Figure 84 clearly demonstrates hoe the relative composition of colony forming and non-colony forming total counts change with treatment in the biofilter and in the foam fractionator. While the colony forming units counts are reduced by about 50% in the foam fractionator and biofilter when the system load is low (non-feeding day), the almost complete removal of colony forming is achieved at feeding days, indicating both the effectiveness of the ozonation process when treating high organic loads and the strong interspecific competition of heterotrophs in the biofilter, depleting colony forming fast. However, the efficacy of the process is largely

influenced by the overall flow rates through the treatment units and it is here where further studies are needed to optimize system performance.

In total the reduction in CFU numbers is negligible at days following a non-feeding period of 24 hours because of the overall low bacterial load while the removal efficiency of the foam fractionator is still substantial (concentrating the bacteria by at least two orders of magnitude). In contrast, the removal efficiency between inlet and outlet of the parallel operating biofilter and foam stripping unit is substantial (one order of magnitude) while the concentration effect of bacteria in the foaming process is massive (about two order of magnitudes), starting from an initial load already one order of magnitude higher than on non-feeding days. The particulate organic matter (POM) in the culture water during feeding days offered more nutrients and substrates for bacterial growth.

Parallel to the experiments on bacterial counts in the treatment units at days with and without feeding, subsamples were also prepared for digital scanning microscopy of the bacterial film in the biofilter (Fig. 86); however, photographs were taken from water samples of inlet and outlet of the foam fractionator, foam condensate and outlet of the biofilter. Bacteria in the inlet of the foam fractionator (Fig. 86a) were found to form massive mats with apparently a firm matrix. Samples taken from the foam condensate showed substantial fewer aggregates of bacteria and POM (Fig. 86b) which is in contrast to the plate counts and this places doubt whether such findings can be used to support quantitative mass balance calculations. The outlet water coming from the foam fractionator tower appeared in less quantity but still with visible POM forming small lumps (Fig. 86c). Small particles were also observed, these without any bacteria attached though. Figure 86 (d) shows the photograph taken from the water sample coming out of the biofilter (nitrification). Free (swimming) bacteria and less POM were observed compared with the water flowing out of the foam fractionator.

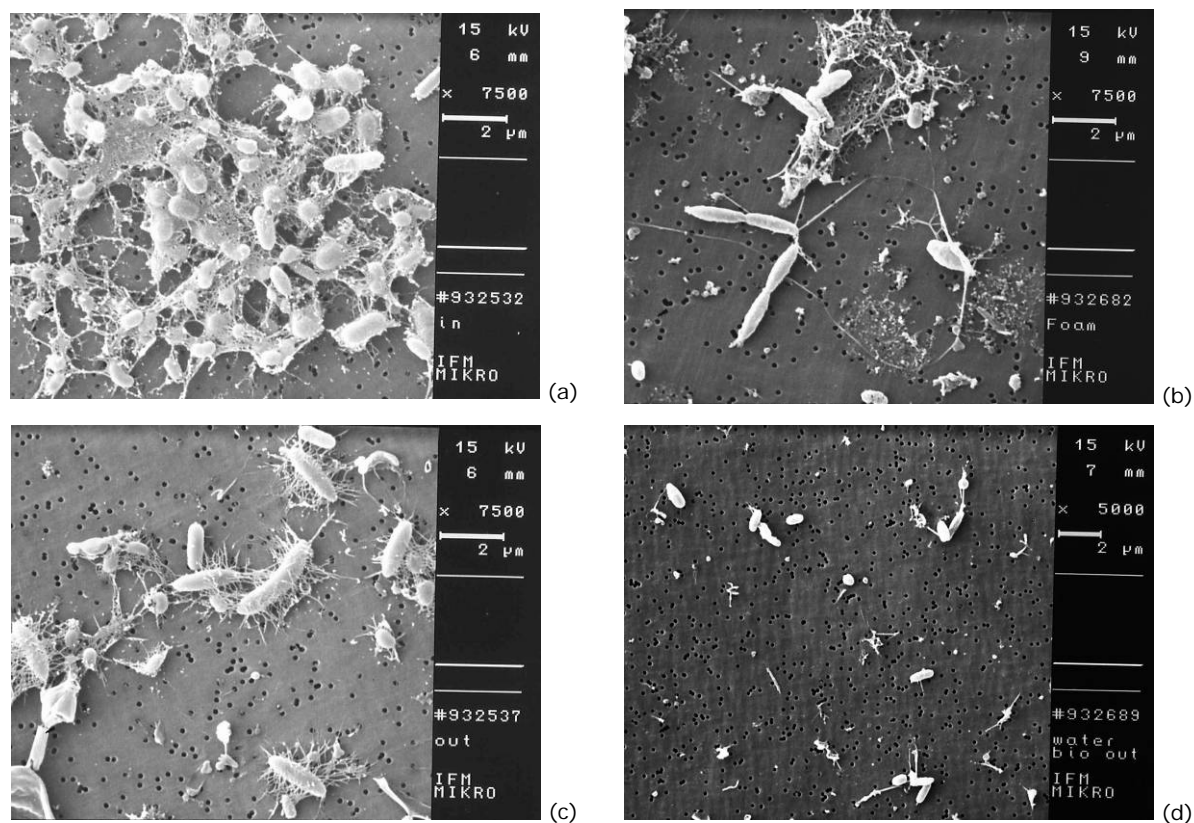


Fig. 86. Digital scanning microscopy photographs showing bacteria and fine solid material found in the inlet (a) and outlet (c) water of the foam fractionator basin; bacteria and fine particles in the foam collected from the foam beaker (b); and (d) shows bacteria and particulate solid matter found in the water coming from the outlet of the biofilter (nitrification). Scaling bars are showed in each picture.

Polyethylene filter media from the biofilter were also prepared for DSM investigations. Filter media substrates were cut longitudinally in two pieces to allow the observation of bacteria settled on the outer and inner surface. Figure 87 (a) presents the data for the outer surface of the biofilter media. One thin layer of bacteria attached to the surface can be observed, as well as small surface areas where no bacteria settled. The surface inside the plastic media showed exhibited different bacteria community structures, probably due to multi-layer formation (Fig. 87b). Long bacterial strings were seen, which formed junctions and bridges between different bacterial layers.

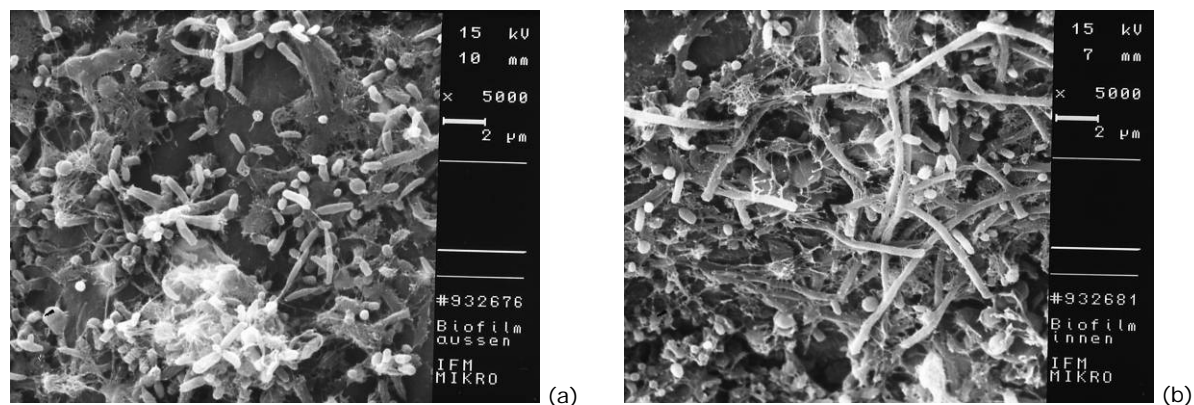


Fig. 87. Digital scanning microscopy photographs taken from the outer (a) and inner (b) surface of the filter media in the biofilter (nitrification), showing the rich bacteria settlement on the polyethylene surface. Scaling bars are showed in each picture.

During the experiments described above, two problems occurred: the staining of bacteria and particles by the acridine orange (AO) dye and the presence of particle agglomerates with high numbers of bacteria attached. Looking after a way to minimize these problems, samples collected and fixed from the foam collector tank between day t_{14} and t_{437} were stained with DAPI and treated with ultrasound. DAPI dye was used to stain the samples because DAPI stains the nucleus of bacteria cells and not the particles. Additionally, every sample was treated with ultrasound to split particles and release bacteria attached to particles. Table 28 shows the results of total bacteria counts and bacteria biomass determined.

Tab. 28. Total bacteria counts (TBC, $n \cdot mL^{-1}$), mean cell volume (μm^3), mean cell biomass expressed as micro grams carbon per litre ($\mu g C \cdot L^{-1}$), mean carbon content ($fg \cdot cell^{-1}$), and percentage of cells in division obtained from water samples taken from the foam flushing beaker. Standard deviation is presented as percentage from the total (% S.D.).

Sampling day	Mean TBC (% S.D.)	Mean cell volume (% S.D.)	Mean cell biomass	Mean carbon content	% of bacteria in division
Units	$n \cdot mL^{-1}$	μm^3	$\mu g C \cdot L^{-1}$	$fg \cdot cell^{-1}$	$n \cdot mL^{-1}$
1 t_{71}	35,863,000 (20.7)	0.017 (52.2)	291.9	8.1	8
2 t_{84}	88,674,000 (25.3)	0.021 (49.5)	834.8	9.4	32
3 t_{97}	67,876,000 (22.4)	0.018 (52.6)	566.4	8.3	20
4 t_{122}	79,630,000 (19.8)	0.033 (86.1)	918.1	11.5	20
5 t_{153}	164,877,000 (29.3)	0.033 (46.4)	1,983.3	12.0	24
6 t_{188}	72,663,000 (23.0)	0.036 (69.6)	899.2	12.4	12
7 t_{224}	103,224,000 (20.7)	0.038 (90.8)	1,285.2	12.5	20

Total bacteria counts were found to be scattered. Nevertheless, bacteria numbers present in the foam condensate had in average the tendency to arise during time. Unfortunately this was statically impossible to valid. It is noteworthy to emphasize that the bacteria growth activity, measured as bacteria in division process, differed significantly between samples. The smallest value was found in the first sample analyzed though (sample took on day t_{71}) (Tab. 28) Cells in division amounted to 8% of the total counts. In subsequent samples, the percentage of bacteria in division fluctuated between 12% and 32%. As noted before, the foaming process is extremely variable and so is the inactivation of bacteria by ozone. If the flow of produced foam is slow, the residence time of bacteria in the foam beaker is longer compared to a smooth and continuous foam stream. In contrast, when the foaming process has totally collapsed and bacteria dropping back into the water column of the foam tower, many previously aggregated in the foam will re-enter the system. Continuity of the foaming process is the key to reliable effectiveness of this treatment unit. Long residence times of bacteria in the upper part of the foam tower does not only concentrate bacteria in the froth, but also extend the contact time with the ozone containing air-water interface and may increase the effects of ozone on the cells. The collapse of the foam varied from day to day. Whether, the percentage of cells that were not in division had an inactive status due to the effects of ozone warrants further study.

Photographs taken with the fluorescence microscope showed the initial stages of bacterial numbers in the foam collector and the solid matter in subsequent samples are presented in Figure 88a to 88i. Total bacterial counts and biomass determinations were possible only until the sample day t_{224} (Fig. 88d). Thereafter, the counting of bacteria was impossible because of too high levels of fine solids in the filtered samples. Some samples exhibited bacteria in two layers (Fig. 88e and 88f = same ocular field but differently focussed). Also, the distribution pattern of bacteria on the filter was highly scattered (Fig. 88e to 88i). Bacteria and particles sometimes formed extended lumps (Fig. 88h). It was suspected that the sonication treatment of the samples could have tear solids apart, causing subsequently bacteria aggregations and the formation of two layers.

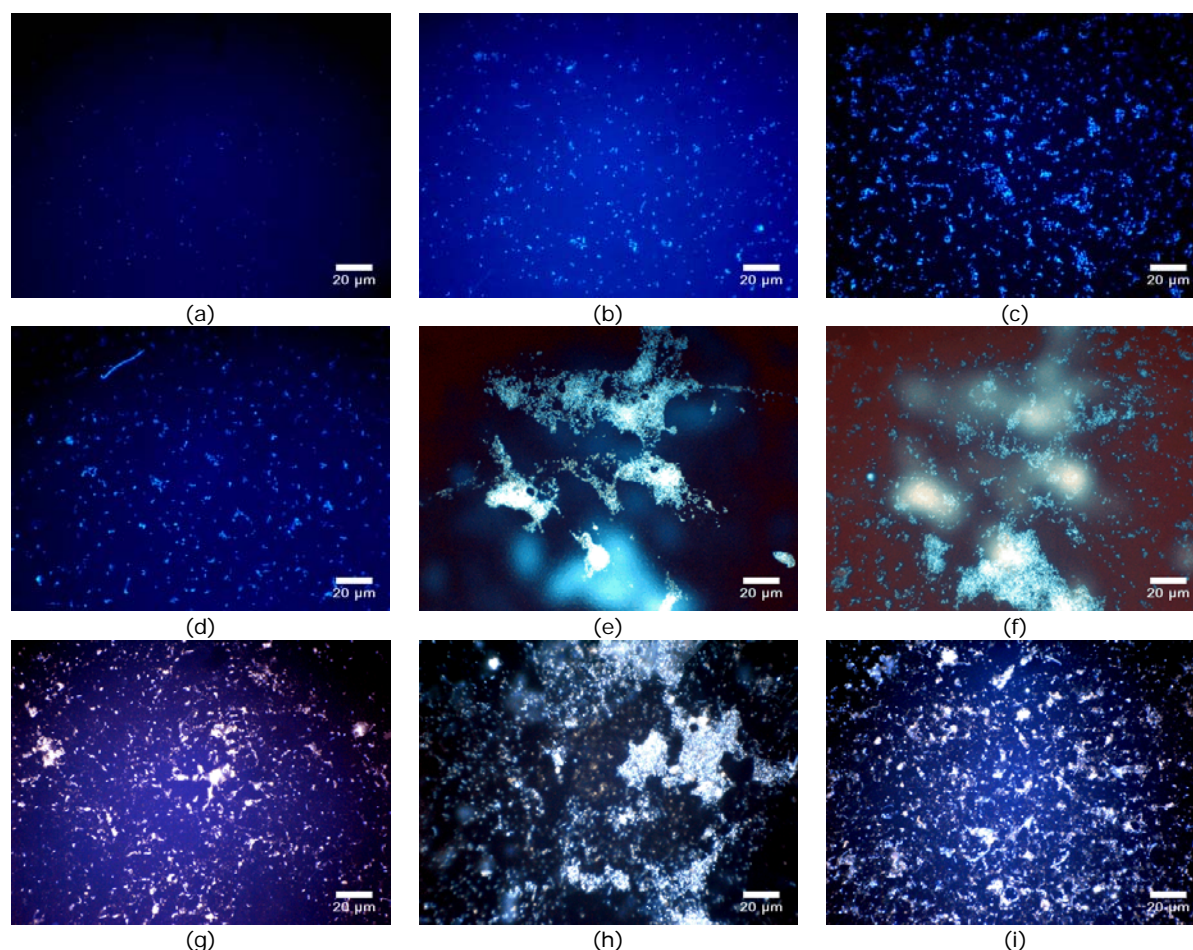


Fig. 88. Fluorescence microscopy photography of bacteria collected from the foam beaker (magnification 63x), stained with DAPI, and treated with an ultrasound stab (50 Hz) for 1 min. These photographs correspond to samples: (a) day t_{14} , (b) day t_{71} , (c) day t_{153} , (d) day t_{224} , (e) and (f) sample of day t_{280} showing bacteria in two layers, (g) sample of day t_{347} with bacteria attached to solid particles and with an uneven distribution pattern, (h) sample of day t_{376} with big solid particles and bacteria lumps and very uneven distributed, and (i) sample of day t_{411} with extremely high bacteria cells attached to fine solid material. Scale bar = 20 μm .

3.4.5 The influence of ozone on particle size distribution and nutrients

The qualitative and quantitative analysis of the dynamics of total suspended solids (TSS) in the RAS under the influence of ozone was investigated in two series of experiments conducted between day's t_{668} and t_{690} . Both series focussed on removal efficacy of particles, when the system was run with ($n = 11$ days) and without ozone ($n = 5$ days). The ozone quantity was adjusted by the ORP control (*i.e.* threshold value set for 350 mV ORP). Nevertheless, the ozone generator was continuously working during the first experiment.

The particle removal efficacy was investigated during this ozonation trial for the swirl separator and the foam fractionator separately. Suspended solids were eliminated from the culture water, specially the fine fraction that is usually difficult to remove. This was also visually noticed by clean and highly transparent water during all days of the experiments. The concentration of solids in the culture water amounted on average to $8 \text{ mg} \cdot \text{L}^{-1}$ (dry weight). The percentages of TSS removed by the swirl separator and the foam fractionator are presented in Figure 89.

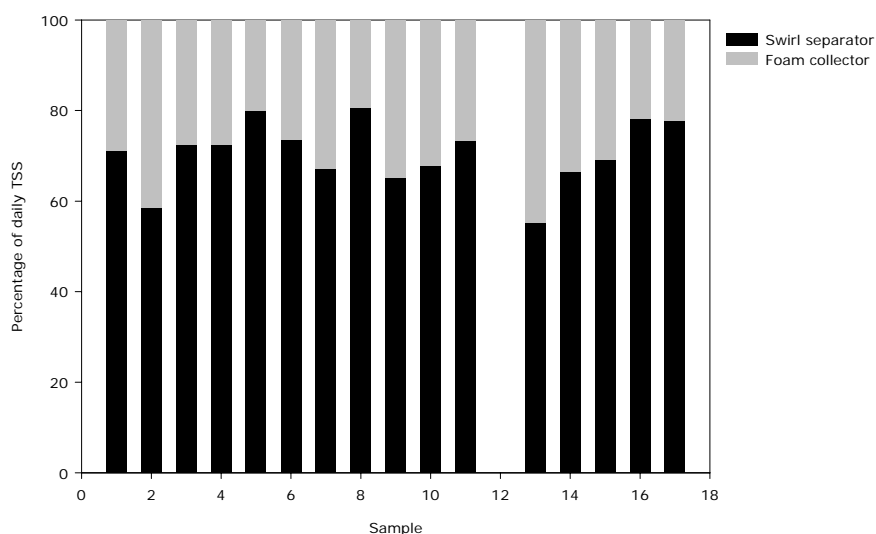


Fig. 89. Total suspended solids collected from the swirl separator and the foam collector tower ($n=16$). The system was run with a biomass of 52 kg Days 1-11 with ozone treatment and days 13-17 without ozone.

The data show an overall suspended solids removal efficacy via the swirl separator of about 65% to 70% of the total, except for one day where almost 80% of the dry weight solids were removed by the swirl separator. The foam fractionator yielded about 35% to 30%. This is a very important and high ratio considering that most of the dry matter

removed via foaming attachment. This is also evident from the results on particle size distribution determined for both removal techniques via the Coulter Counter®.

Figure 90 shows in detail the data on the effectiveness of the two step solid separation and/or elimination. Data are presented as dry weight (g/day) of particle size fractions retained and classified by the various sieves, and set in relation to the corresponding portion retained by the foam collector. The combination of swirl separation and foam fractionation allowed seizing the whole particle spectrum in the recirculation system. The amount removed with the froth is equivalent to that removed in the swirl separator in the larger particle size fractions (above 400 μm). The addition of ozone to the water was found to have a positive effect in the solid separation process, although there was no statistically difference between the samples ($p > 0.05$).

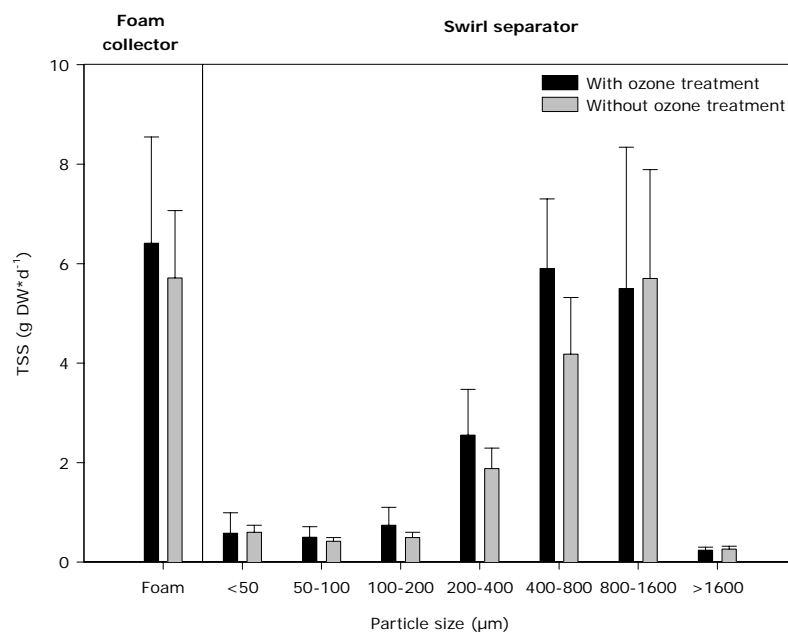


Fig. 90. Size distribution of the daily separated TSS (g DW*d⁻¹) by the swirl separator and the foam fractionator (foam collector tank) with (n=11) and without (n=5) ozone treatment.

Particles in the range of 400 μm to 800 μm removed by the swirl separator were certainly the most dominant ones. Figure 91 shows the cumulative particle size distribution for each filter size category class from below 50 μm to greater than 1600 μm including also the fraction of solids collected by the foam fractionator. It can be seen that both curves followed the same trend and that particles greater than 200 μm but smaller than 1600 μm represented almost 87% of the total.

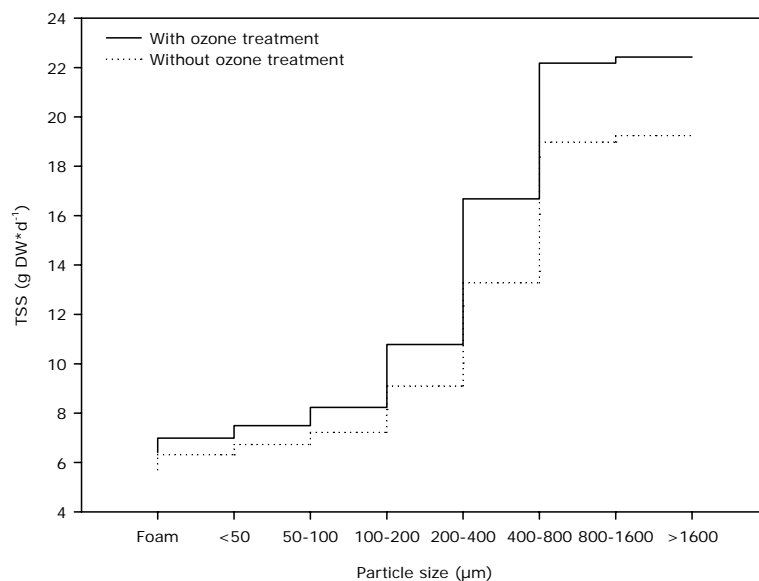


Fig. 91. Cumulative size distribution of the daily separated TSS (g DW*d⁻¹) by the swirl separator and the foam fractionator (foam collector tank). With (n=11) and without (n=5) ozone treatment.

On average the swirl separator removed 15.6 ± 0.7 g and the foam fractionator 6.4 ± 0.7 g dry solids per day when the RAS was running with ozone. During days when the system worked without ozone, the solids removed daily were 13.5 ± 0.2 g and 5.7 ± 0.7 g for the swirl separator and the foam fractionator, respectively. The relation between removal efficacy of swirl separator and foam fractionator remained with $2/3$ to $1/3$ the same.

Figure 92 presents the carbon content expressed in grams dry weight per day as average for days with and without ozone. Unfortunately, due to filtration problems it was impossible to gather enough material for the carbon content analysis of particles below $100 \mu\text{m}$. None the less, no significant differences ($p > 0.05$) were found between the solid size classes for the trials with and without ozone application. An increasing trend was observed while particle size increased though. For small particles ($< 400 \mu\text{m}$) the carbon content was found to be around 35% in average. Larger particles ($> 400 \mu\text{m}$) ranged between 40% and 46% carbon content indistinct if ozone was added or not. In the solid matter collected from the foam flushing tank, the carbon content was in average slightly higher during he experiments without ozone, but not statically difference was calculated. It was observed that the carbon content in the solids eliminated by the foaming process were on the same level as the solid particles found in the swirl separator in the range between $100 \mu\text{m}$ and $400 \mu\text{m}$ when the system was running with ozone. In contrary, the solid gathered from the foam collector tank during the trials without ozone injection were

the highest found during the whole experiment (Fig. 92). Carbon content was found to be lower in small particles than in bigger ones. It was presumed that, because of the negative exponential relationship between particles size expressed as volume and its corresponding surface, small particles leached faster than greater ones. This leaching effect was apparently conducted by heterotrophic bacteria settled on the solid matter, using carbon for growth, as well as carbon being washed out by the influence of mechanical forces.

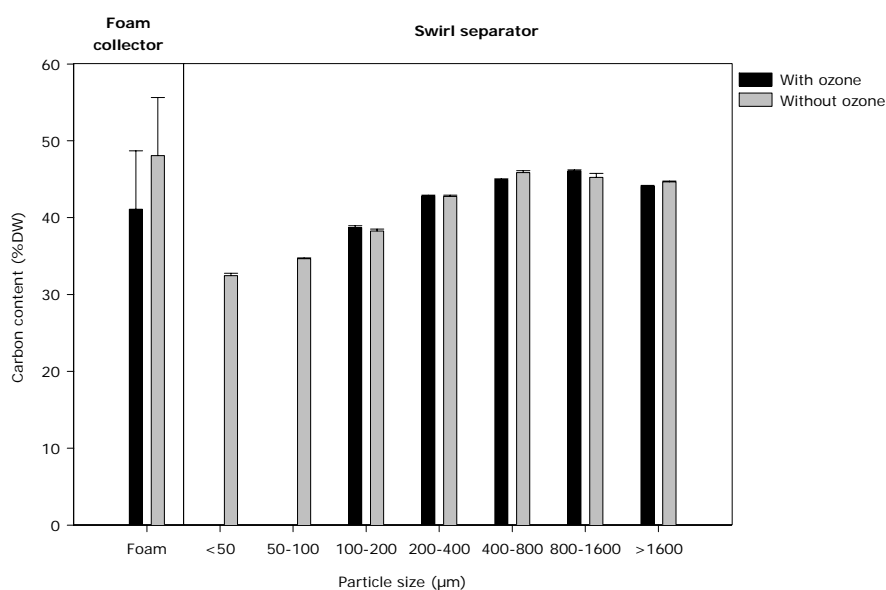


Fig. 92. Carbon content (%DW) of the daily separated TSS by the swirl separator and the foam fractionator (foam collector tank). With (n=11) and without (n=5) ozone treatment.

The amount of ashfree organic material in the samples, which was burned at 540°C, followed the same trend as the carbon content (Fig. 93). In the particles ranging from 100 μm and smaller, the organic content was found to be less in the samples taken during the experiments without ozone. For particles above 100 μm the amount of organics measured showed no difference between the two trials (with and without ozone). The amount of organic content found in the collected foam condensate was on the level of the organics found in the upper three size classes (particles above 400 μm). In this case no difference was found in the organic content between these two trials. But again the amount of organics was smaller in the lower particle size classes, following an incrementing trend while the size of particles was bigger.

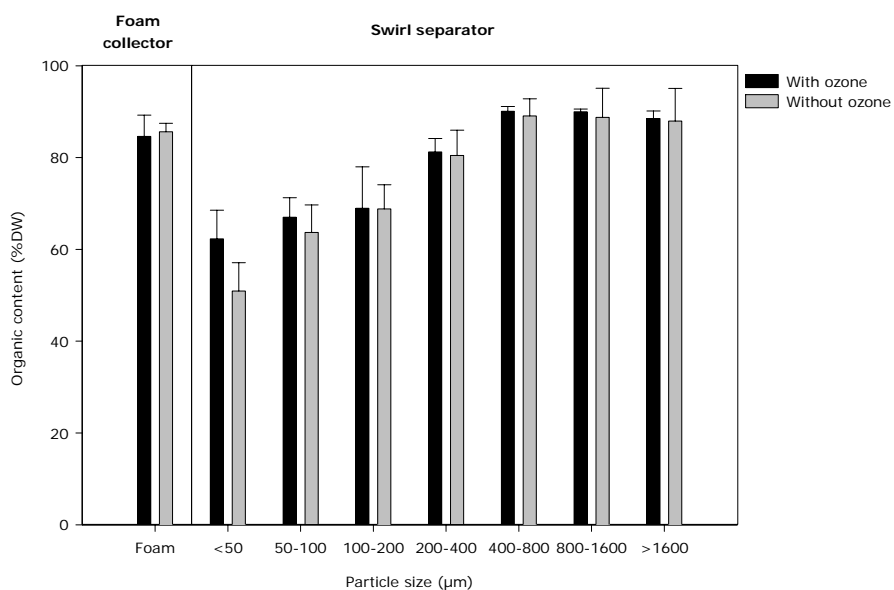


Fig. 93. Ashfree organic content (%DW) of the daily separated TSS by the swirl separator and the foam fractionator (foam collector tank). With (n=11) and without (n=5) ozone treatment.

It was presumed that the same leaching effect affected the measurements *i.e.* the results of organic content in the different particle size classes. Small particles break down faster than bigger ones.

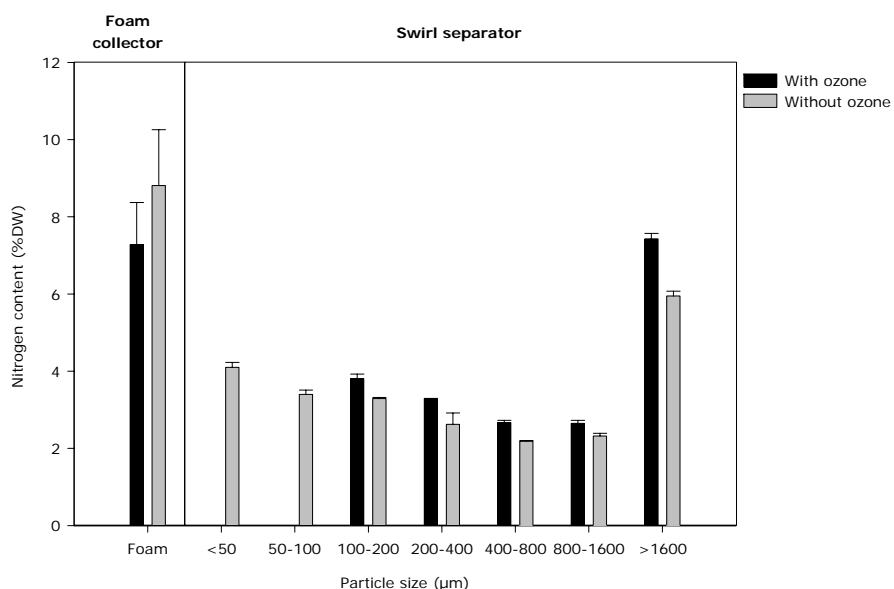


Fig. 94. Nitrogen content (%DW) of the daily separated TSS by the swirl separator and the foam fractionator (foam collector tank). With (n=11) and without (n=5) ozone treatment.

Nitrogen content found in the solid matter collected by the swirl separator basin when ozone was added to the water was found to be not much greater than when the system was running without ozone (Fig. 94). On average the nitrogen content amount 4% dry weight when the system was running with ozone against 3.4% when no ozone was added

to the water. In small particles more nitrogen was measured and a negative trend was observed while particle size increased until the size smaller than 1600 μm . For particles greater than 1600 μm 7.4% and 6% carbon content was found when ozone and when no ozone was given to the system respectively. These last values correspond to particles not consumed by fish and therefore reflect the load from the last feed particles. As well as for the rest of the size classes, particles above 1600 μm had greater nitrogen content when the system was working with ozone. However, There was no statistically difference ($p>0.05$). In contrast to the results observed in the filter fractions capturing different size classes, the solid material collected from the foam flushing basin showed an inverse relationship. Nitrogen content found during those days where no ozone was injected to the system was greater than with ozone treatment, in average 1.5% higher. It was presumed that nitrogen was removed in the foam fractionator through the formation of foam based on surface active substances like proteins with high nitrogen content.

The data for phosphorous content showed, as well as those for nitrogen content, a decreasing trend while particle size increased (Fig. 95). When the system was running with ozone the average phosphorous content was 3.3% for particles below 200 μm . For particles above 200 μm the average phosphorous content was 1.5%. Analogue to the days without ozone treatment, the average phosphorous content for solid matter below 200 μm was 3.8% and 1.5% for particles above 200 μm . Data were found to be fairly scattered. Figure 98 shows a higher phosphorous content when the system was working with ozone in the particle size class between 100-200 μm and for particles greater than 1600 μm . Otherwise, phosphorous content was always higher when no ozone was injected to the foam separation unit. The data obtained from the foam condensate collected from the foam flushing tank showed a greater phosphorous content when no ozone was used.

Irrespective of the addition of ozone, calculating the nitrogen phosphorous relationship, it was observed that for particles greater than 1600 μm the same N/P relationship of 7:1 determined as for the feed pellet. It was assumed that in this size class uneaten feed particles were present in the solid matter trapped in the swirl separator basin.

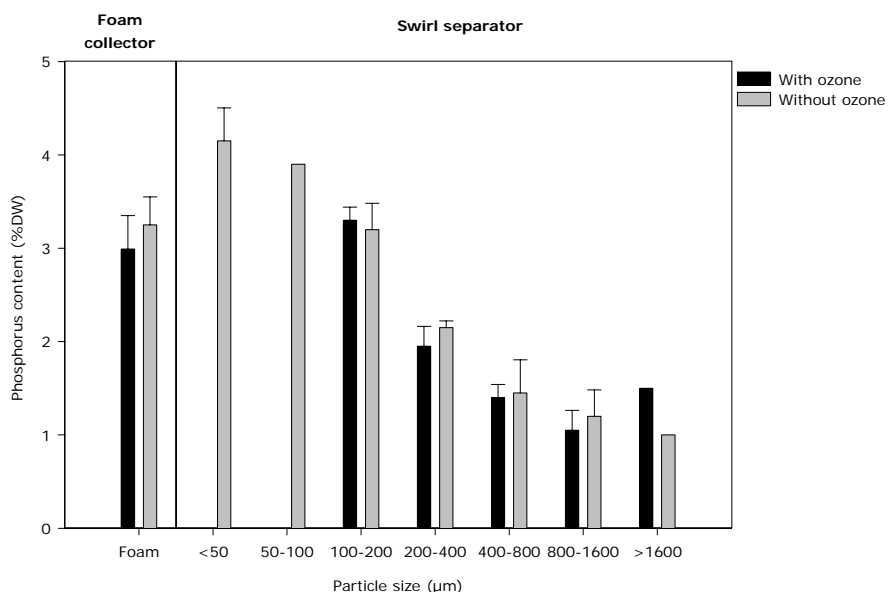


Fig. 95. Phosphorus content (%DW) of the daily separated TSS by the swirl separator and the foam fractionator (foam collector tank). With (n=11) and without (n=5) ozone treatment.

In the particle size classes below 1600 µm it was calculated an N/P ratio of 1:1 for small particles (below 400 µm) up to 2:1 for particles in the range between 400 µm and 800 µm. It was suspected that because nitrogen leach much faster than phosphorous, and because the solid matter stayed in the swirl separator conical bottom once every 24 hours before samples were collected, the leaching effect mentioned above was affecting particulate nitrogen in a higher degree than phosphorous and/or carbon.

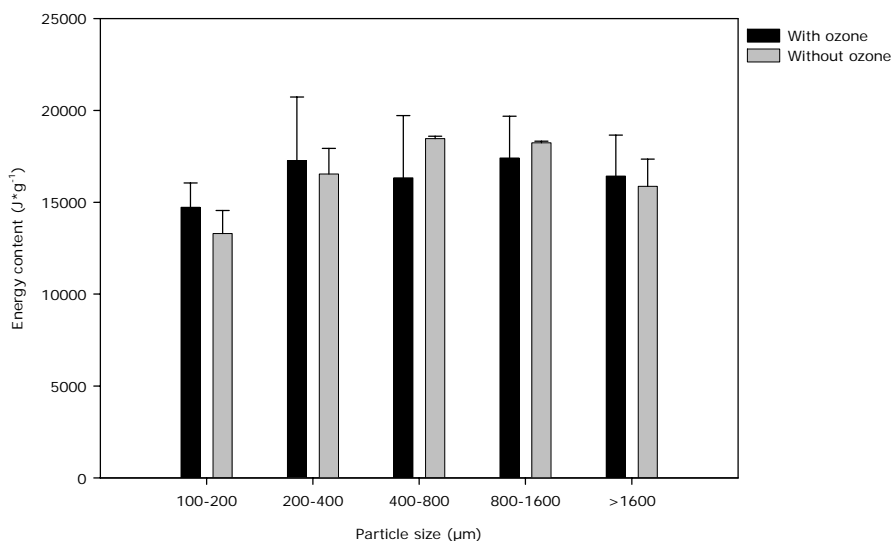


Fig. 96. Energy content (J*g⁻¹) of the daily separated TSS by the swirl separator. With (n=11) and without (n=5) ozone treatment.

The results obtained from the measurements of energy content in the solid matter, sorted by size class are presented in Figure 96. Unfortunately it was impossible to gather enough solids from the foam collector tank and from the particles smaller than 100 μm to measure energy content. The data showed no significant difference between those days with and without ozone ($p>0.05$). It was observed that the amount of energy found in the solid matter about 77% of the energy found in the feed used. The highest energy content was found in the solid particles correspond to the size class between 400 μm and 800 μm during the experiments without ozone, with 18,465 J/g corresponding to 86.7% of the energy contained in the feed.

The effect of ozone in the nutrient and energy composition of particles size classes was found to be slightly. None the less, the relative portion of organic compounds (carbon, nitrogen, and phosphorous) during those days when the RAS was running without ozone were found to be smaller than those found when the system was working with ozone. It was suspected that, without ozone, a higher bacterial activity in the water took place. This bacteria activity was responsible for decomposition processes that affected the concentration of organic compounds in the solid matter.

The experiments without ozone were cancelled after day number 5 from beginning. The quality of the water decreased noteworthy. The culture water became a very intense yellow colour and many bacteria flocks were observed in the water column. The settlement of bacteria films forming big fade-like colonies were observed on the internal wall surface of the swirl separator and in less degree in the fish tanks. The culture water appeared transparent though. No signs of fish stress were observed. Fish feeding and swimming activity in the culture tanks was catalogued as normal.

3.4.6 Particle size analyses during the experiments with and without ozone treatment

3.4.6.1 Particle size analysis with ozone treatment

Particulate matter collected by the swirl separator and by the foam flushing tank was analyzed using the Coulter Counter[®]. Subsamples taken from each basin were measured using the 1000 μm and the 140 μm orifice tube.

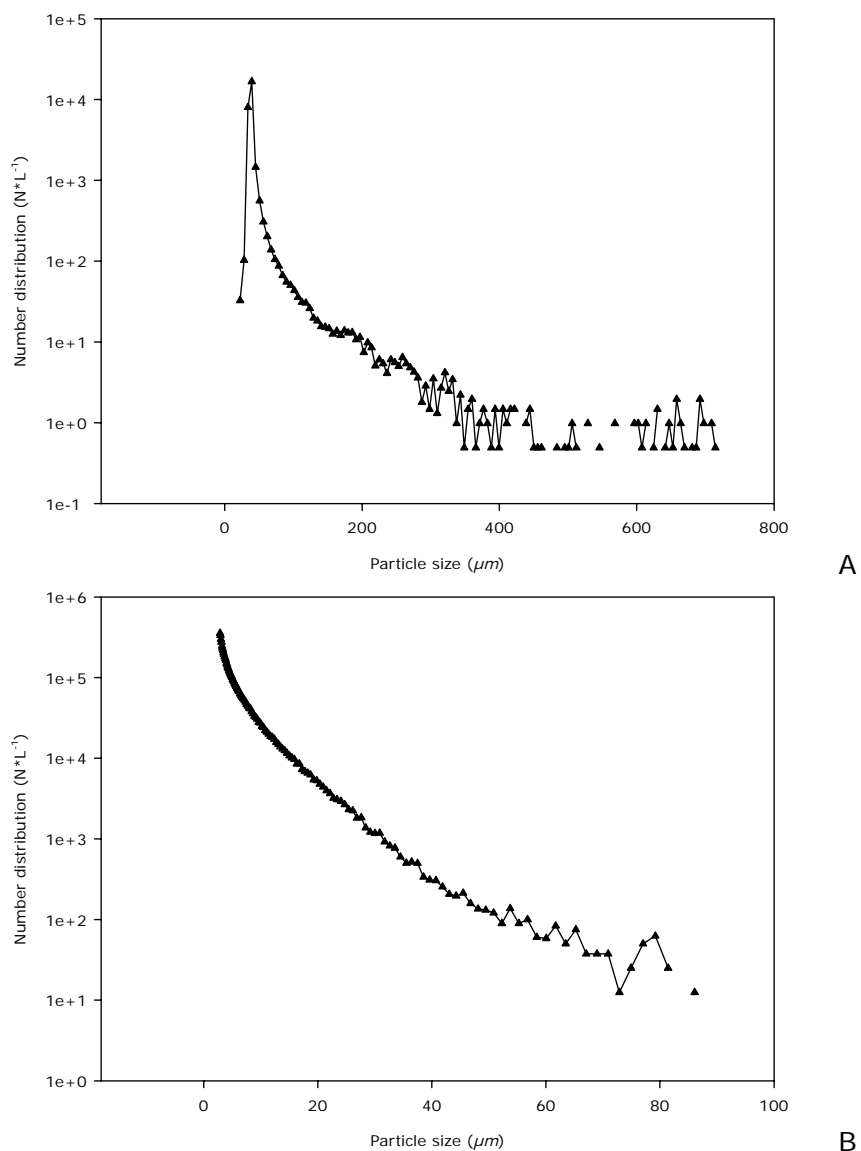


Fig. 97. Performance of the swirl separator receiving the effluents of two fish tanks (water flow $3.2 \text{ m}^3 \cdot \text{h}^{-1}$). Graphics shows the particle size distribution ($\text{N} \cdot \text{L}^{-1}$) for solids collected from the swirl separator during the trials with ozone treatment ($n=5$ days, 3 subsamples). A= size distribution for particles in the range between $22.5\text{--}714.7 \mu\text{m}$ in diameter (Coulter Counter[®] 1000 μm orifice tube). B= size distribution for particles in the range between $2.8\text{--}87.8 \mu\text{m}$ in diameter (Coulter Counter[®] 140 μm orifice tube).

Results obtained for the samples collected from the swirl separator using the 1000 μm orifice tube showed that 92% of the particles ranged between 33.7 μm and 45 μm (Fig. 97A). There was no significant difference ($p > 0.05$) in the particle counts between measurements replicates and between samples. Particle counts peaks were found in average around $28,000 \pm 6,500$. It was observed that particle counts decreased considerably while particles size increased. Some counting had to be aborted because extremely big particles agglomerates obstructed the orifice tube. Nevertheless, this observation was isolated and the realisation of the measurement was conducted normally.

Figure 97B presents the counting data obtained using the 140 μm orifice tube, also for samples collected from the swirl separator's basin. In this case and to avoid the obstruction of the comparable smaller aperture of the measuring device, the sample was previously sieve and only the portion that came after the 100 μm grid size was measured. Particle counts started at a size of 2.8 μm with a high number in particles (in average $355,000 \pm 57,000$). The distribution then followed a negative exponential course. It was impossible to find out if this phenomenon was belonging to a system's measurement error. Particles cumulative distribution showed that 93% of the particles were found in the range between 2.8 μm and 11.4 μm . Particles total counts averaged $5,758,000 \pm 2,269,000$. A significant difference ($p < 0.05$) between samples was found. Although the prior treatment of the sample was the same for every measurement, it was suspected that this might be had an influence in the total counts. Unfortunately this was impossible to validate.

Measurements results indicated that fine suspended material dominated the particle number concentration. Particle numbers counted with the 1000 μm orifice tube were about 10 times lower than the counts obtained with the 140 μm orifice tube. It was assumed that, in relation to the surface/volume relationship subject described in 4.4.5, these fine solids were extremely affected by leaching.

The particle size distribution by number of samples obtained from the foam collector tank is presented in Figure 98A and 98B. Particle number peaks were found in the range between 1,400 and 3,900 particles per litre using the 1000 μm orifice tube (in average $3,100 \pm 1,000$). These counts were found in the size of 40 μm and corresponded to 65% of the total counts. Particles below 34 μm and above 45 μm were found to be of a negligible amount. There was no significant difference ($p > 0.05$) found between counts

and between samples. It was presumed that the counts corresponding to particles above $45 \mu\text{m}$ were associated to particles aggregations more than solids of this size.

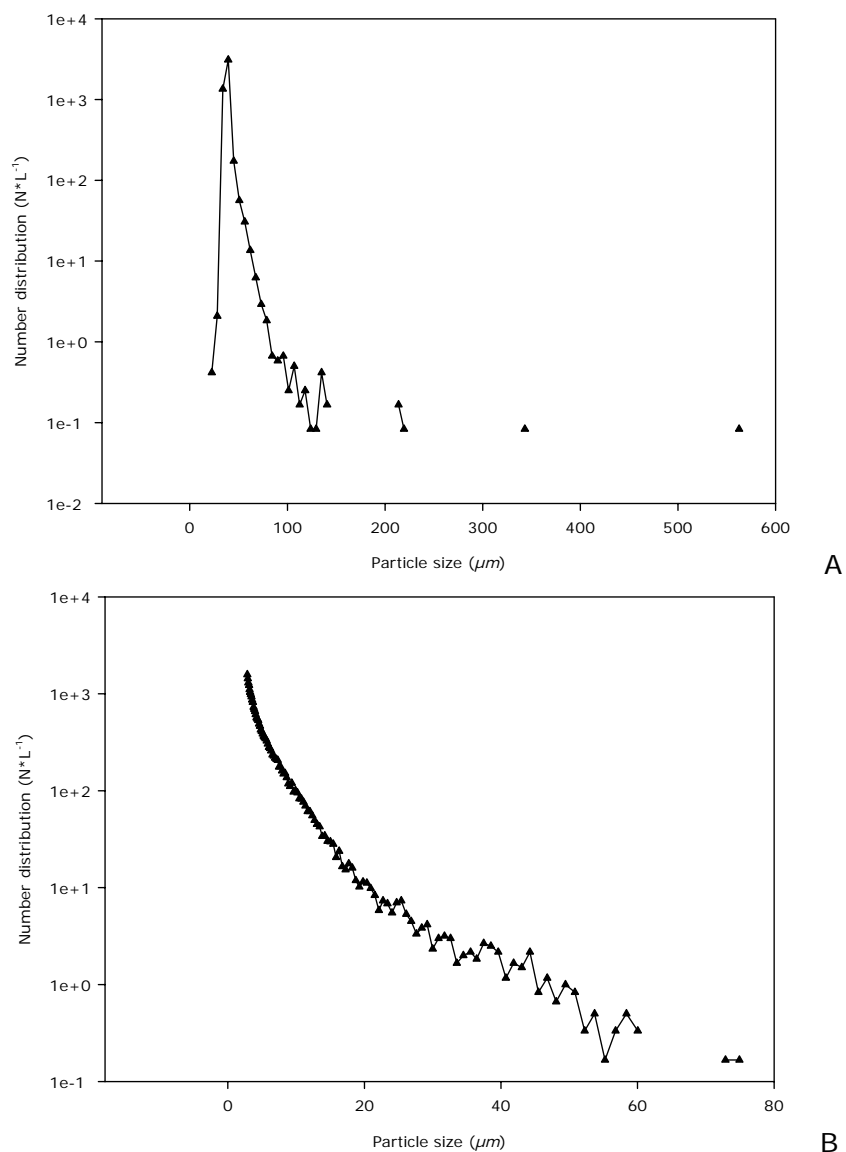


Fig. 98. Performance of the foam fractionator receiving the partially effluents of two fish tanks (water flow $2 \text{ m}^3 \cdot \text{h}^{-1}$). Graphics shows the particle size distribution ($\text{N} \cdot \text{L}^{-1}$) for solids collected from the foam flushing tank during the trials with ozone treatment ($n=4$ days, 3 subsamples). A= size distribution for particles in the range between $22.5\text{--}714.7 \mu\text{m}$ in diameter (Coulter Counter® $1000 \mu\text{m}$ orifice tube). B= size distribution for particles in the range between $2.8\text{--}87.8 \mu\text{m}$ in diameter (Coulter Counter® $140 \mu\text{m}$ orifice tube).

Size distribution for fine solids measured with the $140 \mu\text{m}$ orifice tube is presented in Figure 98B. Data plotted showed an initial averaged count of $1,576 \pm 65$ particles per litre. The curve followed than a negative exponential course. The calculated cumulative distribution described that 95% of the particles were situated in the range between $2.8 \mu\text{m}$ and $10 \mu\text{m}$. Solids above $10 \mu\text{m}$ played a negligible role.

It is noteworthy that the amounts of particle between swirl separator and foam collector tank differed approximately by factor 100. None the less, the counting corresponding to the fine fraction of particles obtained from the foam collector tank, seemed to be more reliable than those from the swirl separator. The water samples collected from the flushed foam were very homogeneous and easy to handle, facilitating the use of the Coulter Counter®.

3.4.6.2 Particle size analysis without ozone treatment

During those days when the ozone generator was turned off (days t_{686} to t_{690}) subsamples taken from the swirl separator and the foam flushing collecting basin were analyzed for the determination of particle size and number distribution. Coulter Counter's® orifice tubes with 1000 μm and 140 μm were used.

The data plotted in Figure 99A represent the particle size distribution for particles collected from the swirl separator in the range between 22.5 μm and 714 μm . Results obtained showed that 97% of the particles were situated in the range between 33.7 and 45 μm . The count peak was at a size of 39.3 μm with $971,000 \pm 134,000$ particles. Particle number concentration decreased rapidly as particle size increased. No significant differences were found between measurements and between samples ($p > 0.05$).

Figure 99B shows the particle concentration in the subsamples from the swirl separator determined using the 140 μm orifice tube. Samples were previously sieved and the portion that was obtained after the 100 μm grid size was analyzed. Particle counts were found to be very scattered and counting above 100,000 particles per litre were found in the size range between 2.8 μm and 4.8 μm . This range covered 71.6% of the size distribution. The highest counts were found in particles with 2.8 μm in diameter ($395,000 \pm 200,000$). The cumulative distribution showed that 95% of the particles were between 2.8 μm and 9.9 μm . The difference between samples was significant ($p < 0.05$).

Results indicated that the portion of fine suspended solids ($< 10 \mu m$) dominated the particle concentration. The counts found with the 140 μm orifice tube were about 10 times lower than those measured with the 1000 μm capillary.

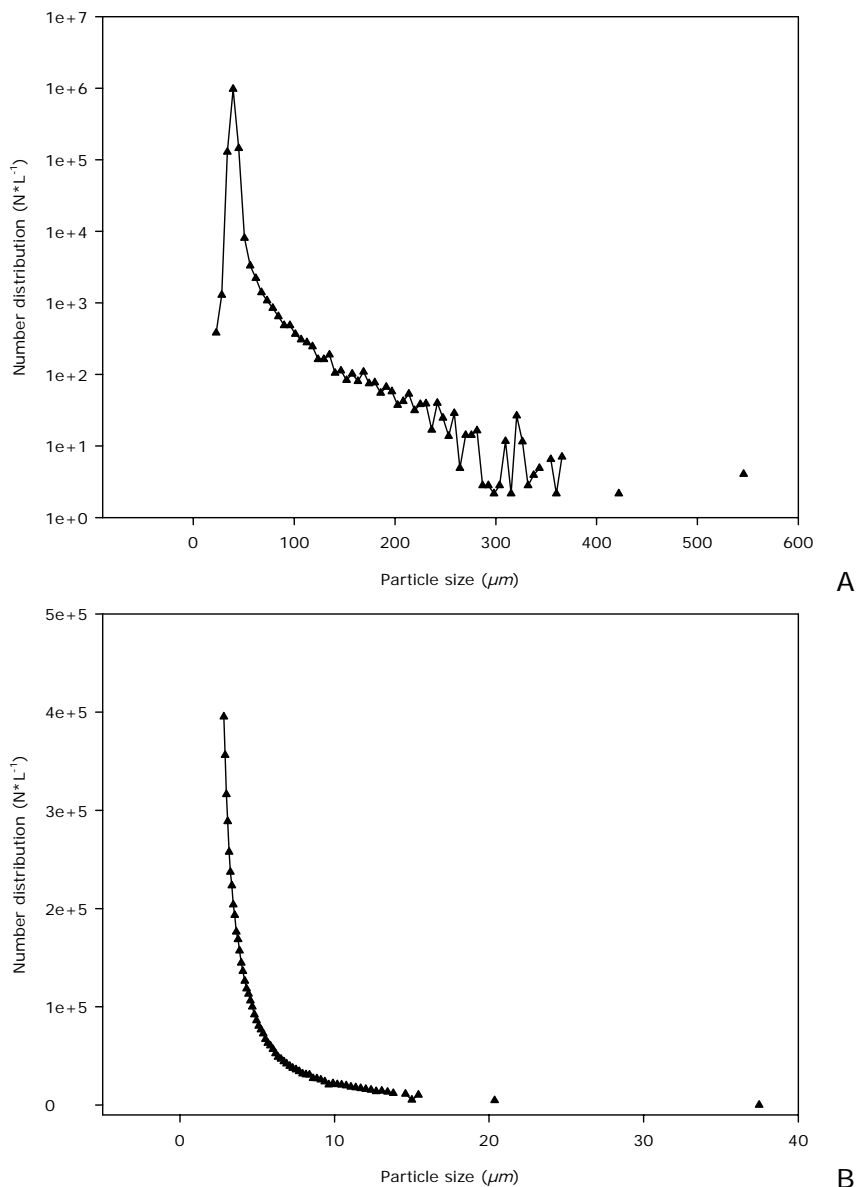


Fig. 99. Performance of the swirl separator receiving the effluents of two fish tanks (water flow $3.2 \text{ m}^3 \cdot \text{h}^{-1}$). Graphics shows the particle size distribution ($\text{N} \cdot \text{L}^{-1}$) for solids collected from the swirl separator RAS during the trials without ozone treatment (n=5 days, 3 subsamples). A= size distribution for particles in the range between $22.5\text{--}714.7 \mu\text{m}$ in diameter (Coulter Counter[®] 1000 μm orifice tube). B= size distribution for particles in the range between $2.8\text{--}87.8 \mu\text{m}$ in diameter (Coulter Counter[®] 140 μm orifice tube).

Results obtained for the samples collected from the foam flushing tank are presented in Figure 100A and 100B. Using the 1000 μm orifice tube particle concentration was in average $108,000 \pm 24,000 \text{ N} \cdot \text{L}^{-1}$. Counting peaks were found in particles with a diameter of $39.9 \mu\text{m}$ ($71,850 \pm 13,000 \text{ N} \cdot \text{L}^{-1}$). The range between $33.8 \mu\text{m}$ and $45 \mu\text{m}$ concentrated 96.8% of the total amount of particles. Particles below $33.8 \mu\text{m}$ and above $45 \mu\text{m}$ represented a negligible amount. It was suspected that the portion of particles above $45 \mu\text{m}$ were associated to particle clumps more than to solids in that size.

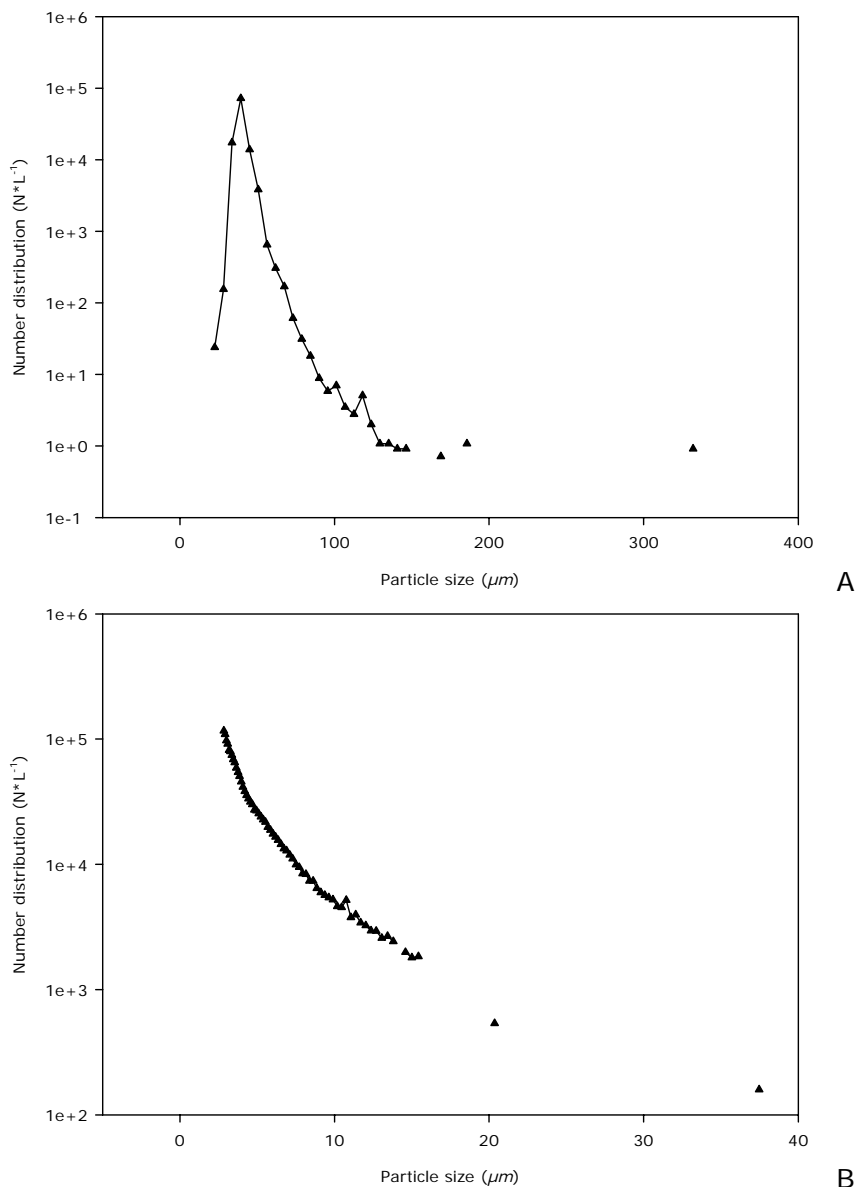


Fig. 100. Performance of the foam fractionator receiving the partially effluents of two fish tanks (water flow $2 \text{ m}^3 \cdot \text{h}^{-1}$). Graphics shows the particle size distribution ($N \cdot L^{-1}$) for solids collected from the foam flushing tank during the trials without ozone treatment (n=5 days, 3 subsamples). A= size distribution for particles in the range between 22.5–714.7 μm (Coulter Counter[®] 1000 μm orifice tube). B= size distribution for particles in the range between 2.8–87.8 μm (Coulter Counter[®] 140 μm orifice tube).

Particle concentration for fine solids measured with the 140 μm capillary is presented in Figure 100B. In average, initial counts were $116,500 \pm 67,000$ particles with a size of 2.8 μm . The calculated cumulative distribution showed that 95% of the counting was situated below 8.8 μm . Solids sized above 8.8 μm played a negligible role. Samples measured with the 140 μm orifice tube were very scattered and a significant difference was found between samples ($p < 0.05$).

Comparing the particle size distribution between the 1000 μm and the 140 μm capillary, the number of particles counted were almost equal (around 100,000), contrary to the results obtained from the swirl separator where a factor 10 was calculated.

3.4.7 Water flow in the RAS

The water flow in the RAS was determined using an ultrasonic flow meter. The system was installed in two places in the system, the outlet pipe coming from the two fish tanks, and the outlet pipe of the biofilter. Data obtained were plotted and are presented in Figure 101.

Data showed that to obtain a maximum water flow through the system of $3.2 \text{ m}^3 \cdot \text{h}^{-1}$, $800 \text{ L} \cdot \text{h}^{-1}$ air flow are needed in the airlift that brings the water to the biofilter (nitrification) (Fig. 101). When the air flow in the airlift was turned off, only $2.0 \text{ m}^3 \cdot \text{h}^{-1}$ circulated through the RAS, corresponding to around 60% of the whole water volume. This was considered to be a too low water flow, and insufficient to satisfied the need of one system's volume flow per hour.

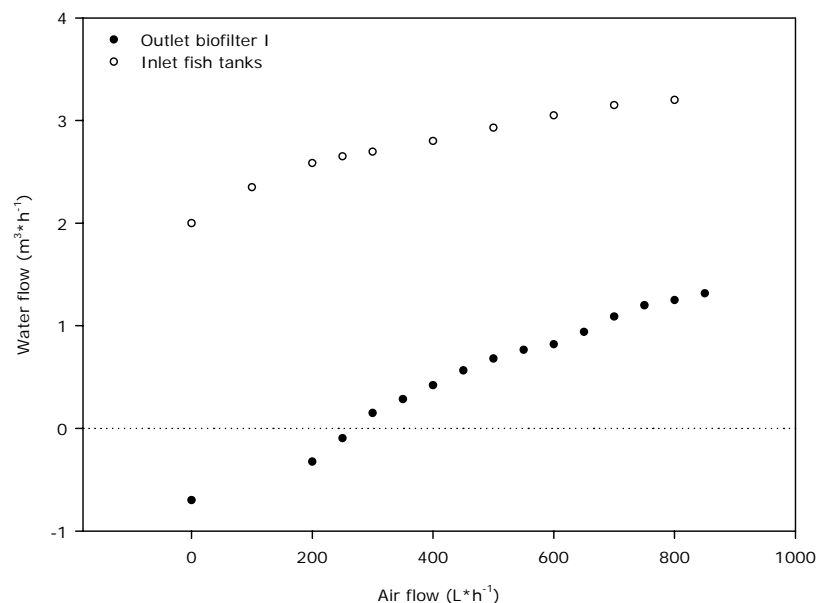


Fig. 99. Water flow ($\text{m}^3 \cdot \text{h}^{-1}$) in the RAS (outlet of the fish tanks i.e. inlet of the swirl separator, solid dots), and at the outlet of the biofilter (clear dots), measured for different air flows ($\text{L} \cdot \text{h}^{-1}$) adjusted in the flow meter installed in the air inlet of the air-lift. Values below zero (below the dotted line) are because of the counter-pressure produced by the air-lift system inside the foam fractionator tower.

Results obtained from the outlet of the biofilter showed that $0.7 \text{ m}^3 \cdot \text{h}^{-1}$ water actually passed from the biofilter basin to the foam fractionator tower when the air in the airlift was turned off. This amount of water returned to the fish tanks indeed through the airlift installed inside the foam fractionator basin.

The air flow inside the foam fractionator tower was not adjusted during the measurements. The compressor delivered $120 \text{ L} \cdot \text{h}^{-1}$ continuously.

4 Discussion

The recirculating aquaculture system (RAS) described in this study was designed and operated with the aim to investigate the fate as well as the qualitative and quantitative dynamics of total suspended solids (TSS) in such systems. Their influence on biological processes can also affect fish welfare (*i.e.* growth, health and quality). The long term sustainable operation of a modern aquaculture unit will increasingly require the integration of cost-effective treatment processes which can include the re-use of water and wastes as new resources. The RAS, under the supervision of the aquaculture working group at the IFM-GEOMAR provided the infrastructure for extended research activities regarding this topic. It allowed the investigation of system components and their interactions with specific biological, physical and chemical processes. The quantification of dissolved and particulate nutrients and their fate in the RAS was possible only because of simultaneous team research activities in two fields: (1) the use of nutrient-loaded system water in another system where macro-algae were cultivated and (2) the subsequent use of particulate wastes removed from the system in a separate detritivorous reactor.

Taking this background into consideration, the type of RAS under study needed special technical approaches in order to evaluate the performance of the system while aiming at low energy consumption (no use of conventional pumps, mechanical filtration exclusively via gravity forces). Additionally, the concept aimed also at low rate of water consumption (renewal). These two aspects were considered as operational key factors, often limiting commercial application in land-based fish farm facilities, because of (a) costs and (b) not providing the anticipated benefit for minimizing the environmental impacts associated the discharge of wastes (including particulate and dissolved matter).

4.1 RAS conception and design in light of the state of the art

The design of the experimental RAS included the following features that will be discussed in terms of operational efficiency such as low energy and water consumption rates, and water quality considerations to derive at desired conditions. From the results it is obvious that:

- The total systems' water flow configuration differs from conventional system designs as the volume passed first the swirl separator while than split in two

streams, one passing with 3/5 through the foam fractionator and the other with 2/5 through the biofilter (nitrification). This is a configuration that is not documented in the literature and therefore, performance can only be indirectly compared and it is argued that it offers a number of advantages and these will be discussed later on.

- Two-step solid separation is a second design element that differs from many other systems but also employed by several studies. Large particle sizes were collected and eliminated via the swirl separator, while fine solids were removed via the foam fractionator who received an independent water stream. Here we will be able to compare the results with studies dealing with each of these components separately.
- The usage of ozone in this study finds several comparative investigations but not with an identical system configuration while in general confirming the enhanced formation of foam, electrostatic adhesion of fines to form larger conglomerates thereby allowing to optimize the particle removal from the water column.
- A novel design of moving bed principle biofiltration was tested to avoid the accumulation of solid matter between the filter media, and this will be discussed in terms of its importance for the overall system performance.
- Low-head construction as employed in this study is an increasingly used concept which is necessitated by the rapidly increasing energy costs and permits to avoid also costly conventional pumps. Thermodynamic problems can also be avoided, including wasted heat energy transmission from the pump.
- Water renewal rates of less than 2% of the system's volume per day are one of the outcomes that indicate the high performance characteristics of the system configuration under study. Although often not practical in large-scale systems, the overall attempt to minimize water exchange has relevance in terms of judging the effectiveness of operational conditions in the system.

4.1.1 Design considerations in terms of efficient water transport and particle removal

The technical modification employed in the study system, in particular the diversion of the water flow from the swirl separator into two separate streams was purposeful to allow the application of higher ozone dosages for more effective control of bacterial populations while the biofilter (e.g. nitrification) was not at risk to be affected by residual ozone concentrations thereby avoiding any exposure of the nitrifier populations inside the biofilter to damaging radicals. A prototype of similar system design was reported by

Waller *et al.* (2001a) while its detailed quantitative assessment on TSS removal is subject of this study. However, the positioning of the foam fractionator and biofilter in the above mentioned study was still in a direct line.

In this study, a two step solid separation technique allowed to maintain clear water conditions over the entire experimental period. While the design of the system, as mentioned previously, was primarily to reduce the energy consumption by using gravity forces and air-lift systems, the side-effect was improved TSS removal, specifically capturing a larger portion of the smaller particle fraction.

Considering effective transport of water alone, it is obvious that the forces that have to be overcome (*i.e.* necessary energy input) is reduced to the expression $E=m \cdot g \cdot H$, where: E is the amount of energy, m is the mass of water that has to be moved (one system's volume per hour, constant), g is the gravitational force (constant), and H is the height that the water has to be lifted to maintain the desired flow. In this case, the only possibility to save energy (minimize E) is to keep H as small as possible. For this reason the RAS tanks in the study system were installed about 0.85 m above the ground and the water outlet from the tanks were at the same height of the inlet from the swirl separator basin. It was necessary than to elevate (lift up) the water approximately between 4-6 cm to maintain flow of one system's volume per hour. This was obtained using the air lift installed in the water inlet of the biofilter and the air lift inside the foam fractionator.

4.2 Growth performance of European sea bass (*Dicentrarchus labrax*)

Because of the team effort to study simultaneously a number of system components and their performance as well as interactions, the temperature regime and salinity had been altered once over the entire 437 day experimental period. This was done to accommodate the specific needs of several studies dealing with other aspects than suspended solids. However, these modifications of two principle operational parameters provided the unique opportunity to compare the performance of fish during subsequent growth periods.

To remember the overall operational mode, the system was at 16.6 °C (average) for the first 70 days (salinity 16) while the longest growth period (353 days) was run at 22.2°C (salinity 23). The growth performance data reported in the results can easily be compared with those obtained from literature operating at similar or identical conditions. As can be seen from Table 29, most of the growth data compare well with our own

findings. For example, at the one end of the spectrum, Person-Le Ruyet (2004) found much lower SGRs than in our study, while Dendrinis and Thorpe (1985) reported higher values. In general our data compare favourably with most of the data reported in Table 25, indicating a reasonable performance of the fish allowing arguing that the overall water quality in the system was adequate despite changing operational conditions which were partly modified for experimental reasons.

Tab. 29. Overall view of specific growth rates (SGR) performed by *Dicentrarchus labrax* reared at different temperatures reported in the literature. Average water temperature, fish weight, and number of data sets are detailed.

Water temperature (°C)	Average weight (g)	SGR (d ⁻¹)	Data sets (n)	Reference
18	140	0.0061	4	Lemarié <i>et al.</i> (1998)
18	10	0.0112	1	Russell <i>et al.</i> (1996)
19	235	0.0102	12	Dendrinis & Thorpe (1985)
19	15	0.0076	4	Papoutsoglou <i>et al.</i> (1998)
20	1000	0.0099	1	Hidalgo <i>et al.</i> (1987)
20	20	0.0099	1	Olivia-Teles <i>et al.</i> (1998)
20	200	0.0034	4	Paspatis <i>et al.</i> (1999)
21	50	0.0071	4	Paspatis <i>et al.</i> (1999)
22	130	0.0047	4	Paspatis <i>et al.</i> (1999)
22	65	0.0115	1	Thetmeyer <i>et al.</i> (1999)
22	410	0.0038	6	Zanuy & Carrillo (1985)
23	10	0.0034	4	Paspatis <i>et al.</i> (1999)
23	400	0.0038	7	Zanuy & Carrillo (1985)
24	105	0.0055	3	Azzaydi <i>et al.</i> (1999)
24	155	0.0063	4	Ballestrazzi & Lanari (1996)
24	160	0.0068	1	Ballestrazzi <i>et al.</i> (1994)
24	60	0.0119	4	Lupatsch <i>et al.</i> (2001)
25	150	0.0063	6	Ballestrazzi <i>et al.</i> (1994)

These data can also be used to arrange a quantitative comparison of the growth performance of *Dicentrarchus labrax*. The literature reports for sea bass two growth characteristics at below and equal to or greater than 20°C. Although this is an arbitrarily chosen classification, it results primarily from practical/commercial farm management experience where seasonal environmental conditions (primarily in the Mediterranean) determine operational schedules for feeding and harvesting. Nevertheless, this classification seems to be useful as the results obtained in this study allow also allocating the experimental periods to the two temperature regimes often compared in the literature. Figure 102 compares the literature and own data sets in terms of specific growth rate from trials below and above 20°C, using most of the references detailed in Table 29.

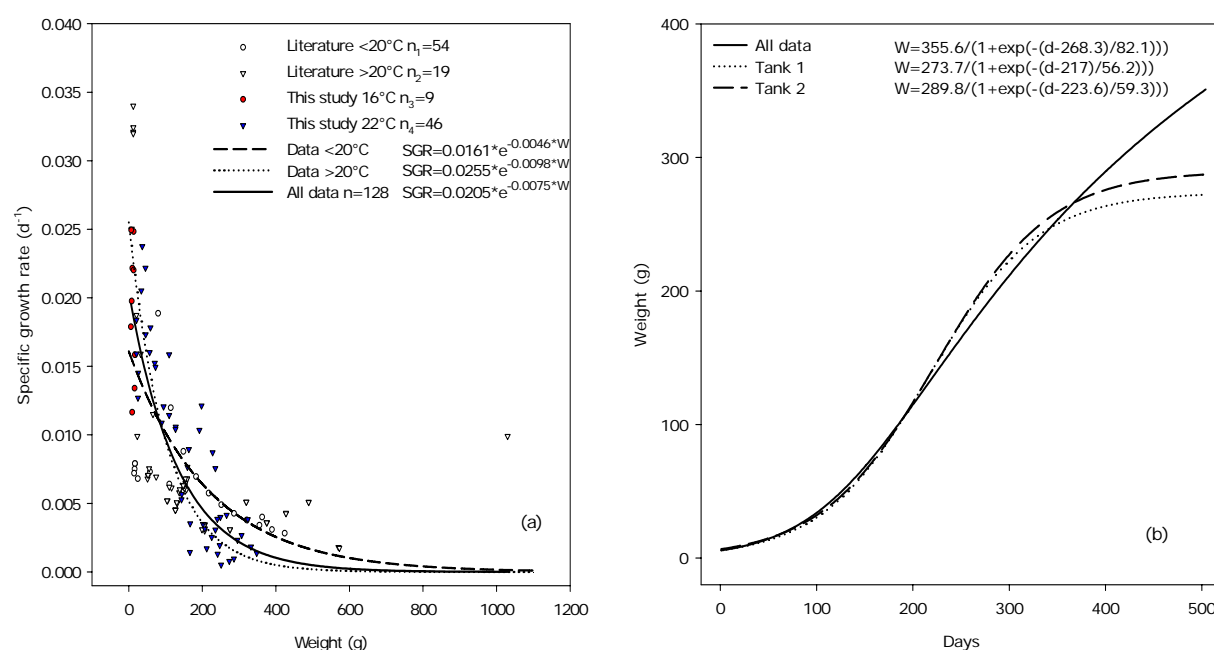


Fig. 102. Comparison of specific growth rates (SGR) for (a) and average weight (W) (b) of European sea bass (*Dicentrarchus labrax*) reared in several aquaculture systems and in our test system at temperatures below and above 20°C. Panel (a) n₁ to n₄ = sample size see insert. Total n for the overall equation = 128. Panel (a) depicts the calculated SGR curves for data below 20°C (dashed line) and above 20°C (dotted line) while the solid line represents all data combined. Panel (b) shows the weight gain over time (days=d) derived from all literature data (solid line) and both replicates of the own study (tank 1 = dotted line; tank 2 = dashed line).

As can be seen in Figure 102a, the data sets compare favourably with each other, leading to surprisingly little differences between the two temperature regimes when considering individual average performance. However, for farm management at large scale these differences are significant.

Figure 102b indicates also good agreement between weight gains over time in our two experimental tanks when compared to literature data. It is worth noting, however, that the growth performance was slightly higher in our experiments for a limited period of time ranging from day 220 to about day 350. Shortly thereafter, towards the end of the study period (about day 350 onwards), a remarkable decline in weight gain did occur. There are good reasons for loss of performance at that time because of (a) sorting which requires at least one day of starving the fish to reduce handling stress (thereby reducing growth), (b) delayed effects of the anaesthetic used on feeding rigor, (c) social stress among fish to re-structure themselves within the group in the new tank environment but foremost because of (d) problems associated with system management and component failures resulting in a period of unstable pH levels because of inappropriate dosing of CaO, occasional overdosing of ozone, and subsequent high TAN concentrations due to temporal system failure (i.e. broken pipe and spillage from the foam fractionator).

These results clearly demonstrate the long-lasting effects of deviations in system performance and/or short-term system failures on growth of the cultured species. The lesson to be learned from such unforeseen system failures also is to stop feeding immediately and accept loss of growth rather than stress related mortality.

Feed conversion ratio averaged 1.8 for both tanks during the growth period at 22°C, between day t_{71} and t_{437} , which is within the range described by other experimental studies. Average FCRs reported ranged from 1.2 to 1.8 for similar ranges of fish size (Ballestrazzi *et al.*, 1998, Dosdat *et al.*, 2003, Eroldogan *et al.*, 2005, Montero *et al.*, 2005, Paspatis *et al.*, 2003, Peres and Oliva-Teles, 1999). Relative low values (1.1) were found by Person Le-Ruyet *et al.* (2004) with sea bass between 120 g and 210 g. Extremely high conversion ratios were determined by Paspatis *et al.* (1999) for different fish sizes with conversion efficiency increasing with fish size. This was partly also observed during the last 100 days of this experiment, where FCRs raised up to values between 2 and 4. Again, these unusual changes to unreasonably high FCR values are due to the ill effects of short-term system failures identified above. Unexplained changes in conversion efficiency should always lead to a retrospect analysis of the system performance in terms of water quality parameters as the problem often finds its origin there.

The investigations about stocking density and feeding efficiency reported by Paspatis *et al.* (2003) showed that the FCR increased while the fish weight *i.e.* culture density rose. Such effects can also be initiated by running systems at too high stocking density. For

example, FCR values were found to increase from 1.4 at fish densities of about $3.0 \text{ kg}\cdot\text{m}^{-3}$ to 2.7 at density of $13.7 \text{ kg}\cdot\text{m}^{-3}$ and finally to FCRs of 4 at about $31 \text{ kg}\cdot\text{m}^{-3}$. Compared to these values the FCRs in our study showed a comparably lower increase in FCRs, and at the time when the tank density reached its maximum ($38.2 \text{ kg}\cdot\text{m}^{-3}$) we found on average the highest FRC value around 3.5. Roncarati *et al.* (2006) suggests from his results that $20 \text{ kg}\cdot\text{m}^{-3}$ is within the optimum rearing density for juvenile sea bass and found much reduced performance data when density reached $40 \text{ kg}\cdot\text{m}^{-3}$. Certainly, while the trend is similar, the absolute values of our study differ from the observations by Roncarati *et al.* (2006).

The condition factor (CF) is commonly used as an indicator of the nutritional condition of fish in both wild and cultured stocks; however, in sea bass and sea bream farming, surprisingly few investigators use this factor in describing fish performance in their studies. Froese (2006), however, also identifies this factor for our species along with determining maturity stages. The CF is very species dependant (Roncarati *et al.*, 2006). Roncarati *et al.* (2006) found a condition factor of 1.2 for fish with a total weight of 310g. This value is comparable to the average condition factor found in this work (1.3). Nevertheless there are no standardized values for the condition factor of *Dicentrarchus labrax* at any given size when being raised in a RAS although this would be a useful tool for practical reasons. Pickett and Pawson (1994) reported condition factor obtained from wild sea bass stocks from the northern, central and southern regions around the UK coast, for males and females collected all year around. Values determined were in the range of 0.8 and 1.4. Unfortunately, these data are difficult to compare because fish were certainly exposed to different environments which exhibit much more variable (*i.e.* seasonal) feeding condition than derived under culture conditions. High content of adipose tissue or fat in reared sea bass will also be partly affecting the condition factor which have a negative repercussion and might be interpreted wrongly.

From an aquaculture point of view, final product quality is also an indicator of system performance. However this is not often a consideration included into scientific studies on recycling systems. In our study we attempt to do so. Among the various aspects that contribute to defining the quality of raw fish, freshness is one of the most important ones. The post mortem degenerative processes that take place lead to a significant and progressive modification of the initial state of freshness (Parisi *et al.*, 2002). Flesh quality is a complex set of characters involving intrinsic factors such as texture, chemical composition, colour, protein and fat content, and is heavily influenced by extrinsic factors such as pre- and post-slaughter handling procedures (Periago *et al.*, 2005).

Sea bass is considered a non-fatty fish (Periago *et al.*, 2005) and the fat content found in the fillets of our fish sampled towards the end of the experimental period was analyzed with 4%. This can be considered as slightly higher than the results obtained by Eroldogan *et al.* (2005) (3.2%) and Person Le-Ruyet *et al.* (2004) (3.9%). Periago *et al.* (2005) compared fat and protein content in wild caught and farmed sea bass indicating that fat content was higher in wild sea bass (9.2%) as in farmed organism (6.7%). In contrary, protein found in farmed fish (23.4%) was higher than in wild specimens (17.6). Protein content in fish fillets collected from the RAS was 20.7%. Comparable results (19.8%) were obtained by Eroldogan *et al.* (2005), but differ from protein content in wild sea bass (17.6%) and from farmed specimens (23.4%) found in the measurements done by Periago *et al.* (2005). It should be considered that the proximate composition depends on feed quality, fish size, environmental conditions, and also genetic factors. In farmed fish, feeding with prepared diets provides a wide range of nutrient composition. This fact determines not only fish growth rate but flesh composition and quality, in particular lipid content. Nowadays, the lipid content in aqua-feeds can be and often are quantitatively and qualitatively modified.

The microbial analysis of the flesh correlates with the characteristics and quality of the handling during and after the slaughter and time of storage (see 3.2.6), more than a direct relation with the nutritional composition of the muscle. The results on CFU, *Enterobacteriaceae* and *E. coli*, together with the absence of *Listeria monocytogenes* on the fish fillets were considered positive and satisfactory in terms of performance of the RAS. Regarding the sensory analysis, the examinations and qualifications used were unfortunately not equivalent to EU standards. None the less, the qualified and experienced personnel of the analytical laboratory gave the highest values for appearance (colour and shape), odour, texture, and taste (steamed) to the fillet samples. In conclusion the fish that were produced in the RAS had an excellent quality.

4.3 Performance of the biofiltration (nitrification)

The RAS and its components should offer save limits to the species in cultivation in terms of TAN, NO_2^- -N and NO_3^- -N concentrations as have been tentatively identified in the scientific literature (Wickins, 1980; Hochheimer and Wheaton, 1997; Malone and de los Reyes, 1997) and by intergovernmental and regional regulatory authorities (EIFAC, 1986). Excessive concentrations of these nitrogen compounds may result in growth depletion, immune depression, and even high mortalities, depending on concentration level and time of exposure. Compared to flow-through or ponds, reuse systems typically

have significantly reduced make-up flows that can result in build-up of unwanted compounds. Also, the ability to independently control parameters such as dissolved oxygen, may allow culture animals to tolerate higher levels of other water quality parameters (compared with other culture types) (Colt, 2006).

The performance of the aerobic biological filter in the present work was satisfactory in terms of the requirements for an intensive fish farm. At the beginning of the experiments the nitrification process was instable and marked by relatively high variability in TAN and NO_2^- -N concentrations. Similar observations were reported by Collins *et al.*, (1975), LaBomascus *et al.* (1987), Nijhof and Bovendeur, (1990), Sander (1998), Olivar *et al.*, (2000), Thoman *et al.*, (2001), and Seo *et al.*, (2001) while the phenomenon is also known for a long time as typical for the start-up phase. Nevertheless, average ($1 \text{ mg} \cdot \text{L}^{-1}$) and maximum ($3.6 \text{ mg} \cdot \text{L}^{-1}$) TAN concentrations measured during the experimental trial were considered within safe limits and far below the sublethal toxicity limits determined for sea bass juveniles (LC_{50} 96-h $40 \text{ mg} \cdot \text{L}^{-1}$ TAN). These values are found in by Person-Le Ruyet *et al.* (1995). Blancheton (2000) considered that TAN concentrations for sea bass adults should be below $2 \text{ mg} \cdot \text{L}^{-1}$ while reduced growth performance was observed in *Dicentrarchus labrax* at values ranging from 6 to $10 \text{ mg} \cdot \text{L}^{-1}$ (Lemarié *et al.*, 2003). Dosdat *et al.* (2003) reported that low total ammonia may even enhance subsequent fish appetite and growth rates and may have a similar effect on growth performance as restricting feeding levels. The non-observable effect concentration (NOEC) was given with $6 \text{ mg} \cdot \text{L}^{-1}$ TAN. Roncarati *et al.* (2006) reported TAN concentrations in the range of 0.3 - $1.5 \text{ mg} \cdot \text{L}^{-1}$ for sea bass reared at three different densities and at high temperatures (26°C - 28°C). It has to be noted that in all of those experiments the variation of ammonia concentration may have greatly varied because of numerous other interfering factors that affect the dissociation of the unionized ammonia fraction (NH_3). The equilibrium between unionized (NH_3) and ionised (NH_4^+) ammonia is highly dependant on water pH, salinity, and other factors. Although the average pH in the present study was relatively low (7.2), the percentage of NH_3 at 22°C is about 1% (Wheaton *et al.* (1994). At lower temperatures (as experienced between day's t_0 and t_{71}) the percentage of NH_3 was around 0.8%. Nitrite-nitrogen concentrations (NO_2^- -N) averaged $0.2 \text{ mg} \cdot \text{L}^{-1}$ (max $0.7 \text{ mg} \cdot \text{L}^{-1}$). These values are concordant with the safe levels reported by Blancheton (2000), and those concentrations measured by Roncarati *et al.* (2006). Nitrite is the ionised form of the relatively strong acid, nitrous acid (Colt, 2006). For a NO_2^- -N concentration of $1.0 \text{ mg} \cdot \text{L}^{-1}$ NO_2^- -N, the concentration of nitrous acid (HNO_2) is $0.17 \mu\text{g} \cdot \text{L}^{-1}$ at a pH of 7.2 (system's average pH). This nitrous acid is freely diffusible across gill membranes while nitrite is not. While the concentration of un-ionised nitrous acid

increases at lower pH, there is no evidence of increased nitrite toxicity at lower pH values (Colt, 2006).

The average TAN removal rate in the biofilter (nitrification) between day's t_{125} and t_{414} was $0.19 \text{ g} \cdot \text{m}^{-2} \cdot \text{d}^{-1}$ TAN, calculated on the basis of the difference between inlet and outlet concentrations. This removal rate was comparable to the results obtained by Nijhof and Bovendeur (1990) who studied also *Dicentrarchus labrax* among other species. The precise dynamics of the nitrification rates could not be described accurately to determine the breakpoint between half order kinetics and zero order kinetics for any given TAN concentration as initially been done by Bovendeur (1989) and later by Nijhof and Bovendeur (1990), Wheaton (1994), Chen *et al.* (2006), Colt (2006), and Malone and Pfeiffer (2006). The data described partly the nitrification process and was definitely limited by high TAN concentrations. However, the data points were very scattered. It was observed, as described by Nijhof and Bovendeur (1990), Wheaton, (1994) and Chen *et al.* (2006) a decrease in the nitrification rate occurred in presence of high TAN concentrations. As the TAN concentrations declined below a certain upper limit, the TAN removal rate suggests dependence on the TAN concentration. It is noteworthy, though, that the relatively low concentration requirement for a biofilter system in aquaculture determines that in most cases the TAN concentration is the rate-limiting factor in biological nitrification. As long as aquaculture biofilters operate at low TAN concentrations, the nitrification kinetics remains satisfactory within the first order reaction model (Chen *et al.*, 2006). Although initially described by Bovendeur (1989) this relationship was also confirmed by Ling and Chen (2005) during the evaluation of three types of biofilters. Consequently, for recycling systems in aquaculture, partial water replacement is a quick solution to bring nitrification back to efficiency once the critical upper TAN concentration has been exceeded. In our study overall TAN concentrations reached never high enough concentrations for sufficiently long periods to establish rates at levels of the zero-order kinetic.

Despite the low TAN and NO_2^- -N concentrations it was suspected that the biofilter did not always work effectively because the packed submerged filter material was collecting solid material which may lead to unsuitable interface conditions between desired autolithotropic bacteria film and the water. There is also the limitation on nutrient supply, the controlling of excessive biofilm development, and the lack of oxygen diffusion. It is actually oxygen diffusion limitations in relation to TAN oxidation in a biofilm that determines the breakpoint for TAN towards the zero order kinetics. Rosenthal and Black (1993) and Sander (1998) explain how such a filter system can silt up causing lower flow

velocities and zones were even no flow passed through. In our trials backwashing the biofilter was not seen as an option because: (1) the performance of the nitrification process was satisfactory, (2) extra water consumption with backwashing, and (3) the disturbance and disruption in the bacteria population structure *i.e.* a loss of bacteria and the need to re-develop a biofilm. Such inconsistencies can lead to uncontrollable and unwanted water quality fluctuations and affect the results on fish growth. Malone and Pfeiffer (2006), describing the various strategies used in the design of biofilters, pointed to submerged packed beds there is no additional biofilm management necessary because of continuous self-control, allowing to operate at a low specific surface area, while also oxygen transfer to the biofilm is maximized by continuous interface exchange.

As reported in Material and Methods (2.2.3) the original biofilters was supplemented by two additional filters on serving each of the two fish tanks. The TAN removal rate in these two additional biofilters operated between days t_{268} and t_{414} was in average $0.28 \text{ g}\cdot\text{m}^{-2}\cdot\text{d}^{-1}$. This performance was higher than in the first biofilter operated during the initial phase of the RAS study. These two biofilters were trickling filters, having a constant oxygen supply (optimal air/water interface) and a continuous hydraulic load controlling the bacteria film from the filter media due to shear forces, thereby avoiding clogging. These two biofilters were operated for a time interval of 146 days and no silt up was observed.

The active submerged surfaces in the system *i.e.* pipes and basins walls, were calculated. Together, the so called passive nitrification surfaces amount 14.6 m^2 . Taking the removal rate calculated for the biofilter, the TAN removal by nitrification on surfaces other than those inside the biofilter, could theoretically have reached about $2.7 \text{ g}\cdot\text{d}^{-1}$, which is 38% of the total nitrification rate. Losordo and Westers (1994) found that TAN removal outside the biofilter has not to be neglected.

It is general consensus that the NO_3^- -N concentrations for marine fish should be not exceed but be less than $500 \text{ mg}\cdot\text{L}^{-1}$ (Colt, 2006). Thoman (2001) described average values of $120.2 \text{ mg}\cdot\text{L}^{-1}$ NO_3^- -N in his 80 days of experiments. He also found some decline in the NO_3^- -N concentrations in the system but presumed that these could have been a result of dissimilatory nitrate reduction, phytoplankton uptake, assimilation by bacteria, or direct denitrification in some spots of the system. The highest concentration measured in the present study was $168.7 \text{ mg}\cdot\text{L}^{-1}$ (day t_{355}) far below the maximum pretended limit reported by Colt (2006). The changes in the NO_3^- -N concentrations were assumed to be more related to water renewal than to the processes described by Colt (2006). None the

less, the so-called “uncontrolled” denitrification may have taken place in parts of the active surfaces in the RAS (explained above), when the thickness of the bacterial mats deposited on tank and pipe walls has become significant. In this context, the internal walls of the fish tanks, although considered “clean” do have an active biofilm as can be felt by the normal slimy surface indicating the thin bacterial film. This biofilm was constantly thinned by contact with the swimming fish. Because of water currents in the tank and additional water movement by the fish, these biofilms experienced good oxygen supply and excellent washout of metabolites. In contrast, the biomass inside the pipes can grow to a relatively thick layer (Fig. 103). This layer settled because the systems’ water flow was not high enough to wash off this thick biomass. It should be remembered that the system operated without conventional pumps and the pressure inside the pipes was only about 0.15 bar. Here in the pipes, biofilm thickness and limited oxygen supply through rapidly changing interface between solid and liquid is the limiting factor. This effect is definitely disadvantageous because the cleaning of pipes is very costly or sometimes impossible to do in case system design did not include the necessary piping access for easy cleaning. The problem with these thick layers is that they can cause the obstruction of a pipe, or the accumulation reaches a certain point when suddenly big amounts of material get loose causing turbidity problems. Modern RAS designed after this low head principle incorporated open channel systems for in- and outlet that are easy to clean.



Fig. 103. Biofilm and solid attachments on the internal wall of the 63 mm in diameter outlet pipe from the biofilter (nitrification) tank. The sludge is approximately between 3 mm and 6 mm thick. The photography was taken on day t_{435} .

The biofilm accumulation inside the pipes has two aspects: (1) the extra bacterial biomass capable of nitrifying dissolved nutrients and (2) the development of an anoxic layer where denitrification can take place despite the rapid water velocity with its high exchange of medium at the interface. This is a matter of biofilm thickness. The dissolved oxygen concentration profile within biofilms with a thickness of approximately $400 \mu\text{m}$

was studied by Zhang *et al.* (1995) (cited by Chen *et al.*, (2006), demonstrating a rapid dissolved oxygen concentration drop within the biofilm. The limiting factor at where denitrification starts to occur is $2 \text{ mg} \cdot \text{L}^{-1}$. The sludge thickness inside the pipes was estimated to be about 3-6 mm (Fig. 103). Hypoxic or totally anoxic micro-niches are certainly present in the accumulated solids inside pipes. This means that, if the organic layer tends to be anoxic in inner layers, the probability of a partial denitrification process is high. However, the source of hydrogen and carbon sources needed for denitrifying bacteria remains limited.

Considerable research has been conducted on the effects of organic compounds on nitrification, however most studies concern domestic or industrial wastewater. Most importantly additional oxygen demand by organics affects nitrification. Particulate and dissolved organics provide ample substrates for heterotrophic bacteria whose growth will compete with nitrifying bacteria for oxygen and growing space. With the addition of organic matter, fast-growing heterotrophic bacteria which use organic carbon as their energy source will out-compete slow-growing nitrifying bacteria, resulting in a decrease in the nitrification rate. It was reported that heterotrophic bacteria have a maximum growth rate of five times and yields of two to three times that of autotrophic nitrifying bacteria (Chen *et al.*, 2006). Michaud *et al.* (2006) stated out that the nitrification efficiency in sea water was strongly impacted by POM: with different C/N ratios, the nitrification efficiency was reduced by 7% when moving from a C/N=1 to C/N=2. More significant was the loss of nitrification efficiency when moving from C/N=0 to C/N=1 (45%), suggesting that the impact of POM became less and less importance as the carbon concentration increased.

4.4 Performance of the suspended solid separation

The swirl separator worked effectively capturing the solids coming from the fish tanks. The amounts of TSS collected were less than the theoretical value of 15% which would be expected based on the digestibility coefficients identified by the feed manufacturer. The TSS quantity was significantly less than reported by Timmons *et al.* (2001) who suggest 25% of the feed fed to fresh water fish. However, samples collected from the swirl separator in our study were taken in the morning of every sampling day. This means that in the conical bottom of the swirl separator the material accumulated for 24 hours and leaching effects as well as partial resuspension may have led to a breakdown of particles with subsequent out washing (Lupatsch and Kissil, 1998). Once released into water, the excreted faeces are subject to gradual changes of nutrient composition due to

disintegration and passive leaching. According to Lupatsch and Kissil (1998) leaching processes come almost to an end after 6 hours in sea water. Therefore, suspended solids should be separated as soon as possible from the main water stream to avoid leaching and nutrient transition into the water. In the present study this was not feasible and would have required an automated and well-timed mechanical removal mechanism. However, depending on the type of RAS it might be desirable to use dissolved nutrients in a secondary production loop as new resource.

The quantity of TSS removed in the present study was on average 5% of the produced solids. TSS expressed as $\text{g} \cdot \text{kg}_{\text{feed}}^{-1}$ are presented in Figure 104, for every feed type *i.e.* size used. These are overall calculations from the detailed data presented in the results section, demonstrating the variability of total amount produced in relation to operational conditions, particularly with changes in feed pellet size. When pellet size becomes too small for on-growing fish, solid output rapidly increases. At larger fish sizes, these changes are not as apparent, although high variability occurs over time. The following comparison with literature data has to be seen with caution as they reflect average values only without indicating variability within a series. Recent published data on solid matter collected from a RAS for the cultivation of sea bass reported amounts of settled solids between $91 \text{ g} \cdot \text{kg}_{\text{feed}}^{-1}$ and $105 \text{ g} \cdot \text{kg}_{\text{feed}}^{-1}$ for sea bass in the size of 60 – 100 g, and $135 \text{ g} \cdot \text{kg}_{\text{feed}}^{-1}$ for sea bass in the range between 500 – 600 g (Franco-Nava *et al.* 2004). These results are somewhat higher than $50 \text{ g} \cdot \text{kg}_{\text{feed}}^{-1}$ found in this study for an average fish size of approximately 70 g and $66 \text{ g} \cdot \text{kg}_{\text{feed}}^{-1}$ for sea bass of approximately 280 g. Differences can possibly be explained by differences in (a) system design, (b) sampling procedures, (c) feed pellet composition, and (d) sampling points and sampling procedures (*i.e.* 3 subsamples). Occasionally, unforeseen short-term events with bulking sludge could have contributed to the inconsistencies in settling characteristics and thereby contributed to some underestimation of the average values. However, this should have accounted to only small fraction of the differences to literature data.

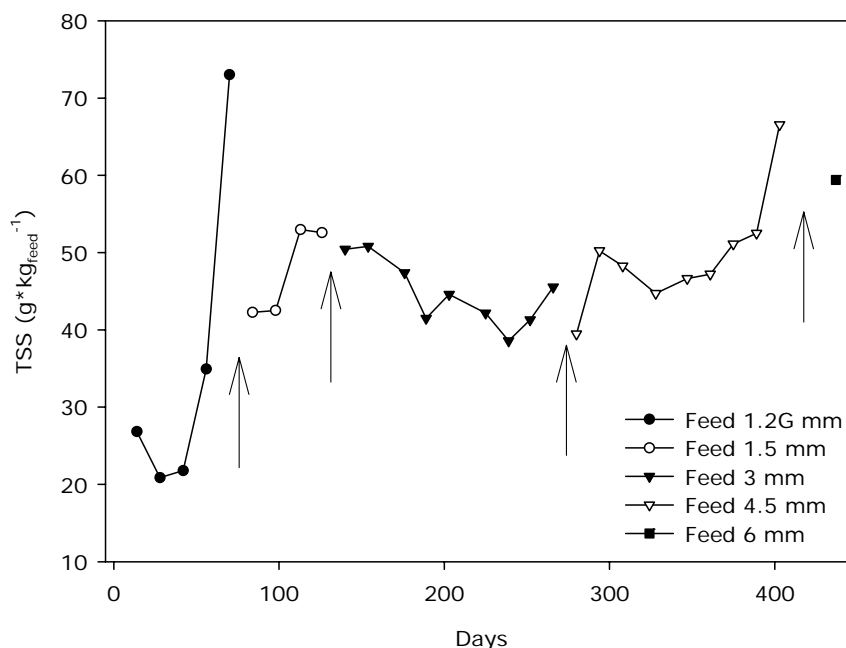


Fig. 104. Distribution of total suspended solids (TSS) in the RAS in relation to feed pellet size as determined from samples collected from the swirl separator between day's t_{14} and t_{437} expressed as grams per kilo feed (dry weight). Arrows indicate the changes in feed pellet size.

The specific gravity of particles plays an important role in the behaviour of solids in various system configurations and this should be considered when designing swirl separators and other particle filtration techniques for RAS. Chen *et al.* (1993) reported particles density of $1,190 \text{ kg}\cdot\text{m}^{-3}$ in three rainbow trout RAS; Timmons *et al.* (2001) found a density of $1,050 \text{ kg}\cdot\text{m}^{-3}$ for tilapia faeces; some other publications cited in Patterson *et al.* (2003) determined values between $1,030$ and $1,100 \text{ kg}\cdot\text{m}^{-3}$. Fact is that the density of particles varied with particle size as reported by Patterson *et al.* (2003) who found that, heavier particles had a mean density of $1,153 \text{ kg}\cdot\text{m}^{-3}$ and that the finer, lighter particles a mean of $1,050 \text{ kg}\cdot\text{m}^{-3}$. It was observed recently (Veerapen *et al.*, 2006) that the solid separation in a swirl separator was mainly due to gravity rather than centrifugal forces. Particles were found uniformly across the swirl tank, and separation was mainly by sedimentation. Small and fine particles will have difficulties to precipitate and will not settle in a swirl separator but stay suspended in the water column.

We collected particulate matter from the conical bottom of the swirl separator and discharge methodology of accumulated sludge may have affected the measurements because removal was intermittent (once a day) to save water needed in this process. Draining of the swirl separator was normally in the morning. The amount of water used for sludge draining was usually in the range of 6 to 8 L. However, when solids were carefully drained for TSS sampling, the amount of water needed ranged between 10 L and 25 L. Taking the regular draining and sampling volumes together, overall water

volume for sludge draining ranged from 16 L to 32 L. These volumes were still negligible with respect to total system volume. It may be unrealistically low for commercial scale RAS as transport distances in larger system with longer pipes may require to install several separators to minimize particles breakdown in turbulent pipe flows. However at commercial scale, even slight increases in discharge volumes might pose a bottle neck because of the scale-up dimension with the discharge counts for solid matter. It is important to design RAS in a way that the energy and matter can be transferred in the most cost-effective way and in large-scale systems where waste amounts reach a critical mass, integration of production systems through a secondary water-loop utilizing the waste right at the source as new resources may be a sustainable mode of operation. In this context it was important to quantify the solids produced and analyse their nutritional content during the entire production cycle of *Dicentrarchus labrax* so that based on these data, a potential secondary production module may be incorporated.

The data collected for carbon, nitrogen, phosphorous and energy content in the solid matter have been divided into seven size classes. The distribution over time was found to be very scattered and highly variable, and besides system instability this may also have been caused by variation in feed quality as feed charges purchased with time may vary in their composition. Recent published data on the faecal composition of sea bass reported contents of 17-26% and 1.2-2.4% for carbon and nitrogen, respectively (Franco-Nava *et al.*, 2004). The results obtained in this study were in the range of those reported by Franco-Nava *et al.* (2004), although their determinations were done based on total sludge material and not on different particles size. Further, the nutrient content in the fish feed will determine the nutrient content of the sludge as does the biology of the species reared. The carbon and nitrogen contents were higher in feed type 1 than in feed type 2 and 3 which had less protein and fat content. The organic matter found in the solids was always higher when using feed type 1. It decreased when feed type 2 was fed and this decline was independent from particle sizes. Although the phosphorous content was constant in all three feed types, the phosphorous content in the particulate matter showed values between 1% and 2% for feed type 1, 2.5% to 4% for feed type 2, and 2% to 5% for feed type 3. The differences can be partly explained by the study on leaching conducted by Lupatsch and Kissil (1998) and Chen *et al.* (2003). Leaching is a significant and very quick process when feeds are exposed to water. Chen *et al.* (2003) reported that after 2.5 min of immersion of pellets in sea water up to 16% of the nitrogen in the solid matter was already dissolved in the water. In conventional RAS this would lead to a tremendous accumulation of dissolved organic nitrogen. The foam fractionator captured also dissolved or colloidal material and it is assume that a fraction

of these originate from proteins leached of feeds. In conventional RAS the accumulation of organic matter may impact biofilter efficiency as heterotrophic bacteria will grow faster compared to autotrophic species. Leaching of organics and nutrients from faeces ranged between 4-14%. Lupatsch and Kissil (1998) found half of the organic content in their solid samples after 6 hours being dispersed in the water. In addition, it was presumed that smaller particles (below 200 μm) have a higher probability to contribute to leaching than particles of greater diameter. Fig. 105 shows the surface/volume ratio of a sphere. Considering that a single particle tends to be of spherical shape, the negative exponential curve shows the dimensions of the potential leaching problem from smaller particles. Heterotrophic bacteria will have an easier game to benefit from these small particles.

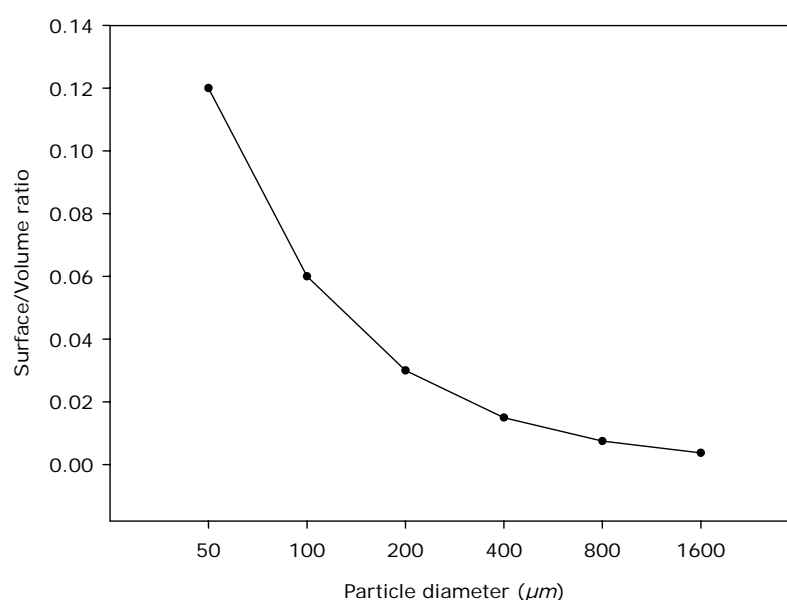


Fig. 105. Relationship between size (diameter) and surface of a sphere, expressed as surface/volume ratio, for particles from 50 μm to 1600 μm in diameter.

The energy content in the solids was more or less evenly distributed through the different size classes but varied with feeds used. Average values were higher ($20,390 \pm 380 \text{ J}\cdot\text{g}^{-1}$) in solids collected when feed type 1 was fed compared to feed type 2 ($17,800 \pm 2,200 \text{ J}\cdot\text{g}^{-1}$) while with feed type 3 the energy content was even lower ($16,710 \pm 2,430 \text{ J}\cdot\text{g}^{-1}$). Interestingly, the variability (SD) increased from feed type 1 to feed type 3, as the overall energy content declined. We do not have an explanation for this phenomenon but speculate that this might be related to variations in fibre content in these feeds. This comparison does not say anything with regard to feed energy utilization but provides simply a base for assessing the quality of suspended solids collected in a RAS and the potential re-use of this resource. Overall, solids content between 76% and 98% of the gross energy content determined in the feed when collected from the swirl separator.

Three assumptions may explain the energy content in solids: (1) the amount (3%) of raw fibre in the feed (long chain polysaccharides) is not retained by the fish, therefore found in the faeces and measured as energy; (2) the fish faeces contained also mucous and bacteria in low quantity which have partly contributed to the energy content; and (3) the solids in the swirl separator might have also contained some feed pellets which have been not taken by the fish.

Recently (Zhu and Chen 2001, Chen *et al.* 2006, Ebeling *et al.* 2006, and Michaud *et al.* 2006) demonstrated that C/N ratios in POM can affect the performance of the water treatment units, specially the biofiltration *i.e.* the composition of the microbial population, an interaction already postulated by Rosenthal (1981). Simulating C/N ratios between zero and two, the above cited authors found that the nitrification process was progressively inhibited by the heterotrophic processes when C/N ratios rise. The addition of sucrose as source with a carbon/nitrogen ratio of 1 or 2 reduced TAN removal rate by nearly 70% as compared to a nitrification process at C/N ratio of zero (Zhu and Chen 2001).

In our study, POM values were not taken from water samples of the culture tank but from the collected solids of the treatment unit (*i.e.* swirl separator). Therefore, the values obtained cannot directly be compared with those reported on the above cited literature. However, for characterizing this sludge for its potential re-use in subsequent (integrated) units, it was of interest to see which level and C/N ratios the treatment process would lead. Further, we distinguished also between gross classes of particles sizes. The C/N ratios obtained in this study were appreciably higher as those reported in culture media. A value of 4 was found in average in particle load ranging 50-100 μm and 200-800 μm when the feed type 1 was used. Maximum C/N ratios of 28 were determined in particles between 400-800 μm during the utilization of the feed type 3.

Chen *et al.* (2006) cited Ohashi *et al.* (1995) who found that the portion of nitrifiers decreased with an increasing C/N ratio. It was also reported that the regulation of nitrification by organic carbon was not only dependant on the quantity but also the quality of organic carbon, where higher quality organic carbon had a stronger negative impact on nitrification (Chen *et al.* 2006).

Ebeling *et al.* (2006) described the reduction in the quantity of TAN removed from the water for several C/N ratios. He also pointed out the fact that autotrophic bacteria are easily to "wash-out" during harvesting of excess bacterial biomass, since the autotrophic

bacteria growth rate is significantly slower than that of heterotrophic bacteria. The stoichiometric calculation of the inorganic carbon demand of heterotrophic bacteria, Ebeling *et al.* (2006) came to the result that the carbon available from the feed is not sufficient to satisfy the requirements of heterotrophic bacteria. This suggests that supplemental carbon may be used from proteins in the feed. Summerfelt and Penne (2005) determined N/P ratios around 2 in solid matter after a high residential time. Similar ratios were found in this study.

4.5 Particle characterization in the effluent of the swirl separator

In order to determine shape and structure of particles samples of suspended solids collected from the swirl separator were classified into seven size classes, and examined under a light and digital electron scanning microscope.

Patterson and Watts (2003) described micro-particles obtained from a cold fresh water site rearing Atlantic salmon (*Salmo salar*). In general, the shape and form of particles observed in this study corresponded well with those characterized by Patterson and Watts (2003). Certainly feed composition and feed processing has an effect on the resulting particle size and form in faeces. The feed ash included bone fragments and the extrusion process gelatinized over 90% of the starches (Patterson and Watts 2003). Additionally, the authors found that heavier particles are composed mainly of wheat-related heavy cellulose from undigested and uneaten fish feed. Lighter material was composed of fine particles which tended to form weak flocs. Heavy material does not necessarily mean big particles and lighter material is not always small solids. In this study, heavy as well as light material was observed in all size classes.

Swirl separation is a process that can be assumed to be non-destructive to large and heavier particles. This is different in other solid separation systems like triangle or drum filters. The suspended solids obtained from the swirl separator were sieved through different mesh sizes to characterize the contribution of various size classes to the total amount of solids. Even this sieving process mechanically altered the solid particles. The image analysis done allowed to determine the percentage of particles that had been above the mesh size of the sieves used for the size differentiation of the solids. On average, $46.5 \pm 19.8\%$ (n=5) of the particles found on the sieve with a nominal square mesh size of $400 \mu\text{m}$ were indeed greater than $400 \mu\text{m}$ in diameter; $21.3 \pm 4.3\%$ (n=5) of the particles retained in sieve of $800 \mu\text{m}$ were bigger than $800 \mu\text{m}$ representing a surface area of over $640,000 \mu\text{m}^2$ (perimeter $3200 \mu\text{m}$); and only $11.5 \pm 3.5\%$ (n=5) of

the particles retained in sieve of 1600 μm were found to be above this size. Although the sieving method can not be directly compared with the filtration process through a drum filter, these results agree reasonable well with the data reported by Langer *et al.* (1996), Patterson and Watts (2003), and Brinker *et al.* (2006). Langer *et al.* (1996) found that drum filtration changed the particle size distribution, resulting in an increase of the smaller particle fraction of the sieved material, thereby indicating a partial breakdown of larger particles during the mechanical filtration process. Patterson and Watts (2003) reported as expected a shift to smaller particles in the filtered water as the larger particles were removed by the drum filtration. Brinker *et al.* (2006) reported that before drum filtration the particle size distribution covered the whole size range while thereafter the particle size was limited to a maximal size of 128 μm as expected from the mesh size used and only 8.1% of the total particle volume was larger than the pore size of 40 μm . The particles larger than 40 μm originated probably from flocculation of small particles or were non-spherical particles that have passed the filter mesh. Aggregations of smaller particles aggregating bigger solids were also observed in this study.

4.6 Particle size analysis

Brinker *et al.* (2006) indicated that the addition of electrolyte to fresh-water samples may alter the original particle size distribution by inducing flocculation or de-flocculation. The subsamples collected in this study were always taken in sea water at 23 psu. It was considered that the addition of electrolyte solution (Isoton II[®], NaCl 7.9 g*L⁻¹) did not alter the size distribution. High velocity and strong shear forces at the aperture of the orifice tube however, may have destroyed fragile particles or particle aggregates (McCave and Syvitski 1991; Hunt 1982 cited by Brinker *et al.* 2006). However, it was impossible in this study to estimate the dimension of this effect. Originally, the Coulter Counter[®] Multisizer was developed to count and size blood cells and other relatively equally-sized and solid micro-particles. One assumption that has to be made is that solid particles tend to be of a spherical form. The microscopic analysis however, suggests that particle size may have been overestimated (*i.e.* the length of a particle was not the diameter of a sphere) and therefore, the Multisizer routine output determines to large means. The breakage of particles resulting in larger overall surface area was negligible against the overestimation of the particle size by the Coulter Counter[®] method. Unfortunately it was impossible to estimate this error by a numerical function. Brinker *et al.* (2006) considered also that electrolyte solution may infiltrate the particles resulting in an underestimate of real particle volume. Finally, Brinker *et al.* (2006) cited Milligan and Kranck (1991) pointing to the required application of different orifice tubes apertures

when measuring a wide range of particle sizes. In this study two orifice tubes apertures were used, 140 μm and 1000 μm covering particles in the range between 2.8 μm to about 715 μm . Difficulties observed utilising the Coulter Counter[®] Multisizer were due to the obstruction of the aperture by particle aggregates. Sucking samples through the orifice tube aperture is possible because of a vacuum pumping. The Coulter Counter[®] Multisizer is equipped with only one suction pump and one small vacuum storage beaker (500 mL) which is suboptimal for the material to be studied in this investigation. It was necessary to install a second pump and a bigger storage beaker (20,000 mL) to achieve the necessary vacuum to collect the sample through the 1000 μm aperture.

The results indicated that fine particles (<45 μm) dominated the particles by numbers. Larger particles were also trapped by the swirl separator. A comparison to other studies is difficult as particle size distribution is definitely influenced by system design, species studied, and feed type used. For example, Chen *et al.* (1993) found that particles smaller than 20 μm were prevalent in the RAS that he considered in his studies. Libey (1993) cited by Langer *et al.* (1996) found that 67% of the particle load were smaller than 30 μm . Langer *et al.* (1996) also reported that the major fraction of the TSS load belonged to particles <20 μm . All these authors reported results coming from RAS equipped with drum filters and/or rotating biological contactor (RBC) while also using centrifugal pumps. Langer *et al.* (1996) reported that an increase in smaller particles (<20 μm) was observed in the particle size distribution after the drum filtration. Interestingly, this study mainly sampled an eel culture system in which feed paste was used known to produce dominantly fines of small particle size. The fraction of extremely fine solid particles recorded with the 140 μm orifice tube showed that 50% of the particles were situated between 4 μm and 7 μm . It was considered that this fraction actually extends the findings done with the 1000 μm orifice tube. These particles were less important in terms of weight but the number was considered to be highly relevant, as they provide extensive surface for bacterial settlement. It remained unsolved the impossibility to separate one solid sample, into several subsamples for being measured with different orifice tube sizes, without mechanically change the particle size distribution. Brinker *et al.* (2006) considered that solid particles had complex characteristics *e.g.* a wide size range, a non spherical form and a non homogeneous composition. Therefore, he and his co-workers developed a laser-based technique to size solids. The application of such a method will help to identify the functionality of RAS components and their design, in particular the effect of system components to produce smaller particle fractions and not only remove particles. Under given configurations (*e.g.* drum-filters, micro-screens, centrifugal pumps, gas exchangers, or water cascades), removal mechanisms can act as particle-

destroying units and the design of sedimentation units or swirls separators should be re-considered in light of these findings. McMillan *et al.* (2003) found that propeller pumps break up larger particles into moderately smaller ones. However, this did not affect the number of very small particles ($<60 \mu m$) that dominated the samples and it is concluded that such pumps may not affect the breakdown into smaller pieces of particles below $60 \mu m$. However, such pumps can only be effectively used for low-head systems.

Overall, whatever which pumping system in a RAS is used, it is important to remove solids as fast as possible from culture water. Therefore, removal seems to be most effective directly after the outlet of fish tanks (nearest to the source). The residential time of particles in the water is crucial and the chance of disintegration of larger particles into much smaller and more soluble ones is high, increasing almost second by second with transport distance. Our knowledge base, to understand the physical and biochemical behaviour of particles needs to be improved to provide better data for RAS designers and users. Modern integrated aquaculture systems will also profit from better health control to optimize the cultivation process while also re-using solid wastes.

4.7 Bacteria in the RAS

4.7.1 Bacteria removal by counter-current foam stripping

Bacterial communities are of similar importance in a RAS as fish because all the processes are directly linked to their metabolic activity and subsequently affecting water quality (Michaud *et al.* 2006). Bacteria are beneficially used in RAS treatment processes and are warranted by design. However, excessive accumulation of non-pathogenic microorganisms may be the initial step of a chain reaction causing serious problems at high fish stocking densities and high quality feeds for optimum fish growth. Some issues regarding these impacts are described by Ebeling *et al.* (2006) for autotrophic and heterotrophic bacteria. This holds in particular for free floating bacteria. Recycling systems with a two step solid separation do have the advantage to harvest an appreciable amount of free floating microorganisms adhered to settleable particles, and free-living bacteria from the culture water primarily through the counter-current foam stripping process.

Total bacterial counts (TBC) determined in the inlet, foam condensate, and outlet of the foam fractionator showed that a continuous bacterial biomass was removed from the system. The continuity of this harvesting process was, however, impaired at every time

the foam collapsed in the foam tower. Schlesner and Rheinheimer (1974) observed the elimination of bacteria through foaming and described the fluctuation of bacterial counts in terms of numbers being partly caused by an “unstable” foam production. The authors explained the instability in the foam with different water levels inside the foaming tower. Because of this repeatedly observed effect, the mechanics of water flow in the study system was designed to maintain the water level constant at any given (preset) height. Lawson and Wheaton (1980) noted that viscosity and surface tension can modify the efficiency of foam stripping. In this study it was suggested that variations in fat content in the reaction chamber altered the surface tension and influenced the formation of foam. The diameter of the air bubbles inside the foam stripping tower became at these times relatively large, an indication that surface tension was high.

The efficacy of bacteria removal in this study reached between 3.6% and 35.5%, and was calculated from the difference between water inlet and outlet of the foam fractionator. It might be an objective for further studies to control the foaming process in order to obtain consistent foam removal over an extended period of time while at the same time minimizing water loss. This is theoretically possible but practically not yet often applied. It was observed how the TBC varied between samples (days) in relation to the feed amount and the presence or absence of feed. It was often immediately after feeding when the foaming process became unstable, indicating a rapid and short-term collapse of the foaming process. Apparently leaching from the fish pellets must cause this short-term change in surface tension. If the foam has a dry and firm consistency, the water losses will be slight and probably the concentration of bacteria in the foam is very high. In contrast, if the foam is “wet” (low surface tension) considerable culture water will be lost, diluting the bacterial mass. Modern RAS are equipped with an automated foaming control system which allows minimizing the loss of culture water even if it's impossible to control the quality (stability) of the foam.

The presence of aggregates of free living microorganisms in the culture medium (outlet biofilter) expressed in TBC per millilitre was in our system maintained at levels of those determined in coastal waters (around 1×10^6 to 4×10^6 , Hoppe pers.com.), and this was despite the fact that fish were at a culture density of $32.2 \text{ kg} \cdot \text{m}^{-3}$. The concentration determined was higher than the data reported by Leonard *et al.* (2000) for a lower culture density (5 to $10 \text{ kg} \cdot \text{m}^{-3}$) and the data found by Leonard *et al.* (2002) for a culture density of 40 to $80 \text{ kg} \cdot \text{m}^{-3}$. Michaud *et al.* (2006) found out that the bacteria concentration inside the biofilter was between 2.3×10^5 and 7.7×10^5 cells per millilitre. It was postulated that the presence of particulate organic matter (POM) and the

availability of carbon (higher C/N ratios) led to a higher abundance of free living bacteria. Nevertheless, the importance of removing excess production of bacteria was observed.

Ozone was used in this study mainly to enhance the foam formation and improve particle aggregation while as a side effect ozone reduced bacterial counts. The application of ozone during foam fractionation was assumed to cause electrostatic polarisation of free floating particles, including bacteria flocs, ultimately leading to larger aggregates which exhibit either better settling characteristics or improved aggregation at the interface between water and air (*i.e.* at the surface of the ascending gas bubble in the foam fractionator), thereby reducing the microbial load in the effluent of the treatment tower. Studies indicating the advantages of using ozone revealed also the inactivation of vegetative cells and spores can be achieved such as for *Bacillus cereus* and *Clostridium perfringens* (Burleson and Pollard 1976), and *Aeromonas sp.* (Ritola *et al.* 2000), although disinfection by ozone is not the primary effect of the process, it is bacterial aggregation and removal of bacterial flocs rather than killing of bacteria. Certainly, whatever the process is, in the end the reduction in CFU by counter-current foam stripped of ozonated water was reported by many investigations, including Schlesner and Rheinheimer (1974), Colberg and Lingg (1978), Rosenthal (1981), Ozawa *et al.* (1991), Kobayashi *et al.* (1993), Liltved *et al.* (1995), Theisen *et al.* (1998), and Suantika *et al.* (2001, 2003). In this study, the percentage of CFU found in the outlet of the foam fractionator was between 4% and 40% compared to the inlet revealing both (a) the effects of ozone (inactivation of cells) and (b) the elimination of cells through the foam separation (skimming). TBC in the foam condensate were found to be between 10^2 and 10^3 times higher than in the inlet or outlet of the foam fractionator. Differences between TBC and CFU in the foam condensate showed an inactivation of bacteria between 93% and 99% (agar media). This is a surprisingly high rate as one would assume that oxygen radicals and ozone would be scavenged by numerous organic compounds and solids before effectively killing bacteria. Apparently, a substantial fraction of the bacterial load may have been killed by ozone and therefore appeared only in the determination of TBC (fluorescent microscopy).

The regular presence of high quantities of POM in the culture water might increase the bacterial load in the system compared to those times when no feed was offered. Assuming that heterotrophic bacteria require POM it is to expect that after a no-feeding day the bacteria may have less organic matter available compared to feeding days. Yanbo *et al.* (2005) found a highly significant correlation between number of particles and epibacteria indicating that the number of bacteria depended on the number of

particles 55% of which had bacteria attached. The great number of fine particles can increase the surface available for bacteria attachment (Kube and Rosenthal, 2006). Bacteria attached to particles reduce the risk of being hit by radicals or ozone because of radical scavenging. Michaud *et al.* (2006) determined a good correlation between the concentration of POM and the bacteria abundance.

There are also some methodological aspects that complicate the evaluation of bacterial agglomerates with suspended solids in the treatment unit. The presence of high quantities of particles in the foam condensate makes it difficult to determine the total bacteria counts (TBC) when acridine orange (AO) is added. It is hard to distinguish bacteria from nonliving particles of similar size such as clay, detritus, or colloids, because they may also be stained or show autofluorescent (Yu *et al.* 1995). Therefore 4,6-diamidino-2-phenylindole (DAPI) was used in direct counts of total bacteria and bacteria biomass in the foam condensate. Posch *et al.* (2001) suggested that the difference in bacterial cell numbers determined from DAPI and AO stained samples were generally not exorbitantly high. However DAPI tends to underestimate the real cell dimensions in freshwater samples (Posch *et al.* 2001). The results obtained in this study showed a negligible difference between the biomass determination factor for AO and DAPI. The use of DAPI was favourable and allowed to differentiate bacteria from particles during counting. Additionally, samples were treated with ultrasound (sonication) to disintegrate particle agglomerates and thereby release bacteria from particles. A positive effect of this procedure was observed in samples taken at the beginning of the experiments. Nevertheless, high amounts of POM in the foam condensate were still confirmed in samples during subsequent times (weeks). Under the fluorescent microscope bacteria and solids were unevenly distributed on filter samples and in many cases two layers of bacteria were found. It was presumed that this effect might appear after sonication because samples with bacteria agglomerates formed organized cells stripes after sonication and zones without any bacteria. Samples that were difficult to count with some levels of confidence were excluded for further evaluation. Samples stained with DAPI should be counted within 24 h (Yu *et al.* (1995) and some of these effects might be because samples were not counted immediately.

Overall, TBC tend to rise with time (true for samples taken between day t_{71} and day t_{224}) and this is probably in relation to fish growth and biological activity in the system. Similar effects were observed by Suantika *et al.* (2003), Rydl (2005), and Yanbo *et al.* (2005). The number of cells in division tends also to rise with time as nutrient conditions for optimal growth were offered. Cell division under optimal conditions takes about 5 hours

(Hoppe pers.com.); however, it was presumed that in the RAS one cells division lasted on average a full day.

4.7.2 The effect of ozone on total suspended solids in a RAS

The primary goal of this part of the experimentations was to observe the effect of continuous ozonation against no ozonation on the amount, size and nutrient composition of TSS collected from the swirl separator and the foam condensate from the fractionation tower. There was a tendency that ozone was beneficial to the suspended solids separation process. However, it was not proven statistically. Certainly ozone was important for the break down and removal of dissolved organic matter that stems from solid matter. The experiments had been terminated when water discoloration reached a level where the water quality could not be maintained, jeopardizing the welfare of the organisms in cultivation. The accumulation of yellow substances was the reason for that. Nevertheless, the results of this study and the benefits observed during ozonation were similar as those reported by Schlesner (1974), Rosenthal and Sander (1975), Rosenthal and Westernhagen (1978), Rosenthal *et al.* (1978), Mathews *et al.* (1979), Otte and Rosenthal (1979), Wheaton *et al.* (1979), Lawson and Wheaton (1980), Rosenthal and Otte, (1980), Williams *et al.* (1982), Sutterlin *et al.* (1984), Ozawa *et al.* (1991), Weeks *et al.* (1992), Chen *et al.* (1993b), Chen *et al.* (1993c), Kobayashi *et al.* (1993), Reuter and Johnson (1995), Summerfelt *et al.* (1997), Hussenot *et al.* (1998), Ebeling *et al.* (2000), Suantika *et al.* (2001), Landau (2002), Tango and Gagnon (2003), Suantika *et al.* (2003), Csordas and Wang (2004), and Liltved (2006).

Considering only the fraction of TSS gathered by the foam fractionator, Reuter and Johnson (1995) reported that the application of ozone was invariably associated with an improvement in TSS removal. When using foam fractionators the application of ozone enhanced the foam forming process, which has already been described in detail by Rosenthal (1980), Sutterlin *et al.* (1984), Kobayashi *et al.* (1993), and Waller (2001). Schlesner (1974) collected 19 times more water from foam coming up the foam collector after ozonation. Otte and Rosenthal (1979) observed that the amount of the decanted foam per day rose with longer ozone treatment. A three times larger amount of effluent water was collected from the so-called "protein skimmer" when ozone was implemented (Suantika *et al.* 2001). In this study, 56% more water was found in the foam flushing tank during the experiments with ozonation. Daily observations on foam quality showed during ozonation a much more consistent and dry foam production. The collapsed foam

turned into a concentrated liquid in the foam collector tower as described by Williams *et al.* (1982).

The weight composition of particle size classes analyzed in this study for the TSS fraction collected from the swirl separator showed an effect of the ozone application elucidated by Reuter and Johnson (1995), with more particle aggregations to be found during times when the water was ozonated. This concurred also with the statement of Summerfelt *et al.* (1997) where changes resulting from ozonation improved the performance of microscreen filters, reducing the TSS in the culture water by 35%. Krumins *et al.* (2001) reported that ozone increased particle coagulation and removal. The amount of total suspended solids through foam fractionation obtained in this study was 12% higher during ozonation. The swirl separator collected 15% more TSS when the ozonation unit was in operation. The particle aggregations found in the swirl separator, based on dry weight, seemed to be represented by the fraction between 200 μm and 800 μm . This might be valuable information when designing RAS with a combination of drum filters and foam fractionator. Drum filters are commonly employed to remove particles sizes down to 60 μm , however their incorporation has design consequences as to differences water levels required for free flow-through.

Ozone has frequently been added to treat culture water to oxidize organic matter that is otherwise not easy to breakdown in biofilters (Otte *et al.* 1977; Otte and Rosenthal, 1978; Otte and Rosenthal 1979; Rosenthal, 1980; Rosenthal 1981; Sutterlin *et al.* 1984; Brazil *et al.* 1998). Particularly Rosenthal (1981b) pointed to the utility of ozonation as support measure for fine particle removal via electrostatic loading and aggregation rather than a disinfection procedure.

The carbon content found in the solid matter collected by the foam fractionation was higher when no ozone was used. Colberg and Lingg (1978) reported that the oxidation of organic matter was very effective at low ozone concentrations. They noted also that the reaction was pH dependant (more efficient at higher pH). Otte and Rosenthal (1978) also demonstrated the chemical oxidation of carbon compounds by free radicals. Summerfelt and Hochheimer (1997) elucidated that pH and temperature has influenced the effectiveness of ozone and the oxidation of carbon compounds. This effect was not observed in this study because this study considers total carbon content only, not distinguishing between BOD and COD loads and conversion of organics in the process. It was assumed that the higher carbon content in the foam condensate without ozonation was due to a higher amount of living bacteria and less oxidized particulate carbon. The

weight distribution of particles analyzed from the swirl separator showed a similar pattern with and without ozonation indicating the considerable effect of the ozonation process on the entire system. However, less carbon was found in smaller particles. It has to be noted that the residence time of the solid matter in the swirl separator was relatively long (leaching effect). Regarding the content of nitrogen and phosphorous in the particulate matter collected by the foam fractionator the results obtained showed that oxidation of these compounds by ozone also took place. The amount of nitrogen despite of the application of ozone was much higher in the foam condensate than in the solids gathered from the swirl separator. The enrichment of nitrogen (proteins) in the foam condensate was also reported by Chen *et al.* (1993). Many authors referred to the elimination of proteins through the foam condensate and/or the use of proteins as surfactants during the foam fractionation process (Lawson and Wheaton 1980; Sugita *et al.* 1996; Lockwood *et al.* 1997; Chen *et al.* 1993; Du *et al.* 2000; Landau 2002). A foam fractionator is also named "protein skimmer" by some scientist presuming that nitrogen compounds eliminated by the foaming process were mainly proteins. The presence of proteins in the culture water at high feeding rates does increase the efficiency of oxidation or removal of organics with and without ozonation, but will be more effective when ozone is applied (Chen *et al.* 1993). The removal of phosphorous through a foam fractionation process seemed to be linked to the removal of organic matter. There is no information in the literature regarding the effects of ozone onto phosphorous containing organics. Nonetheless, the differences in the phosphorous content found in this study with and without ozonation provide some hints on oxidation of phosphorous containing compounds with subsequent removal through foam stripping. The leaching effect determined by Lupatsch and Kissil (1998) showed that the amount of phosphorous remaining in the solid matter was on average 82% after 24 hours, and was much more stable than nitrogen (55%).

The positive effects of ozone on water colour have been reported by Evans (1972), Otte *et al.* (1977), Rosenthal (1981), Sutterlin *et al.* (1984), Huguenin and Colt (1989), Ozawa *et al.* (1991), Chen *et al.* (1994), Summerfelt *et al.* (1997), Brazil *et al.* (1998), Sander (1998), Tango and Gagnon (2003), and Colt (2006). The light yellow to brown colour of the water is a consequence of the accumulation of dissolved organic carbon compounds like fulvic and humic acids. Bailey (1972) describes the ozonolysis of aromatic molecules indicating the breakdown of C=C-double bonds. In this study the accumulation of these substances causing the yellow/brown colour was observed during periods without ozonation. After adding ozone to the system, the water became clear again within 24-48 hours.

The influence of ozone on particle size distribution in a RAS has been investigated by Reuter and Johnson (1995) and Suantika *et al.* (2001). Reuter and Johnson (1995) found that the use of ozone increased the number of larger particles measured. They also found that aggregations of particles were observed after the water was ozonated. Without ozone the particle size distribution was dominated by particles around 31 μm . With ozone the particles formed aggregates of around 100 μm and it is assumed electrostatic loading is one of the mechanisms supporting aggregation. Suantika *et al.* (2001) collected more particles when ozone was used. The particle size distribution found in the swirl separator also showed that the total particle counts per millilitre were higher during the days with ozonation. Larger particles ($>300\mu\text{m}$) were seized with the 1,000 μm Coulter Counter[®] Multisizer orifice tube when ozone was applied. The same was observed when the 140 μm orifice tube was used. The particle size distributions ranged up to 80 μm . Particle counts in the foam condensate were comparably lower. The number of particles per millilitre determined without ozonation was higher but the amount of foam condensate collected was half the amounts compared at days with ozonation. Suantika *et al.* (2001) found three times more foam condensate when ozone was used than without ozone application. Chen *et al.* (1993) found similar particles size distributions in the foam condensate without ozonation. The particle size ranged up to 30 μm . Foam fractionation in conjunction with the application of ozone in the foam reaction tower, demonstrated to be effective in eliminating small particles from the culture water. Small particles ($<20\mu\text{m}$) are potentially dangerous to water quality and fish health and predominate in number in the RAS. Wider particles size spectrum were seized when ozone was used indicating the formation of particle aggregates ($>20\mu\text{m}$). The use of ozone had also a positive impact in the particle size distribution in the swirl separator. The presence of comparable larger particles ($>300\mu\text{m}$) indicated the formation of stable aggregates during ozonation.

4.8 Concluding remarks

Fish growth in the RAS studied was satisfactory and was initially even better than known for commercial systems (particularly during the period at lower temperatures) while during most of the study period growth was well within rates reported in the literature. Overall, feed conversion was also satisfactory so that from an aquacultural point of view the study on system components and their performance was within expected values.

The study demonstrates the importance of suspended solids and their fate in recirculation systems. Particle sizes covered a wide range and seem to tend to disintegrate with time, contributing to dissolved nutrient load via leaching. It can be concluded that the removal of solids should technically be done as close to the source as possible. Although causing higher initial investments for system construction, the removal of larger particles by simple (but cost-effective) settling techniques behind each individual fish tank is highly recommended to avoid leaching from lost feed pellets and faeces that are transported over long distances. Early capture of particles minimizes the organic load for the biofilter.

Mechanical (sieve) filters collect numerous particles that are much smaller than expected by their mesh size. Likewise, large particles that were expected to be retained by a given mesh size, are passing through the filters and this seems to be a very common feature in suspended solids derived from fish culture because of the flexibility in changing shape by external forces. Faeces and particle fractions derived from system solids are being easily „squeezed“ through the filter mesh. It is suspected that these disintegrate further, thereby misleading the particle size readings from mechanical filters. Further studies would be highly desirable to investigate particle behaviour in relation to size and age, thereby greatly assisting to optimize filter engineering.

Bacterial flocs and organic particles derived from faeces seem to be highly instable and capable of quickly breaking down into smaller pieces. Again, early removal of these flocs close to the source is advisable. The study also confirmed that ozonation improves particle aggregation and removal through foam stripping. However, the stability of aggregates is still poorly understood (as experienced by occasional foam collapse and disintegration during and shortly after feeding) and warrants further investigation.

In large commercial recirculation systems piping is extensive to transport the culture medium from a long array of tanks to the central treatment units. The transport distance will ultimately influence particle breakdown, leaching and nutrient load. Our findings

relate to a small laboratory-sized test system. The scale-up problems that may drastically affect particle behaviour needs further study. Inconsistency in the foaming process and removal efficiency of TBCs is one of the findings supporting this conclusion. However, the efficacy of the process is largely influenced by the overall flow rates through the treatment units and it is here were further studies are also needed to optimize system performance.

The data also indicate that ozonation is not necessarily aiming at disinfection but at overall removal of bacteria with organic particles, a function not well understood by practioners.

The study also clearly indicates that a two-step approach for suspended solid removal is reasonable and practical as both techniques capture different particle size classes with different efficiencies.

5 References

- Avnimelech, Y., Mozares, N., Shaher, D., Kochba, M. 1995. Rates of organic carbon and nitrogen degradation in intensive fish ponds. *Aquaculture* 134, 211-216.
- Azzaydi, M., Martínez, F.J., Zamora, S., Sánchez-Vázquez, F.J. and Madrid, J.A. 1999. Effect of meal size modulation on growth performance and feeding rhythms in European sea bass (*Dicentrarchus labrax*, L.). *Aquaculture* 170, 253-266.
- Bailey, P.S. 1958. The reactions of ozone with organic compounds. *Chem. Rev.*, Vol. 58, No. 4, 925-1010.
- Bailey, P.S. 1972. Organic groupings reactive toward ozone mechanisms in aqueous media. *In: Francis L. Evans III (Ed.) Ozone in Water and Wastewater Treatment*, Ann Arbor Science Publishers, Inc., Michigan, 29-59.
- Ballestrazzi, R. and Lanari, D. 1996. Growth, body composition and nutrient retention efficiency of growing sea bass (*Dicentrarchus labrax* L.) fed fish oil or fatty acid Ca salts. *Aquaculture* 139, 101-108.
- Ballestrazzi, R., Lanari, D., D'Agaro, E., Mion, A. 1994. The effect of dietary protein level and source on growth, body composition, total ammonia and reactive phosphate excretion of growing sea bass (*Dicentrarchus labrax*). *Aquaculture* 127, 197-206.
- Ballestrazzi, R., Lanari, D., D'Agaro, E. 1998. Performance, nutrient retention efficiency, total ammonia and reactive phosphorus excretion of growing European sea-bass (*Dicentrarchus labrax* L.) as affected by diet processing and feeding level. *Aquaculture* 161, 55-65.
- Barak, Y. and van Rijn, J. 2000. Biological phosphate removal in a prototype recirculating aquaculture treatment system. *Aquacultural Engineering* 22, 121-136.
- Barnabé, G. 1990. Rearing bass and gilthead bream. *In: Barnabé, G. (Ed.), Aquaculture*. Ellis Horwood, New York, 647-686.
- Baskerville-Bridges, B. and Kling, L.J. 1996. Rearing of cod larvae up to metamorphosis at high stocking densities in a closed recirculating system using artificial seawater. *Bull. Aquacul. Assoc. Canada* 96-3, 27-28.
- Bergheim, A. and Brinker, A. 2003. Effluent treatment for flow through systems and European environmental regulations. *Aquacultural Engineering* 27, 61-77.
- Blancheton, J.P. 2000. Developments in recirculation systems for Mediterranean fish species. *Aquacultural Engineering* 22, 17-31.
- Blogoslawsky, W.J. and Stewart, M.E. 1977. Marine applications of ozone water treatment. *In: Edward G. Fochtman, Rip G. Rice and Myron E. Browning (Eds.) Forum on Ozone Desinfection*. International Ozone Institute, Syracuse, NY, USA, 266-276.
- Boonyasuwat, S., Chavadej, S., Malakul, P., Scamehorn, J.F. 2003. Anionic and cationic surfactant recovery from water using a multistage foam fractionator. *Chemical Engineering Journal*, Vol. 93 (3), 241-252.

- Borges, M.-T., Morais, A., Castro, P.M.L. 2003. Performance of outdoor seawater treatment systems for recirculation in an intensive turbot (*Scophthalmus maximus*) farm. *Aquaculture International* 11, 557-570.
- Bovendeur, J. 1989. Fixed-biofilm reactors applied to waste water treatment and aquacultural water recycling systems. PhD Disseratation, Univ. Wageningen, The Netherlands, 171pp.
- Brazil, B.L., Summerfelt, S.T. and Libey, G.S. 1998. Application of ozone to recirculating aquaculture system. *NRAES-98 Vol. I*, 373-389.
- Brinker, A., Koppe, W., Rösch, R. 2003. Improving waste treatment of aquacultural effluents by increasing fish faeces stability. *European Aquaculture Society Special Publication* 33, 136-137.
- Brinker, A. and Rösch, R. 2005. Factors determining the size of suspended solids in a flow-through fish farm. *Aquacultural Engineering* 33, 1-19.
- Brinker, A., Schröder, H.G., Rösch, R. 2005. A high resolution technique to size suspended solids in flow-through fish farms. *Aquacultural Engineering* 32, 325-341.
- Bullock, G., Herman, R., Heinen, J., Noble, A., Weber, A., Hankins, J. 1994. Observations on the occurrence of bacterial gill disease and amoeba gill infestation in rainbow trout cultured in a water recirculation system. *Journal of Aquatic Animal Health* 6, 310-317.
- Bullock, G.L., Summerfelt, S.T., Noble, A.C., Weber, A.L., Durant, M.D., Hankins, J.A. 1997. Ozonation of a recirculating rainbow trout culture system I. Effect on bacterial gill disease and heterotrophic bacteria. *Aquaculture* 158, 43-55.
- Burleson, G.R. and Pollard, M. 1976. Inactivation of vegetative cells and spores of bacteria by ozone and sonication. *In: Rice, R. G., Pichet, P., Vincent, M.-A. (Eds.) Proceedings Second international Symposium on Ozone Technology, Montreal, Canada, 11-14 may 1975. Ozone Press International, Syracuse, NY, USA, 445-454.*
- Chen, S., Timmons, M.B., Aneshansley, D.J. Bisogni Jr., J.J., 1993a. Suspended solids characteristics from recirculating aquacultural systems and design implications. *Aquaculture* 112, 143-155.
- Chen, S., Timmons, M.B., Bisogni Jr., J.J., Aneshansley, D.J. 1993b. Suspended solids removal by foam fractionation. *The Progressive Fish-Culturist* 55, 69-75.
- Chen, S., Timmons, M.B., Bisogni Jr., J.J., Aneshansley, D.J. 1993c. Protein and its removal by foam fractionation. *The Progressive Fish-Culturist* 55, 76-82.
- Chen, S., Stechey, D., Malone, R.F. 1994. Suspended solids control in recirculating aquaculture systems. *In: Timmons, M.B., Losordo, T.M. (Eds.), Aquaculture Water Reuse Systems: Engineering Design and Management, Developments in Aquaculture and Fisheries Science* 27, Elsevier, 61-100.
- Chen, S., Saucier, B.B., Zhu, J.S., Durfey, E. 2000. Recirculation system design for shellfish wet storage or depuration. *In: National Shellfisheries Association Annual Meeting, Seattle, Washington, March 19-23 2000, 650-651.*
- Chen, S., Ling, J., Blancheton, J.P. 2006. Nitrification kinetics of biofilm as affected by water quality factors. *Aquacultural Engineering* 34, 179-197.

- Chen, Y.-S., Beveridge, M.C.M., Telfer, T.C., Roy, W.J. 2003. Nutrient leaching and settling rate characteristics of the faeces of Atlantic salmon (*Salmo salar* L.) and the implications for modeling of solid waste dispersion. *Journal of Applied Ichthyology* 19, 114-117.
- Colberg, P.J. and Lingg, A.J. 1978. Effect of ozonation on microbial fish pathogens, ammonia, nitrate, nitrite, and BOD in simulated reuse hatchery water. *J. Fish. Res. Board Can.* 35, 1290-1296.
- Collins, M.T., Gratzek, J.B., Shotts, E.B.Jr., Dawe, D.L., Campbell, L.M., Senn, D.R. 1975. Nitrification in an aquatic recirculating system. *Journal of Fish Disease, Board of Canada* 32, 2025-2031.
- Colt, J. 2006. Water quality requirements for reuse systems. *Aquacultural Engineering* 34, 143-156.
- Csordas, A. and Wang, J.-K. 2004. An integrated photobioreactor and foam fractionation unit for the growth and harvest of *Chaetoceros* in open systems. *Aquacultural Engineering* 30, 15-30.
- David, C., Luijckx, R., Hunter, D., West, P., Slaski, R., Hazon, N. 2002. A new recirculation system for rearing juvenile Atlantic halibut. *In: Rakestraw, T.T., Douglas, L.S., Flick, G.J. (Eds.), Proceedings of the Fourth International Conference on Recirculating Aquaculture, Roanoke, Virginia, July 18-21 2002, 393-401.*
- Davidson, J. and Summerfelt, S.T. 2005. Solids removal from coldwater recirculating system – comparison of a swirl separator and a radial-flow settler. *Aquacultural Engineering* 33, 47-61.
- Dendrinou, P. and Thorpe, J.P. 1985. Effects of reduced salinity on growth and body composition in the European bass *Dicentrarchus labrax* (L.). *Aquaculture* 49, 333-358.
- Diaper, E.W.J. 1972. Practical aspects of water and waste water treatment by ozone. *In: Evans, F.L.III (Ed.), Ozone in Water and Wastewater Treatment, Ann Arbor Science Publishers, Inc., Ann Arbor, Michigan, 145-179.*
- Dosdat, A., Person-Le Ruyet, J., Covès, D., Dutto, G., Gasset, E., Le Roux, A., Lemarié, G. 2003. Effect of chronic exposure to ammonia on growth, food utilisation and metabolism of the European sea bass (*Dicentrarchus labrax*). *Aquat. Living Resour.* 16, 509-520.
- Du, L., Loha, V., Tanner, R.D. 2000. Modeling a protein foam fractionation process. *Applied Biochemistry and Biotechnology, Vol. 84-86, 1087-1099.*
- Dwivedy, R.C. 1974. A proposed method of waste management in closed-cycle mariculture systems through foam-fractionation and chlorination. *Proc. of the National Shellfisheries Association, Vol. 64, pp.111-117.*
- Ebeling, J., Krumins, V., Wheaton, F. 2000. Part-day ozonation for nitrogen and organic carbon control in recirculating aquaculture systems. *Aquaculture Engineering* 24, 231-241.

- Ebeling, J.M., Sibrell, P.L., Ogden, S.R., Summerfelt, S.T. 2003. Evaluation of chemical coagulation-flocculation aids for the removal of suspended solids and phosphorus from intensive recirculating aquaculture effluent discharge. *Aquacultural Engineering* 29, 23-42.
- Ebeling, J.M., Timmons, M.B., Bisogni, J.J. 2006. Engineering analysis of the stoichiometry of photoautotrophic, autotrophic, and heterotrophic removal of ammonia-nitrogen in aquaculture systems. *Aquaculture* 257, 346-358.
- EIFAC. 1986. Flow through and recirculation systems. Report of the working group on terminology, format and unit measurements. European Inland Fisheries Advisory Commission, Technical Paper 49, 100pp.
- Eroldogan, O.T., Kumlu, M., Kir, M., Kiris, G.A. 2005. Enhancement of growth and feed utilization of the European sea bass (*Dicentrarchus labrax*) fed supplementary dietary salt in freshwater. *Aquaculture Research* 36, 361-369.
- Espinoza, J.G., Segovia-Quintero, M.A., del Río-Portilla, M.A. 2002. CICESE aquaculture departament returns to recirculation technology. *Aquaculture Magazine*, Nov/Dec 2002, 71-72.
- Evans, F.L. 1972. Ozone technology: current status. *In: Francis L. Evans III (Ed.) Ozone in Water and Wastewater Treatment*, Ann Arbor Science Publishers, Inc., Michigan, 1-13.
- Franco-Nava, M.A., Blancheton, J.P., Deviller, A., Le-Gall, J.Y. 2004a. Particulate matter dynamics and transformations in a recirculating aquaculture system: application of stable isotope tracers in seabass rearing. *Aquacultural Engineering* 31, 135-155.
- Franco-Nava, M.A., Blancheton, J.P., Deviller, G., Charrier, A., Le-Gall, J.Y. 2004b. Effect of size and hydraulic regime on particulate organic matter dynamics in a recirculating aquaculture system: elemental carbon and nitrogen approach. *Aquaculture* 239, 179-198.
- Froese, R. 2006. Cube law, condition factor and weight-length relationships: history, meta-analysis and recommendations. *J. Appl. Ichthyol.* 22, 241-253.
- Hamelin, C. and Chung, Y. S. 1976. Les effets radiomimetiques de l'ozone chez *Escherichia coli*. *In: Rice, R. G., Pichet, P., Vincent, M.-A. (Eds.) Proceedings Second International Symposium on Ozone Technology, Montreal, Canada, 11-14 may 1975.* Ozone Press International, Syracuse, NY, USA. 455-464.
- Han, X., Rosati, R., Webb, J. 1998. Correlation of particle size distribution of solid waste to fish feed composition in an aquaculture recirculation system. *NRAES-98, Vol I*, 257-278.
- Hansen, H.P. and Koroleff, F. 1999. Determination of nutrients. *In: K. Grasshoff, K. Kremling, M. Ehrhardt (Eds.) Methods of Seawater Analysis.* Wiley-VCH Verlag GmbH, Weinheim, Germany. 159-228.
- Hidalgo, F., Alliot, E., Thebault, H. 1987. Influence of water temperature on food intake, food efficiency and gross composition of juvenile sea bass *Dicentrarchus labrax*. *Aquaculture*, 64, 199-207.
- Hochheimer, J.N. and Wheaton, F. 1997. Intensive culture of stripped bass. *In: Stripped Bass and Morone Culture.* Elsevier Science, Amsterdam, The Netherlands, 127-165.

- Honn, K.V. 1979. ozonation as a critical component of closed marine system design. *Ozone: Science and Engineering*, Vol. 1, 11-29.
- House, W. A., Jickells, T. D., Edwards, A. C., Praska, K. E. and Denison, F. H. 1998. Reactions of phosphorus with sediments in fresh and marine waters. *Soil Use and Management* 14, 139-146.
- Huggins, D.L., Piedrahita, R.H., Rumsey, T. 2005. Use of computational fluid dynamics (CFD) for aquaculture raceways design to increase settling effectiveness. *Aquacultural Engineering* 33, 167-180.
- Huguenin, J.E. and Colt, C. 1989. *Design and Operating Guide for Aquaculture Seawater Systems*. Developments in Aquaculture and Fisheries Science No. 20, Elsevier, The Netherlands, 264 pp.
- Hussenot, J., Lefebvre, S., Brossard, N. 1998. Open-air treatment of wastewater from land-based marine fish farms in extensive and intensive systems: current technology and future perspectives. *Aquat. Living. Resour.* 11, 297-304.
- Ingols, R. S. 1978. Ozonation of seawater. *In*: R.G. Rice, J. A. Cotruvo (Eds.) *Ozone/Chlorine Dioxide Oxidation Products of Organic Materials*. Ozone Press International, Cleveland, OH, USA, 77-81.
- Kim, S-K., Kong, I., Lee, B-H., Kang, L., Lee, M-G., Suh, K.H. 2000. Removal of ammonium-N from a recirculation aquacultural system using immobilized nitrifier. *Aquacultural Engineering* 21, 139-150.
- Kobayashi, T., Yotsumoto, H., Ozawa, T. 1993. Closed circulatory system for mariculture using ozone. *Ozone Science & Engineering*, Vol. 15, 311-330.
- Krumins, V., Ebeling, J., Wheaton, F. 2001a. Part-day ozonation for nitrogen and organic carbon control in recirculating aquaculture systems. *Aquacultural Engineering* 24, 231-241.
- Krumins, V., Ebeling, J., Wheaton, F. 2001b. Ozone's effect on power-law particle size distribution in recirculating aquaculture systems. *Aquacultural Engineering* 25, 13-24.
- Kube, N. and Rosenthal, H. 2006. Ozonation and foam fractionation used for the removal of bacteria and particles in a marine recirculation system for microalgae cultivation. *In*: N. Kube, *The integration of microalgae photobioreactors in a recirculation system for low water discharge mariculture*. Dissertation, Mathematisch- Naturwissenschaftlichen Fakultät, Leibniz-Institut für Meereswissenschaften IFM-GEOMAR an der Universität Kiel, 123-146.
- LaBomascus, D.C., Robinson, E.H., Linton, T.L. 1987. Use of water conditioners in water-recirculation systems. *The Progressive Fish-Culturist* 49, 64-65.
- Landau M., Richard, C., Erstfeld, K. 2002. The effect of suspended clay on protein removal during foam fractionation. *North American Journal of Aquaculture* 64, 217-219.
- Langer, J., Efthimiou, S., Rosenthal, H., Bronzi, P. 1996. Drum filter performance in a recirculating eel culture unit. *J. Appl. Ichthyol.* 12, 61-65.
- Lawson, T. B. and Wheaton, F. W. 1980. Removal of organics from fish culture water by foam fractionation. *Proc. Orld. Maricul. Soc.* 11, 128-134.

- Lee, P.G., Lea, R.N., Dohmann, E., Prebilsky, W., Turk, P.E., Ying, H., Whitson, J.L. 2000. Denitrification in aquaculture systems: an example of a fuzzy logic control problem. *Aquacultural Engineering* 23, 37-59.
- Lefevbre S., Bacher, C., Meuret, A., Hussenot, J. 2001. Modelling nitrogen cycling in a mariculture ecosystem as a tool to evaluate its outflow. *Estuarine, Coastal and Shelfish Science* 52, 305-325.
- Lemarié, G., Martin, J-L. M., Dutto, G., Garidou, C. 1998. Nitrogenous and phosphorous waste production in a flow-through land-based farm of European seabass (*Dicentrarchus labrax*). *Aquat. Living Resour.* 11 (4), 247-254.
- Lemarié, G., Dosdat, A., Covés, D., Dutto, G., Gasset, E., Person-Le Ruyet, J. 2003. Effect of chronic ammonia exposure on growth of European sea bass (*Dicentrarchus labrax*) juveniles. *Aquaculture* 229, 479-491.
- Leonard, N., Blancheton, J.-P., Guiraud, J.P. 2000. Population of heterotrophic bacteria in an experimental recirculating system. *Aquacultural Engineering* 22, 109-120.
- Leonard, N., Guiraud, J.P., Gasset, E., Cailleres, J.P., Blancheton, J.-P. 2002. Bacteria and nutrients – nitrogen and carbon – in a recirculating system for sea bass production. *Aquacultural Engineering* 26, 111-127.
- Liao, P.B. and Mayo, R.D. 1974. Intensified fish culture combining water reconditioning with pollution abatement. *Aquaculture* 3, 61-85.
- Liltved, H., Hektoen, H., Efraimsen, H. 1995. Inactivation of bacterial and viral fish pathogens by ozonation or UV irradiation in water of different salinity. *Aquacultural Engineering* 14, 107-122.
- Liltved, H., Vogelsang, C., Modahl, I., Dannevig, B.H. 2006. High resistance of fish pathogenic viruses to UV irradiation and ozonated seawater. *Aquacultural Engineering* 34, 72-82.
- Lin, S.H. and Wu, C.L. 1996. Removal of nitrogenous compounds from aqueous solution by ozonation and ion exchange. *Wat. Res.* Vol. 30, 1851-1857.
- Ling, J. and Chen, S. 2005. Impact of organic carbon on nitrification performance of different biofilters. *Aquacultural Engineering* 33, 150-162.
- Lockwood, C.E., Bummer, P.M., Jay, M. 1997. Purification of proteins using foam fractionation. *Pharmaceutical Research*, 14 (11), 1511-1515.
- Losordo, T.M. and Westers, H. 1994. System Carrying capacity. *In: M.B. Timmons and T.M. Losordo (Eds.), Aquaculture Water Reuse Systems: Engineering Design and Management. Developments in Aquaculture and Fisheries Science, Vol. 27, Elsevier, Amsterdam, 9-60.*
- Lupatsch, I. and Kissil, G.W. 1998. Predicting aquaculture waste from Gilthead Seabream (*Sparus aurata*) culture using a nutritional approach. *Aquat. Living Ressour.* 11, 265-268.
- Lupatsch, I., Kissil, G.W., Sklan, D. 2001. Optimization of feeding regimes for European sea bass *Dicentrarchus labrax*: a factorial approach. *Aquaculture* 202, 289-302.

- Madetoja, J., Nyman, P., Wiklund, T. 2000. *Flavobacterium psychrophilum*, invasion into and shedding by rainbow trout *Onchorhynchus mykiss*. Dis. Aquat. Org., Vol. 43, 27-38.
- Malone, R.F. and de los Reyes Jr., A.A. 1997. Categories of recirculating aquaculture systems. In: M.B. Timmons and T.M. Losordo (Eds.) Advances in Aquacultural Engineering. Aquacultural Engineering Society (AES) Proceedings III, ISTA IV, Orlando, FL, November 9-12 1997. NRAES, New York, 197-208.
- Malone, R.F. and Pfeiffer, T.J. 2006. Rating fixed film nitrifying biofilters used in recirculating aquaculture systems. Aquacultural Engineering 34, 389-402.
- Mathews, A. Bishnoi, P.R., Svrcek, W.Y. 1979. Treatment of oil contaminated waste waters by foam fractionation. Water Research, Vol. 13, 385-391.
- McMillan, J.D., Wheaton, F.W., Hochheimer, J.N., Soares, J. 2003. Pumping effect on particle sizes in a recirculating aquaculture system. Aquacultural Engineering 27, 53-59.
- Michaud, L., Blancheton, J.P., Bruni, V., Piedrahita, R. 2006. Effect of particulate organic carbon on heterotrophic bacterial populations and nitrification efficiency in biological filters. Aquacultural Engineering 34, 224-233.
- Mildenberger, M. 1998. Über den Einfluß der Grenzschicht auf die Kinetik immobilisierter Nitrifikanten. Fortschr.-Ber. VDI Reihe 15 Nr. 204, Düsseldorf: VDI Verlag. 119 pp.
- Montero, D., Robaina, L. Caballero, M.J., Ginés, r., Izquierdo, M.S. 2005. Growth, feed utilization and flesh quality of European sea bass (*Dicentrarchus labrax*) fed diets containing vegetable oils: A time-course study on the effect of re-feeding period with a 100% fish oil diet. Aquaculture 248, 121-134.
- Nijhof, M. and Bovendeur, J. 1990. Fixed film nitrification characteristics in sea-water recirculation fish culture system. Aquaculture 87, 133-143.
- Noble, A.C. and Summerfelt, S.T. 1996. Diseases encountered in rainbow trout cultured in recirculating systems. Annual Review of Fish Diseases, Vol. 6, 65-92.
- Nolting, M. 2000. Einfluß des Salzgehaltes auf die Nitrifikationsleistung von Biofiltern einer experimentellen Kreislaufanlage bei annähernd gleicher Biomasse der Fische (*Oreochromis niloticus*). Berichte aus dem Institut für Meereskunde an der CAU Kiel Nr. 317, 199 pp.
- Olivar, M.P., Ambrosio, P.P., Catalán, I.A. 2000. A closed water recirculation system for ecological studies in marine fish larvae: growth and survival of sea bass larvae fed with live prey. Aquat. Living Resour. 13, Vol. 1, 29-35.
- Oliva-Teles, A., Pereira, J.P., Gouveia, A., Gomes, E. 1998. Utilization of diets supplemented with microbialphytase by seabass (*Dicentrarchus labrax*). Aquat. Living Resour. 11, Vol. 4, 255-259.
- Oliva-Teles, A. and Pimentel-Rodrigues, A. 2004. Phosphorous requirement of European sea bass (*Dicentrarchus labrax* L.) juveniles. Aquaculture Research 35, 636-642.
- Orellana, J., Wecker, B., Sander, M., Waller U. 2005. Particulate matter in a modern marine recirculations system: what, where, and how much. European Aquaculture Society Special Publication 35, 354-355.

- Otte, G. and Rosenthal, H. 1978. Water quality during a one year operation of a closed intensive fish culture system. ICES, C.M. 1978/F:7, 18 pp.
- Otte, G. and Rosenthal, H. 1979. Management of a closed brackish water system for high density fish culture by biological and chemical water treatment. *Aquaculture* 18, 169-181.
- Otte, G., Hilge, V., Rosenthal, H. 1977. Effect of ozone on yellow substances accumulated in a recycling system for fish culture. ICES, C.M. 1977/E:27, 13 pp.
- Ozawa, T., Yotsumoto, H., Sasaki, T., Nakayama, S. 1991. Ozonation of seawater – Applicability of ozone for recycled hatchery cultivation. *Ozone Science & Engineering*, Vol. 13, 697-710.
- Patterson, R.N. and Watts, K.C. 2003a. Micro-particles in recirculating aquaculture systems: particle size analysis of culture water from a commercial Atlantic salmon site. *Aquacultural Engineering* 28, 99-113.
- Patterson, R.N. and Watts, K.C. 2003b. Micro-particles in recirculating aquaculture systems: microscope examination of particles. *Aquacultural Engineering* 28, 115-130.
- Patterson, R.N., Watts, K.C., Gill, T.A. 2003. Micro-particles in recirculating aquaculture systems: determination of particle density by density gradient centrifugation. *Aquacultural Engineering* 27, 105-115.
- Papoutsoglou, S.E., Tziha, G., Vrettos, X., Athanasiou, A. 1998. Effect of stocking density on behaviour and growth of European sea bass (*Dicentrarchus labrax*) juveniles reared in a closed circulated system. *Aquacultural Engineering* 18, 135-144.
- Paspatis, M., Batarías, C., Tiangos, P., Kentouri, M. 1999. Feeding and growth responses of sea bass (*Dicentrarchus labrax*) reared by four feeding methods. *Aquaculture* 175, 293-305.
- Paspatis, M., Boujard, T., Maragoudaki, D., Kentouri, M. 2000. European sea bass growth and N and P loss under different feeding practices. *Aquaculture* 184, 77-88.
- Periago, M.J., Ayala, M.D., López-Albors O., Abdel, I., Martínez, C., García-Alcázar, A., Ros, G., Gil, F. 2005. Muscle cellularity and flesh quality of wild and farmed sea bass, *Dicentrarchus labrax* L. *Aquaculture* 249, 175-188.
- Perry, D.M., Mercaldo-Allen, R., Burgh, S. 2001. Growth and culture of larval and juvenile tautogs in a closed recirculation-seawater system. *North American Journal of Aquaculture* 63, 300-305.
- Peres, H. and Oliva-Teles, A. 1999. Influence of temperature on protein utilization in juvenile European sea bass (*Dicentrarchus labrax*). *Aquaculture* 170, 337-348.
- Person-Le Ruyet, J., Chartois, H., Quemener, L. 1995. Comparative acute ammonia toxicity in marine fish and plasma ammonia response. *Aquaculture* 136, 181-194.
- Person-Le Ruyet, J., Skalli, A., Dulau, B., La Bayon, N., Le Delliou, H. 2004. Does dietary n-3 highly unsaturated fatty acid level influence the European sea bass, (*Dicentrarchus labrax*) capacity to adapt to a high temperature? *Aquaculture* 242, 571-588.

- Peters, G., Hoffmann, R., Jörgensen, L. 1984. Gill and fin lesions in rainbow trout from North German culture facilities. *In: Rosenthal, H. and Sarig, S. (Eds.) Research on Aquaculture. Special Pub. European Maricult. Soc. 8, 103-104.*
- Pickett, G.D. and Pawson, M.G. 1994. Sea bass. Biology, Exploitation and Conservation. Chapman & Hall, Fish and Fisheries Series 12, 337 pp.
- Piedrahita, R.H. 2003. Reducing the potential environmental impact of tank aquaculture effluents through intensification and recirculation. *Aquaculture 226, 35-44.*
- Posch, T., Lofere-Krößbacher, M., Gao, G., Alfreider, A., Pernthaler, J., Psenner, R. 2001. Precision of bacterioplankton biomass determination: a comparison of two fluorescent dyes, and of allometric and linear volume-to-carbon conversion factors. *Aquatic Microbial Ecology, Vol. 25, 55-63.*
- Reuter, J. and Johnson, R. 1995. The use of ozone to improve solid removal during disinfection. *Aquacultural Engineering 14, 123-141.*
- Ricker, W.E. 1979. Growth rates and models. *In: Hoar, W.S., Randall, D.J., Brett, J.R. (Eds.) Fish Physiology, Vol. VIII, Academic Press Inc., 679-743.*
- Ritola, O., Lyytikäinen, T., Pylkkö, P., Mölsä, H. and Lindström-Seppä, P. 2000. Glutathione-dependent defence system and monooxygenase enzyme activities in Arctic charr *Salvelinus alpinus* (L.) exposed to ozone. *Aquaculture 185, 219-233.*
- Roncarati, A., Melotti, P., Dees, A., Mordenti, O., Angellotti, L. 2006. Welfare status of cultured seabass (*Dicentrarchus labrax* L.) and seabream (*Sparus aurata* L.) assessed by blood parameters and tissue characteristics. *J. Appl. Ichthyol. 22, 225-234.*
- Rosenthal, H. 1981a. Ozonation and sterilization. *In: K. Tiews (Ed.), Proc. World Symp. on Aquaculture in Heated Effluents and of Recirculation Systems, EIFAC, Stavanger, Norway, 28-30 May 1980, Vol. I, 219-274.*
- Rosenthal, H. 1981b. Recirculation systems in Western Europe. *In: K. Tiews (Ed.), Proc. World Symp. on Aquaculture in Heated Effluents and of Recirculation Systems, EIFAC, Stavanger, Norway, 28-30 May 1980, Vol. II, 305-316.*
- Rosenthal, H. 1993. The history of recycling technology: a lesson learned from past experience. *In: Reinertsen, Dahle, Jorgensen, Tvinnereim (Eds.), Fish Farming Technology, Balkema, Rotterdam, 341-349.*
- Rosenthal, H. 1994. Aquaculture and the environment. *World Aquaculture 25 (2), 4-11.*
- Rosenthal, H. 1997. Forschungen zur Aquakulturentwicklung: Rückblick & Ausblick. *Fortschr. Fisch. wiss. 13, 53-60.*
- Rosenthal, H. and Sander, E. 1975. An improved aeration method combined with waste-foam removal in sea-water recycling system. *ICES, C.M. 1975/E:14, 16pp.*
- Rosenthal, H. and Westernhagen, H. 1976. Fischzucht im Seewasserkreislauf unter Kombination biologischer und chemischer Aufbereitungsverfahren (Ozonisierung). *Arb. Dtsch. Fisch.-Verb. 16, 208-218.*
- Rosenthal, H. and Otte, G. 1979. Ozonation in an intensive fish culture recycling system. *In: Ozone: Science and Engineering, Vol. 1, Pergamon Press Ltd, 319-327.*

- Rosenthal, H. and Krüner, G. 1985. Treatment efficiency of an improved ozonation unit applied to fish culture situations. *Ozone: Science and Engineering* 7(3), 179-190.
- Rosenthal, H. and Wilson, J. S. 1987. An updated bibliography (1845-1986) on ozone, its biological effects and technical applications. *Can. Tech. Rep. Fish. Aquat. Sci.* 1542, 249 pp.
- Rosenthal, H. and McInerney-Northcott, M.E. 1989. Technology development and transfer & environmental considerations. *In: Boghen, A.D. (Ed.) Cold-Water Aquaculture in Atlantic Canada*, The Canadian Institute for Research on Regional Development, Moncton, New Brunswick, Canada, 275-325.
- Rosenthal, H. and Black, E.A. 1993. Recirculation systems in aquaculture. *In: Wang, J.-K. (Ed.) Techniques for Modern Aquaculture, Proceedings of an Aquacultural Engineering Conference, 21-23 June 1993, Spokane, Washington, USA*, 284-294.
- Rosenthal, H. and Hilge, V. 2000. Aquaculture production and environmental regulations in Germany. *J. Appl. Ichthyol.* 16, 163-166.
- Rosenthal, H., Krüner, G., Otte, G. 1978. Effects of ozone treatment on recirculating water in a closed fish culture system. *ICES, C.M.* 1978/F:9, 16pp.
- Rosenthal, H., Andjus, R., Krüner, G. 1981. Daily variations of water quality parameters under intensive culture conditions in a recycling system. *In: K. Tiews (Ed.), Proc. World Symp. on Aquaculture in Heated Effluents and of Recirculation Systems, Stavanger, Norway, 28-30 May 1980, Vol. I*, 113-120.
- Rosenthal, H., Allen, J.H., Helm, M.M., McInerney-Northcott, M. 1995. Aquaculture technology: its application, development, and transfer. *In: Boghen, A.D. (Ed.) Cold-Water Aquaculture in Atlantic Canada*, The Canadian Institute for Research on Regional Development, Moncton, New Brunswick, Canada, 395-450.
- Rosenthal, H., Scarratt, D.J., McInerney-Northcott, M. 1995. Aquaculture and the environment. *In: Boghen, A.D. (Ed.) Cold-Water Aquaculture in Atlantic Canada*, The Canadian Institute for Research on Regional Development, Moncton, New Brunswick, Canada, 453-500.
- Russell, N.R., Fish, J.D., Wootton, R.J., 1996. Feeding and growth of juvenile sea bass: the effect of ration and temperature on growth rate and efficiency. *J. Fish Biol.*, 49, 206-220.
- Rydl, A. 2005. Sukzession und Analyse des bakteriellen Bewuchses an Fischen und Materialoberflächen in einer geschlossenen Fischzuchtanlage. Diplomarbeit, Leibniz-Institut für Meereswissenschaften and der CAU-Kiel, 102pp.
- Sander, E. and Rosenthal, H. 1975. Application of ozone in water treatment for home aquaria, public aquaria and for aquaculture purposes. *In: Blogoslawski, W. J. and R. G. Rice (Eds.), Aquatic Applications of Ozone, Intern. Ozone Inst.*, 103-114.
- Sander, M. 1998. *Aquarientechnik in Süß- und Seewasser*. Stuttgart, Ulmer, 256pp.
- Schlegel, H.G. 1992. *Allgemeine Mikrobiologie*. Georg Thieme Verlag, Stuttgart, 480pp.

- Schlesner, H. and Rheinheimer, G. 1974. Auswirkungen einer Ozonisierungsanlage auf den Bakteriengehalt des Wassers eines Schauaquariums. *In: Kieler Meeresforschungen aus dem Institut für Meereskunde an der Universität Kiel, Band 30, 117-129.*
- Schreck, C.B. and Li, H.W. 1991. Performance capacity of fish: stress and water quality. *In: Brune, D.E., Tomasso, J.R. (Eds.), Aquaculture and Water Quality. Advances in World Aquaculture Vol. 3, The World Aquaculture Society, 21-29.*
- Scott, K.R. and Allard, L. 1983. High-flowrate water recirculation system incorporating a hydrocyclone prefilter for rearing fish. *Prog. Fish-Cult. 45, no.3, 148-153.*
- Scott, K.R. and Allard, L. 1984. A four-tank recirculation system with a hydrocyclone prefilter and a single water reconditioning unit. *Prog. Fish-Cult. 46, no.4, 254-261.*
- Seo, J.-K., Jung, I.-H., Kim, M.-R., Kim, B.J., Nam, S.-W., Kim, S.-K. 2001. Nitrification performance of nitrifiers immobilized in PVA (polyvinyl alcohol) for a marine recirculating aquarium system. *Aquacultural Engineering 24, 181-194.*
- Sharer, M.J., Summerfelt, S.T., Bullock, G.L., Gleason, L.E., Taeuber, J. 2005. Inactivation of bacteria using ultraviolet irradiation in a recirculating salmonid culture system. *Aquacultural Engineering 33, 135-149.*
- Siman, M. and Azam, F. 1989. Protein content and protein synthesis rates of planktonic marine bacteria. *Marine Ecology Progress Series 51, 201-213.*
- Singh, S., Ebeling, J., Wheaton, F. 1999. Water quality in four recirculating aquacultural system configurations. *Aquacultural Engineering 20, 75-84.*
- Spotte, S.H. 1979. *Seawater Aquariums, the Captive Environment.* Wiley, New York, 413pp.
- Suantika, G., Dhert, P., Rombaut, G., Vandenberghe, J., De Wolf, T., Sorgeloos, P. 2001. The use of ozone in a high density recirculation system for rotifers. *Aquaculture 201,35-49.*
- Suantika, G., Dhert, P., Sweetman, E., O'Brien, E., Sorgeloos, P. 2003. Technical and economical feasibility of a rotifer recirculation system. *Aquaculture 227, 173-189.*
- Sugita, H., Mita, J., Deguchi, Y. 1996. Effect of ozone treatment on amylases in seawater. *Aquaculture 141, 77-82.*
- Summerfelt, S.T. and Hochheimer, J.N. 1997. Review of ozone processes and applications as an oxidizing agent in aquaculture. *The Progressive Fish-Culturist 59, 94-105.*
- Summerfelt, R.C. and Penne, C.R. 2005. Solids removal in a recirculating aquaculture system where the majority of flow bypasses the microscreen filter. *Aquacultural Engineering 33, 214-224.*
- Summerfelt, S.T., Hankins, J.A., Weber, A.L. and Durant, M.D. 1997. Ozonation of a recirculating rainbow trout culture system II. Effects on microscreen filtration and water quality. *Aquaculture 158, 57-67.*
- Sutterlin, A.M., Couturier, C.Y., Deveraux, T. 1984. A recirculation system using ozone for the culture of Atlantic salmon. *Progressive Fish-Culturist, Vol. 46, no. 4, 239-244.*

- Tango, M.S. and Gagnon, G.A. 2003. Impact of ozonation on water quality in marine recirculation systems. *Aquacultural Engineering* 29, 125-137.
- Theisen, D.D., Stansell D.D., Woods, L.C.III. 1998. Desinfection of Nauplii of *Artemia franciscana* by ozonation. *The Progressive Fish-Culturist* 60, 149-151.
- Thetmeyer, H., Waller, U., Black, K.D., Inselmann, S., Rosenthal, H. 1999. Growth of European sea bass (*Dicentrarchus labrax* L.) under hypoxic and oscillating oxygen conditions. *Aquaculture* 174, 355-367.
- Thoman, E.S., Ingall, E.D., Davis, D.A., Arnold, C.R. 2001. A nitrogen budget for a closed, recirculating mariculture system. *Aquacultural Engineering* 24, 195-211.
- Timmons, M.B., Ebeling, J.M., Wheaton, F.W., Summerfelt, S.T., Vinci, B.J. 2001. *Recirculating Aquaculture Systems*. NRAC Publication No. 01-002, 250pp.
- Tucker, C.S. and Martin, J.F. 1991. Environment-related off flavors in fish. *In: Brune, D.E., Tomasso, J.R. (Eds.), Aquaculture and Water Quality, Advances in World Aquaculture, Vol. 3, The World Aquaculture Society, 133-179.*
- Van Gorder, S.D. and Jug-Dujakovic, J. 1998. The effects of feed management on design and production capacity of recirculating aquaculture systems. *NRAES-98, Vol. I, 390-398.*
- Veerapen, J.P., Brooks, M.J., Lowry, B.J., Couturier, M.F. 2002. Solids removal modeling in recirculating aquaculture systems. *In: Proceedings of the 4th International Conference on Recirculating Aquaculture, Roanoke VA (USA), 18-21 Jul 2002, 491-499.*
- Veerapen, J.P., Lowry, B.J., Couturier, M.F. 2005. Design methodology for the swirl separator. *Aquacultural Engineering* 33, 21-45.
- Viadero, R.C.Jr. and Noblet, J.A. 2002. Membrane filtration for removal of fine solids from aquaculture process water. *Aquacultural Engineering* 26, 151-169.
- Waller, U. 2000. Tank culture and recirculating systems. *In: Kenneth D. Black (Ed.) Environmental Impacts of Aquaculture, Sheffield Academic Press, 99-127.*
- Waller, U., Sander, M., Piker, L. 2001. Low energy and low water consumption recirculation system for marine fish: first results from a test run with *Dicentrarchus labrax* in an improved recirculation system and suggestions on an integration into secondary production lines. *European Aquaculture Society Special Publication 29, 265-266.*
- Waller, U., Orellana, J., Schiller, A., Sander, M. 2002. The growth of young sea bass in a new type of re-circulation system. *ICES 2001/Session S.*
- Waller, U., Bischoff, A., Orellana, J., Sander, M., Wecker, B. 2003a. An advanced technology for clear water aquaculture recirculation systems: results from a pilot production of sea bass and hints towards „zero discharge“. *European Aquaculture Society Special Publication 33, 356-357.*
- Waller, U., Attramadal, K., Koppe, R., Orellana, J., Sander, M., Schmaljohann, R. 2003b. The control of hygienic conditions in seawater recirculation systems: the use of foam fractionation and ozone. *European Aquaculture Society Special Publication 33, 354-355.*

- Wecker, B. 2006. Nährstofffluss in einer geschlossenen Kreislaufanlage mit integrierter Prozesswasserklärung über Algenfilter. Disseration, Mathematisch-Naturwissenschaftlichen Fakultät, Leibniz-Institut für Meereswissenschaften IFM-GEOMAR an der Universität Kiel, 156pp.
- Weeks, N.C., Timmons, M.B., Chen, S. 1992. Feasability of using foam fractionation for the removal of dissolved and suspended solids from fish culture water. *Aquacultural Engineering* 11, 251-265.
- Wheaton, F.W. 1977. *Aquacultural Engineering*. John Wiley and Sons, New York, 708pp.
- Wheaton, F.W., Lawson, T.B., Lomax, K.M. 1979. Foam fractionation applied to aquacultural systems. *In: Avault, J.W.Jr. (Ed.), Proceedings of the Tenth Annual Meeting World Mariculture Society, Honolulu, Hawaii, January 22-26 1979, Louisiana State University, Baton Rouge, Louisiana, USA, 795-808.*
- Wheaton, F.W., Hochheimer, J.N., Kaiser, G.E., Krones, M.J., Libey, G.S., Easter, C.C. 1994a. Nitrification filter principles. *In: Timmons, M.B., Losordo, T.M. (Eds.), Aquaculture Water Reuse Systems: Engineering Design and Management, Developments in Aquaculture and Fisheries Science, 27, Elsevier, 101-126.*
- Wheaton, F.W., Hochheimer, J.N., Kaiser, G.E., Krones, M.J., Libey, G.S., Easter, C.C. 1994b. Nitrification filter design methods. *In: Timmons, M.B., Losordo, T.M. (Eds.), Aquaculture Water Reuse Systems: Engineering Design and Management, Developments in Aquaculture and Fisheries Science, 27, Elsevier, 127-171.*
- Wickins, J.F. 1980. Water quality requirements for intensive aquaculture: a review. *In: K. Tiews (Ed.), Proc. World Symp. on Aquaculture in Heated Effluents and of Recirculation Systems, Stavanger, Norway, 28-30 May 1980, Vol. I, 17-37.*
- Williams, R.C., Hughes, S.G. and Rumsey, G.L. 1982. Use of ozone in a water reuse system for salmonids. *Progressive Fish-Coulturist* 44 (2), 102-105.
- Yanbo, W., Zirong, X., Xuxia, Z., Meisheng, X. 2005. Bacteria attached to suspended particles in Northern White Shrimp (*Penaeus vannamei* L.) ponds. *Aquaculture* 249, 285-290.
- Yu, W., Dodds, W.K., Banks, M.K., Skalsky, J., Strauss, E.A. 1995. Optimal staining and sample storage time for direct microscopical enumeration of total and active bacteria soil with two fluorescent dyes. *Applied and Environmental Microbiology*, Vol. 61, No. 9, 3367-3372.
- Zanuy, S. and Carrillo, M. 1985. Annual cycles of growth, feeding rate, gross conversion efficiency and hematocrit levels of sea bass (*Dicentrarchus labrax* L.) adapted to two different osmotic media. *Aquaculture* 44, 11-25.

ANNEX

Some calculations on overall TSS production in a RAS

Ideally it would be an improvement for system management to be able to predict the dynamics of solids produced in a RAS to advice on design and operation of such systems based on mass balance modelling. This would require a comprehensive modelling approach as partly has been done by Wecker (2006) for overall waste output and approximation of total solids when using *Sparus aurata*. However, when specifically looking into the fate of various fractions of faeces and their interaction with system components directly, many highly specific processes that are often interactively influenced by other functional parameters have to be assessed to find detailed solutions on particle management. The study therefore focussed more on the technical aspects rather than primarily presenting data for such comprehensive modelling approaches. Data from this study and from literature have been examined and carefully extracted to assist building the elements for such basic mass balance calculations that may be used at a later date in dynamic modelling. The literature data have all been gained from studies working in differently designed systems which operate under quite different conditions as to the species studied, the temperature regime, the system configurations and most importantly the types of feed used.

The data base generated in this study is also too weak to derive at a sound generalized model on mass balance of solids beyond what is generally known and has recently been presented by Wecker (2006). Therefore, a tentative and partly theoretical approach has been made to derive at a first approximation (not presented in the discussion but attached here as Annex) "of solid production over time in relation to fish growth and system component performance. The results of this exercise need to be seen with caution.

The data of this study were used to estimate growth of the European sea bass in a RAS, and the determination of parameters for calculations of nutrient input (feed), retention (fish growth) and output (soluble and particulate wastes). The overall calculations are valid for the time window between day t_0 and day t_{330} as reliable measurements on growth and some fair data on solid production but less verifiable data on quantitative solid behaviour in such a system were available. Basic physiological parameters

necessary to feed the models were also taken from scientific literature. The calculations are based on individual fish and on a daily basis.

The first set of 10 equations deals with fish growth, feed conversion, feed intake, and the amount of nutrients retained in the fish and these are used to support further mass balance calculations.

[1] Individual fish wet weight (g):

$$W_t = a_w / (1 + \text{EXP}(-(d_t - x_0) / b_w))$$

$a_w =$	281.24
$b_w =$	57.58
$x_0 =$	220.14

Data source:
This study

W_t = wet weight at day t

d_t = day

a_w , b_w , and x_0 = equation parameters

[2] Individual weight increment (g):

$$\Delta W_t = W_t - W_{t-1}$$

Data source:
This study

ΔW_t = weight increment between day t and day t-1

W_t = wet weight at day t

W_{t-1} = wet weight at day t-1

[3] Feed conversion ratio:

$$\text{FCR}_t = a_{\text{FCR}} + b_{\text{FCR}} * (\text{LN}(W_t))^2$$

$a_{\text{FCR}} =$	0.65
$b_{\text{FCR}} =$	0.05

Data source:
This study

FCR_t = feed conversion ratio at day t

a_{FCR} and b_{FCR} = equation parameters

W_t = wet weight at given day t

[4] Feed intake (g):

$$\text{FI}_t = \Delta W_t * \text{FCR}_t$$

Data source:
This study

FI_t = feed intake at day t

ΔW_t = weight difference between day t and day t-1

FCR_t = feed conversion ratio at day t

[5] Nitrogen amount consumed by fish through the feed (mg*d⁻¹):

$$N_{t,feed} = a_{N,feed} * FI_t$$

$$a_{N,feed} = 72$$

Data source:
Feed manufacturer

$N_{t,feed}$ = nitrogen amount consumed by fish through the feed at day t

$a_{N,feed}$ = nitrogen content in the feed (mg*g⁻¹)

FI_t = feed intake at day t

[6] Phosphorous amount consumed through the feed (mg*d⁻¹):

$$P_{t,feed} = a_{P,feed} * FI_t$$

$$a_{P,feed} = 14$$

Data source:
Feed manufacturer

$P_{t,feed}$ = phosphorous amount ingested through the feed at day t

$a_{P,feed}$ = phosphorous content in the feed (mg*g⁻¹)

FI_t = feed intake at day t

[7] Carbon amount consumed through the feed (mg*d⁻¹):

$$C_{t,feed} = a_{C,feed} * FI_t$$

$$a_{C,feed} = 523$$

Data source:
This study

$C_{t,feed}$ = carbon amount ingested through the feed at day t

$a_{C,feed}$ = carbon content in the feed (mg*g⁻¹)

FI_t = feed intake at day t

[8] Nitrogen amount retained in fish tissue (mg*d⁻¹):

$$N_{t,R} = (a_{N,R} + b_{N,R} * W_t) * \Delta W_t * 1000$$

$$a_{N,R} = 0.04$$

$$b_{N,R} = -4.06E-05$$

Data source:
This study

$N_{t,R}$ = nitrogen retained in fish tissue at day t

$a_{N,R}$ and $b_{N,R}$ = equation parameters

ΔW_t = weight difference between day t and day t-1

[9] Phosphorous amount retained in fish tissue (mg*d⁻¹):

$$P_{t,R} = a_{P,R} * \Delta W_t$$

$$a_{P,R} = 7.2$$

Data source:
Lupatsch and Kissil
(1998)

$P_{t,R}$ = phosphorous retained in fish tissue at day t

$a_{P,R}$ = phosphorous content in fish tissue in mg*g⁻¹

ΔW_t = weight difference between day t and day t-1

[10] Carbon amount retained in fish tissue (mg*d⁻¹):

$$C_{t,R} = (a_{C,R} + b_{C,R} * W_t) * \Delta W_t * 1000$$

$$a_{C,R} = 0.20$$

$$b_{C,R} = -1.18E-04$$

Data source:
This study

$C_{t,R}$ = carbon retained in fish tissue at day t

$a_{C,R}$ and $b_{C,R}$ = equation parameters

W_t = wet weight at given day t

ΔW_t = weight difference between day t and day t-1

Equations 11 to 13 describe the output of suspended solid material as derived from calculations on the fish metabolism based on the type of feed (feed composition) used and the approximations for faecal output known for the fish species involved, considering (a) the total amount of faecal production (assuming feed compositions for various sizes will behave similar despite the variation already existing between individual feed packages because of linear programming of the feed industry), (b) estimates on the non-soluble fraction of solids produced in a RAS, and (c) on the soluble fraction of solids released from faeces and lost feed (a highly variable component, changing with each feed lot and pellet size)

[11] Amount of solids (faeces) (g*d⁻¹):

$$SW_t = a_{SW} * b_{SW} * FI_t$$

$$a_{SW} = 0.90$$

$$b_{SW} = 0.33$$

Data source:
Feed manufacturer
Lupatsch and Kissil
(1998)

SW_t = dry weight of solids (faeces) at day t

a_{SW} = dry matter in feed

$b_{SW} = 1 - 0.67 = 0.33$; (0.67 = apparent digestibility coefficient for dry matter)

FI_t = feed intake for given day t

[12] Non-soluble fraction of the solid wastes (g*d⁻¹):

$$W_{t,non-sol} = a_{Wnon-sol} * SW_t$$

$$a_{Wnon-sol} = 0.64$$

Source:
Lupatsch and Kissil
(1998)

$W_{t,non-sol}$ = dry weight of the non-soluble fraction of the solids at day t

$a_{Wnon-sol}$ = remaining dry weight after leaching

SW_t = solids at day t

[13] Soluble fraction of the solid wastes ($g \cdot d^{-1}$)

$$W_{t,sol} = a_{wsol} * SW_t$$

$$a_{wsol} = 0.36$$

Source:
Oliva-Teles *et al.*
(1998)

$W_{t,sol}$ = dry weight of the soluble fraction of the solids at day t

$a_{wsol} = 1 - 0.644 = 0.36$; dry weight loss due to leaching

SW_t = solids at day t

The estimated growth performance of *Dicentrarchus labrax* over time is in good agreement with the data presented in the results section (Figs 28, 29, Chapter 3.1.1) and with literature data. These were also compared with the feed conversion ratio and feed intake (Figure 106) for almost a full year (experimental period between day t_0 and day t_{330}).

Based on the data obtained from fish raised in the experimental RAS (Fig. 108a) the FCR increased gradually and began to level with time instead of declining as would be suggested by literature data. Here, the feeding regime certainly played a decisive role and common feeding regimes in other studies may lead to slightly different overall trends. Fig. 106b, however, depicts the feed intake and FRC in relation to individual body weight. The feed intake declined after the fish reached about 160 g, because the feeding rate in percent body weight was gradually adjusted close to what the commercial feed table suggests. The conversion rate (FCR) on a wet to dry-weight basis, however, did not, indicating for this species that perhaps the feeding regime was not optimal as optimal growth was not the objective of this study. In fact feeding level was reduced after day 220 and this certainly has influenced the performance and this is well reflected in the model.

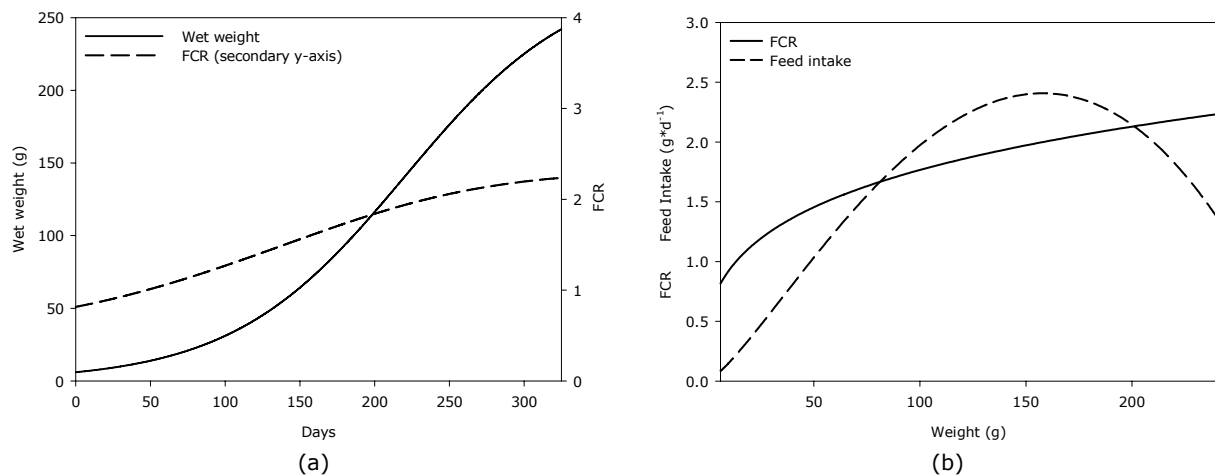


Fig. 106. Growth performance of European sea bass (*Dicentrarchus labrax*) in an experimental RAS between days t_0 and day t_{330} . (a) = Individual fish weight and feeding conversion ratio (FCR) over time (equations 1 and 3); (b) Amount of feed intake and FCR in relation to individual fish size (g) (equations 3 and 4).

Waste output of the fish via excretion of faeces as well as soluble wastes seem to be closely linked to individual feed uptake and biomass gain and the data obtained are in general agreement with the calculations shown in Fig. 106a. Again, after day 220 the fish were not fed the optimum ration (not even every day), while growth was still being observed (see 106a). However, daily weight increment from day 220 onwards is lower, therefore the calculated output of wastes declined for both the solid and soluble fractions. (Fig 107a and 107b).

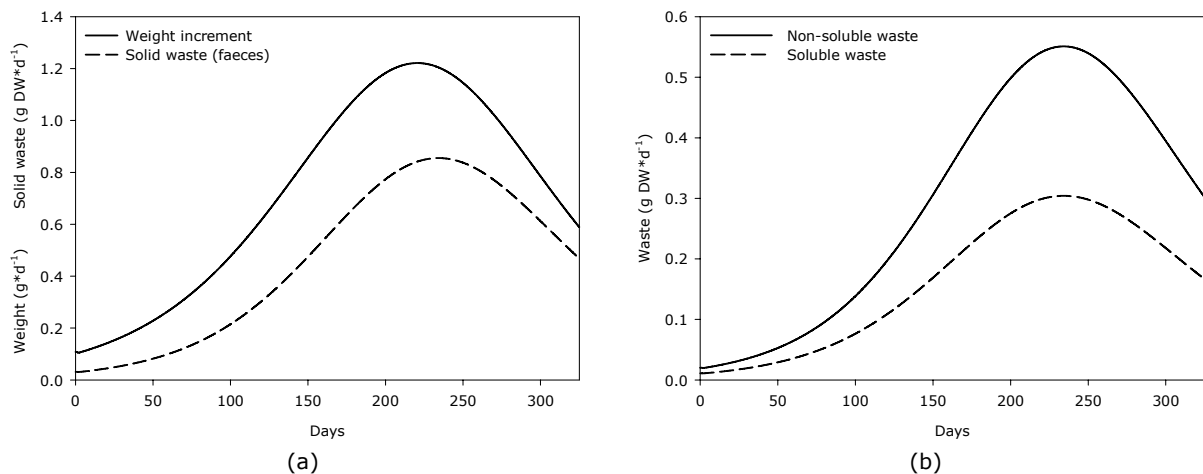


Fig. 107. Performance of the RAS while growing European sea bass (*Dicentrarchus labrax*) between days t_0 and t_{330} . (a) Daily fish weight increment and solid wastes (faeces) produced per day based on equations 2 and 11; (b) Amount of soluble and non-soluble wastes based on equations 12 and 13.

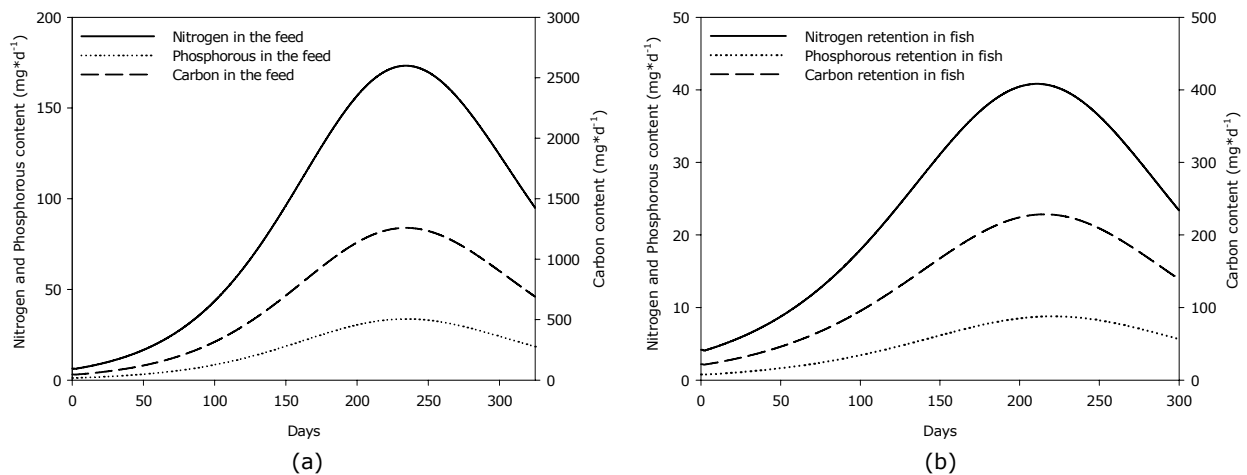


Fig. 108. Performance of the RAS while growing European sea bass (*Dicentrarchus labrax*) between day's t_0 and t_{330} . (a) Changes of nutrient (nitrogen, phosphorous, and carbon) inputs over time from the feed (based on equations 5, 6 and 7). (b) Amount of nutrients (N, P, and C) retained in fish tissue based on determined fish growth and feeding data (equations 8, 9, and 10).

As Figure 108a indicates, there is a clear relationship between total input of nutrients via the feed while the retention of these nutrients over time follow strictly the input curves. The amount retained was approximately 20, 25 and 20% for phosphorus, carbon and nitrogen, respectively (Fig. 108b). These overall retention rates are grossly proportional for the various fish sizes and also in relation to the total biomass of the system.

Equations 14 to 25 address the amounts of various relevant nutrients being retained in fish faeces and being affected by leaching processes during time and the data from own experimental work and literature sources have been used to gain some insight in how much nutrients contained in the solids may remain, leach, or being removed from the system by both, the swirl separator and foam fractionator. These equations are as follows:

[14] Nitrogen amount in fish faeces ($\text{mg}\cdot\text{d}^{-1}$):

$$N_{t,\text{faeces}} = a_{N,\text{faeces}} \cdot N_{t,\text{feed}}$$

$$a_{N,\text{faeces}} = 0.83$$

Source:
Lupatsch and Kissil
(1998)

$N_{t,\text{faeces}}$ = nitrogen amount in fish faeces at day t

$a_{N,\text{faeces}}$ = apparent digestibility coefficient for nitrogen

$N_{t,\text{feed}}$ = nitrogen amount ingested through the feed at day t

[15] Phosphorous amount in fish faeces (mg*d⁻¹):

$$P_{t,faeces} = a_{t,faeces} * P_{t,feed} \quad a_{P,faeces} = 0.48 \quad \text{Source: Lupatsch and Kissil (1998)}$$

$P_{t,faeces}$ = phosphorous amount in fish faeces at day t

$a_{P,faeces}$ = apparent digestibility coefficient for phosphorous

$P_{t,feed}$ = phosphorous amount ingested through the feed at day t

[16] Carbon amount in fish faeces (mg*d⁻¹):

$$C_{t,faeces} = a_{C,faeces} * C_{t,feed} \quad a_{C,faeces} = 0.69 \quad \text{Data source: Lupatsch and Kissil (1998)}$$

$C_{t,faeces}$ = carbon amount in fish faeces at day t

$a_{C,faeces}$ = apparent digestibility coefficient for carbon

$C_{t,feed}$ = carbon amount ingested through the feed at day t

[17] Amount of nitrogen in non-soluble fraction of faeces (mg*d⁻¹):

$$N_{t,faeces \text{ non-sol}} = a_{N \text{ faeces non-sol}} * N_{t,faeces} \quad a_{N \text{ faeces non-sol}} = 0.56 \quad \text{Data source: Lupatsch and Kissil (1998)}$$

$N_{t,faeces \text{ non-sol}}$ = nitrogen amount in the non-soluble fraction of the faeces at day t

$a_{N \text{ faeces non-sol}}$ = remaining nitrogen in the faeces after leaching

$N_{t,faeces}$ = nitrogen amount in fish faeces at day t

[18] Amount of phosphorous in non-soluble fraction of faeces (mg*d⁻¹):

$$P_{t,faeces \text{ non-sol}} = a_{P \text{ faeces non-sol}} * P_{t,faeces} \quad a_{P \text{ faeces non-sol}} = 0.85 \quad \text{Data source: Lupatsch and Kissil (1998)}$$

$P_{t,faeces \text{ non-sol}}$ = phosphorous amount in the non-soluble fraction of faeces at day t

$a_{P \text{ faeces non-sol}}$ = remaining phosphorous in the faeces after leaching

$P_{t,faeces}$ = phosphorous amount in fish faeces at day t

[19] Amount of carbon in non-soluble fraction of faeces (mg*d⁻¹):

$$C_{t,faeces\ non-sol} = a_{C\ faeces\ non-sol} * C_{t,faeces}$$

$$a_{C\ faeces\ non-sol} = 0.58$$

Data source:

Lupatsch and Kissil
(1998)

$C_{t,faeces\ non-sol}$ = carbon amount in the non-soluble fraction of faeces at day t

$a_{C\ faeces\ non-sol}$ = remaining carbon in the faeces after leaching

$C_{t,faeces}$ = carbon amount in fish faeces at day t

[20] Nitrogen amount in the soluble fraction of faeces (mg*d⁻¹):

$$N_{t,faeces\ sol} = N_{t,faeces} - N_{t,faeces\ non-sol}$$

Data source:

This study

$N_{t,faeces\ sol}$ = nitrogen amount in the soluble fraction of faeces at day t

$N_{t,faeces}$ = nitrogen amount in fish faeces at day t

$N_{t,faeces\ non-sol}$ = nitrogen amount in the non-soluble fraction of faeces at day t

[21] Phosphorous amount in the soluble fraction of faeces ((mg*d⁻¹):

$$P_{t,faeces\ sol} = P_{t,faeces} - P_{t,faeces\ non-sol}$$

Data source:

This study

$P_{t,faeces\ sol}$ = phosphorous amount in the soluble fraction of faeces at day t

$P_{t,faeces}$ = phosphorous amount in fish faeces at day t

$P_{t,faeces\ non-sol}$ = phosphorous amount in the non-soluble fraction of faeces at day t

[22] Carbon amount in the soluble fraction of faeces ((mg*d⁻¹):

$$C_{t,faeces\ sol} = C_{t,faeces} - C_{t,faeces\ non-sol}$$

Data source:

This study

$C_{t,faeces\ sol}$ = carbon amount in the soluble fraction of faeces at day t

$C_{t,faeces}$ = carbon amount in fish faeces at day t

$C_{t,faeces\ non-sol}$ = carbon amount in the non-soluble fraction of faeces at day t

[23] Non-faecal nitrogen loss (mg*d⁻¹):

$$NFL_N = N_{t,feed} - N_{t,R} - N_{t,faeces}$$

Data source:

This study

NFL_N = amount of non-faecal nitrogen loss

$N_{t,feed}$ = nitrogen amount ingested through the feed at day t

$N_{t,R}$ = nitrogen retained in fish tissue at day t

$N_{t,faeces}$ = nitrogen amount in fish faeces at day t

[24] Non-faecal phosphorous loss ((mg*d⁻¹))

$$NFL_P = P_{t,feed} - P_{t,R} - P_{t,faeces}$$

Data source:
This study

NFL_P=amount of non-faecal phosphorous loss

P_{t,feed}=phosphorous amount ingested through the feed at day t

P_{t,R}= phosphorous retained in fish tissue at day t

P_{t,faeces}=phosphorous amount in fish faeces at day t

[25] Non-faecal carbon loss ((mg*d⁻¹))

$$NFL_C = C_{t,feed} - C_{t,R} - C_{t,faeces}$$

Data source:
This study

NFL_C=amount of non-faecal phosphorous loss

C_{t,feed}=carbon amount ingested through the feed at day t

C_{t,R}= carbon retained in fish tissue at day t

C_{t,faeces}=carbon amount in fish faeces at day t

Equations 26 to 33 address the amounts of solids removed by the swirl separator and the foam fractionator, and their nutrient composition.

[26] Solids removed by the swirl separator (mg*d⁻¹):

$$SW_{SS,t} = a_{Wnon-sol} * b_{SS} * SW_t$$

$$a_{Wnon-sol} = 0.64$$

$$b_{SS} = 0.73$$

Data source:
Lupatsch and Kissil
(1998)
This study

SW_{SS,t}= dry weight of solids removed by the swirl separator

a_{Wnon-sol}=remaining dry weight in solids after leaching

b_{SS}=share of solids removed by the swirl separator

[27] Solids removed by the foam fractionator (mg*d⁻¹):

$$SW_{FF,t} = a_{Wnon-sol} * b_{FF} * SW_t$$

$$a_{Wnon-sol} = 0.64$$

$$b_{FF} = 0.27$$

Data source:
Lupatsch and Kissil
(1998)
This study

SW_{FF,t}=dry weight of solids removed by the foam fractionator

a_{Wnon-sol}=remaining dry weight in solids after leaching

b_{FF}=share of solids removed by the foam fractionator

[28] Nitrogen in solids removed by the swirl separator (mg*d⁻¹):

$$NSW_{SS,t} = N_{t,faeces\ non-sol} * b_{SS}$$

$$b_{SS} = 0.73$$

Data source:
This study

$NSW_{SS,t}$ =nitrogen amount in solids removed by the swirl separator

$N_{t,faeces\ non-sol}$ =nitrogen amount in the non-soluble fraction of solids at day t

b_{SS} =share of solids removed by the swirl separator

[29] Phosphorous in solids removed by the swirl separator (mg*d⁻¹):

$$PSW_{SS,t} = P_{t,faeces\ non-sol} * b_{SS}$$

$$b_{SS} = 0.73$$

Data source:
This study

$PSW_{SS,t}$ =phosphorous amount in solids removed by the swirl separator

$P_{t,faeces\ non-sol}$ =phosphorous amount in the non-soluble fraction of solids at day t

b_{SS} =share of solids removed by the swirl separator

[30] Carbon in solids removed by the swirl separator (mg*d⁻¹):

$$CSW_{SS,t} = C_{t,faeces\ non-sol} * b_{SS}$$

$$b_{SS} = 0.73$$

Data source:
This study

$CSW_{SS,t}$ =carbon amount in solids removed by the swirl separator

$C_{t,faeces\ non-sol}$ =carbon amount in the non-soluble fraction of solids at day t

b_{SS} =share of solids removed by the swirl separator

[31] Nitrogen in solids removed by the foam fractionator (mg*d⁻¹):

$$NSW_{FF,t} = N_{t,faeces\ non-sol} * b_{FF}$$

$$b_{FF} = 0.27$$

Data source:
This study

$NSW_{FF,t}$ =nitrogen amount in solids removed by the foam fractionator

$N_{t,faeces\ non-sol}$ =nitrogen amount in the non-soluble fraction of solids at day t

b_{FF} =share of solids removed by the foam fractionator

[32] Phosphorous in solids removed by the foam fractionator (mg*d⁻¹):

$$PSW_{FF,t} = P_{t,faeces\ non-sol} * b_{FF}$$

$$b_{FF} = 0.27$$

Data source:
This study

$PSW_{FF,t}$ =phosphorous amount in solids removed by the foam fractionator

$P_{t,faeces\ non-sol}$ =phosphorous amount in the non-soluble fraction of solids at day t

b_{FF} =share of solids removed by the foam fractionator

[33] Carbon in solids removed by the foam fractionator ($\text{mg}\cdot\text{d}^{-1}$)

$$CSW_{FF,t} = C_{t,\text{faeces non-sol}} * b_{FF}$$

$$b_{FF} = 0.27$$

Data source:
This study

$CSW_{FF,t}$ =carbon amount in solids removed by the foam fractionator

$C_{t,\text{faeces non-sol}}$ =carbon amount in the non-soluble fraction of solids at day t

b_{FF} =share of solids removed by the foam fractionator

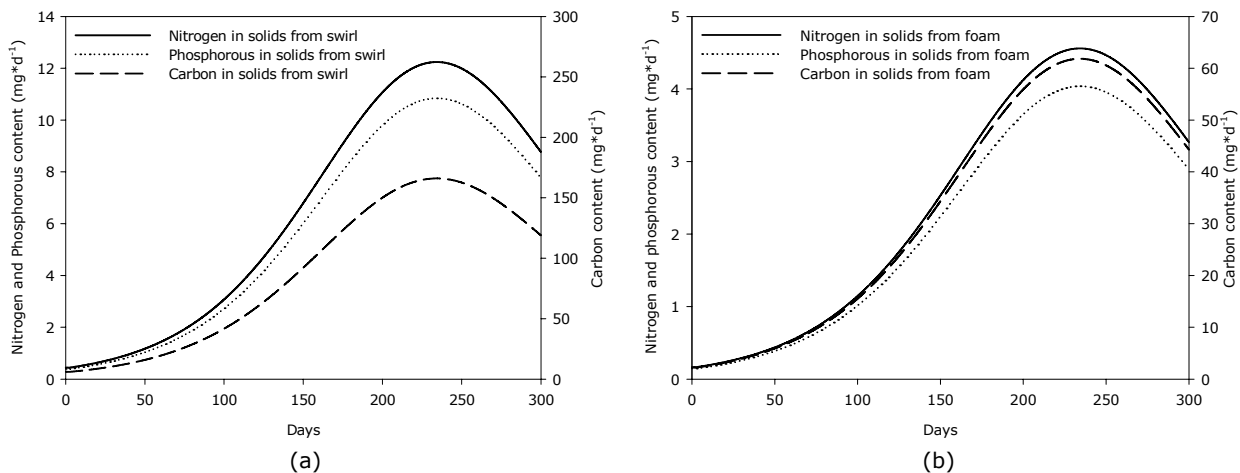


Fig. 109. Performance of the RAS while growing European sea bass (*Dicentrarchus labrax*) between day's t_0 and t_{330} . (a) Amount of nutrients (N, P, and C) in the solid waste (faeces) in the swirl separator (equations 28, 29, and 30); (b) Amount of nutrients (N, P, and C) in the solid matter in the foam condensate equations 31, 32, and 33).

These overall calculations help to understand the changes in the fate of nutrients and solids in the RAS in relation to biomass gain while also allowing to evaluate the incorporation of performance of treatment units in a secondary water loop. One of the interesting findings is that the removal efficiency of both treatment methods for suspended solids (Fig. 109) seems definitely to be linked to the level of feed loading and fish biomass. This observation has certainly consequences from a practical point of view as the performance has cost implications. Although one wishes to see maximum removal efficiency for all size categories of particles, it may not pay off completely if growth performance of fish is not impaired up to a certain level of solid load at which removal efficiency is higher but remaining solid levels in the system are somewhat elevated. This is a matter of further investigation on long-term exposure to solids not at sub-lethal but non-effect levels.

Erklärung

Hiermit erkläre ich, dass die vorliegende Arbeit nach Inhalt und Form und die ihr zugrunde liegenden Versuche meine eigene Arbeit sind. Es wurden – abgesehen von der Beratung durch meine akademischen Lehrer – keine anderen als die angegebenen Hilfsmittel und Quellen verwendet. Wörtlich und inhaltlich aus anderen Quellen entnommene Textstellen sind als solche kenntlich gemacht.

Diese Arbeit wurde weder ganz noch in Auszügen an einer anderen Stelle im Rahmen eines Prüfungsverfahrens vorgelegt. Ferner erkläre ich hiermit, dass ich noch keine früheren Promotionsversuche unternommen habe.

Für die Prüfung wird die Form der Disputation gewählt. Der Zulassung von Zuhörerinnen/Zuhörer bei der mündlichen Prüfung wird nicht widersprochen.

Kiel, den

Jaime Orellana

Danksagung

Ich möchte an erster Stelle Herr Dr. Uwe Waller danken. Sein Engagement diente immer dem innovativen Forschungsinteresse der Arbeitsgruppe. Ich persönlich habe in Herrn Dr. Waller nicht nur einen Freund gefunden, sondern auch einen wertvoller Diskussionspartner und erfahrener Ratgeber und einen ständigen Betreuer meiner Doktorarbeit.

Meinem Fachkollegen und Freund Bert Wecker danke ich für die wertvolle langjährige Zusammenarbeit während der Durchführung unserer jeweiligen Promotionsarbeiten. Mit gemeinsamen Zielen und ergänzenden Fragestellungen haben wir eine sehr gute, entspannte und produktive Atmosphäre geschaffen.

Meinem Fachkollege und Freund Adrian Bischoff danke ich ebenfalls für die wertvolle Zusammenarbeit. Als Diskussionspartner und Kritiker ist er immer präsent gewesen.

Besonders möchte ich mich bei Herrn Prof. Dr. Dr. h.c. mult. Harald Rosenthal herzlich für die Bereitschaft bedanken, sich trotz seines Ruhestandes für die Prüfungen als Verantwortlicher zu zeichnen. Seine konstruktiven Hinweise für wichtige Fragestellungen und die Abfassung wissenschaftlicher Arbeiten, die er uns allen noch während seiner Amtszeit gab, sind mir in guter Erinnerung geblieben und waren mir auch noch bei der Erstellung dieser Arbeit eine Hilfe.

Ganz herzlich möchte ich mich bei Michael Gruber und Egon Glappa vom Aquarium bedanken. Ihr seid eine große Hilfe in der technischen Bereitstellung der Kreislaufanlage gewesen, mit Rat und Tat (und Werkzeug!).

Ich möchte mich bei der mikrobiologischen Arbeitsgruppe in der Hohenbergstraße bedanken. Ganz besonders bei Regine Koppe die in den mikrobiologischen Fragestellungen dieser Arbeit mir ihrer Erfahrung und ihrem Wissen sehr hilfreich und engagiert war und bei Prof. Dr. Hans-Georg Hoppe für seine wertvollen Hinweise. Dr. Ralf Schmaljohann möchte ich danken für die Einführung in der faszinierende Welt der Elektronenmikroskopie.

Kerstin Nachtigall und Thomas Hansen (Durchführung der Nährstoffanalysen), Antje Burmeister, Peter Fritsche und Helge Mempel (Labor und Geräte) und Brigitte Rohloff (Sekretariat) möchte ich danken für ihren jeweiligen Beitrag zu dieser Arbeit.

Der Abteilung Fischereibiologie, besonders Herrn Prof. Dr. Dietrich Schnack, danke ich für die Bereitstellung eines Arbeitsplatzes. Die gesamte Abteilung hat während meiner Aufenthaltszeit eine sehr nette Atmosphäre geschaffen. Ich habe mich vom Anfang an willkommen und wohl gefühlt.

Ich möchte an dieser Stelle der Firma Erwin Sander Elektroapparatebau GmbH danken. Die Firma Sander hat sämtliche Komponenten der Kreislaufanlage kostenlos zur Verfügung gestellt und immer wieder für Reparaturen und technische Unterstützung gesorgt.

Ich danke meinem Vater, Dr. Hernán Orellana, der mich immer geistig und finanziell unterstützt hat. Ohne seine Hilfe wäre diese Arbeit nicht zustande gekommen.

Dieser Arbeit widme ich meiner kleine Tochter Leonie Fischer und meiner Mutter Ana María Hurtado († 1999).

Lebenslauf

JAIME ORELLANA

Limmerstr. 81, 30451, Hannover

PERSÖNLICHE ANGABEN

Geburtstag/ -ort: 23. April 1968, Viña del Mar, Chile
Staatsangehörigkeit: Chilene
Sprachkenntnisse: Spanisch, Muttersprache
Deutsch, fließend
Englisch, fließend

AUSBILDUNG

Schulausbildung

1975-1986 Deutsche Schule Valparaíso, Chile
Grundschule und Oberstufe

1984 Deutsches Sprachdiplom der Kultusministerkonferenz Stufe I

1986 Deutsches Sprachdiplom der Kultusministerkonferenz Stufe II

1986-1987 Schulabschluss, Hochschulaufnahmeprüfung

Studium

1988-1995 (Jul) Katholische Universität Valparaíso, Chile
Institut für Meereswissenschaften
Fischerei- und Aquakultur- Ingenieurwissenschaft

Studienabschluß

1996 (Mär-Dez) Abschlußprüfung
Diplomarbeit: "Technische Durchführung für die Produktion von Knospen der Meeressalge "luche" (*Porphyra columbina*)"

Weitere Ausbildung

1995 (Okt) Katholische Universität Temuco, Chile
Internationaler Fortbildungskurs "Ernährung und Fütterung der Salmoniden"

BERUFLICHE TÄTIGKEITEN

- 1993 (Jan-Mär) Fitz-Roy GmbH, Calbuco, Chile
Mitarbeiter einer Lachszuchtanlage
- 1994 (Jan-Mär) Fitz-Roy GmbH, Calbuco, Chile
Abteilungsleiter einer Lachszuchtanlage
- 1995 (Aug-Dez) Best Salmon GmbH - Ecofeed GmbH, Chiloé, Chile
Leiter der Forschungsabteilung
Forschungsprojekt: "Optimierung der Futterregime für das Wachstum von Atlantischer Lachs (*Salmo salar*) im Meer"
- 1995-1996 Katholische Universität Valparaíso, Chile
Institut für Meereswissenschaften
Leiter und Forschungsassistent des Versuchslabors für Meeresorganismen
Forschungsassistent im Mikroalgenlabor
- 1995-1996 Katholische Universität Valparaíso, Chile
Institut für Biologie
Labor für Tierische Funktionsmorphologie
Forschungsassistent
- 1997-1998 Fitz-Roy GmbH, Calbuco, Chile
Operationsleiter der Lachszuchtanlagen
Operationsleiter der Schlachtungsabteilung
Leiter der Miesmuschelzuchtanlage
- 1998 (März-Jun) Plancton Andino Ltda., Puerto Montt, Chile
Assistent für Umwelt, Aquakultur, und Ozeanographie
- 1998-2000 (Apr) Aquasmart Ltda., Puerto Varas, Chile
Berater und Experte für die Ernährung der Salmoniden
- 2000 (Mai-Nov) Technopress S.A., Santiago, Chile
Wissenschaftlicher Berater der Zeitschrift Aqua Noticias
- 2001- 2004 Leibniz-Institut für Meereswissenschaften, Kiel, Deutschland
Wissenschaftlicher Mitarbeiter, Doktorand
Promotionsthema: "Identification and quantification of suspended solids and their effect in modern recirculation systems"
- 2005-dato Erwin Sander Elektroapparatebau GmbH, Uetze-Eltze, Deutschland
Wissenschaftlicher Mitarbeiter
Technische und biologische Leitung des Projekts
"PISA: Poly Integrierte Seewasser Aquakultur"